A SECRETED FACTOR-BASED MECHANISM FOR OLFACTORY ENSHEATHING CELL-MEDIATED NEURITE OUTGROWTH

by

EDMUND AU

B.Sc. (Biochemistry), The University of British Columbia, 1998

A THESIS SUBMITTED IN PARTIAL FULFILMENT OF THE REQUIREMENTS FOR THE DEGREE OF

DOCTOR OF PHILOSOPHY

in

THE FACULTY OF GRADUATE STUDIES

(Neuroscience)

THE UNIVERSITY OF BRITISH COLUMBIA

September, 2005

Abstract

The olfactory system continually turns over its neuronal population throughout life. As a consequence, newly generated olfactory receptor neurons (ORNs) grow axons centrally towards the olfactory bulb; thus the olfactory system continually accommodates axon growth and does so employing a unique glial cell type, olfactory ensheathing cells (OECs). Because of their involvement in providing a permissive environment for ORN axon growth, OECs have been employed in repair strategies in other parts of the nervous system, most prominently the injured spinal cord. However, little is known about how OECs promote regeneration.

OECs reside in two compartments, the lamina propria and the nerve fibre layer of the olfactory bulb. LP-OECs were examined in vivo and in vitro and compared with what has been reported on olfactory bulb OECs (OB-OECs). LP-OECs are very similar to OB-OECs in vivo and in vitro with several subtle differences. LP-OECs express CD44 in vivo while OB-OECs do not. LP-OECs also proliferate robustly without exogenous mitogens added, suggesting a more immature phenotype. LP-OEC cultures can be purified to greater than 95% and express novel developmentally regulated markers such as p200 and NG2.

Purified cultures of LP-OECs were used to elucidate mechanisms of OEC-mediated neurite outgrowth. Using an embryonic dorsal root ganglion (DRG) culture system, LP-OECs promoted outgrowth in co-culture and also with LP-OEC conditioned media (LP-OCM) alone. LP-OCM from passage 2 and passage 6 LP-OECs were assayed for biological activity using the outgrowth assay and passage 2 LP-OCM was found to have a more effective dose-response curve.

Secreted factors underlying this difference in biological activity were identified using isotope coded affinity tags (ICAT) proteomics, which provides the identity and relative quantity. By correlating biological activity with relative quantity, SPARC (secreted protein acidic rich in cysteine) was identified as a candidate factor. Gain- and loss-of-

function experiments confirmed the important role of SPARC in the outgrowth activity of LP-OCM. In summary, the work in this thesis characterizes a previously poorly understood cell type and uses it as a model system to prospectively elucidate mechanisms of OEC-mediated neurite outgrowth.

Table of Contents

List of Tables

List of Figures

List of Abbreviations

2-DE	2 dimensional gel electrophoresis
ACM	astrocyte conditioned medium
aFGF	acidic fibroblast growth factor, aka FGF-1
amu	atomic mass unit
AraC	cytosine arabinoside
A-type	astrocyte-type OEC
BDNF	brain derived neurotrophic factor
BBB	Basso, Beatie and Bresnahan open field test
bFGF	basic fibroblast growth factor, aka FGF-2
BrdU	bromodeoxyuridine
CBP/p300	CREB binding protein
CCD	charge coupled device
CGRP	calcitonin gene related peptide
CID spectrum	collision-induced spectrum
CldU	chlorodeoxuridine
CNS	central nervous system
CP	cribriform plate
CRE	cre recombinase
CSPG	chondroitin sulphate proteoglycan
CST	corticospinal tract
DAPI	4'6-diamidino-2-phenylindole
DBA	*Dolichos biflorus* agglutinin, a lectin that binds subpopulation of ORNs
DCC	deleted colorectal cancer, the receptor for netrin-1
dhh	desert hedgehog
DMEM	Dulbecco's modified Eagle's medium
DMEM/F12	DMEM in a 1:1 ratio with Ham's F12 medium
DMEM-BS	modified DMEM with Bottenstein-Sato supplements

DREZ	dorsal root entry zone, CNS/PNS boundary of the spinal cord and sensory root
E-C domain	extracellular calcium binding domain
ECM	extracellular matrix
ER	estrogen receptor
FACS	fluorescence activated cell sorting
FBS	fetal bovine serum
FGF	fibroblast growth factor
FGFR	fibroblast growth factor receptor
GFAP	glial fibrillary acidic protein
HGF	hepatocyte growth factor
HPLC	high pressure liquid chromatography
HRGb1	heuregulin b1, a neuregulin-1 isoform
HSPG	heparin sulphate proteoglycan
ICAT	isotope-coded affinity tags
IdU	iododeoxyuridine
IGFBP	insulin growth factor binding protein
IRES	internal ribosome entry site
kDa	kiloDalton
LHRH	luteinizing hormone releasing hormone
LIF	leukemia inhibitory factor
LP	lamina propria
LP-OCM	lamina propria-derived OEC conditioned media
LP-OECs	lamina propria-derived OECs
m/z	mass to charge ratio
MEM-d-valine	minimal essential medium with D-valine (instead of L-valine)
mRNA	messenger ribonucleic acid
MS-MS	tandem mass spectroscopy
NCAM	neural cell adhesion molecule
NFL	nerve fibre layer
NGF	nerve growth factor

NT-3	neurotrophin-3
NT-4/5	neurotrophin-4/5
O4	oligodendrocyte marker 4
OB	olfactory bulb
OB-OECs	olfactory bulb-derived OECs
OCT	optimal cutting temperature
OE	olfactory epithelium
OEC	olfactory ensheathing cell (OECs = olfactory ensheathing cells)
OM	olfactory mucosa
OMP	olfactory marker protein
ONR-OECs	olfactory nerve rootlet-derived OECs
ORN	olfactory receptor neuron
P200	a type V collagen isoform
p75	low affinity nerve growth factor receptor, protein 75 kDa in size
PACAP	pituitary adenylate cyclase-activating peptide
PBS	phosphate buffered saline
PDGF	platelet derived growth factor, two isoforms are PDGF-A and PDGF-B
PEDF	pigment epithelium derived factor
PNS	peripheral nervous system
PSA-NCAM	polysialated neural cell adhesion molecule
SAGE	serial analysis of gene expression
SCI	spinal cord injury
sf9	*spodoptera frugiperda* cell line 9 (insect cell line)
SPARC	secreted protein acidic rich in cysteine
S-type	Schwann cell-type OEC
tris	tris(hydroxymethyl)-aminomethane
trk	tropomycin-related kinase
TRP-like	transient receptor protein-like, putative channel protein
VEGF	vascular endothelial growth factor
WGA	wheat germ agglutinin

Preface

I may not have gone where I intended to go, but I think I have ended up where I intended to be.

- Douglas Adams

Simplicity is the ultimate sophistication.

- Leonardo da Vinci

Acknowledgements

I would like to thank all the members of the Roskams lab, past and present, for their support, help, advice, and friendship. You've made it a pleasure to come to the lab everyday. In particular, I'd like to thank Miranda Richter, co-founder of ΓΛΙΑ, for her hard work on LP-OEC transplantation collaboration with Dr. Wolfram Tetzlaff and members of his lab, without whom all this work would be nothing more than in vitro speculation. Also, thanks to David Dai, an undergraduate student, for his help quantifying neurite outgrowth.

I'd also like to thank the collaborators who made this project possible: Dr. Reudi Aebersold (ICAT proteomic analysis) and Dr. E. Helene Sage (recombinant human SPARC, function-blocking antibodies and SPARC null mice). Thanks also to Drs. David Carey (anti-P200) and Frank Margolis (anti-OMP) for their kind gift of primary antibodies.

To my supervisor, mentor and friend, Dr. Jane Roskams, thank you for deciding to take a chance on me and patiently allowing me to grow. And thank you for your guidance and input, which has helped me to look at problems from a new perspective.

To my family and to Evelyn, thank you for believing in me.

Edmund Au, 2005

Chapter 1: Literature Review and Introduction

1.1 Literature Review

1.1.1 Olfactory Turnover

The mammalian olfactory system is unique in several regards. It receives its primary input not in the form of light or mechanical energy but rather by chemical ligand binding. The gustatory system shares this feature also but without the same magnitude of complexity. With a complement of hundreds to thousands of olfactory receptors each with differential affinities to a given odourant, the olfactory system is capable of discerning seemingly limitless different odours (reviewed in Mombaerts, 2001). Such a system requires a certain degree of flexibility in order to accommodate the changing environment and the evolving needs of the animal. Likely, it is through this need that the olfactory system has retained an unusual feature: the constant turnover of its olfactory neuron population (Graziadei and Graziadei, 1979a; Graziadei and Graziadei, 1979b). By and large, olfactory receptor neurons (ORNs), which reside in the olfactory epithelium (OE) of the nasal cavity (see figure 1.1), have a finite lifespan estimated at approximately four to six weeks (reviewed in Farbman, 1990). They undergo programmed cell death (Holcomb et al., 1995; Michel et al., 1994) and are replaced by newly generated neurons arising from progenitor cells situated in the basal region of the OE (Graziadei and Monti Graziadei, 1976) (see figure 1.2). With their cell body residing in the periphery, ORNs are bipolar neurons that extend a short dendrite out into the nasal cavity to detect odour molecules and a longer axon basally into lamina propria (LP) where they fasciculate with other ORN axons into nerve bundles (Doucette, 1991). The nerve bundles course through the LP, deep to the OE, en route to the olfactory bulb (OB) (see figure 1.3). When the ORN axons reach the outer layer of the bulb, they begin to

defasciculate (Whitesides and LaMantia, 1996) and path find towards their appropriate individual targets known as glomeruli. Thus, as new ORNs are generated to replace dying ones, they must grow axons long distances into the central nervous system (CNS). Since this turnover takes place throughout the life of an animal, it can be said that the olfactory system accommodates CNS axon growth even during adulthood.

1.1.2 Olfactory Ensheathing Cells in the Olfactory System

While the capacity to support axon growth in the adult nervous system is not unique to the olfactory system, the manner in which it occurs is. The peripheral nervous system (PNS) can undergo extensive repair following injury to restore near-normal function (Liuzzi and Tedeschi, 1991). The olfactory system does not undergo repair in a similar fashion but rather replaces its neurons. The other difference is that ORNs target in the central nervous system where, in general, axon growth is severely limited after development (reviewed in Fawcett and Asher, 1999). ORNs undergo constant replacement and regularly grow axons into the CNS and form functional synaptic connections, thus setting them apart.

How the olfactory system continuously re-targets is likely dependent on multiple factors. The fact that ORNs are newly generated and may be more immature or embryonic in nature may contribute to their growth capabilities. There may be additional intrinsic properties of ORNs that make them uniquely capable of successfully navigating the CNS environment. Also, there are likely environmental factors. For example, the outer layers of the olfactory bulb may be especially amenable to axon growth regardless of the nature of the neuron itself whereas everywhere else in the CNS, the environment is less hospitable.

Residing in the outer layers of the OB and also peripherally in the lamina propria are glial cells unique to the olfactory system, olfactory ensheathing cells (OECs) (reviewed in Ramon-Cueto and Avila, 1998) (see figure 1.3). In fact, OECs are in direct contact with ORN axons from where they exit the OE to just before they synapse with mitral cells in

glomeruli – effectively the entire length of the ORN axon (Doucette, 1991). Therefore, OECs are well situated to provide a permissive environment for ORN axon growth. But which factors play a more important role in the unique regenerative capacity of the olfactory system? Is it intrinsic to ORNs or the environment created by OECs?

1.1.3 The Intrinsic Plasticity of ORNs

The idea that olfactory receptor neurons possess an intrinsic degree of plasticity is supported by the observation that ORNs can synapse with and form ectopic glomeruli with parts of the brain other than the olfactory bulb. Several groups have demonstrated this using olfactory bulb ablation studies (bulbectomies, see figure 1.4) as well as embryonic engraftment experiments. In a bulbectomy, the olfactory bulb is surgically ablated leading to a synchronous wave of ORN cell death via distal axotomy, prompting a large scale mobilization of the progenitor population in the OE to replace the dying ORNs (reviewed in Graziadei and Monti Graziadei, 1983). The newly generated ORNs robustly extend axons back towards the OB in an attempt to form new connections (Doucette et al., 1983a). In the case of incomplete bulbectomies, ORNs have demonstrated the ability to synapse inappropriately with other brain structures, stimulating the formation of glomerular structures (the functional synaptic unit normally found within the olfactory bulb) (Graziadei et al., 1978; Graziadei and Monti Graziadei, 1986). This suggests that ORNs exert a degree of influence over the area of the brain with which they interact, molding it to suit their purposes (Gong and Shipley, 1996). It is reasonable to speculate that this ability to direct glomerular formation (Doucette et al., 1983b) may not be confined to the special circumstance of a lesioned bulb but may also occur in the normal state to accommodate the changing needs of the animal's olfactory system. Such changes may be necessary to adapt to a changing environment or changes associated with reaching sexual maturity. Embryonic engraftment studies have also suggested that ORNs can re-model the brain. Isochronic transplantation of olfactory placode (a region of neuroectoderm that gives rise to the olfactory system) in place of the optic vesicle results in an ectopic olfactory nerve that inappropriately establishes glomeruli on the diencephalic wall (Magrassi and Graziadei, 1985). If two-thirds of the

optic vesicle is replaced with donor olfactory placode, the ORNs are able to out-compete the developing optic nerve for the diencephalic target. Therefore, the intrinsic properties of ORNs are likely a contributing factor to the olfactory system's remarkable regenerative abilities.

There is also evidence that ORNs provide trophic support contributing to their growth capabilities in an autocrine manner. Mackay-Sim's group (Hsu et al., 2001) suggest that ORNs are a source of basic fibroblast growth factor, previously demonstrated to promote axon and neurite outgrowth in other systems (Dingwell et al., 2000; Grothe et al., 2000; Kornblum et al., 1990). ORNs also influence the glia with which they interact. When a short length of sympathetic nerve is transplanted into the olfactory system, ORN axons will extend into the nerve graft (Barber, 1982). The ORNs influence Schwann cells of the sympathetic nerve to bundle ORN axons differently than sympathetic nerves; in a manner similar to OEC ensheathement (see section 1.2.1). However there were subtle differences. Schwann cells surrounded each bundle of ORN axons with a basal lamina whereas OECs segregated ORN axons into dicrete bundles called mesaxons that lacked a basal lamina (see section 1.2.1).

There are, however, limitations to the growth and plasticity potential of olfactory receptor neurons. Several groups have autologously transplanted olfactory mucosa (OM, the soft tissue overlying the cartilaginous turbinates; containing both olfactory epithelium and underlying lamina propria tissue layers, see figure 1.1) into other regions of the body. Olfactory mucosa can successfully engraft into the anterior chamber of the eye, become vascularized and maintain both OE and LP tissue layers (Barber et al., 1982). A subset of the transplanted ORNS, presumably newly generated ones, expressed olfactory marker protein (OMP, an antigen specific to ORNs) and grew moderate distances into and along the connective tissue of the iris. This was confirmed in a separate study using carnosine to specifically label the graft (Novoselov et al., 1983). OM was also transplanted in apposition to neuronal tissue in various regions of the brain including the fourth ventricle, parietal cortex, and the cerebellum (Amemori et al., 1987; Monti Graziadei and Morrison, 1988). Pieces of OM were transplanted into the parietal cortex but the transplant was

exposed via a removable plastic lid. Even three weeks post transplant, the olfactory mucosa was electrophysiologically responsive to odourant stimulation (Amemori et al., 1987). The authors found that the OM transplant was unable to form glomerular-like structures. In an attempt to direct glomerular formation using OM transplants, OM was transplanted directly into its corresponding olfactory bulb (Monti Graziadei and Graziadei, 1989). Even then, ORNs did not form new glomeruli or interact with existing glomeruli in the OB. Furthermore, the transplants all contained OECs making it difficult to discern the growth capabilities of the ORNs themselves. More recently, an antibody against PDGF-B (platelet derived growth factor isoform B) was used to identify OECs from pieces of embryonic olfactory bulb transplanted into a bulbectomized neonate host. They found close association of OECs with growing bulb neurons (Kott et al., 1994). It appears that, at the very least, the intrinsic capabilities of ORNs are linked to the unique spatial context and likely the environment of the olfactory system.

When the olfactory system is intact and in the correct spatial context, even then there are limitations to its regenerative capabilities. Work by Doucette and coworkers has called into question the ability of ORNs to regenerate in the injured state (Doucette et al., 1983b). In their study, they made a small lesion on the dorsal surface of the olfactory bulb, effectively creating a distal axotomy to a small subset of ORNs but leaving the target organ intact. The regenerating ORNs were traced by horseradish peroxidase to follow where they re-targeted. They found that newly generated ORNs, while able to create new glomeruli and synapse with existing ones, were largely unable to cross the small glial scar formed when lesioning the bulb surface. Thus, like other CNS neuronal populations, an astrocytic scar barrier also obstructs ORN growth.

In summary, ORNs exhibit a great deal of plasticity in the olfactory system by robustly extending axons following injury, re-targeting and directing the formation of new glomeruli. When transplanted, strips of OM can successfully engraft, become vascularized, express OMP and respond to odourants. However, there are limitations to ORN plasticity. Strips of OM cannot direct glomerular formation (suggesting that this ability may be lost in adulthood), ORNs cannot overcome the glial scar formed after a

microlesion on the surface of the olfactory bulb and finally the transplantation studies cannot parse apart the contributions of ORNs versus OECs.

1.2 Olfactory Ensheathing Cells

The other factor contributing to the regenerative capacity of the olfactory system is the environment in which the ORN axons reside. This environment is generated and regulated by the glia of the olfactory system, olfactory ensheathing cells.

1.2.1 OEC Introduction

The glial environment of the olfactory system is made up of a unique cell type found only in the primary olfactory pathway: olfactory ensheathing cells, OECs. Olfactory ensheathing cells, as their name implies, ensheathe ORN axons virtually along their entire length: from where they exit the olfactory epithelium up to where they synapse with mitral cells at the glomerulus (see figure 1.3) (Doucette, 1991). OECs associate with many ORN axons in nerve bundles, each bundle typically containing over one hundred axons each. The outside of the bundle is entirely surrounded by OECs and is further sub-compartmentalized into sub-fascicles (mesaxons) by involuting OECs processes (Doucette, 1991). It is in this configuration that axons traverse through the lamina propria, the extracellular matrix (ECM) rich tissue layer deep to the olfactory epithelium. Separate nerve bundles begin to coalesce as they approach the cribriform plate (CP), a specialized portion of the skull that separates the olfactory mucosa from the olfactory bulb. En masse, the nerve bundles weave through the porous surface of the CP to contribute to the most superficial layer of the olfactory bulb, the nerve fibre layer (NFL) (Doucette, 1989; Valverde et al., 1992). The nerve fibre layer is structurally complex with tens of thousands of nerve bundles coursing every which way along the surface of the bulb. Ultimately, individual ORNs arrive at the appropriate glomerulus and form a synapse with mitral cell dendrites. OECs are directly in contact with ORN axons until just before the ORN axon terminal enters the glomerulus (Doucette, 1989).

It is interesting to speculate exactly what role the close association of OEC and ORN axon plays in the setting up and maintenance of the primary olfactory pathway. Clearly, the nature of the olfactory system poses a unique set of requirements. For instance, there is a precise targeting of millions of ORNs (see figure 1.5) (reviewed in Mombaerts, 2001), to their appropriate target glomeruli; ORNs target to just one glomerulus among hundreds or even thousands depending on the species. In addition, the mature olfactory system contains ORNs at all different stages of their life cycle and there must be a mechanism in place for newly generated ORNs to find their way to the correct glomerular target to replace ORNs undergoing apoptosis. While there is a wealth of data to support an olfactory receptor-based mechanism of glomerular specificity, it does not address how receptor expression translates meaningfully into a pathfinding mechanism. With the ORN axons arranged into discrete nerve bundles and mesaxons by OECs, it is an attractive hypothesis that ensheathing cells are the first order 'sorting station' for olfactory axon targeting. One could envision a mechanism where like ORNs are brought together into nerve bundles and the sorting process is further refined by arrangement into mesaxons. Additionally, OECs may be contributing to the development and maturity of each individual ORN by providing growth factor trophic support (see section 1.2.3) and helping immature ORNs reach electrophysiological competence (Hegg et al., 2003).

1.2.2 OEC Development

One way to examine the role of OECs in the olfactory system is to follow them developmentally. What is their role in the initial setup of the primary olfactory neuraxis and initial synapse formation in the olfactory bulb? It is well established that OECs, like the rest of the primary olfactory system, originate from the olfactory placode (Chuah and Au, 1991; Doucette, 1989; Farbman and Squinto, 1985; Marin-Padilla and Amieva, 1989). The placode is a disc-like neuroectodermal structure originally part of the antero-lateral neural ridge (Couly and Le Douarin, 1985). At about embryonic day 10 (E10) in the mouse, the OP invaginates to form the olfactory pit, a structure that continues to deepen and convolute to make up both the respiratory and olfactory epithelia that line the

nasal cavity. By E11.5, the olfactory epithelium is a pseudostratified epithelium with a clear basal lamina separating it from the underlying lamina propria (Farbman and Squinto, 1985). Olfactory neurons have already differentiated and in concentrated areas throughout the basal lamina, holes form through which axons exit the OE. Shortly afterwards, cells from the basal layer of the primitive OE begin to migrate through these same holes and closely associate with ORN axons (Marin-Padilla and Amieva, 1989). The work of Doucette and others indicate that these migrating basal layer cells are the precursors of olfactory ensheathing cells (Doucette, 1990; Tennent and Chuah, 1996). The OEC precursors migrate along with the ORN axons, and divide in situ; collectively they are referred to as the migratory mass (MM). By electron microscopic analysis, Valverde and coworkers suggest that the precursors also differentiate as they divide and migrate; the more differentiated OECs are situated peripherally and arise from OEC precursors found within the nerve bundle (Valverde et al., 1992). While these structures are not arranged as well-defined nerve bundles and mesaxons, OECs are ensheathing these pioneer ORN axons (Doucette, 1990). Meanwhile centrally, a pocket of the cerebral vesicle has evaginated and will ultimately become the olfactory bulb (Doucette, 1989). Making its way through the mesenchyme, the MM along with the first ORN axons reach the cerebral vesicle (by E14 in rat) and proceeds to cover its surface forming the nerve fibre layer of the OB (see figure 1.6).

Several salient points about the developing olfactory system at this stage should be highlighted. First, the embryonic origin of OECs sets them apart from all other glial cell types. In the peripheral nervous system, Schwann cells (reviewed in Jessen and Mirsky, 2002) derive from the neural crest along with enteric glia (reviewed in Gershon et al., 1993). In the central nervous system, astrocytes arise from radial glia of the subventricular zone (Malatesta et al., 2003) and oligodendrocytes from the ventral neural tube (reviewed in (Liu and Rao, 2004)). That OECs arise separately from the olfactory placode (Chuah and Au, 1991; Doucette, 1989; Farbman and Squinto, 1985; Marin-Padilla and Amieva, 1989) which may account for some of their hybrid-like characteristics (Doucette, 1990) (see section 1.2.4). Second, it does not appear that OECs facilitate the exit of the ORN axons through the basement membrane of the OE. Farbman

and Squinto suggest however that nearby endothelial cells may aid in this process (Farbman and Squinto, 1985). Third, even at the earliest stages, OECs are closely associated with the developing olfactory nerve and are therefore well situated to help ORNs pathfind towards their target. In twirler knockout mice, Gong found severe deficits in ORN pathfinding coincident with defasciculation (Gong, 2001). It is possible that failure of proper OEC ensheathement contributes to this phenotype. Unfortunately with the twirler mouse, the genetic defect has only been characterized at the chromosome locus level so molecular mechanisms cannot readily be ascertained.

Over the next 24 hours of mouse embryonic development, the nerve fibre layer remains a separate entity from the developing olfactory bulb. ORNs, OECs and OEC precursors accumulate at the nerve fibre layer increasing its thickness and breadth until it covers nearly the entire surface of the bulb. Also, the meningeal layer overlying the OB is remodelled by OECs (Doucette, 1989); where once there was a continuous meningeal layer (produced by leptomeningeal cells) covering the entire surface of the developing OB, ORNs have penetrated through and OECs have fused the basal lamina covering the outside of the nerve bundles with the meningeal layer of the OB (see figure 1.7). This rearrangement, while subtle, is likely key to the regenerative capacity of the olfactory system: OECs, in effect, are the glia limitans of the olfactory system. In fact, with the meningeal layer now continuous with the basal lamina covering the nerve bundles, it can be said that the CNS/PNS boundary of the olfactory system is continuous along the length of the ORN axon from the point that it exits the OE to when it crosses the cribriform plate. This is a unique arrangement found only in the olfactory system. Everywhere else with a CNS/PNS boundary, there is a clear delineation that separates CNS glia from PNS glia (reviewed in Fraher, 1992). As such, OECs can be thought of as both CNS and PNS glia; no boundary is formed and there is no barrier to growing axons throughout life.

As with their perforation of the basal lamina, separating the OE from the LP, ORNs are the first to break through the pial surface that separates the olfactory bulb from the developing nerve fibre layer. However Marin-Padilla and Amieva observed that ORNs

may make their first synaptic contacts prior to infiltrating the OB (Marin-Padilla and Amieva, 1989). Via a series of EM studies where they found synaptic vesicle assemblies before ORN infiltration into the bulb, they suggest that ORNs may in fact form temporary 'synapses' with OECs or OEC progenitors first. They further suggest that, in this manner, OECs may aid in the refinement of ORN subsets as they form their initial glomerular targets. Once ORNs have penetrated the pial surface, OECs follow closely and associate with ORN axons to the point just before they form glomeruli. At this stage of development, astrocytes are just beginning to be generated. OECs in the bulb and astrocytes interact and form a poorly defined boundary (not delineated by a basal lamina) at the interface between nerve fibre layer and glomerular layer, a process that continues well into postnatal development (Doucette, 1984; Doucette, 1993).

In summary, OECs play a significant role in the development of the primary olfactory neuraxis. While not directly involved in breaking the barriers at the basal lamina or the bulb pial surface, OECs follow closely behind. In their wake, self-contained and continuous conduits are formed from the base of the OE to the nerve fibre layer. In addition to providing a 'highway' for subsequent axon growth, these OEC conduits may aid in the initial sorting of ORNs to their target glomeruli. OECs in the nerve fibre layer may also aid in the initial refinement of ORN sorting prior to initial glomerular formation (reviewed in Key and St John, 2002). Furthermore, OECs and astrocytes interact to form a diffuse border (Doucette, 1990) in contrast to the definitive and solid barrier formed between astrocytes and Schwann cells at the CNS/PNS interface (reviewed inFraher, 1992). In this manner, OECs help in establishing and maintaining the physical arrangement of the primary olfactory system in addition to contributions made via cell surface and secreted molecules.

1.2.3 Molecules Implicated in OEC-Mediated Axon Growth and Pathfinding

OECs help regulate ORN axon extension via molecular cues both cell surface and secreted. Many of these molecules also have a known role in regulating neuronal development in other parts of the nervous system as well and are reviewed below:

1.2.3.1 Neurotrophin Family

The neurotrophins are the most well characterized family of growth factors related to neuronal growth and survival. Nerve growth factor (NGF) was the first member identified (as reviewed in Cowan, 2001) and was in fact one of the first proteins to be sequenced (Angeletti et al., 1971). The other family members include BDNF (brain derived neurotrophic factor), NT-3 (neurotrophin-3) and NT-4/5 (neurotrophin-4/5) (reviewed in Bothwell, 1995). Neurotrophins have high affinity receptors known as the tropomycin-related kinase (trk) receptors with trkA binding to NGF, trkB binding to BDNF and NT-4/5, and trkC binding to NT-3. In the olfactory system, trkB and trkC have been found in ORNs at different stages of maturity. Roskams and coworkers (1996) found trk B expression in both immature and mature ORNs and trk C only in the mature population. This pattern was re-capitulated following bulbectomy with newly generated ORNs expressing first trkB and then trkB and C together at later timepoints. The expression of trkA in ORNs is, however, unclear. One group (Miwa et al., 1998) found trkA in both horizontal basal cells and ORN axons and another group detected trkA only in horizontal basal cells (Roskams et al., 1996). Olfactory ensheathing cells, in different contexts, have been reported to express NGF, BDNF and NT-4/5 (summarized in table 1.1). NGF was found in OECs shortly after bulbectomy in response to ORN injury (Roskams et al., 1996) and was detected in an olfactory bulb ensheathing cell line (Goodman et al., 1993) by RT PCR and ELISA (Boruch et al., 2001). Woodhall and coworkers (2001) also found NGF by ELISA in the conditioned media and cell lysates of neonate OB OECs. BDNF, which could affect immature ORN survival (reviewed in Calof et al., 1996; Carter and Roskams, 2002), has been found in OECs by several groups (Boruch et al., 2001; Lipson et al., 2003; Woodhall et al., 2001). All three groups detected low levels of BDNF in OEC conditioned media. In vivo, BDNF has been

detected in the glomeruli of the olfactory bulb and it is possible that the source of BDNF are neighbouring OB-OECs. Boruch and coworkers also found NT-4/5 present in their olfactory ensheathing cell line (Boruch et al., 2001) however the expression of NT-4/5 in the olfactory system in vivo has not been described. These data indicate that neurotrophins are important in the ORN maturation process and that OECs may supply at least some neurotrophins to ORNs in vivo. In vitro studies have been somewhat contradictory, suggesting that OEC production of neurotrophins may depend on ORN axon contact or an ORN-derived signal.

1.2.3.2 Low Affinity Nerve Growth Factor Receptor, p75

Many groups have reported p75 expression by olfactory ensheathing cells (Barnett et al., 1993; Gong et al., 1994; Koh et al., 1989; Yan and Johnson, 1988). It is in fact one of the most widely recognized antigens for OECs (reviewed in Ramon-Cueto and Avila, 1998). The functional significance of p75 is not well understood. p75 is the low affinity neurotrophin receptor and has approximately equal binding activity for all four neurotrophins (Rodriguez-Tebar et al., 1990; Rodriguez-Tebar et al., 1992; Squinto et al., 1991). Its function in neurotrophin signalling is still a contentious issue and to date it has been implicated in modulating neuron survival, growth, death and differentiation (reviewed in Bothwell, 1995; Nykjaer et al., 2005). While the expression data for neurotrophins in the olfactory system is incomplete, it is possible that p75 binds and presents neurotrophins to aid ORN survival and growth thereby acting as a signal enhancer (reviewed in Bibel et al., 1999; Ramon-Cueto and Avila, 1998). Recent studies also indicate that the pro-form of NGF (proNGF) binds preferentially to p75 to induce apoptosis (Lee et al., 2001). Whether such a pathway initiates OEC turnover in response to ORN turnover remains to be tested.

There is evidence of a functional correlation between p75 expression and OEC-mediated neurite outgrowth. In a recent study, Kumar and coworkers examined two subpopulations of olfactory ensheathing cells in the olfactory bulb (Kumar et al., 2005).

The authors found that OECs residing along the outer edge of the OB and coursing through the cribriform plate, olfactory nerve rootlet (ONR) OECs, contained a higher proportion of p75 positive cells and performed better in promoting retinal ganglion cell (RGC) outgrowth. If both populations, ONR-OECs and OB-OECs, are immunoselected for p75 expression, the difference in outgrowth promotion disappears. The authors propose that the p75-expressing population of OECs is functionally distinct (Kumar et al., 2005). Perhaps this is due to neurotrophin presentation by p75, which enhances signalling, as mentioned above. The functional significance of p75 expression by OECs is not well understood, although there is some evidence that both p75-positive and p75-negative populations of OECs exist and cooperate in mediating neuronal regeneration (see section 1.2.6.1.2 for more details).

1.2.3.3 Fibroblast Growth Factor

Two forms of fibroblast growth factor have been described in the olfactory system: FGF-1 (also known as acidic fibroblast growth factor) and FGF-2 (also known as basic fibroblast growth factor). Both forms of FGF have been reported to promote neurite outgrowth, survival and neural development (Dono, 2003; Hossain and Morest, 2000; Pataky et al., 2000). FGF-1 has been detected in the developing olfactory system (Key et al., 1996) and both ORNs and OECs demonstrated a morphological response to FGF-1. Expression of FGF-1, however, is downregulated postnatally coincident with its upregulation in mitral cells. With its transient expression in OECs coincident with mass ORN axon growth, FGF-1 may be an important neurotrophic factor during the initial set-up of the primary olfactory neuraxis. As its expression switches postnatally to mitral cells, FGF-1 may become a target-derived survival/growth factor. FGF-2 has also been detected in OECs (Chuah and Teague, 1999; Matsuyama et al., 1992) in vivo and in OB-OECs in vitro (Chuah and Teague, 1999). FGF-2 has a mitogenic effect on olfactory ensheathing cells (Alexander et al., 2002; Au and Roskams, 2003; Chuah and Teague, 1999) and this effect is dependent on perlecan (Chuah and Teague, 1999). Whether FGF-2 is important in promoting ORN axon growth is uncertain but there is abundant evidence

that FGF-2 promotes axon/neurite outgrowth in other systems (reviewed in Dono, 2003). Fibroblast growth factor receptor isoform FGFR-1 is highly expressed throughout the OE including in OECs (Hsu et al., 2001) suggesting perhaps that FGF-2 may be acting in an autocrine mitogenic manner on OECs and paracrine manner mediating ORN growth. It has also been proposed that FGF-2 produced by cells in the OE may be involved in controlling neuronal differentiation (Calof et al., 1996; Hsu et al., 2001; Mackay-Sima and Chuahb, 2000).

1.2.3.4 Other Growth Factors

Additionally, many other growth factors and their receptors have been reported in the olfactory system (Mackay-Sima and Chuahb, 2000). Of particular interest are platelet derived growth factor (PDGF) and hepatocyte growth factor (HGF). PDGF has two isoforms PDGF-A and PDGF-B, which form the homodimers PDGF-AA and PDGF-BB and the heterodimer PDGF-AB. Sasahara and coworkers have reported OECs expressing PDGF-B in vivo (Kott et al., 1994; Sasahara et al., 1992) and embryonically PDGF-A is expressed by cells of the developing olfactory system (Orr-Urtreger and Lonai, 1992). The homodimer PDGF-BB has been found to have mitogenic effects on OECs in vitro (Alexander et al., 2002; Yan et al., 2001a). Intriguingly, the heterodimer PDGF-AB has been found to promote the survival of differentiating ORNs in vitro (Newman et al., 2000). The biological significance of this finding remains to be seen as the source of PDGF-A in the olfactory system has not been described.

Hepatocyte growth factor has been reported as a potent mitogen for OECs in vitro (Yan et al., 2001a; Yan et al., 2001b) and the expression of HGF mRNA in the lamina propria (Thewke and Seeds, 1996) has been interpreted as belonging to OECs (Mackay-Sima and Chuahb, 2000). The receptor for HGF, c-met appears to be confined to the OE in vivo (Thewke and Seeds, 1996) and the activator for HGF expression, tissue plasminogen activator (tPA) appears to be neuronal: ORNs, mitral cells and periglomerular cells. HGF, in addition to its mitogenic effect on OECs, has been implicated in neuronal

development (Jung et al., 1994) and in the specific axon growth of thalamic but not cortical neurons in vitro (Powell et al., 2003). The expression patterns suggest an interesting interplay whereby tPA is mediated by ORNs at the glomerulus, which could be regulating HGF expression by OECs that then regulates ORN growth and OEC division.

1.2.3.5 Extracellular Matrix Molecules

Extracellular matrix (ECM) proteins can have a profound effect on axon growth and certainly the environment within ORN nerve bundles and the olfactory nerve fibre layer is rich in ECM. Julliard and Hartmann examined the expression of three ECM molecules in the developing and adult rat olfactory system: laminin, fibronectin and type IV collagen (Julliard and Hartmann, 1998). The authors found all three ECM molecules in the basement membrane separating the OE and the LP, which fragments as ORNs and OECs begin to course towards the olfactory bulb (see section 1.2.2). The expression of the three molecules coincides with migrating OECs and with their establishment of a self-contained basal lamina continuous from the NFL to the OE (see section 1.2.2). They report that the expression of laminin and type IV collagen persists into adulthood whereas fibronectin levels drop perinatally. There is considerable evidence that laminin (reviewed in Grimpe and Silver, 2002) is involved in neurite and axon growth in various contexts. Collagen has been found to be permissive (Joosten et al., 2004), inhibitory (Hermanns et al., 2001; Kawano et al., 2005), or as a potential scaffold to promote axon growth (Itoh et al., 2001). Fibronectin, like laminin is also thought to be permissive (Zhang et al., 2005) if not actively promoting axon growth (Robinson et al., 2004). Taken together, the basal lamina created by OECs during development and, in the case of laminin and collagen, maintained throughout life likely facilitates ORN turnover and growth (Carter et al., 2004). In addition to affecting ORN growth directly, ECM molecules may also influence the efficacy with which OECs promote axon growth (Tisay and Key, 1999). In their study, Tisay and Key cultured E19.5 rat OE explants on a variety of substrates and found differential neurite outgrowth. Suspecting modulation of OECs by the different

substrates, they examined OEC cultures from neonate rat LP grown on various substrates and found differences in morphology. OECs grown on matrigel (a basement membrane cognate, made up of various ECM molecules including type IV collagen (Kleinman et al., 1986) and laminin were considerably more spindle-shaped with longer processes. It is, however, difficult to interpret whether ECM interaction switches OECs to an axon growth-promoting state, as the authors assert, since their outgrowth assays were co-cultures.

1.2.3.6 Cell Adhesion Molecules

Olfactory ensheathing cells also express cell adhesion molecules that may be important in mediating ORN axon growth including L1, NCAM (neural cell adhesion molecule) and PSA-NCAM (polysialated-NCAM) (Miragall et al., 1989). L1 and NCAM are both implicated in neurite outgrowth and axon growth in vivo (reviewed in Kiryushko et al., 2004). L1 can bind homophillically and to other cell adhesion molecules such as NCAM, ECM molecules and integrins (Brummendorf and Rathjen, 1995). NCAM binds homophillically and also interacts with ECM molecules such as chondroitin sulphate proteoglycan (CSPG) and heparan sulphate proteoglycan (HSPG) (Brummendorf and Rathjen, 1995). The polysialated form of NCAM, PSA-NCAM is expressed developmentally and downregulated in adulthood (Miragall et al., 1989). Due to its bulky polysialic acid moiety, PSA-NCAM has weaker binding affinity due to steric hindrance. It is generally assumed that this less adhesive form of NCAM accommodates neuronal plasticity during development and is replaced by NCAM as synaptic connections become stable in adulthood. Mechanistically, L1 and NCAM signal via the FGF receptor (FGFR1) in a calcium-dependent manner (Williams et al., 1994) and are dependent on the MAP kinase pathway (Schmid et al., 1999; Schmid et al., 2000). Likely, both L1 and NCAM promote ORN growth as it has been demonstrated that ORNs express FGFR1 (Hsu et al., 2001). PSA-NCAM appears to be important in olfactory development as well with respect to the olfactory bulb since mice treated with endoneuranimadase-N (to cleave PSA moieties) have much smaller olfactory bulbs (Ono

et al., 1994). The result was effectively a phenocopy of the NCAM-180 null mouse (NCAM 180 kDa variant) (Tomasiewicz et al., 1993). Defects in the primary olfactory neuraxis of NCAM-180 null mice were examined by Treloar and coworkers (1997). The authors found fewer and smaller glomeruli in the olfactory bulb in a subset of ORNs labelled with DBA (*Dolichos biflorus* agglutinin, a lectin that specifically labels a subset of ORNs). The authors suggest that the ORNs are less able to fasciculate within the nerve fibre layer and form glomeruli. It is possible that NCAM-positive OECs in the nerve fibre layer may aid in this sorting/fasciculating process. Functionally however, there have been conflicting reports as to the olfactory discrimination abilities of the NCAM-180 null mouse (Gheusi et al., 2000; Schellinck et al., 2004).

1.2.3.7 Ion Channels

An intriguing new mechanism for regulating OEC-mediated neurite outgrowth is by manipulation of intracellular calcium. It has been proposed that a TRP-like (transient receptor protein-like) Ca^{2+} channel may be involved in switching OECs to a growth promoting state (Hayat et al., 2003b). By increasing intracellular calcium in OECs via release of intracellular stores, the authors report increased neurite outgrowth in RGC/OEC co-cultures. In a follow-up study, OECs were treated with pertussis toxin to block $G_{i/o}$ protein activity (Hayat et al., 2003a). Pre-incubation with pertussis toxin increased OEC ability to promote RGC outgrowth in co-culture. Furthermore, the effect could be ablated by Ca^{2+} depolarization by treating OEC with KCl. With the putative TRP-like Ca^{2+} channel being affected by potassium depolarization in the same manner, it suggested that the G-protein and TRP-like channel mechanisms may be linked. In a comparison of olfactory nerve rootlet OECs with OB-OECs (see section 1.2.3.2) it was found that the p75-negative OECs in their population were the ones responsive to pertussis toxin (Kumar et al., 2005).

1.2.3.8 Guidance Molecules

Since OECs co-migrate with ORNs developmentally and ensheathe ORN axons into nerve bundles and sub-sort them into mesaxons, it is an attractive hypothesis that OECs are involved in ORN axon guidance. During the initial set-up of the olfactory neuraxis, OECs migrate along with neurons and possibly respond to guidance cues on their way to the olfactory bulb (Key and St John, 2002). Perhaps OEC migration leads ORN axons towards the bulb by acting as a preferred substrate for ORN growth. Key and St John (Key and St John, 2002) propose that since OECs avoid CSPG in vitro (Tisay and Key, 1999), they may also do so in vivo and respect CSPG boundaries such as the one rostral to the OE and in the marginal zone of the developing bulb prior to ORN infiltration (Treloar et al., 1996). In reality, however, the situation is likely more complex. Storan and Key made OE/OB cocultures where a subpopulation of ORNs expressing P2 (an odorant receptor (Mombaerts et al., 1996)) project caudally then turn dorsally, independent of OEC migration as visualized by S100β-dsRed (Storan and Key, 2004).

One candidate for OEC-mediated ORN axon guidance is the netrin family of guidance molecules (Manitt and Kennedy, 2002). There is evidence that luteinizing hormone releasing hormone (LHRH) neurons (a neural cell type also derived from the olfactory placode) rely on netrin-1 (Schwarting et al., 2004) and its receptor DCC (deleted colorectal cancer) (Schwarting et al., 2001) to migrate towards the forebrain. DCC is expressed by developing ORNs embryonically but the expression drops off by birth (Astic et al., 2002). The expression of netrin-1 was detected directly beneath the basement membrane and in the lamina propria, it has been attributed to OECs (Astic et al., 2002). Netrin expression in the mesenchyme was not uniform, with a tendency for higher expression dorsally towards the cribriform plate but no expression in the developing olfactory bulb. Like DCC, netrin-1 expression levels dropped perinatally. However, unlike DCC, netrin-1 levels increased bilaterally in the lamina propria following a unilateral bulbectomy (Astic et al., 2002). It is possible that netrin-1 expression by OECs during development and following bulbectomy could aid in ORN pathfinding towards the olfactory bulb. The nasal septum expresses the repulsive

guidance cue, slit (Pini, 1993) which may prevent ORN mistargeting to the contralateral bulb. Also, the olfactory bulb expresses slit as well as its receptor Robo1 (Nguyen Ba-Charvet et al., 1999; Yuan et al., 1999). While there is evidence of slit-1 being necessary for vomeronasal axon targeting (Cloutier et al., 2004), slit/Robo involvement in olfactory guidance has not been described. In an in vitro study by Patel and coworkers, the authors co-cultured embryonic OE explants with nasal septum (Patel et al., 2001). While they found repulsion of OE neurites, it could not be blocked by competitive inhibition with soluble Robo.

During embryonic development, OECs appear to play a role in ORN guidance through a semaphorin-mediated pathway (Renzi et al., 2000). In their study, the authors blocked semaphorin-3A signalling in ORNs by electroporating soluble neuropilin-1 extracellular domain into chick olfactory placode. Neuropilin-1, a pan receptor for class 3 semaphorins (Feiner et al., 1997) can act as a dominant negative receptor for semaphoring-3A and 3C signalling in its soluble truncated extracellular form (Renzi et al., 1999). By blocking semaphorin-3A, ORNs did not stop at the olfactory bulb and accumulate as a nerve fibre layer (see section 1.2.2) but instead overshot deep into the telencephalon. Semaphorin-3A expression was examined by in situ and the staining pattern coincided with OECs lining the olfactory bulb (Renzi et al., 2000).

Another likely candidate for OEC-mediated ORN guidance are Eph/ephrins. Eph/ephrins are generally repulsive contact-mediated guidance molecules (O'Leary and Wilkinson, 1999). There are two forms of the receptor, Eph: EphA and EphB. Generally, EphA binds to ephrinA and likewise EphBs bind to ephrinBs. Binding is generally promiscuous between the various forms of EphB/ephrinB and EphA/ephrinA but in the case of EphA4, it can also bind to ephrinB2 and ephrinB3 (see figure 1.8). Many members of the Eph/ephrin family are found in the olfactory system (St John and Key, 2001; St John et al., 2002). ORNs express a number of ephrin ligands: A2, A5 and B1 and the Eph receptors A3, A4 and A5 (Cutforth et al., 2003; St John et al., 2002). Ensheathing cells express ephrin B2 (St John and Key, 2001) but only in the nerve fibre layer of the bulb. Two potential mechanisms can be gleaned from this expression profile.

One, ORNs expressing EphA4 may be facilitated in defasciculation and sorting in the nerve fibre layer by OECs expressing ephrinB2. Two, in the lamina propria there is also EphA4 expression, although it cannot be determined if it is in the OECs (St John et al., 2002). Perhaps EphA4/ephrinB2 signaling also aids in OEC migration away from the OE towards the olfactory bulb and, by extension, aiding ORN axon growth towards the OB.

1.2.4 OEC Antigenic Profile

There is still much work to be done to elucidate the molecular cues and growth factors employed by OECs. In fact, what even what defines them as a discrete cell population is not entirely clear. While anatomically and ontogenically OEC are distinct (Chuah and Au, 1991; Doucette, 1989; Farbman and Squinto, 1985; Marin-Padilla and Amieva, 1989), there has been a degree of controversy over the antigenic profile of olfactory ensheathing cells and there is a paucity of definitive markers that uniquely identify them. The most widely agreed upon markers are: p75 (Gong et al., 1994; Ramon-Cueto and Nieto-Sampedro, 1992), GFAP (glial fibrillary acidic protein) (Barber and Lindsay, 1982; Barnett et al., 1993), and S100 (Astic et al., 1998; Doucette, 1993). Other markers that have been described in OECs include O4 (oligodendrocyte marker 4) (Barnett et al., 1993; Franceschini and Barnett, 1996), NCAM (Chuah and Au, 1994) and nestin (Barnett et al., 1993; Doucette, 1993). There are many more antigens reported in the literature concisely summed up by Ramon-Cueto and Avila (1998). None of the markers listed above or additional markers reviewed by Ramon-Cueto and Avila definitively identifies OECs by themselves. However, in combination they distinctly identify OECs from other glial populations as well as other cell types found in the olfactory system. Heredia and coworkers have reported on two monoclonal antibodies that can identify OECs found in the nerve fibre layer (Heredia et al., 1998). However, the specificity of these two antibodies are is age-dependent and exhibit cross reactivity with radial glia in the case of monoclonal antibody 1.9.E and sciatic nerve-derived Schwann cells in the case of monoclonal antibody 4.11.C. Also, neither monoclonal has been verified by other

groups. The purification and full characterization of OEC cultures is vital prior to their use in experiments.

1.2.5 Comparison of OECs with Other Glial Cell Types

Since OECs reside in both the central and peripheral nervous systems, an obvious question is how similar are OECs to Schwann cells and astrocytes?

1.2.5.1 OECs vs. Schwann cells

OECs and Schwann cells are very similar in most respects. They are derived embryonically from different origins, the olfactory placode in the case of OECs (Chuah and Au, 1991; Doucette, 1989; Farbman and Squinto, 1985; Marin-Padilla and Amieva, 1989) and the neural crest in the case of Schwann cells (Jessen and Mirsky, 2002). However, the origins are similar in that the neural crest and the olfactory placode are both derived from the neural ridge, in the case of the olfactory placode, the anterolateral neural ridge (Couly and Le Douarin, 1985). Both OECs and Schwann cells express the low affinity nerve growth factor receptor, p75 (see section 1.2.3.2). Schwann cells can myelinate axons under the appropriate circumstances (Lobsiger et al., 2002), and while this issue is contentions, there is considerable evidence that OECs can also myelinate axons in vitro (Devon and Doucette, 1992) and in vivo (Franklin et al., 1996; Imaizumi et al., 2000b; Imaizumi et al., 1998; Smith et al., 2002; Smith et al., 2001) (see section 1.2.6.2 for more details). The manner in which the two cell types myelinate is also strikingly similar (Franklin, 2003). OECs and Schwann cells also share several mitogens in common including FGF-2 (Alexander et al., 2002; Au and Roskams, 2003; Chuah and Teague, 1999; Watabe et al., 1994), neuregulin (Alexander et al., 2002; Lobsiger et al., 2002; Yan et al., 2001a) and hepatocyte growth factor (Alexander et al., 2002; Krasnoselsky et al., 1994; Lobsiger et al., 2002; Yan et al., 2001a; Yan et al., 2001b).

However, in the absence of mitogens, OECs can proliferate in serum-containing media (Au and Roskams, 2002; Au and Roskams, 2003; Hayat et al., 2003a; Hayat et al., 2003b; Kumar et al., 2005; Nash et al., 2001; Ramon-Cueto and Nieto-Sampedro, 1992; Ramon-Cueto and Nieto-Sampedro, 1994) whereas Schwann cells do so very slowly (Brockes et al., 1979). The two cell types interact with astrocytes differently both in vivo (Doucette, 1990) and in vitro (Lakatos et al., 2000). In the in vitro Lakatos study, a direct comparison was made between OEC and Schwann cell interactions. The authors found that Schwann cells induced astrocyte hypertrophy and tended to stay away from astrocytes in culture. OECs on the other hand, freely mingled with astrocytes. Another difference between OECs and Schwann cells is the manner in which they ensheathe axons. Schwann cells, even non-myelinating ones, are surrounded by a basal lamina. OECs on the other hand lack a basal lamina and ensheathe much larger bundles of axons (Barber, 1982). Finally, the response to injury is different between the two glial types. In the case of Schwann cells, nerve injury is followed shortly by rapid proliferation and migratory to rearrange and form a 'growth channel' to guide regenerating peripheral nerves (Liuzzi and Tedeschi, 1991). This also occurs in non-myelinating Schwann cells (Clemence et al., 1989). However, in response to a zinc sulfate lesion of the OE where all ORNs are eliminated, OECs are largely quiescent, maintaining the integrity of existing axon conduits (Williams et al., 2004). The fact that the conduits remain may underscore the importance of OECs in maintaining proper ORN targeting during adulthood.

1.2.5.2 OECs vs. Astrocytes

While there are similarities between OECs and astrocytes, they are not as similar as OECs and Schwann cells (Vincent et al., 2005). OECs, like astrocytes express GFAP and both upregulate its expression in response to injury (Barber and Dahl, 1987). GFAP is typically not expressed by Schwann cells (Jessen and Mirsky, 1985). Also, in both OECs and astrocytes, each individual cell is not encased in its own basal lamina (Doucette, 1990) which is not the case with myelinating or non-myelinating Schwann cells. Finally, OECs contribute to the glia limitans of the olfactory bulb (see section 1.2.2) in a

cooperative manner with astrocytes (Doucette, 1991), unlike the CNS/PNS boundary anywhere else in the body formed only by astrocytes (reviewed in Fraher, 1992). Such cooperativity may suggest a greater similarity between OECs and astrocytes. In vitro interactions between the two cell types also support this claim (Lakatos et al., 2000). In the olfactory bulb, OECs and astrocytes may be differentiated by expression of glutamate transporters only in the astrocytes (Roskams lab unpublished observations).

1.2.6 OEC-mediated Neuronal Repair

OECs can provide an appropriate environment for continual ORN axon growth throughout adult life. It was a natural progression of logic that OECs placed in other environments may do the same for other neuronal populations. Perhaps OECs can help neuronal regeneration in areas where repair is problematic and severely limited. To this end, many studies have been performed to assay the ability of OECs to mediate neuronal repair and regeneration.

Following injury, the central nervous system is only capable of limited repair. The major obstacles to regeneration are: (1) the atrophy and death of injured neurons, (2) formation of a glial scar at the lesion site that persists as both a physical and biochemical barrier to regenerating axons and (3) the non-permissive environment of the adult CNS to axon growth (Fawcett and Asher, 1999; Kwon and Tetzlaff, 2001; Ramer et al., 2005). Many groups have attempted to use OEC transplantation as a means of alleviating and circumventing the above issues with some limited success. Their assessment of repair can be loosely placed in two categories: axon growth/sprouting/regeneration and axon re-myelination.

1.2.6.1 OEC mediated Axon Growth/Sprouting/Repair in Transplantation Studies

1.2.6.1.1 The Injured Dorsal Root Entry Zone and OEC Transplantation

The first study using OECs for transplant-mediated repair were performed by Ramon-Cueto and Nieto-Sampedro using a rhizotomy (crush) of the sensory root as a lesion model (Ramon-Cueto and Nieto-Sampedro, 1994). This type of lesion, while performed in the periphery, is considered a CNS lesion because the injured sensory axons are unable to cross the dorsal root entry zone (DREZ), to re-form connections in the spinal cord (Bradbury et al., 2000). Since OECs and astrocytes appear to share the duty of forming the CNS/PNS boundary in the developing olfactory system (Doucette, 1989; Doucette, 1991), it was of interest to Ramon-Cueto and Nieto-Sampedro to see if OECs could alter the CNS/PNS boundary of the dorsal root entry zone (DREZ) (Ramon-Cueto and Nieto-Sampedro, 1994). The authors found that in the absence of OEC transplantation, sensory axons could grow up to the CNS/PNS boundary between the sensory rootlet and the spinal cord but no further. However, with OEC transplantation, many DiI-labeled sensory axons appeared to cross the boundary and grow into the dorsal horn. Some axons were reported to cross the midline into the contralateral dorsal horn while others even reached the ventral horn. The authors concluded that OECs were able to manipulate the dorsal root entry zone in such a way that sensory neurons were now able to grow robustly into the spinal cord. These findings were supported by three follow-up studies lesioning the lumbar (Li et al., 2004; Navarro et al., 1999) and lumbo-sacral (Pascual et al., 2002) dorsal roots. In the Navarro study, electrophysiological tests were performed on treated and control animals and the authors found significant functional recovery with OEC transplantation. In the case of Pascual and coworkers, the authors also reported a behavioural outcome in response to OEC treatment with respect to bladder control (Pascual et al., 2002). These findings are not without controversy. Two subsequent studies by other groups and another study by the Nieto-Sampedro group, show no significant regeneration across the DREZ (Gomez et al., 2003; Ramer et al., 2004b; Riddell et al., 2004). The Gomez study performed the dorsal root transection at the cervical level and by multiple visualization methods (including cholera toxin B, calcitonin gene related peptide (CGRP) antibody, P2X3 antibody) found minimal axon growth across the DREZ into the spinal cord. The authors did find a minimal level of

small diameter unmyelinated axons positive for CGRP and P2X3 crossing the lesion but were unable to rule out axon sparing (Gomez et al., 2003). The Riddell study (Riddell et al., 2004) directly examined many aspects of the Navarro study (Navarro et al., 1999) but their findings are contradictory. Riddell and coworkers observed negligible functional recovery, and axon growth across the DREZ was not significantly better than controls. Ramer and coworkers also found that OEC transplantation failed to promote significant axonal growth into the CNS following dorsal root crush (Ramer et al., 2004b). The authors noted however, an affinity of small and medium diameter axons for OEC laminin-rich channels, however the axons were not able to exit the channel into the dorsal horn. Additionally, increased angiogenesis and a general loosening of the astrocytic scar were noted. The studies generally agree that if any there is any regeneration of axons across the DREZ, they tended to be small diameter CGRP positive axons. It is however, difficult to reconcile the disparate results of these studies. The results of the Ramer and coworkers study suggest that if the DREZ was disrupted by the injection of OECs, the axons could progress further, although not outside of the OEC channel. Perhaps it was this disruption coupled with spared fibres from an incomplete lesion that explains the regeneration in the Nieto-Sampedro studies (Navarro et al., 1999; Pascual et al., 2002; Ramon-Cueto and Nieto-Sampedro, 1994). In the case of OEC transplantation at the injured DREZ, the astrocyte/Schwann cell boundary had long ago been established and is not permissive to regeneration (Bradbury et al., 2000). Developmentally, OECs, arrive at the CNS/PNS boundary of the olfactory bulb before astrocytes and the two cell types successfully and cooperatively form a glia limitans permissive to ORN axon growth (Doucette, 1991; Doucette, 1993). So in the context of OEC development (see section 1.2.2), it may be asking too much for OECs to penetrate and create a channel for sensory regeneration in an adult organism.

1.2.6.1.2 The Injured Spinal Cord and OEC Transplantation

OECs have shown promise in mediating repair, to varying extents, after spinal cord injury. The first studies transplanting OECs following spinal cord injury (SCI) were

performed by Raisman's group (Li et al., 1997) and Franklin and Barnett's group (Franklin et al., 1996). The Franklin and Barnett study focuses on OEC-mediated re-myelination and will be reviewed in the next section (see section 1.2.6.2). In the Li and coworkers study (1997), the researchers transplanted OECs into an electrolytic lesion of the corticospinal tract (CST). They found remarkable directed robust growth that they termed a 'continuous bridge of OECs and axons' across the lesion. They further found a correlation between the presence of an OEC/axon bridge and behavioural recovery as assayed by a food pellet-reaching test. In a follow up study, they more thoroughly examined the OEC-mediated regeneration histologically (Li et al., 1998). In this study, they also suggest cooperativity between p75-positive 'S-type' (Schwann cell type) and fibronectin-positive 'A-type' (astrocyte type, later called olfactory nerve fibroblasts (Li et al., 2003a) OECs in the ensheathement of regenerating axons. S-type OECs, the authors claim, myelinate axons through the lesion site and pass them off to be myelinated by oligodendrocytes. A-type OECs cover the outside of the S-type myelin sheaths. The group suggest in a subsequent study that a similar arrangement also exists in the olfactory system (Field et al., 2003) although these finding are not consistent with reported ECM expression patterns with respect to fibronectin downregulation postnatally (Doucette, 1996; Julliard and Hartmann, 1998). Other studies by this group suggest behavioural recovery following OEC transplantation as assayed by food pellet reaching in a chronic CST electrolytic lesion (Keyvan-Fouladi et al., 2003) and behavioural recovery as assayed by climbing and breathing after lateral hemisection of the cervical spinal cord (Li et al., 2003b). Remarkably, the climbing and breathing study found a behavioural recovery in climbing ability in as little as ten days post-procedure. It is important to note that in all of the Raisman group studies, all lesions were performed unilaterally. It is possible that sprouting of contralateral spared fibres could account for some behavioural recovery. Another notable factor is that only the Raisman group uses the electrolytic lesion paradigm in OEC transplant studies. This type of lesion can be prone to axon sparing with temporary loss of conduction due to demyelination (Wolfram Tetzlaff, personal communication).

The Bunge group, in collaboration with Ramon-Cueto, used Schwann cells together with OECs in transplant studies of SCI (Ramon-Cueto et al., 1998). In this study OECs were transplanted as 'caps' on the ends of a Schwann cell/matrigel filled channel. The lesion was a full transection and wheat germ agglutinin (WGA) labelled axons were found growing into the Schwann cell channel into which the OEC 'caps' were also found migrating. The authors suggest that the OECs have facilitated axon growth through the Schwann cell channel by modulating the astrogliotic scar. They argue this may occur because OECs migrated long distances away from the injection site. This finding is not consistent with later studies using genetically labelled OECs (Boyd et al., 2004; Li et al., 2003b; Ramer et al., 2004a) which found very limited migration of OECs. The discrepancy could be explained by the labelling method. Since the OECs were Hoechst-labelled, and ED-1 positive macrophages were present at the lesion site, the Hoechst detected at long distances could be due to macrophage phagocytosis of labelled OECs which then migrated. Ramon-Cueto and coworkers performed a similar study without the Schwann cell channel but retaining the rostral and caudal injection strategy and assessed behavioural recovery (Ramon-Cueto et al., 2000). This study reported significant axon growth across the lesion and, strikingly, found treated rats climbing up 80^{o} inclined ramps several months after injury after treatment with OECs.

Since these initial OEC transplantation studies, there have been numerous other studies performed, many of which await replication by other groups. Some studies have found quantifiable regeneration and recovery following transplantation (Garcia-Alias et al., 2004; Imaizumi et al., 2000a; Nash et al., 2002; Plant et al., 2003). However, not all studies reported promising results. In a study by the Bunge group, Takami and coworkers performed a direct comparison between OECs, Schwann cells and OEC/Schwann cell combination (Takami et al., 2002). The authors found improved re-myelination and limited hindquarter movement recovery following contusion injury only in treatment groups receiving Schwann cells. Guntinas-Lichius and coworkers found OEC mediated facial nerve regeneration, however much of this represented inappropriate sprouting of select populations of motoneurons (Guntinas-Lichius et al., 2001). No motor (whisking) recovery was detected.

Some groups have attempted to augment OECs by having them deliver additional neurotrophic factors into the lesion site (Cao et al., 2004; Ruitenberg et al., 2005; Ruitenberg et al., 2003). In the two Ruitenberg studies, OECs were transduced by adenovirus to deliver BDNF, NT-3 or BDNF and NT-3 into the SCI. In the 2003 study, the authors found improved rubrospinal axon growth with BDNF and better ropewalking behaviour recovery with neurotrophin expressing OECs and OECs alone (Ruitenberg et al., 2003). In the 2005 study, NT-3 expressing OECs increased traced CST axon regeneration over OECs without NT-3 (Ruitenberg et al., 2005). Cao and coworkers found similar results with OECs delivering GDNF after retroviral transduction (Cao et al., 2004). The authors found limited CST and rubrospinal axon regeneration by retrograde tracing in OEC-treated animals. The regeneration was increased modestly with GDNF expression.

Another trend in the OEC field that has recently emerged is the potential cooperation of different cell types from the olfactory system (reviewed in Barnett and Chang, 2004). This idea was first introduced by the Raisman group (Li et al., 1998). In that study, they described their OEC population as an approximately 50:50 ratio of p75-positive, fibronectin-negative and fibronectin-positive, p75-negative cell types, working cooperatively to mediate repair. The Franklin and Barnett group found that meningeal cells (lining the outside of the olfactory bulb), when co-transplanted with O4-positive OECs, synergistically improved OEC myelination (Lakatos et al., 2003b). The Mackay-Sim group has reported positive effects from transplanting strips of lamina propria (Lu et al, 2001) or unpurified LP constituent cell types (Lu et al., 2002) into SCI. A replication study of these two works has recently been performed and the results are not consistent (Steward lab, manuscript submitted). Guntinas-Lichius also used strips of LP and found that it promoted facial nerve targeting and regeneration (Guntinas-Lichius et al., 2002) whereas dissociated OECs promoted growth but in an inappropriate manner (Guntinas-Lichius et al., 2001). Testing this mixed cell theory, Andrews and Stenzler transplanted purified p75-positive OECs and 50:50 p75- and fibronectin-positive cells but reported no difference in their lesion paradigm – a dorsal column crush injury very similar to the

Koscis group lesion (Imaizumi et al., 2000b) - (Andrews and Stelzner, 2004). Unfortunately, the authors did not quantify the amount of regeneration and sprouting so that an objective comparison could be made. More work will need to be done to parse apart the subtleties of this particular issue.

With many different groups performing different spinal cord lesions, using OECs from different cell preparations and assessing recovery by a variety of methods at different times post-operation, it is difficult to compare their findings and come away with a well-defined effect of OEC transplantation. There appears, however, to be common themes that have been reported by various groups in spite of their differences in experimental approach, method and materials. (1) OECs can mediate a limited amount of regeneration. Whether this regeneration has functional consequences is debatable since very few of the studies claim more than modest behavioural improvement. Thus, it can be safely stated that OECs do not by themselves mediate targeted functional recovery. (2) OECs are effective in minimizing tissue loss after injury (Plant et al., 2003; Ramer et al., 2004a; Ruitenberg et al., 2003; Takami et al., 2002). This effect has largely been overlooked as a positive effect of OEC-mediated repair. With reduced cavitation, regenerating axons have more substrate through which to grow. It should be noted however, that reduction in cavity size following injury is not the unique property of OECs. Schwann cells (Takami et al., 2002), bone marrow cells (Ankeny et al., 2004) and even fibroblasts (Franzen et al., 1999) can aid in tissue sparing following SCI. (3) OECs can mediate Schwann cell infiltration at the lesion site (Boyd et al., 2004; Ramer et al., 2004a; Ruitenberg et al., 2003; Sasaki et al., 2004; Takami et al., 2002). This theme is clearly demonstrated by xenotransplantion using a host-specific p75 antibody (Ramer et al., 2004a) and by immunohistochemistry with electron microscopy (Boyd et al., 2004; Sasaki et al., 2004). Likely all three of these themes are interrelated, with Schwann cell infiltration potentially contributing to regeneration and reduced cavitation. (4) OECs can modify the astrogliotic environment at the lesion site (Andrews and Stelzner, 2004; Garcia-Alias et al., 2004; Lakatos et al., 2003a; Ramer et al., 2004a). In an in vitro study, Fairless and coworkers propose that this may have to do with differential N-cadherin signalling between OECs and Schwann cells (Fairless et al., 2005). When N-cadherin

activity was inhibited by a cyclic peptide inhibitor or by siRNA, Schwann cell adhesion to astrocytes was reduced. Down regulation of N-cadherin activity had no effect on OEC interactions with astrocytes. (5) There is a strong body of evidence that OEC transplantation results in re-myelination. Whether this is a direct or indirect effect is a contentious issue in the field (see section 1.2.6.2).

1.2.6.2 Re-Myelination by OECs Following Spinal Cord Lesion

In addition to promoting sprouting and regeneration, OEC transplantation has also been accompanied by remyelination (reviewed in Franklin, 2003). The initial interest in employing OECs for transplant re-myelination came from pioneering studies by the Doucette group. ORN axons are very small in diameter, often less than 0.5 μm (Doucette, 1990) and there is a well-documented correlation between axon diameter and myelination (reviewed in Jessen and Mirsky, 1991). While in their native environment OECs are in contact with axons below the minimal diameter threshold for myelination, perhaps exposure to axons of the appropriate size could promote a myelinating phenotype. By electron microscopy, Doucette noted OEC ensheathement of both ORN and myelinated trigeminal axons in the lamina propria (Doucette, 1990). In a subsequent study, Devon and Doucette co-cultured OECs with dissociated dorsal root ganglion sensory neurons and found that OECs could myelinate large diameter axons in vitro (Devon and Doucette, 1992). In a study by the Bunge group, the authors suggest that this phenomenon may be attributed to Schwann cell and satellite cell contaminants in the culture (Plant et al., 2002).

Different groups have also drawn different conclusions when it comes to OEC-mediated re-myelination of the spinal cord. An initial study used a temperature-sensitive OEC cell line in a focal demyelination lesion using ethidium bromide and x-irradiation (Franklin et al., 1996). The authors found Schwann cell-like peripheral myelination and reasoned the transplanted OECs seeded into the focal lesion were myelinating. In a follow-up study,

Smith and coworkers examined OEC-treated focal lesions for the expression of promyelinating transcription factors (Krox-20 and SCIP) normally found in myelinating Schwann cells (Smith et al., 2001). They found expression of Krox-20 and low levels of SCIP by in situ at the lesion as well as the morphogen desert hedgehog (dhh). Dhh, the authors hypothesize, is expressed by myelinating OECs to direct non-myelinating OECs to form fascicles analogous to the perineural sheath in myelinated peripheral nerves. This finding fits well with a subsequent study by the group that found better myelination when OECs and olfactory bulb meningeal cells were co-transplanted (Lakatos et al., 2003b). The authors reported that the meningeal cells, while not able to myelinate axons, formed a perineural sheath-like structure around myelinating OECs. The mixed cell phenomenon (see section 1.2.6.2.1 for more examples) may also be a contributing factor in work by the Kocsis group. OECs used in their transplantation studies are prepared fresh without a purification regimen and they also found remyelination after OEC transplantation (Imaizumi et al., 2000b; Imaizumi et al., 1998; Sasaki et al., 2004). The Imaizumi study (1998) used the ethidium bromide X-irradiation lesion like the Franklin and Barnett group. They were able to repeat the results of the Franklin et al. study (Franklin et al., 1996) and found faster conduction velocities across the lesion site in the OEC treated group versus controls. Imaizumi and coworkers also examined re-myelination following bilateral dorsal column transection of the spinal cord (Imaizumi et al., 2000b). While the authors observed only modest regeneration, both with Schwann cell and OEC-treated groups, conduction velocity across the lesion site was increased versus controls. In fact, the authors report faster than normal conduction, which they ascribe to preferential myelination of large, and fast conducting axons.

It has been suggested that endogenous Schwann cells, not OECs, infiltrating from the periphery are responsible for re-myelination in the above studies (Boyd et al., 2004; Takami et al., 2002). Schwann cell infiltration has been reported by other groups as well following OEC transplantation (Ramer et al., 2004a; Ruitenberg et al., 2003). Two studies, one by the Franklin and Barnett group and one by the Kocsis group, strongly suggest that at least some of the re-myelination is performed by OECs. In the Franklin and Barnett group's study (Smith et al., 2002), canine OECs were xenotransplanted into

rat focal de-myelinated lesions. In nude or immunosuppressed rats, the canine OECs were able to mediate re-myelination while non-immunosuppressed animals receiving OECs were not re-myelinated. It is possible to infer from these findings that OECs are directly responsible for re-myelination. However, there remains the possiblility that OECs must be present in order for Schwann cells to integrate with the host cord - a possibility that cannot be discounted by the Smith et al. study. The Kocsis group recently published a paper to more directly tackle this issue (Sasaki et al., 2004). In this study, Sasaki and coworkers transplanted OECs from GFP rats into a transected dorsal column lesion similar to an earlier study (Imaizumi et al., 2000b). By electron microscopy, the authors identified GFP-positive and GFP-negative cells myelinating axons in the lesion site accompanied by some behavioural recovery assessed by the Basso Beatie and Bresnahan open field test. Sasaki and coworkers suggest that OECs and host Schwann cells share the duty of re-myelinating the spinal cord. In the Boyd et al. study, the authors also used genetically labelled OECs and EM microscopy to examine the source of re-myelination (Boyd et al., 2004). They did not find Lac-Z-positive OECs actively myelinating axons or even OECs directly contacting axons. As such, the authors concluded that all of the re-myelination was due to host Schwann cells. These contrary results may be due to culture conditions, the age of the donor animal and the lesion paradigm. In the Boyd study, they used a spinal cord compression injury (Fehlings and Tator, 1995) and the OECs were obtained from embryonic rats and cultured long-term (Boyd et al., 2004) while Sasaki and coworkers used adult rat OECs without culturing into a dorsal column transection injury (Sasaki et al., 2004). Regardless of the cell type or whether the effect is primary, secondary or both, all groups agree that OEC transplantation is coincident with re-myelination following spinal cord injury.

In summary, OECs are a promising candidate cell for transplantation to treat neural injury. Data from animal models suggest that OECs can, at least to a limited degree, translate their ability to promote ORN axon growth into promoting regeneration in other systems. Also, there is strong data to suggest that they possess the latent ability to myelinate when interacting with appropriate diameter axons, thus expanding their potential application to treating demyelinating disorders such as multiple sclerosis. More

work will need to be done to bridge the current research, however promising, to lesion paradigms and model systems that more closely mimic human neuronal dysfunction.

1.3 Thesis Rationale

At the start of this thesis (September 1999), there were many outstanding issues to be addressed in the olfactory ensheathing cell field. One such issue was the anatomical delineation between OECs derived from the nerve fibre layer of the OB, OB-OECs and the OECs derived from lamina propria of the periphery, LP-OECs. By following the two populations developmentally (see section 1.2.2), it would make sense that they are very similar, if not identical since they are both derived from the same tissue, the olfactory placode (Chuah and Au, 1991; Doucette, 1989; Farbman and Squinto, 1985; Marin-Padilla and Amieva, 1989). But then again, so too are ORNs, sustentacular cells and LHRH neurons (Schwanzel-Fukuda and Pfaff, 1989) – a fairly disparate cell population. It is possible that there are subtypes of OECs along the olfactory neuraxis; their function and phenotype varying depending on where they are along the length of the ORN axon. There is evidence that such a situation exists within the nerve fibre layer itself. Heterogeneity in the OEC population between inner and outer layers of the NFL has been reported with respect to antigenicity and degree of ORN bundling by OECs (Au et al., 2002). Could there be differences between the OECs found on the periphery versus the ones found along the nerve fibre layer? From a clinical aspect, this question is also relevant since OECs from the lamina propria are far more accessible for autologous transplantation strategies.

Another issue in the field is, mechanistically, how do OECs mediate axon growth? There have been a number of studies examining the presence of various factors that could contribute to OEC function (see section 1.2.3). However, the presence of a factor does not demonstrate function and there is little evidence correlating the presence of say, a neurotrophic factor and said factor's relative contribution to OEC-mediated axon growth. It can be said that, to date, the ability of OECs to (A) provide a permissive and promotive environment for ORN axon growth and (B) mediate axon growth in other systems such as SCI is not well understood. It can only be assumed that the ability to do (A) is related to OEC ability to do (B) but there is no definitive evidence to show that that is the case.

The need to understand OEC function is necessary to more effectively use this cell type in therapies to treat neuronal dysfunction. In light of clinical trials currently underway to treat SCI and amyotropic lateral sclerosis with OECs, it is incumbent upon the field to understand how OECs work. That way we can assess what useful aspects OECs can provide, and perhaps just as importantly, what potential negative effects can arise.

1.4 Thesis Objectives

My attempt to address these two issues form the basis of this PhD thesis and can be summarized by the following objectives and aims:

Objective 1: Characterization and Purification of Lamina Propria-Derived Olfactory Ensheathing Cells

STATEMENT: OECs from the lamina propria can be directly compared with OECs from the olfactory bulb to determine the similarities and differences between the two cell populations. The comparison will help characterize a poorly understood cell type and be informative about OECs and how they relate to other glial cell types.

- Examine the antigenic profile of olfactory ensheathing cells residing in the nerve fibre layer and lamina propria in vivo
- Culture and purify olfactory ensheathing cells from the lamina propria, LP-OECs
- Examine the antigenic profile of cultured LP-OECs and compare with what has been reported in the literature about bulb-derived OECs in vitro
- Examine the expansion characteristics of LP-OECs
- Describe differences between LP-OECs and OB-OECs

Objective 2: The Neurotrophic Properties of Olfactory Ensheathing Cells in an In Vitro Assay for Neurite Outgrowth

HYPOTHESIS: Secreted factors generated by LP-OECs will promote neurite outgrowth. As the LP-OECs senesce, their combination of secreted factors will be less effective, thereby allowing for a comparison of conditioned media from fresh and senescent cells to identify individual factors responsible for the biological activity.

- Establish an assay system to quantify neurite outgrowth
- Examine the effect of LP-OECs on the outgrowth assay
- Establish different culture conditions whereby OEC-mediated neurite outgrowth is differentially effective
- Use the different culture conditions as a means to isolate candidate factors that may be responsible for OEC-mediate neurite outgrowth

Objective 3: The Identification and Functional Validation of the Candidate Factor

HYPOTHESIS #1: Conditioned media samples with different biological activities can be analysed using ICAT proteomics to determine the identity of constituent proteins as well as their relative quantity. By correlating activity with the results of the ICAT dataset and a priori data on the proteins detected, a shortlist of candidate factors can be assembled.

HYPOTHESIS #2: Candidate factors can be tested individually using the same neurite outgrowth assay and their relative contribution to the conditioned media as a whole can be determined using function-blocking reagents.

- Employ isotope-coded affinity tagged (ICAT) proteomics to determine the protein constituents and their relative quantities of the differentially bioactive OEC samples
- Identify candidate factors from the ICAT results based on relative quantity, abundance and a priori data
- Confirm the presence of the candidate factor identified by the ICAT run
- Test the bioactivity of the candidate factor by adding the factor to the assay and also carry out function-blocking antibody studies
- Identify the cellular target of the candidate factor – is the promotion of neurite outgrowth a direct or indirect effect?

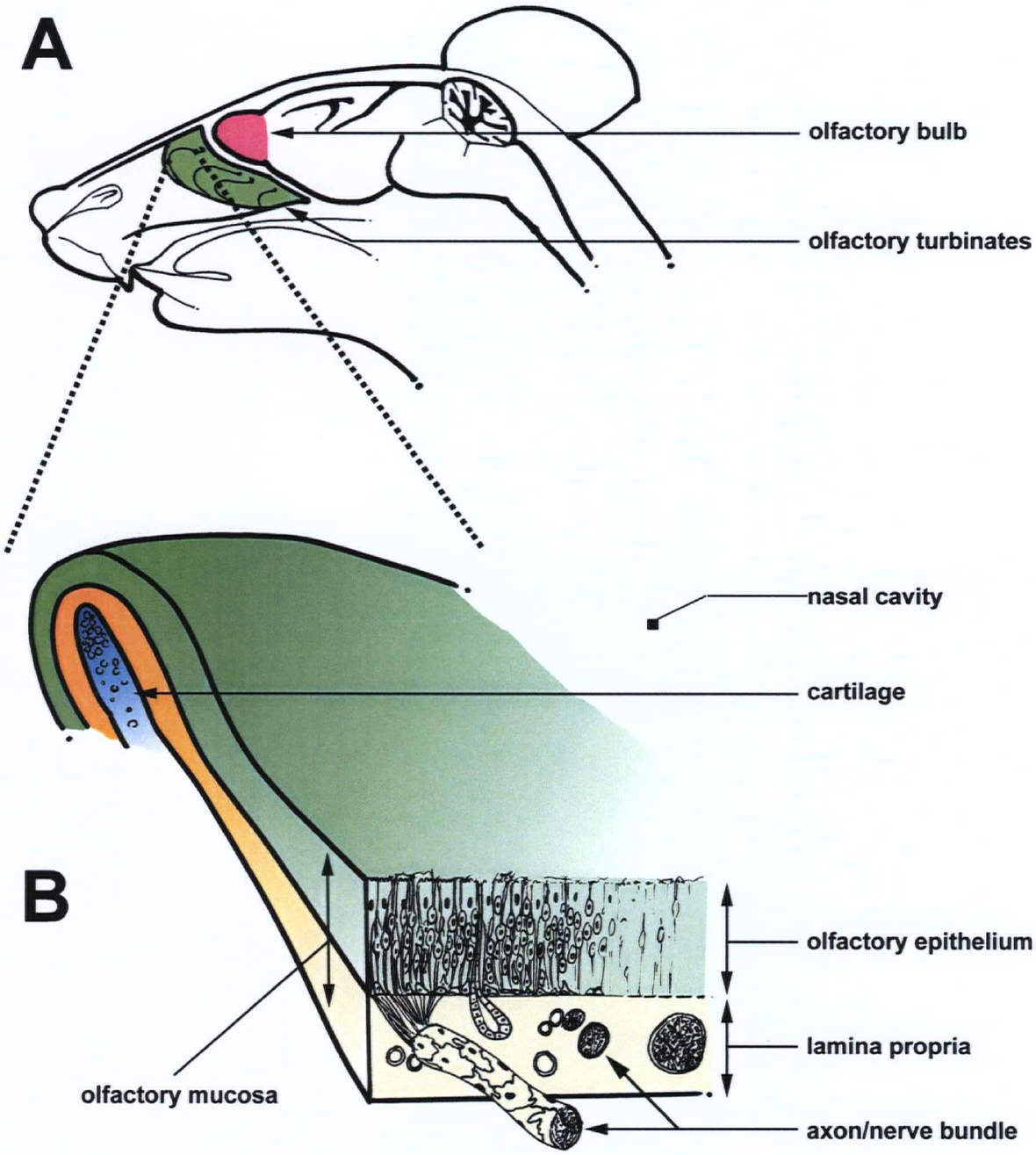

FIGURE 1.1
Neuroanatomy of the Primary Olfactory System to the Histology of the Olfactory Mucosa
(A) Mid-sagittal view of mouse head depicting the primary olfactory system. Olfactory turbinates in green and olfactory bulb in pink. (B) Cut away of one olfactory turbinate exposing layers of soft tissue overlying cartilage. Olfactory epithelium in green, underlying lamina propria in orange and cartilage in blue.

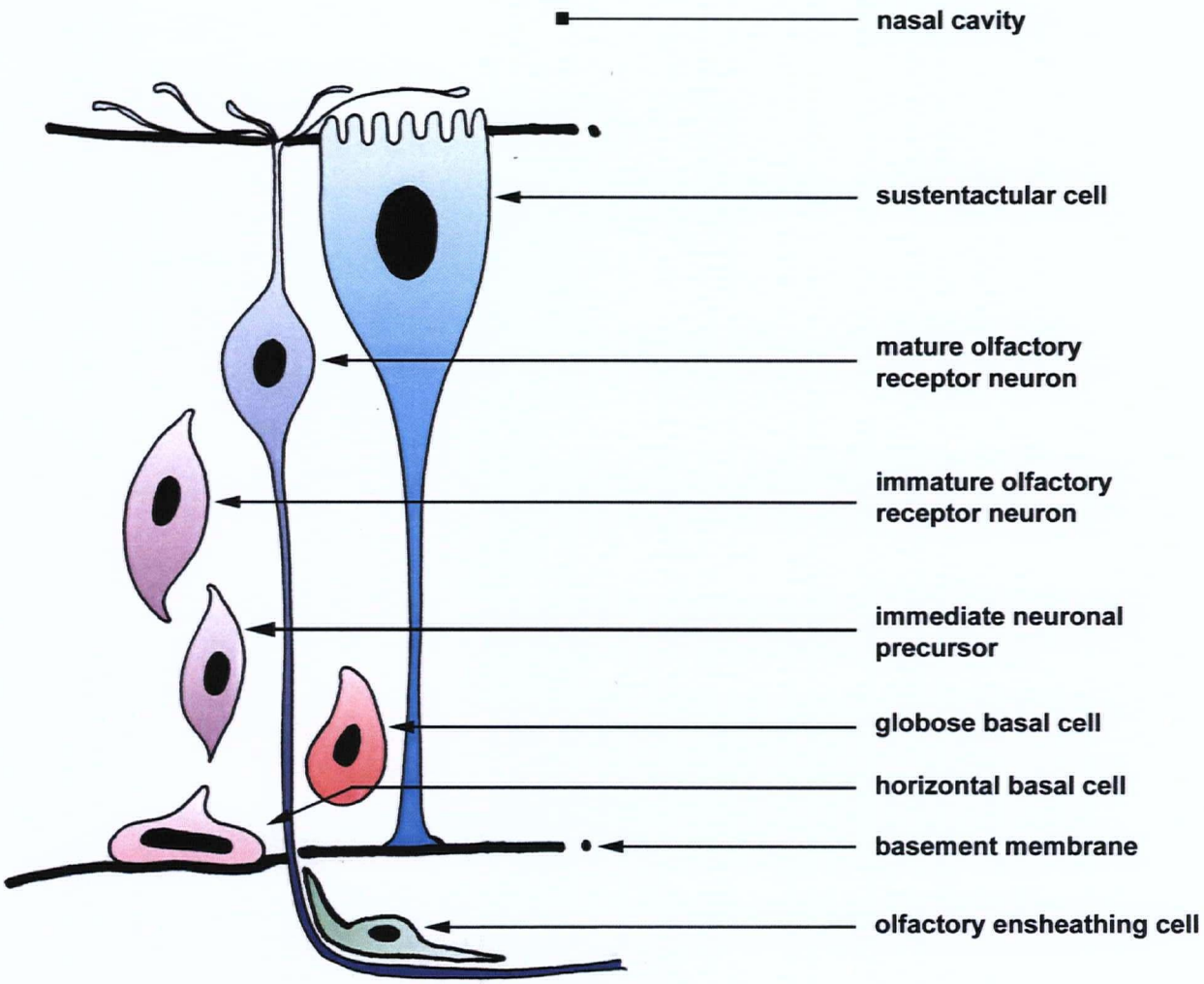

FIGURE 1.2
Various Cell Types of the Olfactory Epithelium and Lamina Propria
Diagram depicts various cell types found in the olfactory epithelium (OE) and lamina propria (LP). Basal cells (horizontal basal cell, pink; globase basal cell, red) give rise to neuronal progenitors. Progenitors differentiate into immature neurons (light purple) that mature into olfactory receptor neurons, ORNs (dark purple). Sustentacular cells (blue) span the height of the olfactory epithelium. ORN axons are ensheathed by olfactory ensheathing cells (green) once they enter the lamina propria through the basement membrane.

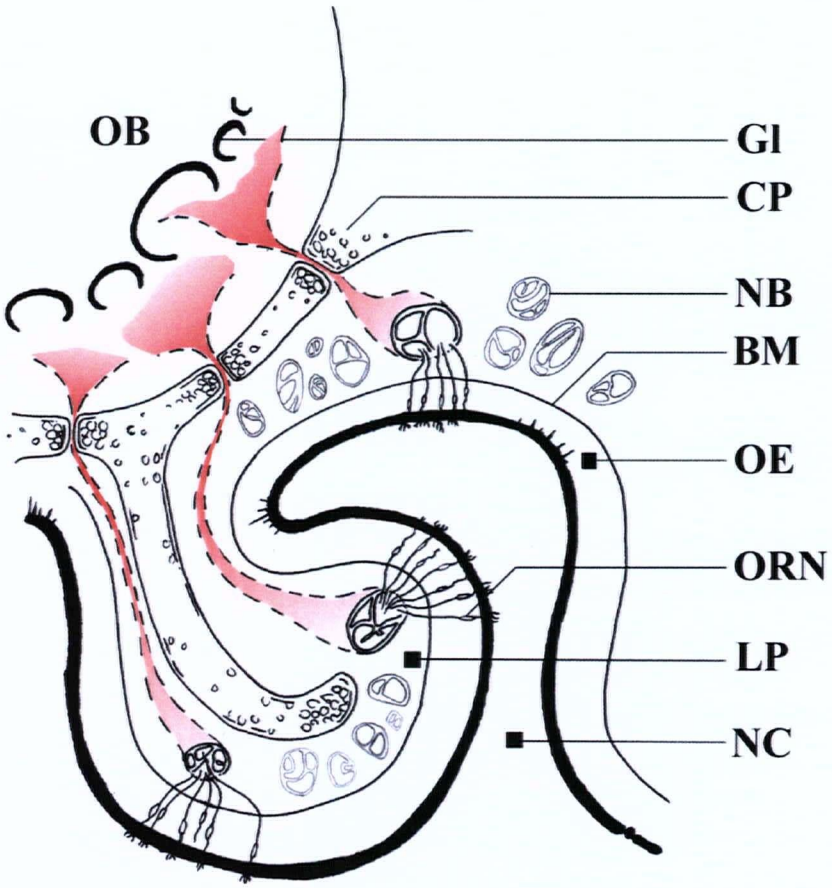

OB	**olfactory bulb**
Gl	**glomerulus**
CP	**cribiform plate**
NB	**nerve bundle**
BM	**basement membrane**
OE	**olfactory epithelium**
ORN	**olfactory receptor neuron**
LP	**lamina propria**
NC	**nasal cavity**
- - -	**OEC ensheathment**

FIGURE 1.3
Olfactory Ensheathing Cells are Found Throughout the Olfactory Neuraxis
Olfactory ensheathing cells (OECs) ensheathe the olfactory nerve from the basement membrane (BM of the olfactory epithelium (OE) all the way through to the glomerular layer (Gl) of the olfactory bulb (OB). Ensheathement depicted in red with dashed lines. Modified from Au and Roskams (2003) Glia 41(3):224-236.

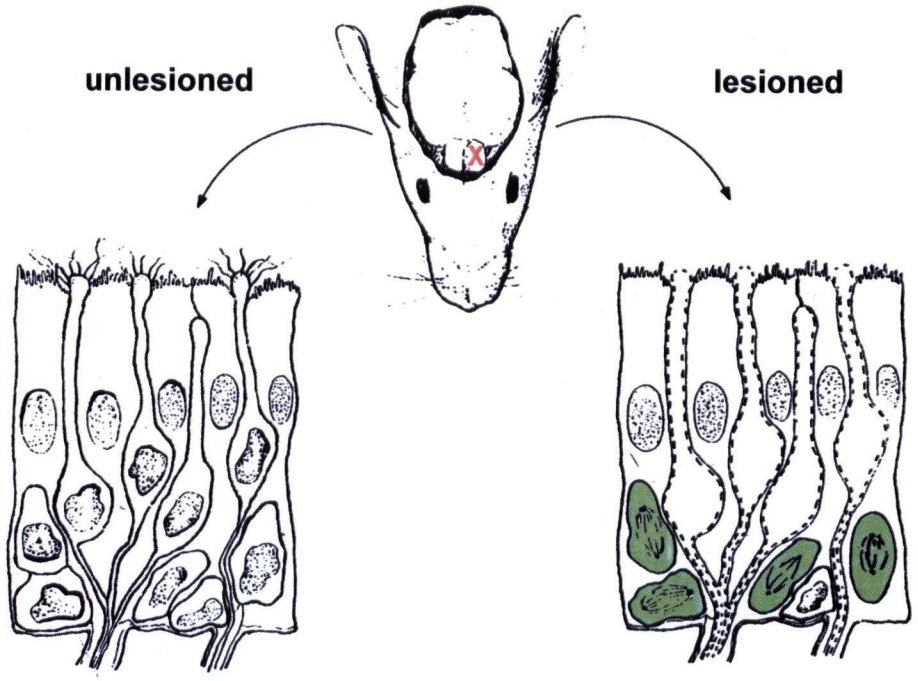

FIGURE 1.4
Bulbectomy Lesion Model and its Effect on the Olfactory Epithelium
Diagram depicting a unilateral bulbectomy. Unlesioned bulb is on the left, lesioned bulb is on the right marked with a red "X". The removal of the olfactory bulb causes a distal deafferentation of all ORNs that have reached the nerve fibre layer of the olfactory bulb. Due to injury ORNs synchronously degenerate and die as shown in the olfactory epithelium on the right. Concurrently, neural progenitors (green) are mobilized to divide and replace the dying ORNs. Modified from Calof et al (1996) Ciba Foundation Symposium 196: 188-205.

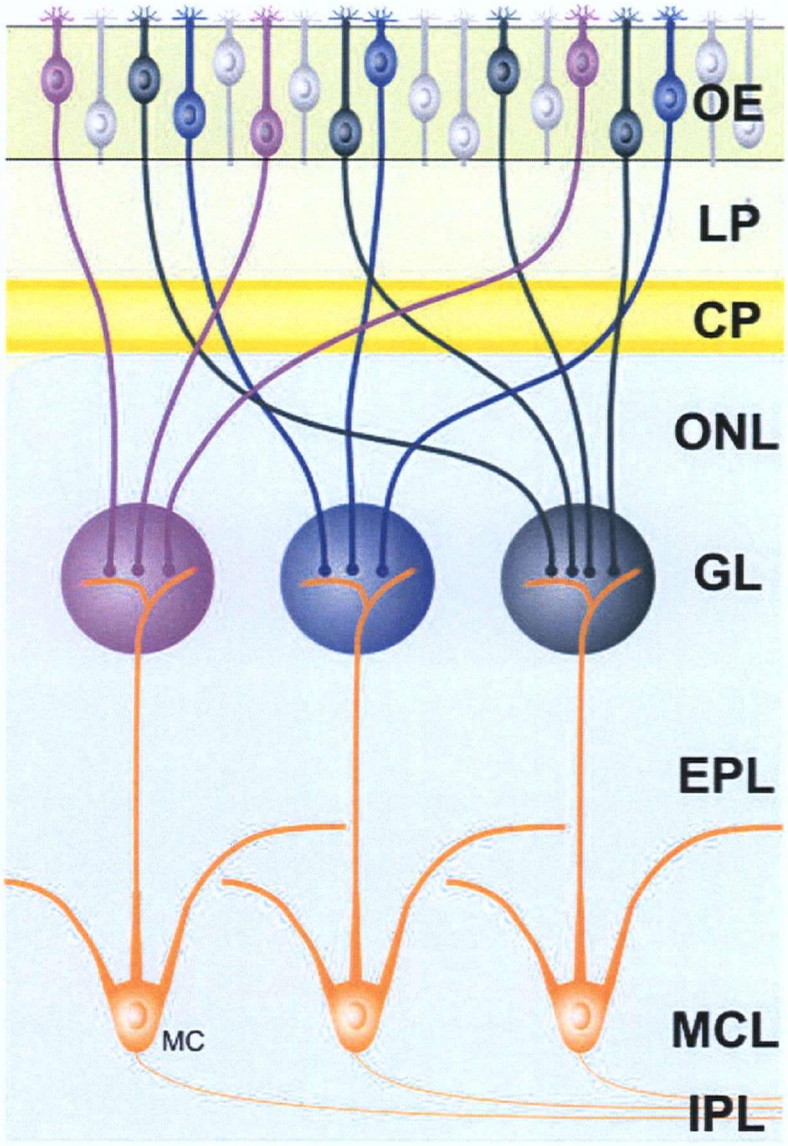

FIGURE 1.5

Circuit Diagram of Olfactory Receptor Neuron Target Specificity to Glomerular Target

Olfactory receptor neurons expressing the same odourant receptor have the same colour. They all specifically target to the same glomerulus of the corresponding colour. Modified from Shipley, M.T., Puche, A.C., and Ennis, M. (2003) The olfactory system. In The Rat Nervous System. George Paxinos Ed., Academic press, NY).

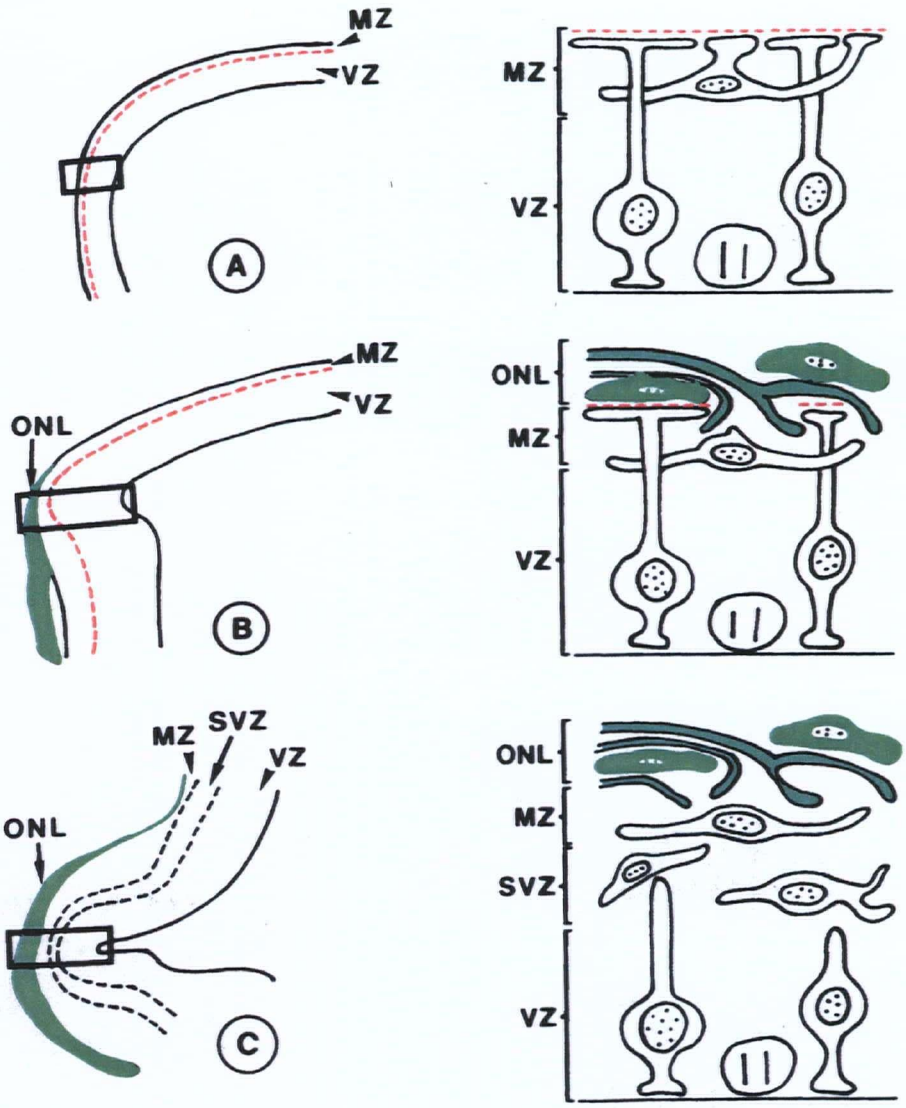

FIGURE 1.6
Migration of the Migratory Mass over the Telencephalon to Form the Olfactory Nerve Fibre Layer

Three stages of early olfactory bulb (OB) development are shown. The left column is a sagittal view and the right column is a diagram showing the cell layers of the OB found within the rectangular box on the left. (A) Radial glia form the basal lamina of the glia limitans (red dashed lines) in the rostral cerebral vesicle (mouse embryonic day 12). (B) The migratory mass made of ORN axons and OECs (in green) moves over the surface of the cerebral vesicle and partially breaks down the glia limitans (mouse embryonic day 15). (C) New glia limitans is formed by OECs of the nerve fibre layer (ONL) (E 18-perinatal). Abbreviations: MZ = marginal zone; VZ = ventricular zone; ONL = olfactory nerve fibre layer (migratory mass becomes of the olfactory nerve fibre layer); SVZ = subventricular zone. Modified from Doucette (1990) Glia 3(6): 433-449.

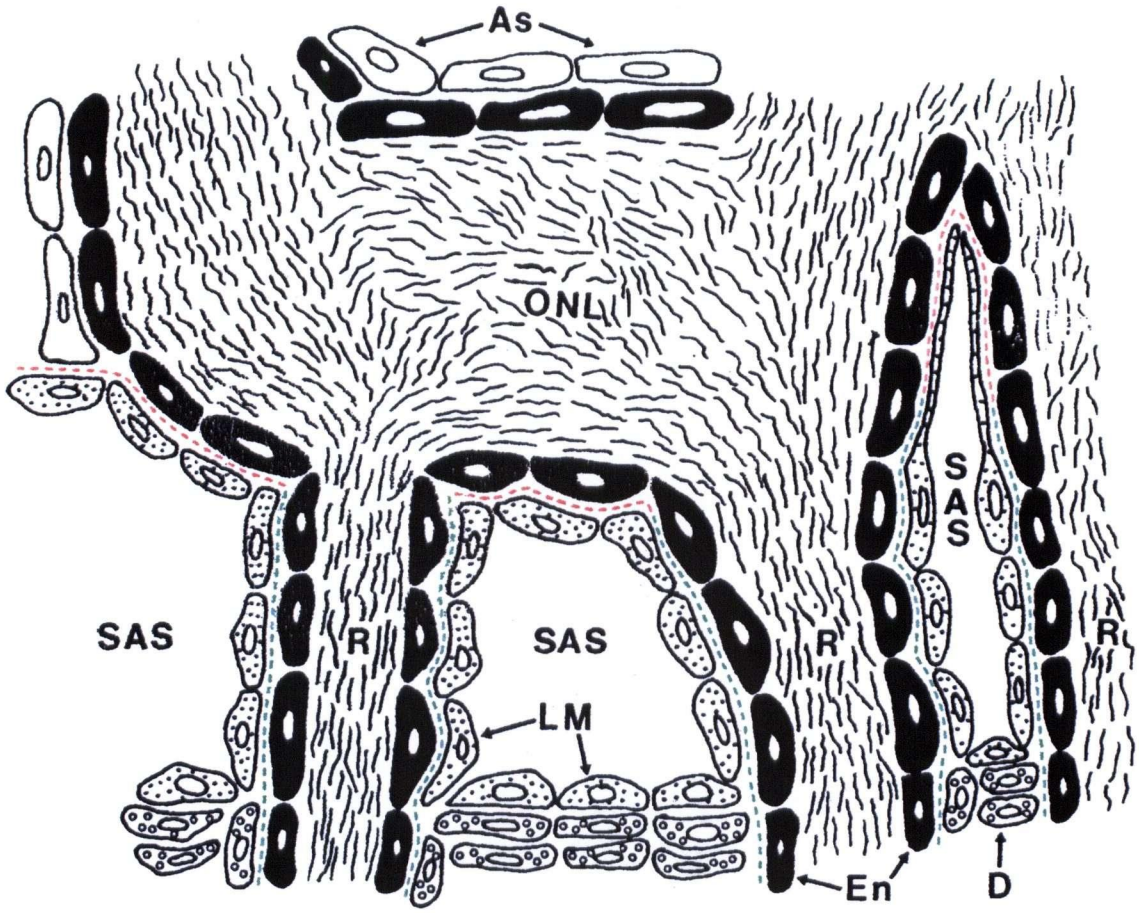

FIGURE 1.7
The Olfactory Nerve Fibre Layer of the Olfactory Bulb
A schematic diagram of the olfactory nerve fibre layer showing the various constituent cell types. Three olfactory rootlets (ORN axon bundles merge to form rootlets prior to passing through the cribriform plate) are shown merging with the olfactory nerve fibre layer (ONL). Note the fusion of the basal lamina covering the olfactory rootlet (green) is continous with the basal lamina of the glia limitans of the olfactory bulb (red). Abbreviations: SAS = subarachnoid space; As = astrocyte; R = olfactory rootlet; LM = leptomeningeal cell; D= dura mater. Modified from Doucette (1991) The Journal of Comparative Neurology 312(3): 451-466.

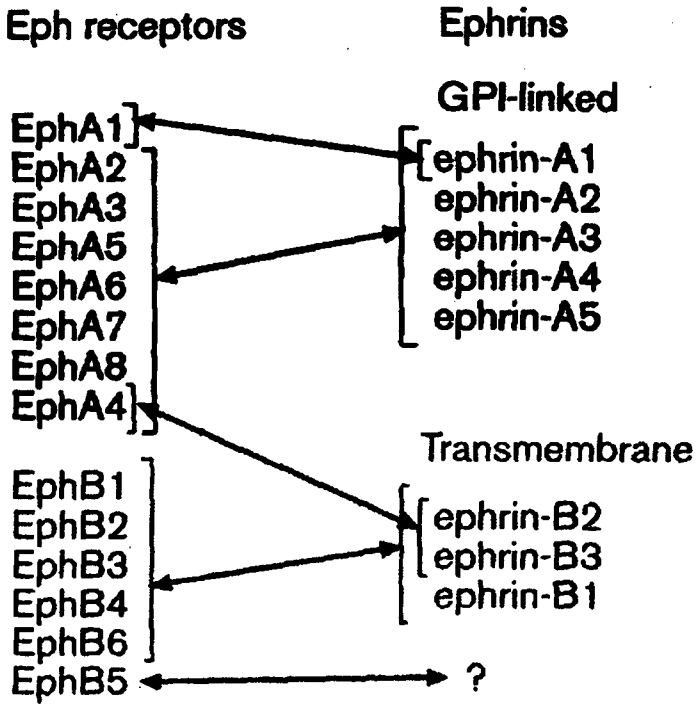

FIGURE 1.8

Eph Receptor – ephrin Ligand Binding Specifities

Generally, EphA receptors bind ephrin-A ligands and EphB receptors bind ephrin-B ligands. The exceptions are: EphA1 is specific to ephrin-A1, EphA4 can also bind ephrin-B2 and ephrin-B3 and the ligand for EphB5 is unknown. From O'Leary and Wilkinson (1999) Current Opinion in Neurobiology 9(1): 65-73.

TABLE 1.1 Expression of Growth-Promoting Molecules by OECs

OEC factors	NFL	LP	in vitro	species	reference(s)
growth factors					
NGF	nd	+	+	rat	Roskams et al, 1996; Woodhall et al, 2001
BDNF	+	nd	+	rat	Woodhall et al, 2001; Boruch et al, 2001; Lipson et al, 2003
FGF-1	+	+	nd	rat	Key et al, 1996
FGF-2	+	+	+	rat	Chuah and Teague, 1999; Matsuyama et al, 1992
FGFR-1	+	+	+	rat	Chuah and Teague, 1999; Hsu et al, 2001
PDGF	+	nd	-	rat	Sasahar et al, 1992; Kott et al, 1994
HGF	nd	+	nd	rat	Thewke and Seeds, 1996
ECM					
laminin	+	+	+	rat	Julliard and Hartmann, 1998; Kafitz and Greer, 1998; Ramon-Cueto and Nieto-Sampedro, 1992
collagen IV	+	+	nd	rat	Julliard and Hartmann, 1998
fibronectin	+	+	nd	rat	Julliard and Hartmann, 1998
CAMs					
L1	+	+	+	rat	Miragall et al, 1989; Ramon-Cueto and Nieto-Sampedro, 1992
NCAM	+	-	+	rat	Miragall et al, 1989; Franceschini and Barnett, 1996
PSA-NCAM	+	nd	+	rat	Miragall et al, 1989; Kumar et al, 2005

+ = present, nd = not described, - = not present

Chapter 2: Materials and Methods

2.1 Animals Used in Experiments

LP-OECs were cultured from postnatal day 5 mice, predominantly outbred CD-1 strain. The exceptions were the green fluorescence protein-expressing LP-OECs used for spinal cord transplantation (strain: C57/black6 x SVJ/ICR) and SPARC null mice (kind gift from Dr. E Helene Sage) for generating SPARC null conditioned media (strain: C57/black6). All DRG explants were cultured from E13.5 CD-1 mouse embryos. Bulbectomy experiments were performed on male CD-1 mice 8-10 weeks old. All animal housing and experimental protocols were approved by the University of British Columbia Committee on Animal Care.

2.2 Culturing Lamina Propria-Derived Olfactory Ensheathing Cells

A detailed protocol for the culture of OECs from neonatal mouse lamina propria can be found in Au and Roskams (2002). The following is a brief description of the procedure. Postnatal day 5 mouse pups are decapitated and their heads are split in the mid-sagittal plane. Using a pair of curved number 7 forceps, the olfactory mucosa and underlying cartilaginous turbinates are dissected out and transferred into DMEM (Dulbecco's modified Eagle's medium, Gibco, Burlington ON). The tissue is chopped into fine pieces with a razor blade, transferred into a 50 ml conical tube and spun at 120xg for 10 minutes at room temperature. The supernatant is removed, 3 ml of fresh DMEM is added and the tissue is triturated with a P1000 pipet tip (enlarged by cutting last 5 mm off the end). The resulting slurry is spun again at 230xg for 5 minutes. A digestion mix containing dispase I (Roche, Baie D'Urfe QC), collagenase D (Sigma, St Louis MO), hyaluronidase (Sigma) DNAse (Invitrogen, Burlington ON) and bovine serum albumin (Sigma) is added to the

tissue pellet. The pellet is resuspended and incubated in digestion mix for 60 minutes at 37°C. The tissue is triturated with a serum-coated glass Pasteur pipet and passed through a 40μm nitex filter (Becton-Dickenson, Mississauga ON). The cells are spun down at 230xg for 5 minutes and plated in MEM-d-valine (minimal essential medium supplemented with d- instead of l-valine, US Biological, Swampscott MA). For the next two passages, the cells are purified by complement-mediated lysis using an anti-Thy1.1 hybridoma antibody (American Type Culture Collection, Manassas VA). Briefly, the complement (rabbit complement, Sigma) and anti-Thy1.1 are added to the cell pellet after trypsinization and incubated for 30 minutes at 37°C. The cells are then re-plated at 5600 cells/cm^2.

2.3 Immunohistochemistry and Immunocytochemistry

Mice were anesthetized, cardially perfused, their heads were carefully dissected of skin, lower jaw, teeth and muscle. The dissected head was cryoprotected by stepwise increasing concentrations of sucrose in PBS (10% then 30%) and then embedded in Tissue Tek (Sakura Finetek, Torrance CA) and the olfactory mucosa and olfactory bulb were sectioned between 8 and 14 μm using a HM500 OM cryostat (Microm International GmbH, Walldorf Germany). Tissue sections were mounted onto charged Superfrost Plus glass slides (Fisher, Edmonton AB) and stored at –20°C in a non-frostfree freez6er.

LP-OECs were grown in Lab-Tek 4 chambered glass slides (Nalge Nunc, Naperville IL) at 37°C in 5% CO_2. When they achieved the appropriate density, the cells were fixed in 4% paraformaldehye (Fisher) in PBS and washed twice with PBS for 5 minutes each. They were then stored at 4°C in 0.05% azide (Sigma) in PBS sealed with Parafilm (Pecheney, Menasha WI).

2.3.1 Immunofluorescence

Tissue sections (of OE and OB) were first thawed on a slide warmer (Lab-Line Instruments Inc., Melrose Park IL) at a setting of 3 for 10 minutes and post-fixed in 4% paraformaldehyde in PBS for 10 minutes. This was followed by 2 PBS washes for five minutes each and permeablization in 0.1% triton X-100 (Sigma) in PBS for 30 minutes. Two more rinses with PBS follow and the sections are then blocked in 4% normal serum in PBS for 20 minutes. Following block, the tissue is incubated with primary antibody (see table 2.1) in 2% normal serum in PBS at 4°C for 12 to 16 hours. Then the sections are washed twice with PBS and incubated with secondary antibody (see table 2.2) in 2% normal serum in PBS for 1 hour at room temperature. Two more washes with PBS follow and then the sections coverslipped with Vectashield (Vector Laboratories, Burlingame CA) before viewing. Images were captured using a Retiga 1.3 megapixel CCD camera (QImaging, Burnaby BC) mounted to an Axioplan2 Imaging microscope (Zeiss, Jena Germany) using Northern Eclipse 6.0 imaging software (EMPIX Imaging Inc., Mississauga ON).

2.3.2 Immunochemistry developed with VIP

The procedure is identical to immunofluoresence up to the primary incubation step. After incubation with primary antibody, the sections are washed twice with PBS and incubated with biotinylated secondary antibody in 2% normal serum in PBS for 30 minutes at room temperature. The sections are then washed twice in PBS, blocked with 0.5% hydrogen peroxide (Sigma) in PBS followed by another 5-minute wash with PBS. They are then conjugated to avidin using the Vectastain ABC kit (Vector Laboratories) for 30 minutes at room temperature. Two more washes with PBS follow and then the sections are developed with VIP (Vector Laboratories). Developing is stopped by a 10-minute wash in ddH_2O and the sections are coverslipped in Aqua Poly/Mount (Polysciences Inc., Warrington PA). Imaging is the same as in section 2.3.1.

2.3.3 DAPI

For some sections, DAPI (Sigma) was used to label nuclei. The sections were incubated in DAPI at a concentration of 0.5 ng/ml for 5 minutes at room temperature. This was done after the two PBS washes that follow the secondary incubation. After DAPI, the sections are washed twice more with PBS before coverslipping with Vectashield.

2.4 Neurite Outgrowth Assay

To set up timed pregnancies, female mice were checked each morning for the presence of a vaginal plug. The time the plug was detected was deemed E0.5. At E13.5, the dame was anesthetized with xylaket (25% ketamine (Biomeda-MTC, Cambridge ON) and 12.5% xylazine (Bayer Inc., Toronto ON), and tested for nociception by pinching the tip of the tail and the toes using forceps. Once the dame was unresponsive, a horizontal incision was made along the abdomen and the uterus was isolated. The embryos were freed from the uterus and the amniotic sac under a Stemi DV4 dissecting microscope (Zeiss) using 5/45 forceps (Fine Science Tools, North Vancouver BC). The DRGs were dissected from the embryos using the methods described in Banker and Goslin, (1998). The six largest lumbar DRGs are cleaned of spinal and peripheral rootlets and plated onto 15 mm circular glass coverslips pre-coated with poly-L-lysine (50 μg/ml, Sigma) and laminin (Chemicon, Temecula CA). The coverslips are placed in wells of a 24 well plate with 225 μL of media in each well. The media was a DMEM base supplemented with 1% penicillin/streptomycin (Gibco, Hamilton ON), 2 mM l-glutamine (Sigma), 1.5 g/L D-glucose (Sigma), 1% FBS (Gibco) and 1.5 ng/ml recombinant human NGF (gift from Regeneron, Vancouver BC). The explants were grown for 48 hours at 37°C in 5% CO_2 and then fixed in 4% paraformaldehyde in PBS for 10 minutes, washed twice with PBS and stored in 0.05% azide in PBS at 4°C.

2.4.1 Variations on the Basic Neurite Outgrowth Assay

In order to test different aspects of LP-OEC mediated neurite outgrowth, modifications were made to the outgrowth assay for different experiments. These modifications are outlined below:

2.4.1.1 LP-OEC Co-Culture

LP-OECs were plated on poly-L-lysine and laminin coated coverslips at a density of 15 000 cells/cm^2 the day before the assay. They were grown in DMEM with 1% FBS. On the day of the assay, the media was switched to that described in section 2.5 before the explant was added directly on top of the LP-OEC monolayer.

2.4.1.2 LP-OEC Conditioned Media Added to the Outgrowth Assay

Conditioned media was added to the baseline media at various concentrations normalized to the number of cells generating the media (see section 2.6.1). The explants were plated into the conditioned media-supplemented media for the entire duration of the assay.

2.4.1.3 SPARC and SPARC Function-Blocking Antibodies

As with conditioned media, SPARC was added to baseline media and the explants were grown in the SPARC-supplemented media for the duration of the assay. For the function-blocking antibody studies, a twenty molar excess of function-blocking antibody was added to SPARC in 200 μL of DMEM. The mixture was incubated on a rocker platform at 4°C for 1 hour and then added to the baseline media for assay with explants.

2.4.1.4 Antimitotic Regimen to Remove Dividing Cells

Explants were plated in media supplemented with 10 μM cytosine arabinoside (Sigma) and grown for 48 hours. The media was removed and the explants were gently rinsed with DMEM to wash off any remaining AraC. New media was then added without AraC and the explants were grown with or without SPARC for 48 hours prior to fixing.

2.4.1.5 Inhibitor Studies

The MAPK inhibitor PD 98059 (Calbiochem, San Diego CA) was added to the media at a concentration of 100 μM and the pan trk inhibitor k252a (Biosource, Camarillo CA) was added at 100 nM. The explants were grown in the presence of the inhibitor for the entire duration of the assay.

2.4.2 Canvassing and Montaging the Neurite Outgrowth Assay

Fixed explants were processed for analysis by immunofluoresence using neurofilament heavy chain antibody (see section 2.3.1). The only difference was the explants were transferred from step to step by inverting them onto 80μL droplets on Parafilm. 200x z-stacked images of the explant were captured using the equipment described in section 2.3.1. Each z-stack was 100 nm and 10 steps were captured per image. The steps were combined using an X-Y maximum intensity algorithm. The entire explant was canvassed in this fashion and then pieced together as separate layers using Photoshop 7.0 (Adobe, San Jose CA).

2.4.3 Quantifying Neurite Outgrowth

The outgrowth was quantified using four different methods, the primary method being skeletonization (section 2.4.3.1) to quantifiy total outgrowth. The other method commonly used was average neurite carpet radius (section 2.4.3.2). Measuring axon carpet surface area (section 2.4.3.3) and total neurite signal (2.4.3.4) were used primarily as a basis for comparison. Carpet surface area was also used to determine DAPI nuclei density.

2.4.3.1 Skeletonization to Determine Total Neurite Length

Canvassed and montaged images were processed using Northern Eclipse running the macro "Neurobinary". Neurobinary reduces the image, originally an 8-bit grayscale image to a purely black and white image after user-specified thresholding. The ganglion is omitted from analysis and the image is skeletonized by comparing each pixel to its 8 neighbours and eliminating them one by one until the continuous signal is reduced to one pixel width. All of the pixels above a user-defined threshold of 25 pixels are counted and in this way, the number of pixels correlates with the total neurite outgrowth.

2.4.3.2 Average Neurite Carpet Radius

The montaged DRG was processed using Northern Eclipse running the macro "Neuroquant". In this macro, the user defines the centre of the ganglion and then outlines the outer edge of the explant. A series of equidistant points are laid along the outline and the computer measures the distance from the centre of the ganglion to each of the points. The distances are averaged to produce an average outer radius (R1 in figure 4.3B). A similar analysis is performed outlining the ganglion itself to give the inner radius (R2 in figure 4.3B). R2 is subtracted from R1 to give the average neurite carpet radius.

2.4.3.3 Axon Carpet Surface Area

The montaged DRG was processed using Photoshop 7.0 (Adobe) to determine axon carpet surface area. The magic wand tool was used to select the area surrounding the explant and then the selection was inverted to select the entire explant. Using the polygon tool, the ganglion was deselected to only select the axon carpet. The total number of pixels was determined in the histogram dialog box (see Appendix 2)

2.4.3.4 Total Neurite Signal

The same processing used for carpet surface area (see section 2.4.3.3) was used in this method. After selecting the carpet, the image was posterized into 4 bins. The top three bins were selected in the histogram dialog box to give a measurement in pixels (see Appendix 3).

2.4.4 Error Analysis

Outgrowth measurements of a given experimental group were pooled, averaged and the standard deviation was determined. Error bars were reported as standard error of the mean ($s.d/\sqrt{n}$). Statistical significance was determined using a two-tailed Student's T test assuming normal variance. ANOVA was performed using the same parameters. Number of replicates for each experimental group can be found in table 2.2.

2.5 Generating Conditioned Media Libraries

LP-OECs were cultured as described in Au and Roskams (2002) (see section 2.2). The only difference was for passage 2 conditioned media where the primary culture was plated in MEM-d-valine containing 5% FBS instead of 10% FBS. For passage 6 LP-OCM (LP-OEC conditioned media), the culture and purification protocol is the same as that described previously (Au and Roskams, 2002). For passage 2 conditioned media, the

cells were grown in 5% FBS initially and stepped down to 2.5% FBS two days later. When the cells reached confluency, they were passaged and complement lysed and re-plated in 2.5% FBS. Two days later the cells were stepped down to 1% FBS, passaged, complement lysed and re-plated in 1% FBS. Two days later, the cells were switched to serum-free DMEM-BS (DMEM Bottenstein-Sato) media which contains: DMEM supplemented with 0.5 nM bovine pancreatic insulin, 100 μg/ml human transferrin, 0.2 nM progesterone, 0.1 nM putrescine, 0.49 nM triiodo-l-thyronine, 0.45 nM l-thyroxine, 0.224 nM sodium selenite and 2 mM l-glutamine (all supplements from Sigma). The cells were grown in DMEM-BS for 96 hours prior to harvesting conditioned media. For passage 6 LP-OCM, the serum step regimen began at passage 4 when the serum concentration was dropped from 10% FBS to 5% FBS two after plating. The regimen is then the same as passage 2 conditioned media without the complement lysis during passage (see figure 4.7 for a schematic representation).

2.5.1 Axon Membrane-Stimulated Conditioned Media

Axon membrane fragments (axolemma) were harvested from 60 mm plates containing 150 DRG explants each using the method of Salzer and coworkers, (Salzer et al., 1980). Briefly, under a dissecting scope the ganglia were excised using a fine scalpel, leaving behind neurite carpets. The carpets were scraped off and gently disrupted using a Dounce homogenizer (Kontes Glass Co., Vineland NJ). The mixture was centrifuged at 35 000xg for one hour at 4°C in silanized Corex tubes (Corning Glass, Corning NY). The resulting pellet was resuspened in 0.1% bovine serum albumin and contained the enriched membrane fraction. One 60 mm plate of axolemma was added to the media for each T175 (175 cm^2 flask) of LP-OECs in DMEM-BS. LP-OCM was then generated as per usual.

2.5.2 Harvesting and Concentrating Conditioned Media

LP-OCM was removed from the cells and transferred into 50 ml conical tubes. The tubes were spun at 280xg for 5 minutes at 4°C to remove cellular contaminants. The supernatant was carefully removed and added to an Ultrafiltration Cell (Millipore, Billerica MA) using a 1 kDa molecular weight cut-off membrane (Millipore). Under 50 psi N_2 pressure, the conditioned media was forced through the membrane, concentrating the protein constituents greater than 1 kDa. The concentrate was filtered using a syringe-driven 0.22 μm filter (Millipore) and stored at –80°C. Concurrently, the LP-OECs that generated the conditioned media were trypsinized, counted and stored at –80°C. By measuring the volume of the filtrate, the x concentration of the media was determined. Each batch of conditioned media was standardized by the number of cells generating 1 ml of LP-OCM and the x concentration after ultrafiltration. In this fashion, each batch of conditioned media could be directly cross-compared by the number of cells generating the media. Arbitrarily, full strength conditioned media was set at 30 000 cells/ml LP-OCM, 1:2 media would then be 15 000 cells/ml LP-OCM, etc.

2.6 Recombinant Mouse SPARC and Recombinant Human SPARC

Recombinant human SPARC was a gift from Dr. E. Helene Sage (University of Washington). Details of its production can be found in Bradshaw et al. (Bradshaw et al., 2000). Recombinant mouse SPARC was generated using the RT-PCR product of passage 2 LP-OECs as a template (figure 2.1). The full length mRNA was amplified by PCR and confirmed by on-campus DNA sequencing (UBC NAPS unit). Flanking the N- and C- termini were the restriction sites HindIII and XhoI respectively and appropriate nucleotide overhang for efficient endonuclease digestion. Downstream of the HindIII site, an Ig κ-chain leader sequence was added to facilitate secretion (Coloma et al., 1992). An extra nucleotide was inserted upstream of XhoI to accommodate the reading frame for

C-terminus epitope tags. Upstream of the extra nucleotide was a short glycine hinge CCACCAC to minimize steric hindrance from the epitope tags. The insert was directionally ligated into a pcDNA-V5/His plasmid using T4 DNA ligase (Roche). The vector was transformed into heat-competent DH5α bacteria (Invitrogen) and selected for by ampicillin resistance. Clones were selected and sequenced to test for the presence, correct orientation and reading frame of the insert. DNA from verified clones were purified using a Plasmid Midi Kit (Qiagen, Mississauga ON).

Plasmids were lipofected into cos-7 cells using Lipofectamine (Invitrogen) and successful transfectants were selected for using 400 μg/ml neomycin. The cos-7 cells were selected for 3 weeks to obtain stable transfectants. Cell lysates and conditioned media were tested for the presence of the V5 epitope by Western blotting. Recombinant mouse SPARC was purified using Ni-NTA (nickel nitriloacetic acid) agarose resin (Qiagen).

Concentrated cos-7 conditioned media (by ultrafiltration, see section 2.5.1) was added to Ni-NTA resin and incubated for 2 hours at 4°C, washed with low salt tris (tris(hydroxymethyl)-aminomethane) buffer (200 mM NaCl), high salt tris buffer (400 mM NaCl) and eluted with 300 mM imidazole in low salt (100 mM NaCl). The fractions were assayed for protein content using a BCA kit (Pierce, Rockford IL) and selected fractions were pooled and dialysed in 10% glycerol in PBS for 18 hours at 4°C to remove tris. A BCA protein assay was performed after dialysis to quantify the dialysed, sterile filtered sample.

2.7 Lesion Paradigms

2.7.1 Bulbectomy

The unilateral bulbectomy procedure is described in greater detail in Roskams et al. (1996). Briefly, an adult CD-1 mouse (8-10 weeks old) was anesthetized with xylaket (4.5 ml/kg). A 1.4 mm diameter hole was drilled through the skull directly above the olfactory bulb and the bulb was ablated by suctioning. The wound was filled with Gelfoam (Pharmacia & Upjohn, Kalamazoo MI) and the skin sealed with VetBond (3M, Minneapolis MN). Twelve days after the procedure, the mouse was processed for sectioning (see section 2.3).

2.7.2 Rubrospinal Crush and Cell Transplantation

The details of the rubrospinal crush injury and transplantation of LP-OECs can be found in greater detail in Ramer et al. (2004). Briefly, a hemilaminectomy was performed at cervical spinal cord section C4 of a 225 g Sprague-Dawley rat host and a crush injury was performed on the dorsolateral funiculus using a pair of fine forceps. Immediately after injury, 1.5 μl of OEC cell slurry was injected directly into the lesion site, 100 000 cells in total. The rat was immune suppressed for two days prior and throughout the duration of the experiment with cyclosporin A (Novartis Pharmaceuticals, Mississauga ON). 7 days after injury the animal was prepared for sectioning.

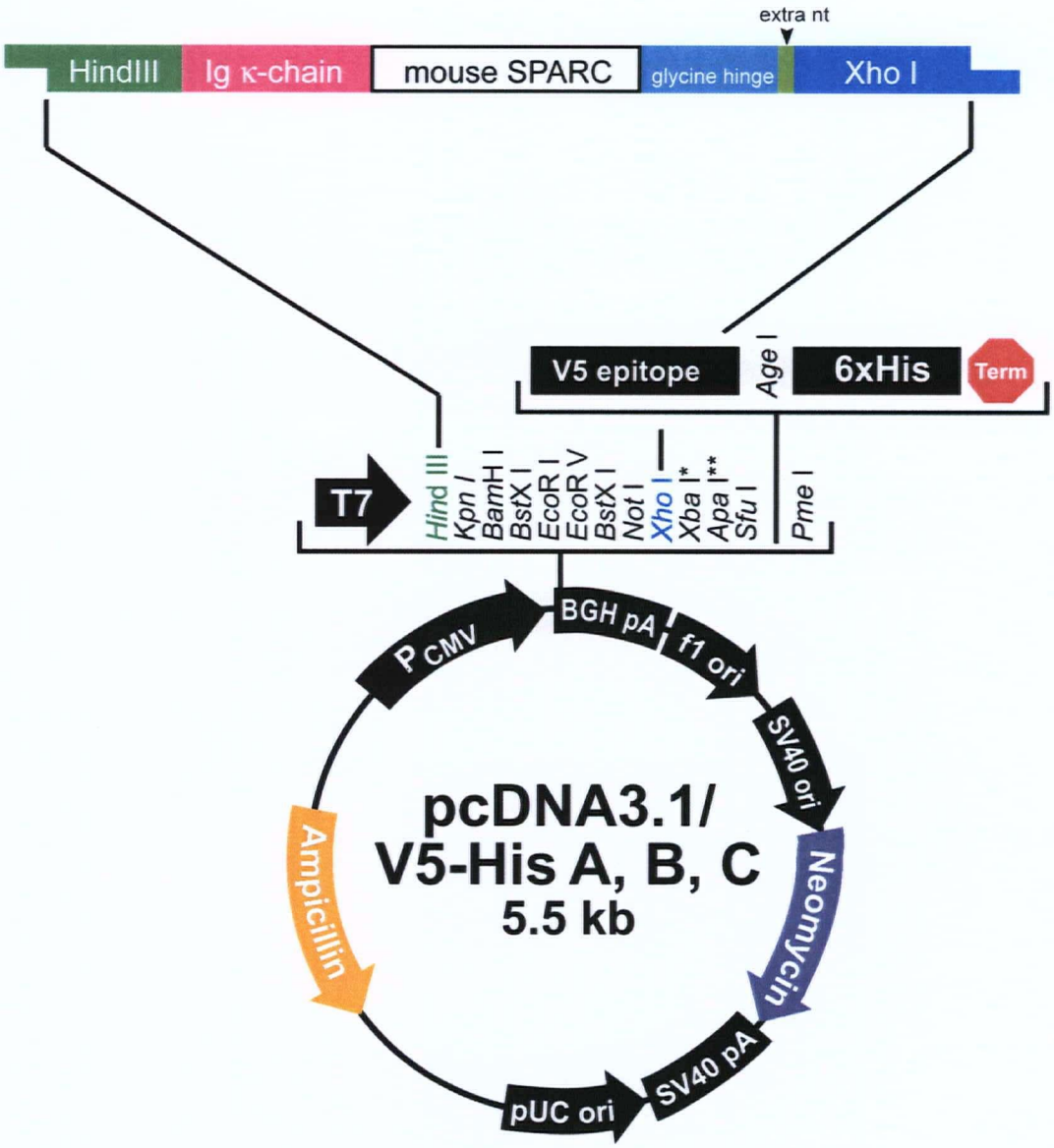

FIGURE 2.1

Schematic Representation of Recombinant Mouse SPARC Insert and pcDNA Vector

Flanking the insert are Hind III (green) and Xho I (blue) restriction sites with appropriate over-hangs to facilitate endonuclease digestion. Downstream of the Hind III site is an Ig k-chain leader sequence to facilitate secretion (pink). Upstream of the Xho I site are a glycine hinge (light blue) and an extra nucleotide (light green) to reduce steric hindrance and maintain the proper reading frame respectively. On the C-terminus of recombinant mouse SPARC are a V5 epitope and 6xHis tag. pcDNA 3.1/V5-His provides two selection genes, ampicillin resistance (orange) and neomycin resistance (purple). To facilitate DNA sequencing of the insert, T7 and BGH flank the multiple cloning site. Adapted from the user's manual for pcDNA 3.1/V5-His A, B and C from Invitrogen.

TABLE 2.1 Antibody Suppliers and Dilutions

Primary Antibody	Supplier	Dilution
β1 integrin	Pharmingen	1/500
CBP 300	Santa Cruz	1/50
CD44	Pharmingen	1/250
DAPI	Sigma	1/10000
GAP-43	Chemicon	1/250
GFAP	Diasorin	1/500
laminin	Sigma	1/1000
NCAM	Chemicon	1/500
nestin	Chemicon	1/100
Neurofilament heavy chain	Serotec	1/500
Notch 3	Santa Cruz	1/100
O4	Chemicon	1/100
OMP	gift (Dr. Frank Margolis)	1/10000
p200 (type V collagen)	gift (Dr. David Carey)	1/500
p75	Chemicon	1/500
PACAP	Penninsula Laboratories	1/250
rat-specific p75	Chemicon	1/1000
S100β	Sigma	1/500
SPARC	R&D Systems	1/1000
thy 1.1	American Type Culture Collection	1/125
VEGF	US Biological	1/250
vimentin	Accurate	1/50

Secondary Antibody	Supplier	Dilution
Alexa 594 (various hosts, specificities)	Molecular Probes	1/100
Alexa 488 (various hosts, specificities)	Molecular Probes	1/100
Biotinylated anti-IgG (various hosts)	Vector Laboratories	1/200
Cascade Blue goat anti-mouse	Molecular Probes	1/100

TABLE 2.2 Outgrowth Assay Experimental Groups and Replicates

Experiment	# Experimental Groups	Total Replicates
NGF controls		
NGF baseline	8	34
NGF + heat denatured LP-OCM	3	9
NGF + Ab236	3	10
NGF + Ab255	3	13
NGF + AraC	3	16
NGF + PD 98059	3	18
NGF + K252a	3	18
LP-OEC co-culture	4	22
P2 LP-OCM		
1x	4	15
0.5x	4	14
0.25x	4	16
0.1 x	3	12
0.05x	3	10
0.025x	3	10
1x + Ab255	3	13
P6-LPOCM		
1x	4	13
0.5x	4	12
0.25x	4	14
1x + Ab255	3	13
SPARC null LP-OCM 1x	3	16
rhSPARC		
1 ng/ml	3	16
2.5 ng/ml	3	15
5 ng/ml	5	25
10 ng/ml	3	18
5ng/ml + Ab236	3	14
rmSPARC		
1 ng/ml	3	14
2.5 ng/ml	3	16
5 ng/ml	3	17
10 ng/ml	3	15
5 ng/ml + Ab 255	3	15
		Total: 463

Chapter 3: Purification and Characterization of Olfactory Ensheathing Cells In Vivo and In Vitro

Note: The majority of Chapter 3 was published as Au and Roskams (2003) Glia 41(3): 224-236 with the following additions and modifications: It has been formatted to match the style of the thesis, the Introduction has been revised, expanded and updated and the Materials and Methods section has been integrated into Chapter 2.

3.1 Introduction

3.1.1Background

OECs reside within the two main regions of the primary olfactory neuraxis: the lamina propria (LP) in the periphery and along the olfactory nerve fibre layer (NFL) of the olfactory bulb centrally (Figure 1.3). OECs of the lamina propria ensheathe ORN axons as they exit the olfactory epithelium through the basal lamina, fasciculating them into nerve bundles (Doucette, 1990). OECs also secrete the extracellular matrix of the lamina propria and its basal lamina (Barnett et al., 1993; Gong and Shipley, 1996; Kafitz and Greer, 1998; Li et al., 1997; Li et al., 1998; Raisman, 2001; Treloar et al., 1996). Ensheathement of ORN axons stops just short of the ORN synapse at the mitral cell glomerulus of the olfactory bulb. In this context, OECs are the only glial population that can continuously ensheathe axons from the periphery into the central nervous system (see figure 1.3 and 1.6; section 1.2.2).

To deal with their dynamic environment, OECs possess characteristics that are both peripheral (Schwann cell-like) and central (astrocyte-like) (Li et al., 1997; Li et al., 1998; Raisman, 2001) (see section 1.2.5). OECs also express developmentally regulated

proteins normally found in immature or progenitor cell populations, such as nestin, vimentin and PSA-NCAM, throughout adulthood (Imaizumi et al., 2000b; Imaizumi et al., 1998).

Because of their versatility, OECs have been transplanted into lesioned areas of the nervous system and can promote the regeneration of PNS and CNS axons *in vivo* (reviewed in Bartolomei and Greer, 2000) (see section 1.2.6.1). While OECs do not normally myelinate ORN axons, they can myelinate axons in a demyelinating lesion, restoring near-normal conduction properties (Barnett et al., 1993; Farbman and Margolis, 1980; Yan and Johnson, 1988) (see section 1.2.6.2). OECs used in these transplantation paradigms, for the most part, have been derived from the olfactory bulb, a structure that is surgically inaccessible in a live rodent or human as a source of cells for autotransplantation (Barber and Lindsay, 1982). As an alternative, OECs of the olfactory mucosa are more accessible and less invasive in both rodent and human. Here, we provide a simple method for purifying and characterizing OECs from the olfactory mucosa. In so doing, we have expanded the developmental characterization of OECs, and reveal additional gene expression patterns that may yield insight into the remarkable degree of plasticity they exhibit.

3.1.2 Review of OEC Culture Approaches by Other Groups

There are a number of methods employed by different groups to culture and study OEC function. The age of donor, source of tissue, rat strain, purification process, and expansion regimen are unique to each method and there has yet to be a consensus as to which method is best. An examination of the OEC literature reveals that this confounding issue has not been scrutinized and reviewed to any great detail. In the context of this results section (introducing yet another new method for culturing and purifying OECs) it is appropriate to summarize the main methods of OEC culture and the experimental context in which they have been employed.

3.1.2.1 The Chuah Method

At about the same time, three groups began to prospectively culture and purify OECs, all of them from the nerve fibre layer of the olfactory bulb. The Chuah group obtained OECs from neonate rat olfactory bulbs by careful dissection of the nerve fibre layer followed by enzymatic digestion in trypsin and collagenase (Chuah and Au, 1993). The cells were initially maintained in DMEM (Dulbecco's modified Eagle's medium) with 10% fetal bovine serum (FBS), MEM (minimal essential medium) vitamin supplement and penicillin/streptomycin. Originally, the group removed fibroblast contaminants by treatment with cytosine arabinoside (AraC) and immunoadsorption to anti-Thy 1.1-coated plates. More recently, the protocol has been modified so that OECs, which the authors claim are less adherent than fibroblasts, are detached earlier by trypsinization during passaging. By carefully monitoring the trypsinization procedure, the more adherent fibroblasts are left on the plate and the OECs can be preferentially isolated (Chuah and Teague, 1999). After the purification regimen, OECs are supplemented with bovine pituitary extract (BPE) to enhance proliferation (Chuah and Au, 1993). The Chuah group has mainly used their OECs for in vitro studies (for example: Chuah et al., 2000; Chuah and Teague, 1999; Liu et al., 1995). To date they have published one transplantation study directly comparing OECs and encapsulated OECs in a spinal cord injury model (Chuah et al., 2004). A modified version of this protocol is employed by the Kocsis group for their transplantation studies (see section 1.2.6.2). Instead of enzymatic digestion, however, the group cuts the dissected nerve fibre layer into small chunks and triturates them into a cell slurry to be used immediately for transplantation.

3.1.2.2 The Doucette Method

Dr. Ronald Doucette obtained OECs from Theiler stage 23 rat embryos (rat embryonic day 18). At this stage, the nerve fibre layer is not firmly attached to the telencephalon (developing olfactory bulb) and can be peeled off of it (Devon and Doucette, 1992). By electron microscopy, the authors claim that astrocytes and Schwann cell contaminants are

not present at this stage. The dissected tissue is dissociated through a 75μm mesh and plated onto tissue culture plastic in DMEM/F12 (DMEM in a 1:1 ratio with Ham's F12 medium) with 10% FBS (Smale et al., 1996). The Doucette group has used this preparation for studying OEC-mediated myelination of dorsal root ganglion neurites (Devon and Doucette, 1992; Devon and Doucette, 1995) and in transplantation studies into the brain (Smale et al, 1996) and the injured spinal cord (Boyd et al., 2004). A similar approach was used in an OEC in vitro study by Dr. Charles Greer except that the rats used were embryonic day 15 instead of 18 (Kafitz and Greer, 1998; Kafitz and Greer, 1999) (see section 4.1.1 for more details).

3.1.2.3 The Ramon-Cueto Method

The Ramon-Cueto group obtained OECs from adult rat olfactory bulbs. The nerve fibre layer was dissected and the tissue was minced and digested in trypsin. In their original characterization paper (Ramon-Cueto and Nieto-Sampedro, 1992), the authors noted fusiform (fibroblast) and 'fried-egg' (macrophage) shaped cell contaminants. The cells are maintained in DMEM with 10% FBS on poly-L-lysine coated tissue culture plastic. After the cells achieved confluency, they are a trypsinized in step similar to Chuah (Chuah and Teague, 1999) where the fried-egg shaped macrophages were left behind. Transfer of the cells to a poly-L-lysine coated glass slide prevented fusiform-shaped fibroblasts from adhering leaving only OECs behind. This observation is at odds with another OEC characterization paper by Nash and coworkers which found fibroblast contaminants were preferentially adherent even to uncoated glass slides (Nash et al., 2001).

This original protocol but without the purification step is the method used by the Raisman group. Their description of p75 and fibronectin positive populations (Li et al., 1998) in their culture is consistent with Ramon-Cueto and Nieto-Sampedro's original observations (Ramon-Cueto and Nieto-Sampedro, 1992). Although it is not explicitly stated in the earlier studies (Li et al., 1997; Li et al., 1998), the Raisman group does not passage the

OECs until just prior to transplantation approximately two weeks after primary culture. At this point, the cells are reported to be extremely confluent, approximately 20μm thick (Li et al., 2003b) before being scraped off the flask with a cell scraper, ready for transplantation. Also, without the purification step, it stands to reason that the ED-1 positive macrophage contaminants reported by Ramon-Cueto and Nieto-Sampedro are still present in the Raisman OEC cultures. There was a recent report of macrophage-mediated axon growth via galectin-1 activation (Horie et al., 2004) and it is possible that this macrophage population could be contributing the remarkable degree of regeneration reported by the Raisman group (see section 1.2.6.1).

Since the original characterization paper, the Ramon-Cueto group has changed their purification procedure. Now the cells are immunopanned twice with anti-p75 antibody (clone Ig192) and the maintenance medium is supplemented with bovine pituitary extract (Ramon-Cueto and Nieto-Sampedro, 1994). Many groups employ the Ramon-Cueto and Nieto-Sampedro newer method of purifying OECs (for example, recently: Gomez et al., 2003; Ruitenberg et al., 2005; Sasaki et al., 2004) including the Bunge group (see section 1.2.6.2.2) who additionally supplements their OECs with forskolin (Ramon-Cueto and Avila, 1998). In fact, it can be argued that this is the most common method for OEC transplantation to mediate spinal cord regeneration, with the exception of re-myelination studies.

3.1.2.4 The Barnett Method

The Barnett group employed fluorescence activated cell sorting (FACS) to select for O4-positive, GalC-negative cells from whole olfactory bulbs of neonate rats (Barnett et al., 1993). The cells are grown in serum-free media DMEM-BS (modified DMEM with Bottenstein-Sato supplements (Bottenstein et al., 1979)) supplemented at 20% with astrocyte conditioned medium (astrocytes were also grown in DMEM-BS). Later, the group developed a clonal temperature-sensitive cell line using this method (Barnett and Roskams, 2002; Franceschini and Barnett, 1996). Because of the large T antigen driving

cell division, the cell line can proliferate efficiently without astrocyte-conditioned media (ACM). This cell line has been used by Franklin and coworkers in the original OEC re-myelination study (Franklin, 2002). Using this purification method, the Barnett group has since examined OEC and Schwann cell interaction with astrocytes (Fairless et al., 2005; Lakatos et al., 2003a; Lakatos et al., 2000) and collaborated with Dr. Robin Franklin on a number of transplantation studies examining OEC-mediated re-myelination (Franklin et al., 1996; Lakatos et al., 2003b; Smith et al., 2002; Smith et al., 2001).

3.1.2.5 The Wigley Method

Olfactory ensheathing cells have also been cultured from nerve rootlets entering the nerve fibre layer (see figure 1.7). The Wigley group obtained OECs from adult rats (Sonigra et al., 1996). To obtain rootlets, the OB was dissected out and the meninges removed. The rootlets hanging off the bulb surface were isolated, digested in trypsin and plated on poly-L-lysine and laminin. The cells were maintained in DMEM with 10% FBS. An OEC cell line termed RolfB1.T was generated by spontaneous transformation (Sonigra et al., 1996) using this method. However the Wigley group's subsequent studies have been from fresh nerve rootlet OEC cultures (Hayat et al., 2003a; Hayat et al., 2003b; Kumar et al., 2005).

3.1.3 Olfactory Ensheathing Cell Mitogens

Because of their potential therapeutic value, it has been of interest to several groups to find optimal expansion conditions for OECs. The Chuah group demonstrated that bFGF was a mitogen for OECs (Chuah and Au, 1993) and they suspect that the active ingredient in the bovine pituitary extract used to expand their OECs (see section 3.1.2.1) is basic fibroblast growth factor (Chuah and Teague, 1999). Similarly, the Barnett group found that neuregulin-1 was an important component in astrocyte conditioned media and was a potent mitogen for OECs (Pollock et al., 1999). The two groups also reported that

OECs can produce bFGF (Chuah and Teague, 1999) and neuregulin-1 (Thompson et al., 2000) in vivo and in vitro. OECs are also responsive to forskolin (Alexander et al., 2002; Ramon-Cueto and Avila, 1998; Yan et al., 2001a) and Yan and coworkers reported that forskolin can synergize with other OEC mitogens such as the neuregulin-1 isoform heuregulin β1 (HRGβ1), platelet-derived growth factor (PDGF) and insulin growth factor-1. The Kocsis group reported that hepatocyte growth factor is a potent OEC mitogen (Yan et al., 2001b). The Barnett group reported that while astrocyte conditioned media promotes OEC proliferation, it did not do so indefinitely. In an attempt to rescue the drop-off in proliferation, Alexander and coworkers found that a cocktail of HRGβ1, forskolin and FGF2 was successful in that regard (Alexander et al., 2002). It was not made clear in their study, however, the passaging regimen for the OECs as contact-mediated inhibition would likely be a factor over the long timescale of their assay. A summary of this section can be found in table 3.1.

It was in the context of previously established approaches for culturing OB-OECs from the nerve fibre layer of the olfactory bulb, coupled with their mitogenic response to various growth factors, that I began to culture, purify and characterize the ensheathing cell population from the lamina propria, LP-OECs. The general approach was to compare what had previously been described in OB-OECs with LP-OECs and correlating this data both in vivo and in vitro.

3.2 Results

3.2.1 Lamina Propria olfactory ensheathing cells express the same characteristic proteins as olfactory bulb-derived ensheathing cells in vivo

Olfactory ensheathing cells within the lamina propria *in vivo* have not been directly compared, with respect to their antigenicity, to OECs from the bulb. The olfactory epithelium and bulb were therefore examined at neonatal postnatal day five (P5 - the same time point chosen for *in vitro* isolation) for the expression of the low affinity nerve growth factor receptor/ p75 (Barnett et al., 1993) and olfactory marker protein (OMP), which is expressed in mature olfactory receptor neurons (ORNs) (Carey and Stahl, 1990). Expression of p75 was detected in processes in both the lamina propria and olfactory nerve fibre layer, with no co-localization of p75 in mature ORN axons expressing OMP (Figures 3.1A and 3.1B). Given that p75 could ostensibly be expressed by immature ORNs (which do not express OMP), we examined the co-expression of p75 with two other OEC markers, the oligodendrocyte lineage marker, O4 and the astrocytic marker, glial fibrillary acidic protein (GFAP) (Alexander et al., 2002; Yan et al., 2001a). Both p75 and O4 detected immunoreactivity in glial processes surrounding and penetrating nerve bundles, and also along the outer layer of the olfactory nerve fibre layer, (NFL; Figure 3.1C). Although O4 and GFAP clearly recognized cell processes outside axon bundles in the lamina propria, the expression of the two markers overlapped in only some instances. Whereas GFAP was mainly in processes surrounding mesaxons (the subcompartments of the nerve bundles delineated by OEC processes), thinner O4-positive cell processes were found chiefly around the outside of whole nerve bundles (Figure 3.1C). Both antigens could be detected in glial processes streaming across the cribriform plate into the NFL. O4 and the calcium binding protein, S100β displayed comparable expression patterns and neither displayed significant overlap of expression with GFAP (Figures 3.1C and 3.1D).

3.2.2 Lamina Propria-derived olfactory ensheathing cells express the same characteristic proteins as bulb-derived ensheathing cells in vitro

Using the *in vivo* OEC antigenic profile as a guide to identify cell fractions from the OE enriched in OECs, we developed a paradigm to culture OECs from the P5 lamina propria. These cells were first examined for retention of expression of the characteristic bulb OEC markers examined *in vivo*. The majority of the cells obtained using this approach expressed p75 (Figure 3.2A), S100β (Figure 3.2B) and GFAP (Figure 3.2C). Cells expressing each of these antigens were bi- and tripolar Schwann cell-like (S-type) and also flat, astrocyte-like (A-type), morphologies previously described in cultured bulb-derived ensheathing cells (Yan et al., 2001b) (Figure 3.2). Using double immunofluorescence, the OECs demonstrated co-expression of O4 and p75 (Figure 3.2D), vimentin and p75 (Figure 3.2E) and nestin and p75 (Figure 3.2F). At 5 DIV, cells within our cultures were also negative for the neuronal marker beta-III neuron-specific tubulin (TuJ1, data not shown).

3.2.3 Optimizing the purity of cultured olfactory epithelium-derived ensheathing cells

After 5 days in vitro (5DIV), although many of the cells displayed an OEC phenotype with negligible neuronal contamination, it was evident that there was significant contamination with fibroblasts. Therefore, a concerted effort was made to actively select against fibroblast growth first by plating initially in MEM d-Valine (to minimize fibroblast mitosis) followed by cytotoxic lysis of remaining fibroblasts by Thy 1.1-mediated complement lysis (Pollock et al., 1999), an approach that has been effective in eradicating fibroblasts from Schwann cell cultures. Following 1, 2 and 3 successive complement lyses, we assayed for the percentage of cells (DAPI-stained nuclei = 100%) expressing S100β, for co-expression of S100β and p75 (Figure 3.3A), and co-expression of S100β and GFAP (Figure 3.3B). The efficacy of the complement-mediated removal of fibroblasts was thus quantified by assaying % S100β+/DAPI+ cells per complement lysis. Prior to any complement lyses, 81±3% of the enriched population of cells was S100β -positive. Following the third complement lysis, 97±3% of the cells expressed

S100β (Figure 3.3C, 3.3D), 97±2% of the purified LP-OEC population expressed p75, 69±3% expressed GFAP (Figure 3.3D).

To determine if there were any cells that were S100β+/P75- or S100β-/P75+, overlap of the two markers was also assessed in these cells. Virtually all S100β positive cells examined co-expressed p75 (99±2%; Figure 3.3A).

3.2.4 Assessing the proliferative capacity of purified LP-OECs

Olfactory ensheathing cells derived from the olfactory bulb have exhibited a wide variety of expansion rates under a number of growth conditions, many of which are dependent on the addition of exogenous growth factors (Ikeda et al., 1996); (Chernousov et al., 1999; Wang and Barres, 2000; Zanger et al., 2001). We tested both the effect of plating density and different media conditions on LP-OEC proliferation. In order to determine maximal expansion characteristics for the LP-OECs, proliferative rate was primarily measured by a standard ^{3}H-thymidine uptake assay. Maximum proliferation was achieved at a plating density of 5800 cells/cm^2, 24 hours after plating (Figure 3.4A). Thus in all subsequent experiments, the LP-OECs were plated at a standard density of 5800 cells/cm^2. At this standard density, the proliferative rates of LP-OECs were compared between the following media conditions: DMEM with 10% FCS, DMEM-BS (a serum-free medium), and DMEM-BS with 10 ng/mL basic fibroblast growth factor, a known OB-OEC mitogen. LP-OECs had an average doubling time of 60 hours in DMEM-10% FCS. By supplementing the serum-free media with bFGF the proliferative capacity of the cells was comparable to that of 10% FCS (Figure 3.4B). To confirm the validity of the ^{3}H-thymidine uptake assay, a growth curve assay with haemocytometer counts was performed in parallel with the same cells and the same media conditions (Figure 3.4C). The resulting growth curves were consistent with the proliferation assays. The mitogenic effect of bFGF, however, was found to tail off over time whereas serum did not (Figure 3.4D). An additional control media condition (DMEM/F12 with 10%FCS) was used in the growth curve to confirm that DMEM DMEM/F12 would comparably support the growth of OECs. DMEM was used in all uptake assays, because F12 media contains a

high concentration of endogenous thymidine, which will decrease the sensitivity and accuracy of the thymidine uptake assay. Finally, the proliferative capability of the LP-OECs was assessed as a function of their passage number, where proliferative capacity was assessed at passage 3, 6 and 9. The ability of LP-OECs to divide diminished with increased time in culture (Figure 3.4D) Passage 6 cells had 74% of the proliferative rate of cells at passage 3 and decreased to 34% by passage 9. From a standard preparation (1 litter of mice, average 10 pups per litter), it was possible to generate 20 million purified LP-OECs by 14 DIV.

3.2.5 Novel markers in vitro and in vivo

OECs from the lamina propria antigenically resemble OECs from the olfactory bulb, but appear to have a greater capacity for expansion and passage under standard culture conditions (DMEM/10% FCS, no exogenous growth factors). Because of this, and their established functional plasticity, we wished to test whether these OECs might express additional proteins of a more developmental nature than other mature glial cells. By immunocytochemical detection, LP-OECs expressed the ECM receptors CD44 (hyaluronic acid receptor) and the β1 integrin subunit, which can form laminin and collagen receptors, *in vitro* (figure 3.5A and 3.5B) and *in vivo*. Both of these receptors are also expressed by embryonic, but not mature, Schwann cells (Chuah and Au, 1991). LP-OECs (probed for co-expression of either S100β or p75) also secrete the ECM components P200 (a type IV collagen) and the secreted proteoglycan NG2 (Doucette, 1993) (figure 3.6C and 3.6D). OB-OECs have been shown to produce some secreted neurotrophic factors; sub-populations of LP-OECs also express the vascular endothelial growth factor (VEGF) and the neuropeptide, pituitary adenylate cyclase-activating peptide (PACAP) (Figure 3.6E and 3.6F).

The Notch family of receptors has been implicated in a number of developmental functions, including over-riding pro-neurogenic mechanisms and instructing bipotential cells towards a glial fate. When activated at the cell surface by their preferred cell surface

ligands, these receptors are cleaved and translocated to the nucleus to influence transcription (Ramon-Cueto et al., 1993). The Notch 3 receptor is highly expressed in the processes of a sub-population of OECs *in vitro* (Figure 3.5G) and *in vivo* (Figure 3.6), but is not found in their nuclei. The CREB binding protein, CBP/ p300, however, is found in the nucleus. It binds to the cyclic amp response element binding protein, and can be activated by a number of developmentally-regulated pathways, including growth factor stimulation (Barnett et al., 1993). CBP/p300 exhibits a nuclear localization in most (but not all) OECs (Figure 3.5H).

Several of the novel markers were found not only in purified LP-OEC cultures *in vitro* but also yielded a clear glial labeling pattern *in vivo* (Figure 3.6). CD44 immunoreactivity was detected in ensheathements around nerve bundles and demonstrated partial overlap with p75 (Figure 3.6A) in the lamina propria. While p75 antibody labels OECs in the outer olfactory nerve fibre layer, no CD44 expression was detected anywhere in the olfactory bulb (Figure 3.6B). CD44 immunoreactivity could however be found in the overlying skull and cribriform plate. Pituitary adenylate cyclase activating polypeptide (PACAP) signal was detected in OECs of the lamina propria as well as some ORN axon bundles (Figure 3.6C). GFAP expression in the lamina propria was restricted to OECs and virtually overlapped with PACAP positive LP-OECs. Notch 3 was present in a subpopulation of GFAP-positive OECs of the lamina propria (Figure 3.6D).

3.3 Discussion

OECs from the olfactory bulb have demonstrated significant promise in transplantation paradigms, to stimulate repair of the lesioned CNS. For the practical purposes of generating cells for transplantation, the lamina propria offers a more attractive source of OECs than the olfactory bulb, but relatively little is known about OECs from the lamina propria. Given that the OECs throughout the length of the olfactory nerve are all derived from the same embryonic origin – within the olfactory placode, it is possible that LP-OECs and OB-OECs are identical in nature (Barber and Lindsay, 1982; Vickland et al., 1991). In the neonatal and adult olfactory system, however, LP-OECs reside in a peripheral cellular compartment vastly different from their CNS-based olfactory bulb counterparts. It is therefore not guaranteed that LP-OECs will demonstrate the same cellular characteristics as OB-OECs, given the differences *in vivo* environments (Figure 1.3). The four most established OB-OEC markers, p75 (Gong et al., 1994), O4 , S100 (Astic et al., 1998) and GFAP (Chuah and Au, 1991), demonstrated an *in vivo* expression profile within the olfactory lamina propria that directly reflects that seen in the OECs of the olfactory bulb (Figure 3.1). Prior to this study, p75 and S100β were the only established OEC markers to display a dynamic glial-specific expression pattern in the developing olfactory system (Barnett et al., 1993; Chuah and Teague, 1999; Doucette, 1993). The peripheral expression patterns for p75, O4, S100β and GFAP, were restricted solely to the lamina propria component of the olfactory mucosa, primarily on ensheathing cell processes within and around ORN nerve bundles. Thus, the co-expression of these proteins should be useful, in combination in the mouse to definitively distinguish OECs from other cells derived from the olfactory mucosa.

Olfactory ensheathing cells, (also known as olfactory Schwann cells or olfactory ensheathing glia) have remained a poorly understood cell type. Their origin – the olfactory placode - (Yan et al., 2001a), is separate from that of neural crest-derived peripheral glia and neural tube-derived central glia and yet OECs share properties of both central and peripheral glia. Furthermore, OECs from the olfactory bulb exhibit a variety

of morphological and expression phenotypes *in vitro*, depending largely upon the purification and/or expansion procedures used to culture them (Alexander et al., 2002; Barnett et al., 1993; Dong et al., 1997; Nash et al., 2001; Ramon-Cueto and Nieto-Sampedro, 1994). This variation could arise either as an *in vitro* artefact or because the expression of some of these proteins is dependent on interaction with neurons or other glial cells. The subcellular distribution of gene products within a population of OECs can be more easily monitored *in vitro*. Expression of the cytoskeleton-associated calcium binding protein S100β, the diffuse cell surface expression of p75 and O4, and the intracellular expression of the developmentally-regulated intermediate filaments, vimentin, GFAP and nestin can be distinctly seen in LP-OECs (Figure 3.2). In addition, the co-expression of GFAP and O4, with either p75 or S100 β is a pattern that has only been reported for OECs, and not other glial cells (Smale et al., 1996).

When purifying olfactory ensheathing cells from the periphery, we had to take pains to eradicate fibroblasts from the cultures. The combination of initial plating in MEM-d-Valine coupled with Thy 1.1-mediated complement lyses appears to be an inexpensive and effective method to yield a pure preparation of OECs (Figure 3.3). Although it has been suggested that OECs from the olfactory bulb may express Thy 1.1 (Franklin et al., 1996), it does not appear to be the case with this cell population as the majority of LP-OECs are resistant to complement-mediated lysis. Cell density had a significant effect on the rate of proliferation of LP-OECs. By using a standard optimal plating density (5800 cells/cm), LP-OECs (Unlike OB-OECs), expanded rapidly in DMEM/10%FBS without addition of exogenous growth factors as measured by thymidine uptake or haemocytometer counts of viable cells (Figure 3.4). When serum was removed and replaced with BS defined media, the expansion rate dropped considerably, but was restored by the addition of bFGF to DMEM-BS. OB-OECs (which do not expand well in serum) also exhibit a significant mitogenic response when grown in the presence of bFGF, whereas Schwann cells do not. Although the LP-OECs will continue to expand over several passages (as many as 12 passages, data not shown), expansion rate dropped after P6 (Figure 3.4), and by passage 5 the OECs assumed a morphology that was predominately A-type.

It is not out of the question that the OEC cultures derived from the lamina propria may have minor Schwann cell contamination from the extrinsic innervation of the nasal cavity. Although the classic OEC expression profile is not normally reflected in non-embryonic Schwann cells, each of the proteins used to identify OECs (Figures 3.1, 3.2 and 3.3) could be expressed by Schwann cells at some stage in embryonic development that could be re-established when SCs are placed in an *in vitro* environment. The culture conditions used in this study that readily expand and characterize the OE-OECs (DMEM/F12 with 10% FCS) do not promote Schwann cell proliferation which requires exogenous factors that upregulate cAMP levels (Li et al., 1997). Although this does not negate the possibility of SC contamination, it is unlikely the contamination is significant since olfactory ensheathing cells constitute the vast majority of glia in the olfactory mucosa where they ensheathe several million ORNs.

Although important milestones have been reached in studies involving OEC transplantation (Barnett et al., 2000; Chernousov et al., 1999; Chernousov et al., 2001; Ikeda et al., 1996; Imaizumi et al., 2000a; Imaizumi et al., 2000b; Schwartz, 2001), the question of mechanistically how OECs promote neurite outgrowth, myelinate neurons and achieve the general level of plasticity that they do when introduced into a foreign environment have yet to be addressed fully. The degree of plasticity exhibited by OECs both within and outside the olfactory system indicates that they have a more immature phenotype than that of other glial cells in the adult CNS.

We have identified several novel proteins, previously unreported in OECs, which are expressed by LP-OECs *in vitro* and may shed some light as to how OECs interact with their cellular and extracellular environment and also in promoting regeneration (Figure 3.6). CD44 recognizes a receptor for hyaluronic acid, a major component of cartilaginous ECM, which is prevalent within the lamina propria. *In vivo*, CD44 is expressed by LP-OECs (but not OB-OECs) and is also expressed by Schwann cells during embryonic development (Levine and Stallcup, 1987). Of particular interest, CD44 expression could only be detected in OECs residing in the lamina propria. As CD44 is a hyaluronic acid

receptor, the difference in CD44 expression may indicate a difference between the hyaluronic acid-rich environments of the periphery compared to the olfactory bulb. The β1 integrin isoform (CD 29) can form heterodimers with many different α-integrin subunits (Levine et al., 1993) to form laminin, collagen and fibronectin receptors and is expressed robustly by OE-OECs *in vitro*. Purified OECs also express two ECM molecules normally associated chiefly with developing glia. The alpha 4 type V collagen isoform p200 (Boruch et al., 2001) is expressed by Schwann cells embryonically and re-expressed in SCs following peripheral lesion where it has been shown to play a role in Schwann cell migration and nerve fasciculation (Hsu et al., 2001). NG2, a chondroitin sulphate proteoglycan transiently expressed by developing oligodendrocytes (Hiraizumi et al., 1993; Lacroix and Tuszynski, 2000) is also expressed by OECs, but has not been reported on SCs. Cultured OECs from the bulb express a number of secreted factors with neurotrophic activity (Illing et al., 2002; Skold et al., 2000; Zhang and Guth, 1997). *In vitro*, LP-OECs also express vascular endothelial growth factor, (VEGF) and pituitary adenylate cyclase activating polypeptide, (PACAP) (Figure 3.6). VEGF is an important mediator of angiogenesis and may be part of a mechanism whereby increased vascularization could assist in promoting neuronal growth and survival in a transplant paradigm (Hansel et al., 2001; Vaudry et al., 1998; Wang and Barres, 2000). PACAP is a neuropeptide implicated in the stimulation of neurogenesis, neuroprotection and the stimulation of mature ORN electrophysiology (Lundkvist and Lendahl, 2001). PACAP expression *in vivo* was found not only in the glia of the lamina propria but also the ORN axon bundles. A neurostimulant, PACAP may be secreted to specific populations of ORNs to mediate neuronal maturation and survival (Chan and La Thangue, 2001; Li et al., 2002; Morrison et al., 2000; Zanger et al., 2001). Little is known about the transcriptional mechanisms that define the developmental state of OECs, and what their downstream effects may be when OECs are shifted from one environment into another. A role for Notch 3 has yet to be identified in developing glial populations but it is highly expressed by LP-OECs *in vitro*. *In vivo*, only subpopulations of OECs were positive for Notch3 and, in all cases examined, these glia did not appear to be actively ensheathing ORN axon bundles. When activated appropriately by an environment that contains a DSL ligand, the interaction may drive a transcriptional switch within the OECs which

will allow them to respond differentially to a new environment (Lundkvist and Lendahl, 2001; Morrison et al., 2000; Wang and Barres, 2000). Similarly, CBP/p300 has been implicated in glial developmental gene regulation as a transcriptional co-activator either directly as a histone acetyl transferase or by its ability to complex with and either activate or inhibit other transcription factors (Chan and La Thangue, 2001; Li et al., 2002; Zanger et al., 2001). Some of the proteins expressed by LP-OECs (e.g. CBP/p300, Nestin, NG2) are also suggested to be characteristic markers of a new class of glia – aldynoglia – that exist as growth-promoting glia within the mature nervous system (Gudino-Cabrera and Nieto-Sampedro, 1999).

Collectively, these data establish LP-OECs as cells that are highly similar to OB-OECs, both morphologically and antigenically with the exception of CD44 expression *in vivo*. Their *in vitro* expansion characteristics, however, set them apart from either OB-OECs or SCs. Finally, the expression of a set of developmentally-regulated proteins more commonly found within the embryonic nervous system appear to place LP-OECs in a class of their own as a readily accessible growth-promoting class of glia which exist in the mature nervous system.

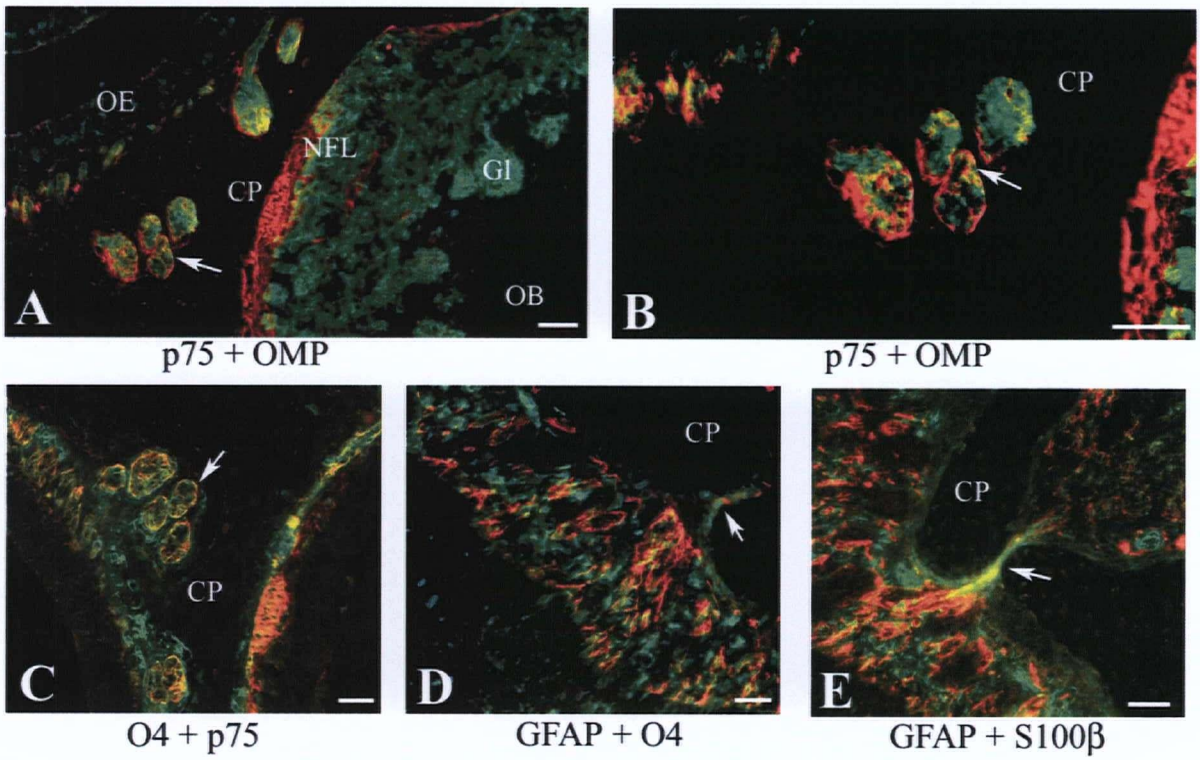

FIGURE 3.1

Olfactory Ensheathing Cells From the Lamina Propria (LP-OECs) Express the Same Characteristic Markers as Olfactory Bulb Ensheathing Cells In Vivo

(A) The low affinity nerve growth factor receptor, p75 (red, arrow) is expressed in ensheathements of olfactory marker protein (OMP) positive olfactory receptor neuron (ORN) axons (green) on both sides of the cribriform plate (CP). (B) p75 positive ensheathments (red, arrow) are more clearly seen at higher magnification. (C) Peripheral OECs also express the oligodendrocyte marker 4 (O4; green) which partially overlaps (yellow, arrow) with p75 expression (red). (D) O4 expression (green) in LP-OECs only partially overlaps with OEC expression of glial fibrillary acidic protein, GFAP (red). (E) GFAP expression (red) partially overlaps (yellow, arrow) with expression of S100β (green). In all cases, LP-OECs exhibit close association to nerve bundles leading up to the olfactory bulb. Scale bars represent 50 microns. Abbreviations: OE = olfactory epithelium; CP = cribriform plate; NFL = nerve fibre layer; Gl = glomerulus; OB = olfactory bulb.

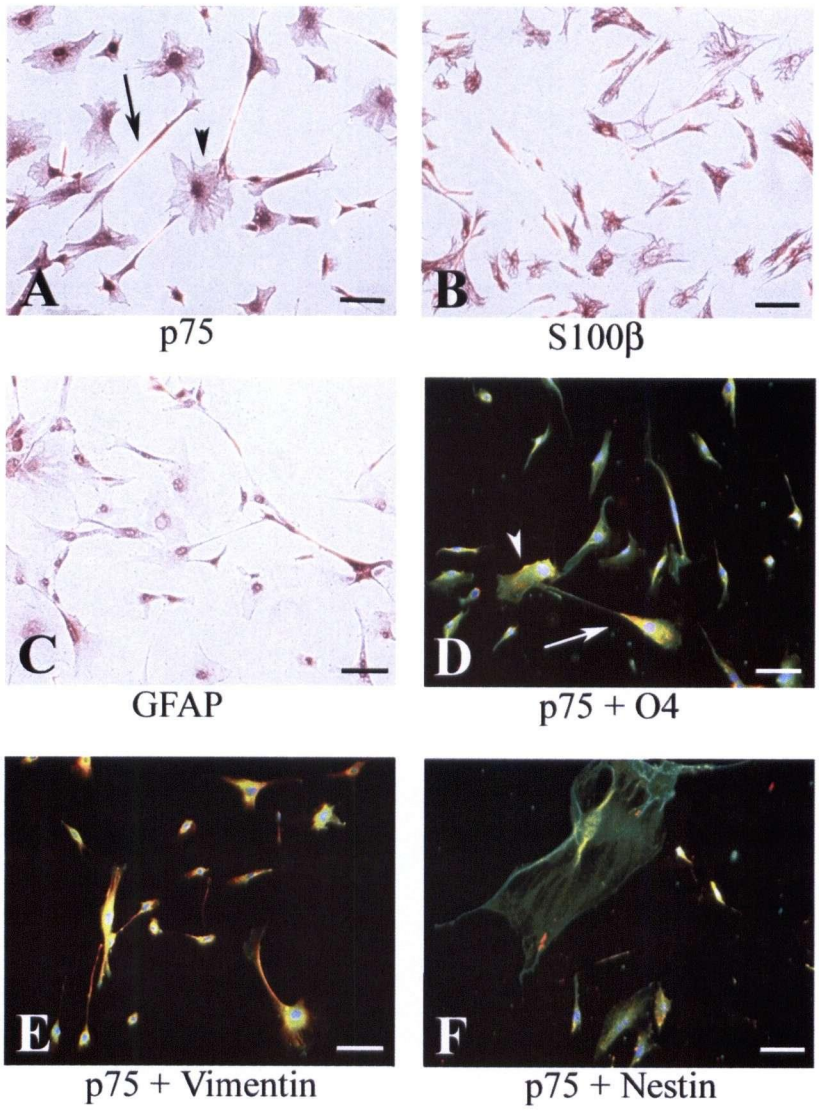

FIGURE 3.2
OECs Purified from the Lamina Propria Express Characteristic Ensheathing Cell Markers In Vitro
When cultured in vitro, lamina propria olfactory ensheathing cells express (A) the low affinity nerve growth factor receptor, p75, (B) S100β and (C) glial fibrillary acidic protein (GFAP) as demonstrated by horseradish peroxidase VIP immunocytochemistry. Cells expressing p75 (green) also co-express the OEC markers (D) O4, (E) vimentin and (F) nestin (all in red). In all cases, cells co-expressing these proteins exhibit both astrocyte-like (A-type, denoted by arrow head) and Schwann cell-like (S-type, denoted by arrow) morphologies (A). Scale bars represent 50 microns.

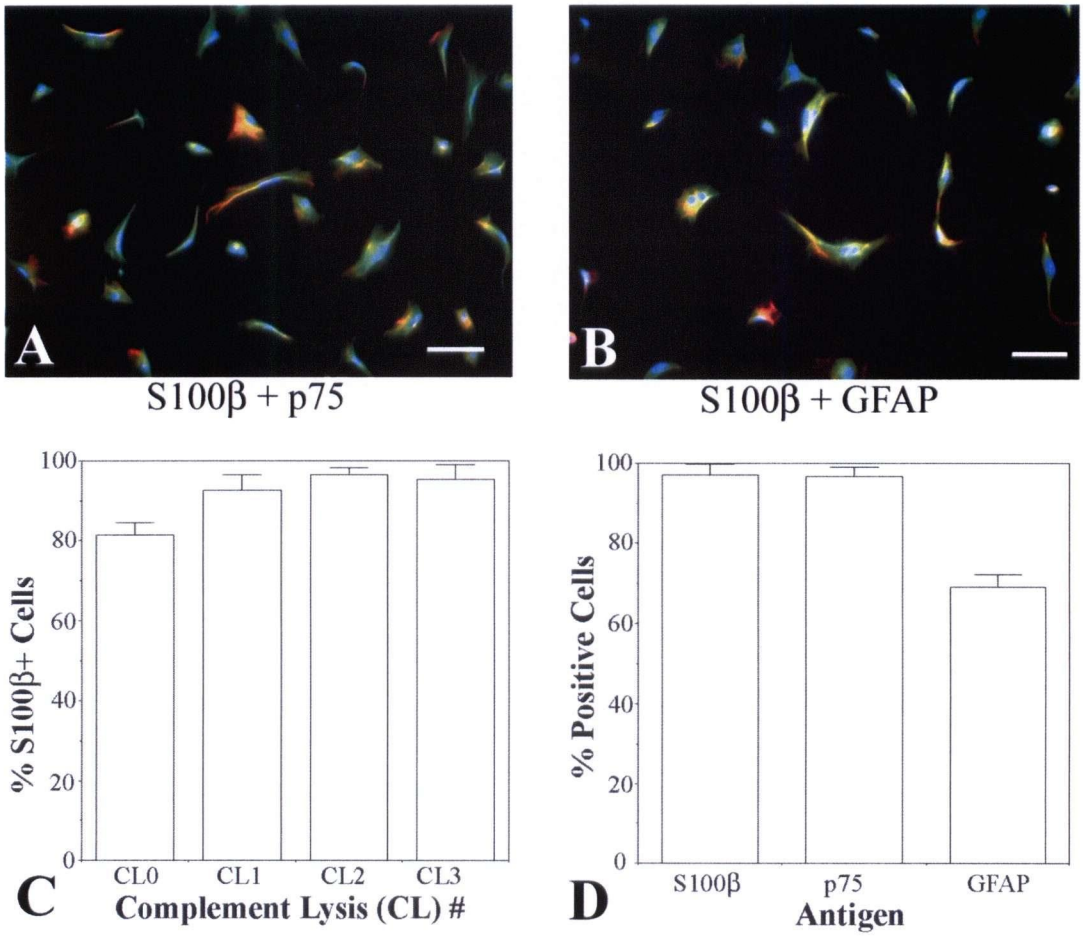

FIGURE 3.3

Purification and Antigenic Characterization of LP-OECs

When plated at 5800 cells/cm, lamina propria-derived olfactory ensheathing cells co-express (A) S100b and p75 and (B) S100β and GFAP. Because S100b exhibited strongest immunoreactivity, it was used to assess (C) the % of S100β-positive glial cells following each complement lysis. (D) Immunoreactivity to S100β, P75 and GFAP was used collectively to assess both the purity of the glial population and the relative % of cells expressing each antigen following the third round of complement lysis. Scale bars represent 50 microns.

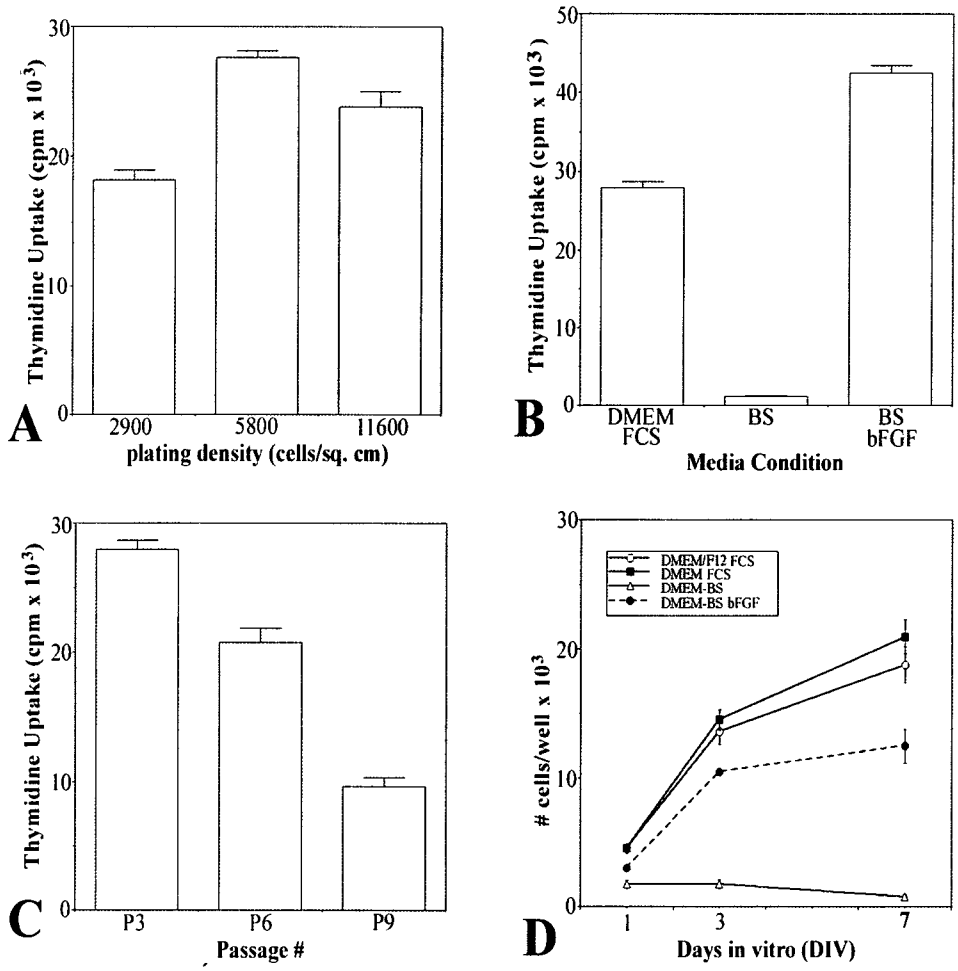

FIGURE 3.4

LP-OECs Demonstrate a Significant Proliferative Capacity

(A) LP-OECs were plated at three successive densities (2900, 5800, 11,600 cells per cm2) and their proliferation capacity measured for 24 hrs using a 3H-thymidine uptake assay. (B) LP-OECs were plated at a standard density of 5800 cells/cm2 in 3 different media conditions: DMEM with 10% FCS, serum-free DMEM-BS and DMEM-BS with basic FGF, and assessed for proliferative capacity over 24 hrs using a thymidine uptake assay. (C) The proliferative capacity of LP-OECs was measured in LP-OECs plated at 5800 cells/cm2 following by measuring thymidine uptake for 24 hrs following passage 3, 6 and 9 of LP-OECs grown in DMEM with 10% FCS. (D) Growth curves of the 3 media conditions tested in B were determined by haemocytometer counts at 1, 3 and 7 days post-plating.

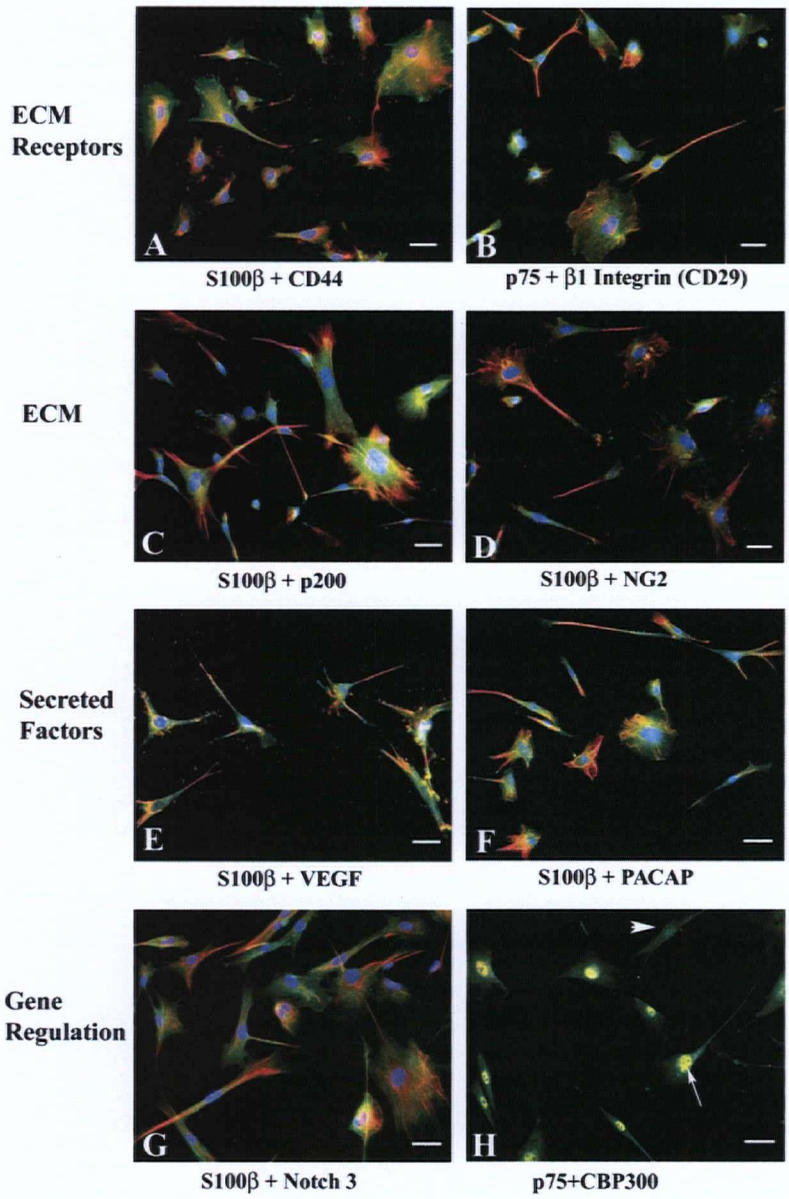

FIGURE 3.5

Novel Proteins Expressed by LP-OECs In Vitro.

LP-OECs were fixed following plating at passage 3 and were examined for the co-expression of the extracellular matrix receptors (A) CD44 (green) with S100β (red) (B) b1 integrin (CD29; red) with p75 (green). LP-OECs also co-expressed the extracellular matrix (ECM) components (C) alpha 4 type V collagen (p200; green) with S100β (red) and (D) NG2 (green) with S100β (red). LP-OECs also co-express the secreted factors (E) vascular endothelial growth factor, (VEGF; green) with S100β (red) and (F) pituitary adenylate cyclase activating polypeptide (PACAP; green) with S100β (red). LP-OECs also co-express the transcriptional regulators (G) Notch 3 (green) with S100β (red) and (H) nuclear expression of the CREB binding protein (p300; red) with p75 (green), found chiefly on the cell surface. Scale bar represents 50 microns.

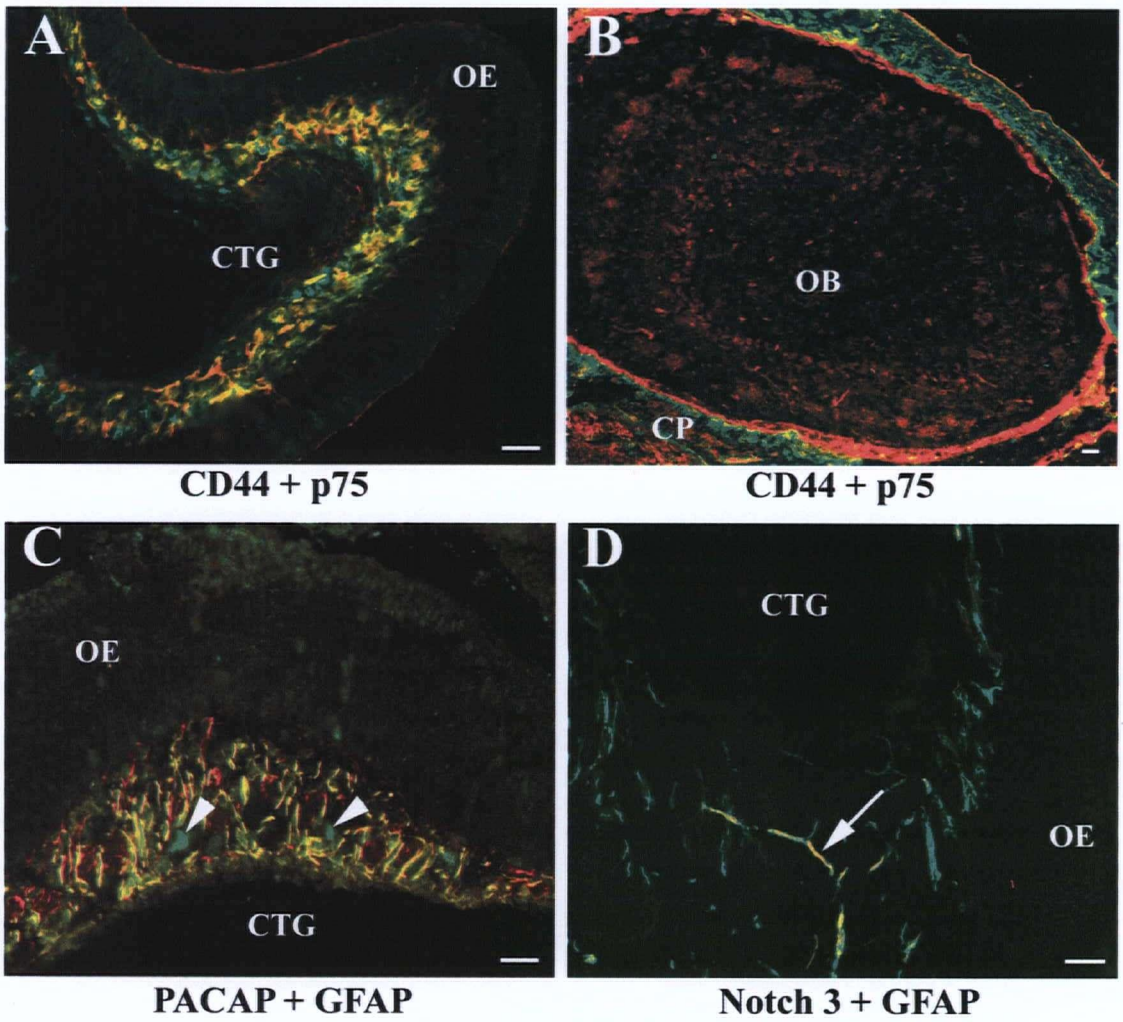

FIGURE 3.6
Novel Markers Expressed by LP-OECs In Vivo
(A) OECs situated in the lamina propria, between the cartilage (Ctg) and the olfactory epithelium (OE), express CD44 (green) and p75 (red). (B) p75 expression (red) could be detected in the olfactory bulb (OB) whereas CD44 (green) could only be detected up to the cribriform plate (CP). (C) LP-OECs also express PACAP (green) and GFAP (red). (C) PACAP signal was also found in ORN nerve bundles (arrow heads). (D) A subpopulation of GFAP (green) positive LP-OECs also expressed Notch 3 (red) (arrow).

TABLE 3.1 OEC Mitogens

Mitogen	Concentration	Reference
bovine pituitary extract	100 ug/ml	Chuah and Au, 1993
		Chuah and Teague, 1999;
FGF-2	10 ng/ml	Yan, Bunge et al, 2001
forskolin	1 uM	Alexander et al, 2002
glial growth factor 2	50 ng/ml	Alexander et al, 2002
heuregulin β1 (HRG β1)	5-50 nM	Yan, Bunge et al, 2001
heuregulin β1 (HRG β1)	50 ng/ml	Alexander et al, 2002
IGF-1	50 ng/ml	Alexander et al, 2002
IGF-1	5 ng/ml	Yan, Bunge et al, 2001
neuregulin-1	1-100 ng/ml	Pollock et al, 1999
	forskolin, FGF-2,	
olfactory mitogen medium	HRG β1	Alexander et al, 2002
PDGF-AA	50 ng/ml	Alexander et al, 2002
PDGF-AA	10 ng/ml	Yan, Bunge et al, 2001

Chapter 4: Assessing Neurite Outgrowth Promotion by Lamina Propria-Derived Olfactory Ensheathing Cells

4.1 Introduction

I have established culture conditions that generate a highly pure population of olfactory ensheathing cells derived from neonate mouse olfactory mucosa (see Chapter 3). This cell population is an ideal model system to study OEC function. The cultures are robust, reproducible and can proliferate sufficiently to generate a sizeable starting material from which to proceed. With this model system in place, I decided to study the mechanisms by which OECs promote axon growth. As reviewed in Chapter 1, OECs appear to play a major role in providing a permissive and promotive environment for ORN axon growth (see section 1.2). On a mechanistic level however, it is poorly understood how this occurs.

4.1.1 Olfactory Ensheathing Cell Interaction with Neurons In Vitro

To study OEC-mediated axon growth, I developed an in vitro model system to study neurite outgrowth. There are several distinct advantages to this type of approach over in vivo analysis: (1) it is a well-defined system where many of the variables can be manipulated to ask different questions. (2) In vitro models can readily accommodate large numbers of replicates and can be set up for rapid analysis. (3) Because of the well-controlled conditions and the number of replicates possible, in vitro systems are well suited to quantitative analysis and comparisons between treatment groups.

Previously, there have been studies examining OEC interactions with neuronal cultures in vitro. Devon and Doucette were the first to examine purified OEC-neuron co-cultures (Devon and Doucette, 1992) and the authors reported OEC myelination of dissociated

embryonic dorsal root ganglion neurons by electron microscopy. A more recent study has questioned whether this myelination might be due to residual Schwann and satellite cell contamination (Plant et al., 2002). Whether OECs can or cannot themselves myelinate axons is controversial (see section 1.2.6.2).

In vitro studies of OEC-ORN interactions reveal ORNs from embryonic OE explants grew preferentially on adult OB-OECs and that the p75-positive subpopulation of cells were the ones responsible for ensheathing the ORN axons (Ramon-Cueto et al., 1993). In a comparison of adult ORN growth on neonate OB-OECs versus astrocytes, better growth was found on OECs and the beginnings of axon ensheathement by OECs after two days (Chuah and Au, 1994). The authors also found that conditioned media from OECs alone did not promote ORN growth. However, they also reported that ORNs would only grow on cell monolayers and not the underlying substrate so it is difficult to interpret the significance of this finding. Conversely, dissociated ORNs from embryonic rats were able to grow neurites on various substrates including poly-L-lysine and laminin (Kafitz and Greer, 1998; Kafitz and Greer, 1999). These two studies report the longest neurite lengths with OEC co-culture or when grown in the presence of OEC conditioned medium. The authors found no significant difference in ORN neurite length between co-culture on an OEC monolayer or in the conditioned medium with both conditions producing greater neurite length than on a laminin substrate.

OECs have also been examined in co-culture with other neuronal populations. Glial cells (not specified or characterized as being OECs) from neonate olfactory bulb promoted greater neurite outgrowth in embryonic dopaminergic projection neurons than astrocytes (Denis-Donini and Estenoz, 1988). OB-OECs increased dendritic density in embryonic cortical neurons either in co-culture or when grown in conditioned media (Le Roux and Reh, 1994). In co-culture, OB-OECs increased retinal ganglion cell frequency for producing neurites. The length of the neurites was not reported, however (Sonigra et al., 1999; Sonigra et al., 1996). Follow up studies from the same group have used the same method for assessing outgrowth (Davies et al., 2004; Hayat et al., 2003a; Hayat et al., 2003b; Kumar et al., 2005) (see sections 1.2.3.2 and 1.2.3.7). OEC conditioned media

was found to promote PC12 cell differentiation and survival (Wang et al., 2003). However, another study found that OEC conditioned media had no effect on peripheral ganglion explant outgrowth even though known neurotrophic factors were detected in OECs by a ribonuclease protection assay (Lipson et al., 2003). In an in vitro model of brain injury, OECs mediated cortical neuron re-growth after a scratch injury to an astrocyte/cortical neuron monolayer (Chung et al., 2004). When OECs were seeded or conditioned media was added following injury, there was increased cortical neuron sprouting at the scratch site. Seeded OECs were found to be more effective than conditioned media.

While these studies do not agree on the efficacy of OEC conditioned media, there is a general consensus that OECs promote neurite outgrowth in vitro. Based on these data, I developed an in vitro model system to study the neurotrophic properties of lamina propria-derived olfactory ensheathing cells.

4.1.2 Neurite Outgrowth Assays

Even within the OEC field, there is a great variety in neurite outgrowth assays employed, each with their advantages and disadvantages. In an ideal system, one would want the following features in a neurite outgrowth assay: (1) the neuronal population would be directly relevant to the question of interest. For example, both Chuah and Au, and Kaftitz and Greer were interested in how OECs mediate ORN growth (Chuah and Au, 1994; Kafitz and Greer, 1998; Kafitz and Greer, 1999) and both assayed ORN primary cultures. The Chuah and Au study used adult ORNs, which were not adherent to the substrate and, according to the authors, neurite length was difficult to assess. Kafitz and Greer had a far more robust ORN culture system derived from embryos. While both groups used ORNs, the adult population, which may be more relevant to the question of how OECs facilitate ORN turnover, appears to be less than ideal as an outgrowth assay. (2) The assay would have a broad sensitivity range so as to detect subtle differences between treatment groups. (3) The neurons would demonstrate robust growth to minimize variability between replicates. (4) The analysis would be simple, comprehensive and rapid, allowing for

accurate measurements of large numbers of assays. This criterion is particularly problematic because simple and rapid analyses often come at the expense of comprehensive and accurate measurement. Careful balance between the two considerations is necessary for an effective neurite outgrowth assay. For example, the Sonigra et al. study assessed retinal ganglion cell neurite outgrowth by only one criteria: whether the neuron was process-bearing or not (Sonigra et al., 1999). While this method allows for more rapid assessment, no information was provided for how long the neurites were and so it was a less comprehensive and informative.

In spite of recent advances in image capture, computer processing speed and imaging software, the methods of quantifying neurite outgrowth remain fundamentally unchanged (reviewed in Connolly, 2001). The process ultimately involves three main stages: (1) Preparing the neurites for visualization, (2) capturing images of the neurites and (3) quantitation and analysis of neurite growth. The process of preparing neurites for visualization broadly varies. Live neurons have been labeled by molecules transported anterogradely down its axon length such as tritiated leucine (Edstrom et al., 1986) and crystallized horseradish peroxidase (Bewick et al., 1991). More recently, neurons have been genetically modified to express fluorescent proteins such as green fluorescent protein and Ds-red (Klimaschewski et al., 2002). Fixed neurons have been labeled by immunocytochemistry of neurite-specific antigens such as PGP 9.5 (Wilson et al., 1988), neurofilament (Fryer et al., 1997) and β-III tubulin (Chakrabortty et al., 2000). With dense neurite outgrowth, as in the case of dorsal root ganglion explants, the neurite can simply be visualized by phase contrast microscopy with darkfield optics (Tonge et al., 1998). Images of the neurites are then commonly captured by a charge-coupled device (CCD) digital camera connected to a computer system with an imaging software suite, which leads to the third phase: data processing and analysis. Computer programs still have difficulty defining the often convoluted and complex shapes of neurites and it is often necessary for the user to define neurites to be analyzed. Many options are available including time lapse imaging of growth cones (Saxod and Bizet, 1988) and morphometric analysis which can quantify neurite length and density by pixel counts and assign shape factors to neuronal soma (Klimaschewski et al., 2002). Another method is to apply

concentric circles on a captured and processed image to measure neurite length and branching at each successive circle (Studer et al., 1994).

4.1.3 Development of a Neurite Outgrowth Assay

4.1.3.1 Embryonic Dorsal Root Ganglia

In order to examine and elucidate the mechanisms of OEC-mediated axon growth, I needed to develop a robust in vitro model system. The model ideally would use a relevant neuronal population that would repeatably give a baseline level of growth, upon which the effect of OECs could be assessed. Preferably, the model would also be modular, flexible and easy to analyze. Ultimately, I wanted to use the model to study how OECs can be better used to mediate regeneration, especially in the context of spinal cord injury. With this in mind, I decided on a neuron population with a wealth of literature and precedent behind it: dorsal root ganglion sensory neurons. The reasoning behind this is that DRGs are simple to grow, grow robustly, there are widely accepted protocols for their culture, and much is known about DRG neurite outgrowth allowing me to change variables in their growth conditions to test various aspects (i.e. good modularity). Also, dorsal root ganglion axons project into the spinal cord and transplantation studies have demonstrated that sensory sprouting is enhanced in the presence of OECs (for example, Ramer et al., 2004a). In vivo spinal cord transplantation studies to validate the in vitro findings can be examined directly by lectin tracing of DRG axons (such as cholera toxin B, wheat germ agglutinin and IB4).

I decided to use an embryonic population of DRGs for two reasons. One, I wanted to maximize the robustness of the assay in order to attain the greatest dynamic range of neurite outgrowth. That is, I wanted to work with the widest range of growth in order to establish the lowest possible baseline condition. With such conditions I hoped to achieve the greatest amount of assay sensitivity. Second, embryonic neurons chosen at the

correct age are dependent on few growth factors. In an assay designed to test for OEC-derived factors that influence neurite outgrowth, it was important to simplify the baseline growth conditions of the neuronal population. With dorsal root ganglion neurons, approximately 80% are NGF-dependent embryonically after E13 (Mu et al., 1993; Ruit et al., 1992) (embryonic day 13). From E10-E13, dorsal root ganglion neurons are predominantly NT-3 dependent in vitro and in vivo (Baudet et al., 2000; McMahon et al., 1994). Thus, by adding NGF alone to embryonic DRG neurons, a large percentage can be expected to survive and grow. This simplifies the parameters of the assay allowing me to examine OEC-mediated neurite outgrowth in a simple, controllable, low background.

The choice of mouse E13.5 for the age of the DRG is partly based on the NT-3 to NGF dependency switch and partly to do with practicality. This particular age is uniquely suitable to dissection of the dorsal root ganglia because the developing vertebral bodies surrounding each DRG have formed enough for the ganglia to pull free along with the spinal cord. And at the same time, a fibrous capsule has yet to form around the ganglion, minimizing fibroblast contamination (Banker, 1998). Also, at both younger and older ages, the dissection of DRGs is not as simple and, as a result, not as clean and repeatable.

4.1.3.2 Outgrowth Assay Configuration

Several different assay systems were explored during the development of the outgrowth model system. Many of these were largely unsuccessful in that they lacked robustness, repeatability or simply did not work. They will be mentioned here only briefly. Initially, I wanted to develop a purely neuronal culture with which to test OEC function. I hoped to dissociate the ganglia and enrich for neurons by size separation using the method of Delree et al. (1989). This method took advantage of the observation that neurons have larger cell bodies (17-100 μm in diameter) and are retained on a 10 μm filter. Using this method, dissociated neurons were plated in a concentrated region, one region per coverslip. It was my intention that the concentrated neuron region would acts a 'pseudo explant': one that did not include fibroblasts and Schwann cells but retained the geometry

of an explant, facilitating quantitation because the neurites would radiate from a single region and their lengths could be assessed all at once.

Dissociated, enriched neuron fractions were plated in several ways, trying to keep them all in small confined area. First, I attempted to plate the neurons into the centre of a glass cylinder, hoping the cells would have had time to settle to the bottom and plate onto the substrate. Several internal diameter glass cylinders were tried and the time allowed for plating down was also varied all without much success. There were problems with surface tension that kept the neurons from settling to the bottom effectively. Second, I attempted to resuspend the neurons in a concentrated slurry of matrigel or collagen gel and plate droplets of the mixture onto collagen-coated coverslips. While the cells were more successful in settling to the bottom, this technique also had technical issues. For one, the neuronal survival was poor unless high concentrations (15 ng/ml) of NGF were added to the matrigel or collagen gel. At this concentration, the neurites grew robustly in the gel and tended to stay within the droplet. I also suspect that the diffusion of nutrients from the media to the gel was not very efficient as the neurons would die over the course of a week. And since their neurites rarely exited the droplet, retrograde uptake of NGF from the media was minimal. I did not fully explore the underlying reasons why the culture conditions were unsuccessful largely because I deemed the starting point too inconsistent to be worth further pursuit.

After working through various 'pseudo explant' models, none of which displayed the robustness and repeatability I wanted in a neurite outgrowth assay, I decided to go with a straightforward DRG explant. I initially considered using AraC to kill off the dividing cells but decided against it. First, it gave me the freedom to test the effect of OECs on Schwann cells and if I so chose, I would simply eliminate the Schwann cells to test the effect on the neurites themselves. Secondly, in the context of the question I was interested in, namely how OECs mediate axon growth in the spinal cord and the olfactory system, glial cells are present in the vivo environment. There is good evidence that Schwann cells are present at the spinal cord lesion when OECs are transplanted (Boyd et al., 2004; Ramer et al., 2004a; Ruitenberg et al., 2003; Sasaki et al., 2004; Takami et al.,

2002) (see section 1.2.6.1.2 for more details). Therefore, it was biologically relevant to keep the dividing cells in the baseline conditions.

4.2 Results

4.2.1 Quantitation of Neurite Outgrowth

In order to work out the best method for quantifying neurite outgrowth, I generated a series of DRG explants grown in increasing concentrations of NGF – a dose response curve. The NGF concentration varied from 1 ng/ml to 20 ng/ml with 4 replicates per condition. NGF acted as a positive control with increasing concentrations of NGF resulting in increasing neurite outgrowth. Four quantitative methods were assessed for their sensitivity to differences in NGF concentration (see figure 4.1). The explants were labelled with anti-neurofilament antibody and detected by fluorescent secondary. All of the quantitative methods measured the same explants, which were canvassed and montaged at 200X magnification (see section 2.4.3).

(1) In the first method (see figure 4.1A), I defined the region to be ignored by the computer (the ganglion itself). The neurite carpet was processed by an eight-direction regression algorithm, which reduced the signal to 1 pixel width, a process known as skeletonization (for a more detailed image of an explant after skeletonization, see Appendix 1). The total pixel number was counted with a minimum cut-off to screen out background signal. The total pixel count was then converted to microns to give the total outgrowth from the entire explant. (2) In the second method (see figure 4.1B), I defined the centre of the explant and drew a polygon around the outside edge of the neurite carpet. A computer program calculated the radius from hundreds of evenly spaced points along the polygon from the defined soma (ganglion) centre. These radii are averaged to give the average total radius. A second average radius is taken by drawing another

polygon around the outside edge of the soma. A similar average radius is determined. The average total radius is subtracted from the average soma radius to give the average neurite radius. (3) The third method measured the surface area of the axon carpet (see figure 4.1C). The whole explant was selected and then the soma was subtracted from the selection. The total pixels within the selection were converted to μm^2. (4) In the fourth method (see figure 4.1D) as in the third method, the explant was selected and the soma was excluded. The signal within the neurite carpet was then binned into four sections based on intensity. The top three bins were taken as being above background and measured in pixels. This effectively measures the total number of pixels represented by the neurite carpet. More details on the quantitation methods 3 and 4 can be found in the Appendix (see Appendix 2 and 3).

4.2.2.1 Cross-Comparison of the Four Different Methods of Quantitation

Neurite outgrowth was quantified using the four methods described above (see section 4.2.1.3). Using a linear Y-axis, the data is represented in figure 4.2. 4.2A shows quantitation by skeletonization (see figure 4.1A and figure 4.2A), 4.2B shows average neurite radius (see figure 4.1B and 4.2B), C shows neurite carpet surface area (see figure 4.1C and 4.1C) and D shows neurite signal (see figure 4.1D and 4.2D). All graphs were fit to natural log curves. The formula and R^2 value for each curve is also displayed. In the low range of NGF (1ng/ml to 5 ng/ml), there are noticeable differences between the methods. In 4.2A, there is fairly even separation between 1, 2.5, 5 and 10 ng/ml. This is in contrast to 4.2D where the method appears to be less sensitive at low ranges of NGF. Also 4.2A appears to have the least overlap in error bars (representing standard error of the mean) compared with the other quantitation methods. ANOVA is an indication of the quantitation method's ability to discern differences in outgrowth between NGF concentrations. By single variable ANOVA analysis, the p values for the four methods were: skeletonization (p=0.003398191), radius (p=0.036618973), surface area (p=0.0274756) and neurite signal (p=0.000234). Therefore by ANOVA, neurite signal and skeletonization, with the smallest p values, were the most sensitive quantitation

methods. This observation is further confirmed by plotting data for all four methods on the same graph after taking the natural log of each y value (figure 4.3). Each dataset was fit to a best-fit line. The slope of each line is an indication of the sensitivity of each method. Once again, both skeletonization (m=0.305) and neurite signal (m=0.415) had the steepest slopes. Next, I binned the natural log data points into three categories: low- (1-5 ng/ml NGF; figure 4.4A), mid- (2.5-10 ng/ml NGF; figure 4.4B) and high- (10-20 ng/ml NGF; figure 4.4C) range NGF. Best-fit lines were applied to each binned data set (figure 4.4). By this analysis as well, skeletonization and neurite signal had the steepest slopes in low and midrange. At high range, there was little difference between the four methods reflecting the fact that NGF-induced growth plateaus in this range (more clearly seen in figure 4.2). At the low range of NGF (figure 4.4A), the slope was slightly steeper for the skeletonization method (m=0.554) than neurite signal (m=0.479). The trend was reversed in the midrange of NGF (figure 4.4B) with neurite signal (m=0.446) having a steeper slope than skeletonization (m=0.394). Thus, it is possible that between the two methods, skeletonization may be more sensitive at low ranges whereas quantifying neurite signal has a broader dynamic range. This makes sense because skeletonization underestimates dense neurite growth, as large fascicles of neurites will be reduced to one pixel width. In contrast, with total neurite signal, all pixels are counted. Therefore a more conservative estimate of OEC-mediated neurite outgrowth will be measured using skeletonization.

Choosing between total neurite signal and skeletonization, I decided to quantify my outgrowth assay using the skeletonization method. I did so for two reasons: One, skeletonization gives a concrete measurement (total neurite length) of outgrowth whereas neurite signal gives pixels. An increase in pixel count can be interpreted as thicker neurites or longer neurites. With skeletonization, length is the only measurement and is the more conservative method so it more stringently assays the effect of OECs on neurite outgrowth. However, I did not discount the value of the average neurite radius method. It can provide an added dimension of information not provided by total neurite outgrowth. Average neurite radius was also used to complement the skeletonization data for some of the conditions tested.

4.2.3 Co-Culture of Dorsal Root Ganglion Explants with OEC Monolayers

As a preliminary test of LP-OEC mediated neurite outgrowth, dorsal root ganglion explants were plated directly onto LP-OEC monolayers. The assay ran for 48 hours after which time the co-culture was fixed with paraformaldehyde and labeled with anti-neurofilament antibody. The explant was then imaged and montaged and the outgrowth quantified by skeletonization (figure 4.1A). Representative images to scale are shown in figure 4.5A and B. LP-OEC co-culture (figure 4.5B) greatly increases neurite outgrowth versus baseline conditions (figure 4.5A). The quantified total outgrowth is shown in figure 4.5C. In co-culture with an LP-OEC monolayer, approximately 3 times as much total growth is measured (166682 μm for co-culture versus 52632 μm for baseline NGF condition). These findings agree with other studies that also demonstrate OEC-mediated neurite outgrowth in co-culture with neurons (reviewed in section 4.1.1).

4.2.4 Experimental Rationale

The co-culture of LP-OECs with DRG explants provided a proof-of-principle that this model system could be used to study OEC mechanisms of axon growth. However, a co-culture system is complex and almost certainly multifactorial. Also, there could be feedback communication between the OECs and the neurites, further complicating analysis. The system required further simplification in order to isolate and identify individual mechanisms. Several general hypotheses were considered as to how OECs mediate axon growth (diagrammed schematically in figure 4.6). The first possibility is that OECs express cell surface factors to which axons preferentially adhere. Their preferential adherence may activate intracellular pathways that drive neurite extension (figure 4.5A). A second possibility is that OECs secrete factors that are received by the neurites, which then transduce pathways leading to neurite extension (figure 4.6B). The third possibility is that OECs secrete factors, which bind to the substrate, such as an ECM

molecule. The secreted molecules then act as a preferred substrate for neurites and may also activate intracellular pathways that drive neurite extension (figure 4.6C).

For this study, hypotheses two and three were chosen for a purely practical reason: It is much more difficult to assay the cell surface factors expressed by OECs in a controlled manner. This is because cell surface factors are anchored to the cell membrane, introducing three difficult problems: (1) it could be difficult to store and normalize samples of OEC plasma membranes due to its hydrophobic nature. (2) Adding the plasma membrane fraction of OECs to the neurite outgrowth assay means that, statistically, half of the membrane fragments will be inside out and biologically inactive. (3) To further complicate the problem, cell surface factors may require a unique spatial context in order to function biologically. That is, a protein embedded in a membrane may require clustering of several other factors in order to mediate neurite outgrowth.

In contrast, OEC secreted molecules, whether they act directly on neurites (figure 4.6B) or indirectly as a preferred substrate (figure 4.6C), can easily be isolated by harvesting the conditioned media from LP-OEC cultures. The media can be normalized to the number of cells generating a given volume making it easy to add controlled doses of conditioned media back to the outgrowth assay. The potential drawback to this approach is that there are conflicting findings concerning the bioactivity of OB-OEC conditioned media (section 4.1.1). However, no data have been reported about the outgrowth promoting properties of LP-OECs and I have already demonstrated that in a co-culture, LP-OECs robustly promote DRG outgrowth (figure 4.6). Given the potential upside for analyzing OEC secreted factors over cell surface factors, the bioactivity of LP-OEC conditioned media was tested.

The purpose of my study, however, was not only to test if LP-OECs promote neurite outgrowth but also to use them as a model system to elucidate mechanisms. Therefore, instead of just testing whether LP-OEC conditioned media promoted outgrowth, a more prospective approach was taken. An assumption was made that LP-OEC conditioned media (LP-OCM) would be neurotrophic and it was anticipated that a detailed analysis of

the constituents of LP-OCM would be necessary to infer mechanism; But a major stumbling block would be the analysis of LP-OCM, more specifically generating a short list of candidate factors with which to validate function. Thus, instead of generating one sample of conditioned media, two different samples were generated (passage 2 and passage 6 LP-OEC conditioned media). Ideally, I wanted to have two samples that were very similar to one another (to simplify analysis) but distinct in terms of their biological activity. That way I could focus on the constituents that were different between the two samples with the rationale that they were likely responsible for the difference in biological activities. Therefore, assuming that LP-OCM indeed promotes neurite outgrowth and that variants of LP-OCM with different biological activities could be generated, here was a way to meaningfully elucidate mechanisms of OEC-mediated axon growth.

4.2.5 LP-OEC Conditioned Media Samples

To try and simplify the analysis, ideally the conditioned media samples would be very similar to one another. This could be accomplished by changing how the LP-OECs are cultured prior to harvesting their conditioned media. I did not want to change the culture conditions drastically because this could introduce unwanted variables such as affecting the general health of the cells. I also could not add factors to the media that could not be removed prior to assaying the outgrowth activity otherwise, the factor itself could confound the results. Finally, I wanted to generate repeatable libraries of conditioned media so I needed a simple, repeatable method of changing culture conditions to reduce variability between batches of LP-OCM.

With these considerations, an observation while characterizing the LP-OECs proved particularly useful: As the cells are successively passaged, their proliferative capacity diminishes (figure 3.4C). The hypothesis was that as the cells lose their proliferative capacity and senesce in culture, the biological activity of their conditioned media would also diminish. This is a simple way to generate two forms of LP-OCM from the same

primary preparation in a controlled and reproducible manner. The samples should be very similar because I would only be analyzing secreted factors produced by the same cell population grown for different amounts of time in culture. I proceeded to work out conditions for generating conditioned media from early passage and late passage cells (schematically represented in figure 4.7) and chose passage 2 for the early passage media based on my purification data for the LP-OECs. It was demonstrated that the cell purity based on S100β antigenicity plateaus by the second round of complement-mediated cell lysis (figure 3.3C). Thus, passage 2 was the earliest time point when I was confident that the cells were of high purity. Passage 6 was chosen as my late passage time point. Originally, I had wanted to use passage 9 LP-OECs but there were concerns about their overall health when grown in serum-free conditions (figure 4.7). Also by passage 6, as shown in figure 3.4C, the proliferative capacity of the cells is significantly diminished compared to passage 3.

4.2.6 Early Versus Late Passage Conditioned Media

Conditioned media from OECs was harvested and the number of cells generating the media was counted. Abitrarily, full strength conditioned media was taken to be 30 000 cells generating 1 ml of conditioned media. In this way, I could normalize between batches of conditioned media and also between passage 2 and passage 6 LP-OCM. This was important because as the cells aged in culture, they became larger and grew less densely, therefore normalizing media by volume alone would bias towards passage 2 LP-OCM. Representative montages of DRGs grown in NGF baseline alone or supplemented with full strength passage 2 conditioned media are shown in figure 4.8A and B. The total outgrowth quantified by skeletonization is shown in figure 4.8C. Passage 2 LP-OCM (P2 LP-OCM, green) was added at full strength (1:1) and at lower concentrations (1:2, 1:4, etc.) to NGF baseline conditions and the outgrowth is compared with NGF baseline (blue) and heat denatured P2 LP-OCM control (red). In a dose-dependent fashion, passage 2 conditioned media increases neurite outgrowth to a maximum of 155315 μm total growth which is nearly three-fold more than baseline NGF (52632 μm). It required

diluting the P2 LP-OCM 1:40 before the outgrowth effect was no longer statistically significant. The heat-denatured control had very little outgrowth (11321 μm) so it appears that boiled P2 LP-OCM was actually deleterious to outgrowth, likely due to heat precipitated proteins. As a further control, DMEM-Bottenstein Sato (the baseline serum-free media with which LP-OEC conditioned media was generated, see section 2.6 for more details DMEM-BS constituents and how LP-OCM was generated) components were added to NGF baseline conditions. No effect on outgrowth was detected and the data were added to the rest of the NGF baseline dataset.

Passage 6 LP-OCM was added to NGF baseline conditions. Representative montages of DRGs grown in NGF baseline and P6 LP-OCM at 1:1 concentration are shown in figure 4.9A and B. The total outgrowth of the various conditions assessed by skeletonization is shown in figure 4.9C. P6 LP-OCM (purple) was added at various concentrations from 1:1 (full strength) to 1:4 (one quarter strength). Full strength (1:1; 104502 μm) and half strength (1:2; 76656 μm) P6 LP-OCM both increased neurite outgrowth over NGF baseline conditions (blue). However, by 1:4 concentration (34497 μm), P6 LP-OCM neurite outgrowth was statistically indistinguishable from baseline; in fact, its mean was considerably less than baseline.

The difference between passage 2 and passage 6 LP-OCM is highlighted in figure 4.10. Again, total outgrowth by skeletonization is shown in both 4.10A and 4.10B. While P2 LP-OCM (green) needed to be diluted to 1:40 before the outgrowth activity was statistically insignificant compared to baseline, P6 LP-OCM (purple) needed only be diluted 1:4. While it appears that full strength P2 LP-OCM is considerably more effective than full strength P6 LP-OCM, the difference is not statistically significant (figure 4.10B). There is a statistically significant difference at the lower concentrations, 1:2 and 1:4 however. Figure 4.10B also highlights how much more dilute P2 LP-OCM can be before its outgrowth activity is no longer detectable, as represented by baseline NGF (blue stripe).

4.2.7 LP-OEC Mediated Neurite Outgrowth Summary

LP-OECs can promote the growth of dorsal root ganglion explants in co-culture and when grown in conditioned media. A summary of all of the total outgrowth data is shown in figure 4.11. There is a clear difference in the biological activity between early and late passage conditioned media. Thus the two samples are suitable for ICAT analysis to try and find the protein factor(s) responsible for the discrepancy in biological activity. However, the outgrowth found in P2 LP-OCM 1:1 versus co-culture with an LP-OECs monolayer is somewhat deceptive. While by skeletonization, the total amount outgrowth is similar between the two groups; there is a significant difference in neurite length. Figure 4.12 shows the average neurite radius between NGF baseline (blue), P6 LP-OCM 1:1 (purple), P2 LP-OCM 1:1 (green) and co-culture with LP-OEC monolayer (orange). Here the difference between P2 LP-OCM and co-culture is clearly illustrated. In fact, the difference in neurite radius between P2 LP-OCM and NGF baseline is only just statistically significant ($p=0.0216$). Also, in the co-culture group, the DRG neurites are highly fasciculated (compare figure 4.5B and 4.8B). As I made reference to earlier, skeletonization will underestimate highly fasciculated explants (section 4.2.1.4).

4.3 Discussion

I have developed an in vitro assay to quantify LP-OEC mediated neurite outgrowth. The assay itself is highly dependent on its repeatability and sensitivity. With respect to repeatability, the baseline values can fluctuate to a degree. Baseline NGF conditions are 1.5 ng/ml and the mean is 52633 μm. Comparing this mean with figure 4.2A, one can see that there is some degree of variability (1 ng/ml measured 66612 μm total growth). That value, however, was determined with only four replicates whereas NGF baseline values were determined with 30 replicates, n=6 (see table 2.2 for a summary of replicates and n). In an attempt to minimize variation, I used the same six DRGs for each outgrowth assay – lumbar DRG 2-4 on both sides. Slight differences in dissection and culturing conditions from assay to assay and the stochastic nature of neurite outgrowth

probably accounts for any remaining variability. The degree of variability does not however invalidate the outgrowth observed when co-cultured with LP-OECs or grown in P2 or P6 LP-OCM. Nor does it invalidate the difference in biological activity observed between P2 and P6 LP-OCM. The statistical analysis between the groups clearly shows a difference in outgrowth.

A comparison of figure 4.11 and 4.12 highlights the deficiencies of the skeletonization method. Total outgrowth can be informative but it does not paint a complete picture of LP-OEC mediated outgrowth. However, in terms of sensitivity, this quantitation method was shown to be quite effective (section 4.2.1.3). Skeletonization can more distinctly discern the difference between P2 LP-OCM and NGF baseline levels (compare figure 4.11 with 4.12). If neurite radius was the only measure of outgrowth used, I may well have concluded that LP-OCM had only a marginal effect on neurite outgrowth. I may also have concluded that there was a negligible difference in biological activity between P2 and P6 LP-OCM. This may explain why Lipson and coworkers did not find a noticeable effect with OEC conditioned media on sensory or autonomic ganglion explants (Lipson et al., 2003).

The difference in outgrowth promotion between LP-OCM and LP-OEC co-culture bears extra commentary. There is a striking difference in neurite radius when DRG explants are grown on LP-OEC monolayers (figure 4.12). Neurites are fasciculated and grow straight and long. This is likely due to OEC cell surface interactions with DRG neurites as has been reported previously (Devon and Doucette, 1992). In conditioned media a similar level of total outgrowth was measured (figure 4.11). While there may have been slightly more fasciculation of neurites over NGF baseline, the most obvious difference was the density of the neurite carpet. This density difference rather than neurite radius had the largest effect on the measured increase in total outgrowth. In this chapter I have not examined whether the increased neurite density arises from increased neuronal survival or increased neurite branching. To a certain degree, I address this in the next chapter (see section 5.2.7). As an additional comment on survival, I have attempted to grow DRG explants in LP-OCM without NGF. No DRG explants survived under these

conditions. The explants appear to be dependent on NGF for survival and any NGF that may be present in the conditioned media was insufficient for DRG survival and growth. I also found that to a limited degree NT-3 could also support the growth of DRGs at this stage. Perhaps, a similar conclusion can also be drawn about the presence of NT-3 in LP-OCM.

The difference in biological activity between passage 2 and passage 6 conditioned media is interesting. There are several possible explanations as to how this could be taking place. (1) There are more kinds of neurotrophic factors present in P2 LP-OCM than P6 LP-OCM. With additional factors present, P2 LP-OCM has different dose response curves and can support increased outgrowth at lower concentrations than P6 LP-OCM. (2) Both LP-OCM types have the same complement of neurotrophic factors but P6 LP-OCM contains more kinds or higher levels of an outgrowth inhibitor. Thus, at lower concentrations, the inhibitory effect overtakes the neurotrophic activity. This would certainly account for the below baseline mean of 1:4 P6 LP-OCM (figure 4.9). (3) Perhaps the simplest explanation, P2 and P6 LP-OCM have the same complement of neurotrophic factors but P2 LP-OCM contains higher levels of them leading to a more effective dose response curve. Likely, the effect of the conditioned media is multifactorial with promoters and inhibitors of outgrowth at play. With a clear difference in biological activity and ostensibly a high similarity between the two LP-OCM types, I decided that these samples were suitable for further analysis to identify key secreted factors that may underlie the biological activity.

Finally, these data underscore the importance of how LP-OECs are cultured and the potential effect that this could have on their ability to promote growth. I reviewed previously that there is a great deal of heterogeneity in how the OECs are prepared, expanded and harvested for transplantation studies (section 3.1.2). With just a difference of four passages, I have demonstrated a quantifiable difference in the biological activity of LP-OECs. Perhaps the differences in culture conditions used by various groups can help to account for the differences in their findings. This also demonstrates the need for

standardization in the OEC field and careful characterization of the cells themselves prior to experimentation.

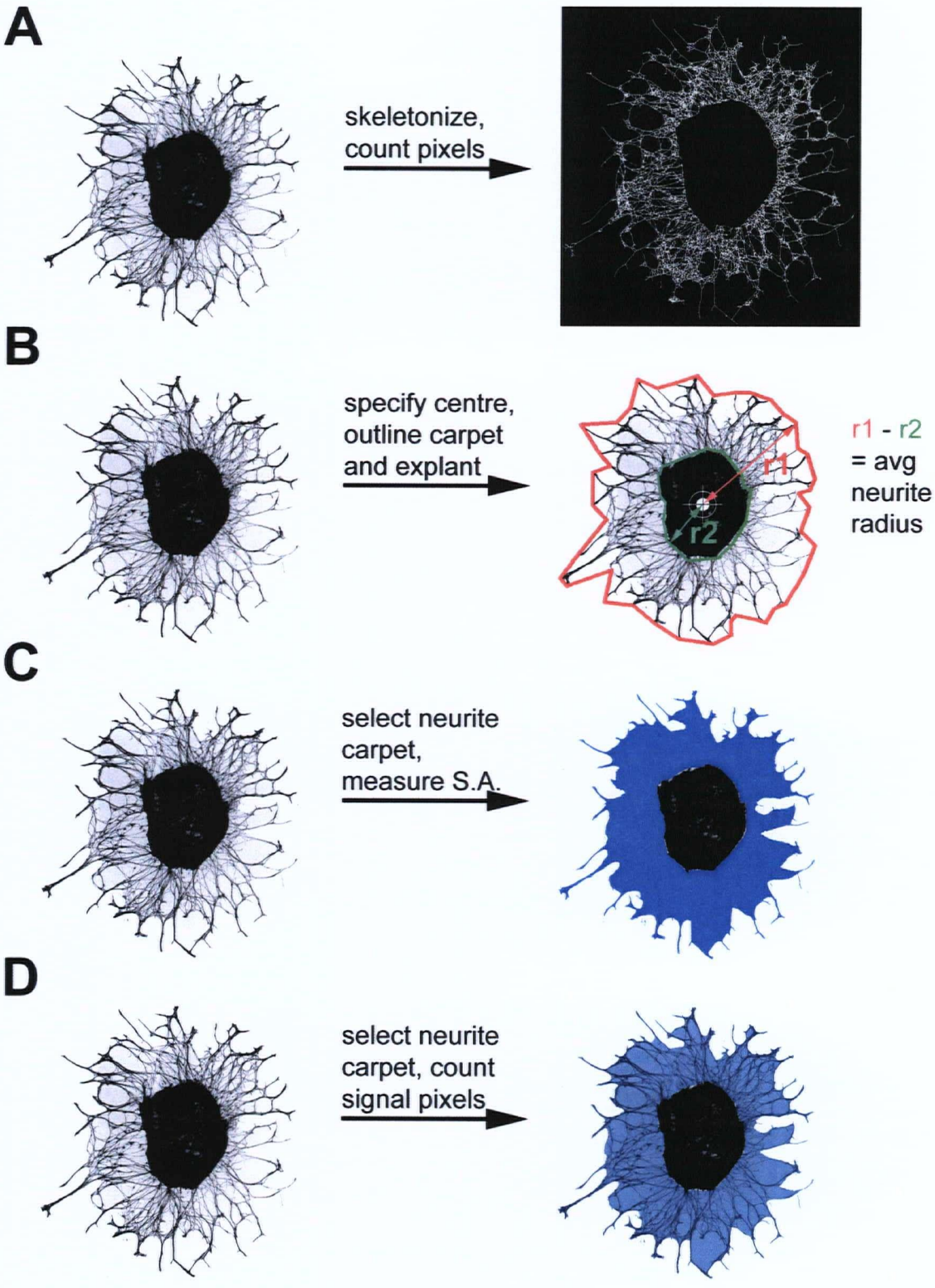
A
skeletonize,
count pixels
B
specify centre,
outline carpet
and explant
r1
r2
r1 - r2
= avg
neurite
radius
C
select neurite
carpet,
measure S.A.
D
select neurite
carpet, count
signal pixels

FIGURE 4.1

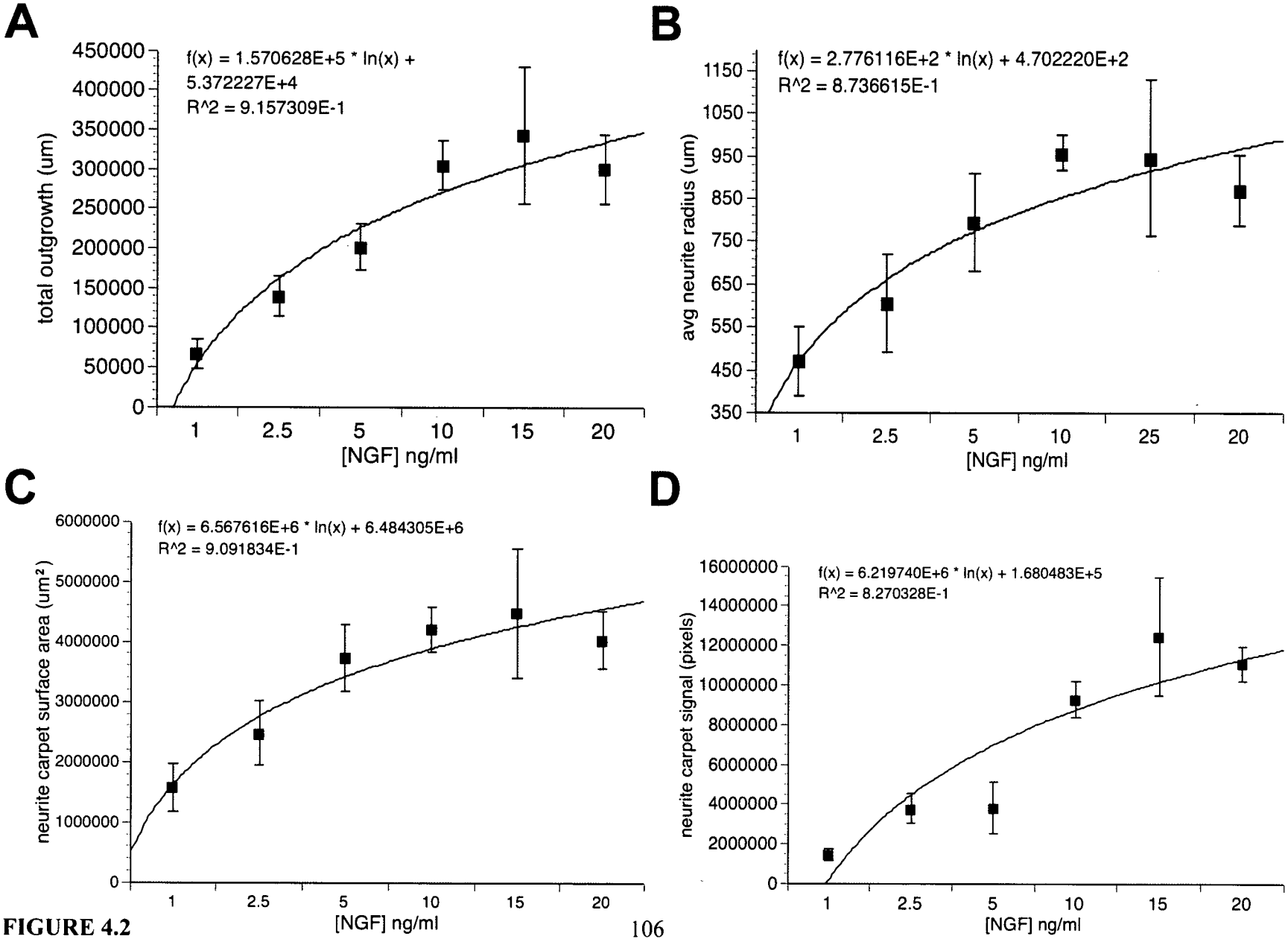
A
f(x) = 1.570628E+5 * ln(x) + 5.372227E+4
R^2 = 9.157309E-1
total outgrowth (um)
450000
400000
350000
300000
250000
200000
150000
100000
50000
0
1
2.5
5
10
15
20
[NGF] ng/ml
B
f(x) = 2.776116E+2 * ln(x) + 4.702220E+2
R^2 = 8.736615E-1
avg neurite radius (um)
1150
1050
950
850
750
650
550
450
350
1
2.5
5
10
25
20
[NGF] ng/ml
C
f(x) = 6.567616E+6 * ln(x) + 6.484305E+6
R^2 = 9.091834E-1
neurite carpet surface area (um²)
6000000
5000000
4000000
3000000
2000000
1000000
0
1
2.5
5
10
15
20
[NGF] ng/ml
D
f(x) = 6.219740E+6 * ln(x) + 1.680483E+5
R^2 = 8.270328E-1
neurite carpet signal (pixels)
16000000
14000000
12000000
10000000
8000000
6000000
4000000
2000000
0
1
2.5
5
10
15
20
[NGF] ng/ml

FIGURE 4.2

FIGURE 4.2
NGF Dose Response Curve Quantified by Four Different Methods
Embryonic dorsal root ganglion explants grown in increasing concentrations of nerve growth factor. Neurite outgrowth is assessed by four quantitative methods. Data fit to best-fit natural log line. (A) Skeletonization of explant excluding cell bodies, total pixels converted to microns. (B) Average neurite radius measured in microns. (C) Neurite carpet surface area measured in μm^2. (D) Total signal of neurite carpet measured in pixels.

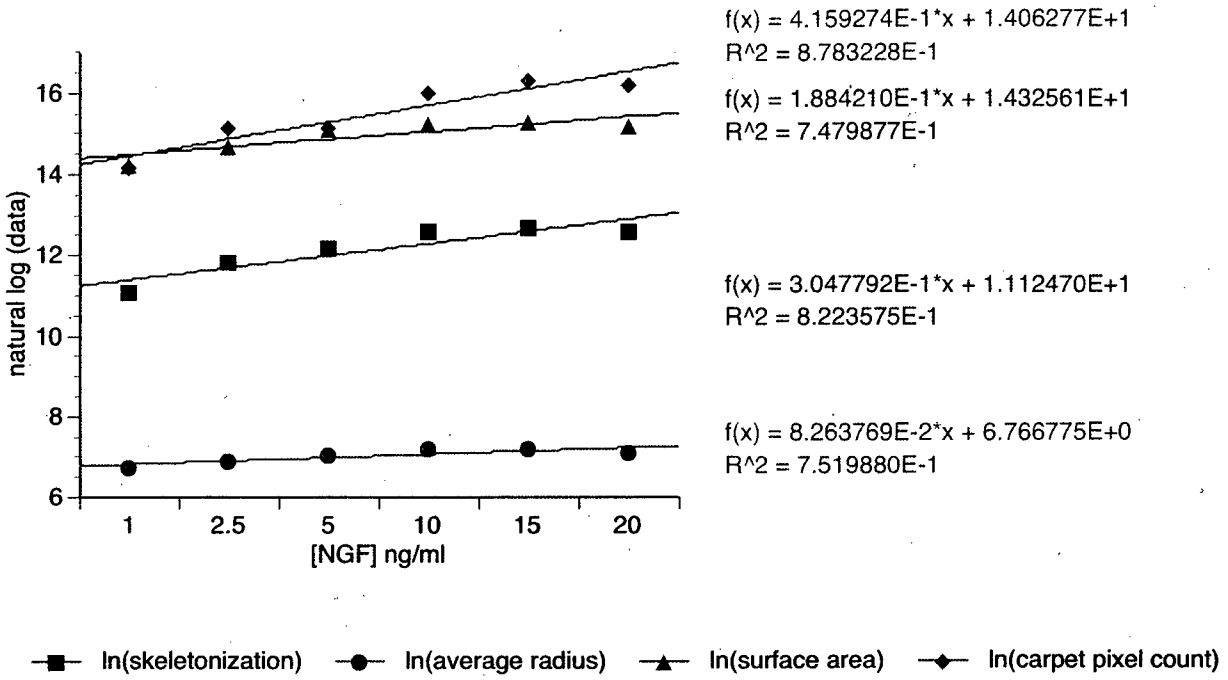

FIGURE 4.3

Natural log of NGF Dose Response Curve Quantified by Four Different Methods

Natural log of data from figure 4.4 re-plotted on a single graph. Skeletonization analysis in blue, average neurite radius in red, neurite carpet suface area in green, neurite carpet total signal in purple.

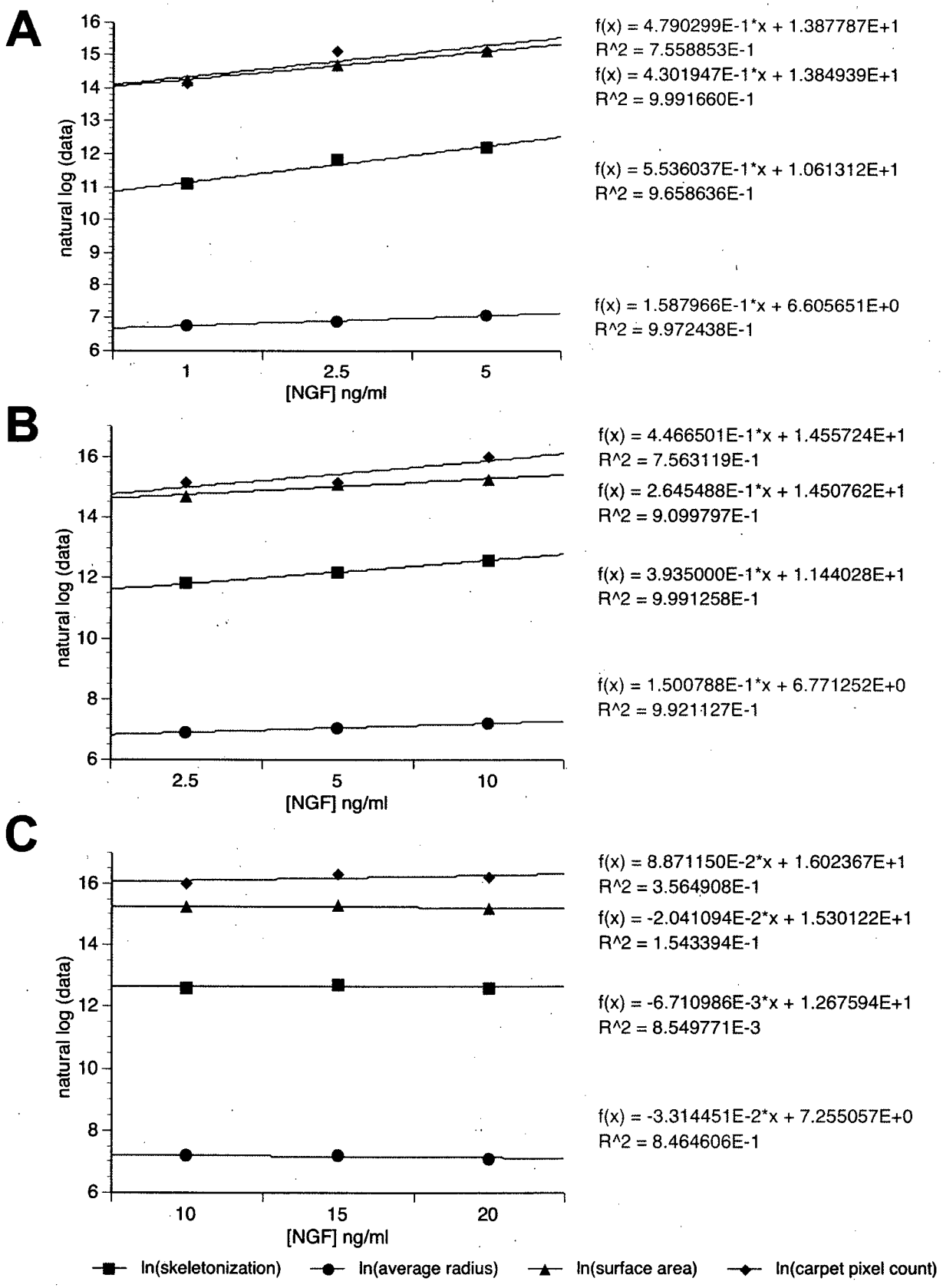
A
16
15
14
13
12
11
10
9
8
7
6
natural log (data)
1
2.5
5
[NGF] ng/ml
f(x) = 4.790299E-1*x + 1.387787E+1
R^2 = 7.558853E-1
f(x) = 4.301947E-1*x + 1.384939E+1
R^2 = 9.991660E-1
f(x) = 5.536037E-1*x + 1.061312E+1
R^2 = 9.658636E-1
f(x) = 1.587966E-1*x + 6.605651E+0
R^2 = 9.972438E-1
B
16
14
12
10
8
6
natural log (data)
2.5
5
10
[NGF] ng/ml
f(x) = 4.466501E-1*x + 1.455724E+1
R^2 = 7.563119E-1
f(x) = 2.645488E-1*x + 1.450762E+1
R^2 = 9.099797E-1
f(x) = 3.935000E-1*x + 1.144028E+1
R^2 = 9.991258E-1
f(x) = 1.500788E-1*x + 6.771252E+0
R^2 = 9.921127E-1
C
16
14
12
10
8
6
natural log (data)
10
15
20
[NGF] ng/ml
f(x) = 8.871150E-2*x + 1.602367E+1
R^2 = 3.564908E-1
f(x) = -2.041094E-2*x + 1.530122E+1
R^2 = 1.543394E-1
f(x) = -6.710986E-3*x + 1.267594E+1
R^2 = 8.549771E-3
f(x) = -3.314451E-2*x + 7.255057E+0
R^2 = 8.464606E-1
ln(skeletonization)
ln(average radius)
ln(surface area)
ln(carpet pixel count)

FIGURE 4.4

FIGURE 4.4
Natural log of NGF Dose Response Curve Quantified by Four Different Methods Bracketed into Low-, Mid- and High-Range
Natural log of data from figure 4.2. (A) showing only the low range (1-5 ng/ml) of NGF, (B) showing only the mid range (2.5-10 ng/ml) of NGF and (C) showing only the high range (10-20 ng/ml) of NGF. Skeletonization analysis in blue, average neurite radius in red, neurite carpet suface area in green, neurite carpet total signal in purple.

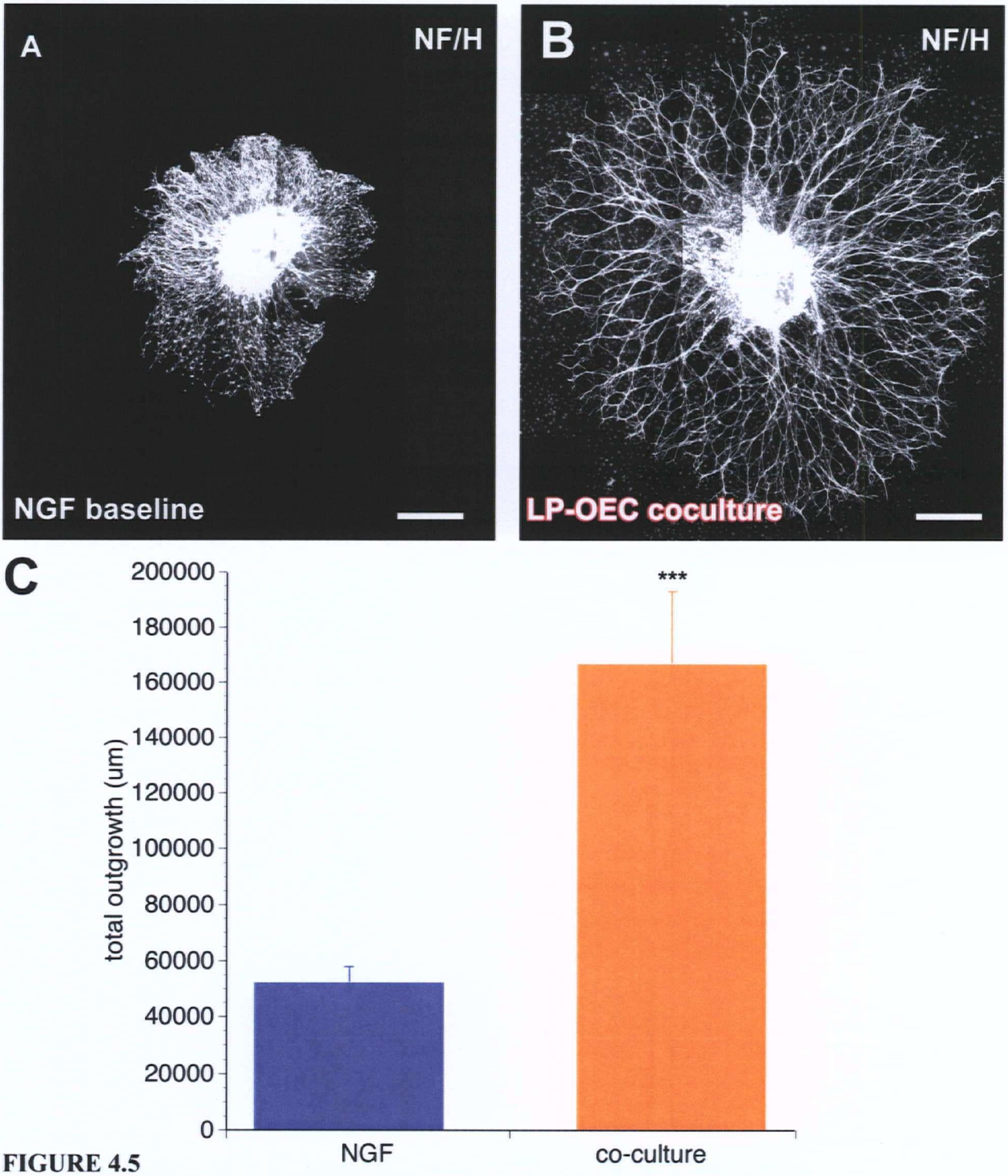

FIGURE 4.5

Comparison of Baseline NGF conditions with Co-culture with LP-OECs

Embryonic DRG explants were cultured in baseline NGF (1.5 ng/ml) on (A) poly-L-lysine/laminin substrate or (B) on poly-L-lysine/ laminin with a monolayer of LP-OECs and labeled with neurofilament heavy chain antibody (NF/H). (C) Total outgrowth quantified for baseline NGF (blue) and LP-OEC co-culture (orange). Scalebar represents 500 microns. Asterisks: * is $p < 0.05$; * is $p < 0.005$; *** is $p < 0.0005$.

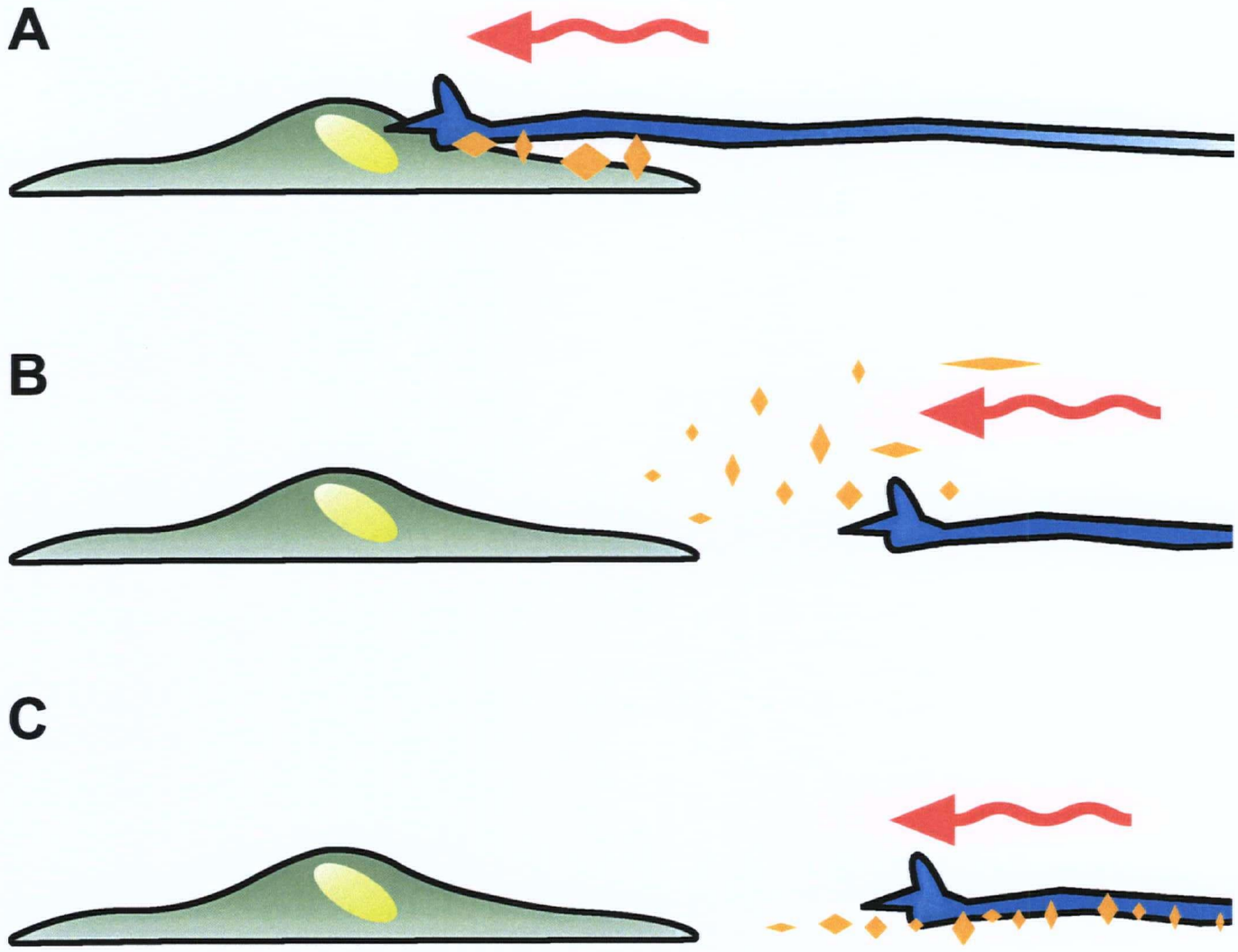

FIGURE 4.6
Three Potential Mechanisms of Olfactory Ensheathing Cell-Mediated Neurite Outgrowth
(A) Olfactory Ensheathing Cell (OEC, green) expresses cell surface factors (orange) that act as a preferential substrate and/or growth-promoting signal for neurites (blue). (B) OEC releases factors (orange) that promote growth of neurites. (C) OEC releases factors (orange) that settle and act as a preferential substrate and/or growth-promoting signal for neurites.

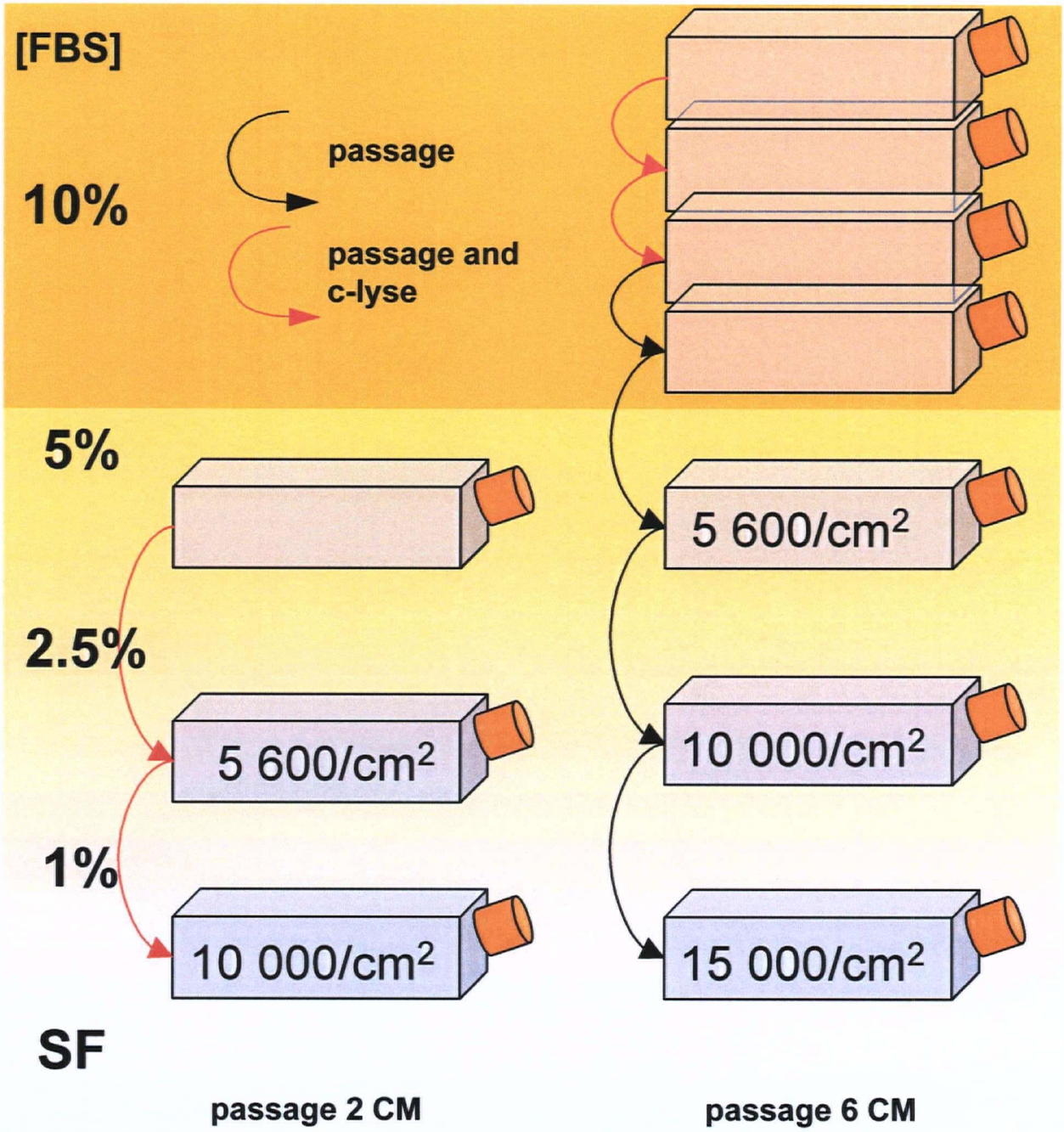

FIGURE 4.7
Schematic of Generating Conditioned Media Samples from Passage 2 and Passage 6 LP-OECs
Over the course of passage and purification, LP-OECs are weaned off of serum by gradual step-down and increasing plating density. Purified LP-OECs are grown in serum-free media for 5 days before harvesting conditoned media at either passage 2 or passage 6. Media is then concentrated to 10-30X using an ultrafiltration cell with a 1 KDa MWCO filter. To fairly cross compare early and late passage media, the samples are normalized to the number of cells generating a given volume of media.

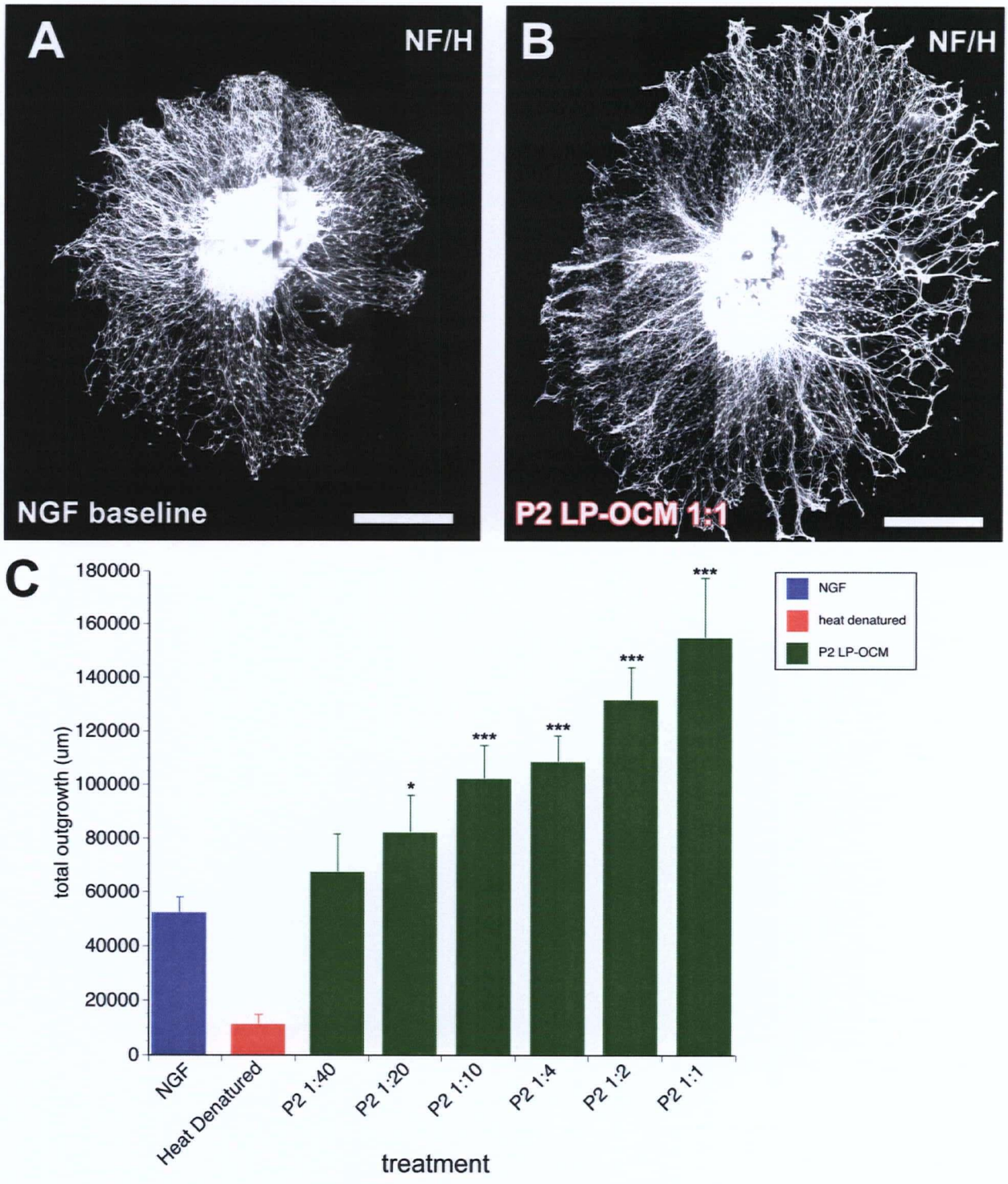
A
NF/H
NGF baseline
B
NF/H
P2 LP-OCM 1:1
C
total outgrowth (um)
180000
160000
140000
120000
100000
80000
60000
40000
20000
0
NGF
heat denatured
P2 LP-OCM
*
***
***
***
***
NGF
Heat Denatured
P2 1:40
P2 1:20
P2 1:10
P2 1:4
P2 1:2
P2 1:1
treatment

FIGURE 4.8

FIGURE 4.8
Comparison of Baseline NGF conditions with Baseline Supplemented with Passage 2 Conditioned Media
Embryonic DRG explants were cultured in (A) baseline NGF (1.5 ng/ml) or (B) baseline NGF supplemented with passage 2 conditioned media (1:1 concentration). (C) Total outgrowth quantified for baseline NGF (blue), heat-denatured conditioned media (red) and various concentrations of passage 2 conditioned media (green). All explants were labeled with neurofilament heavy chain antibody (NF/H). Scalebar represents 500 microns. Asterisks: * is $p < 0.05$; * is $p < 0.005$; *** is $p < 0.0005$.

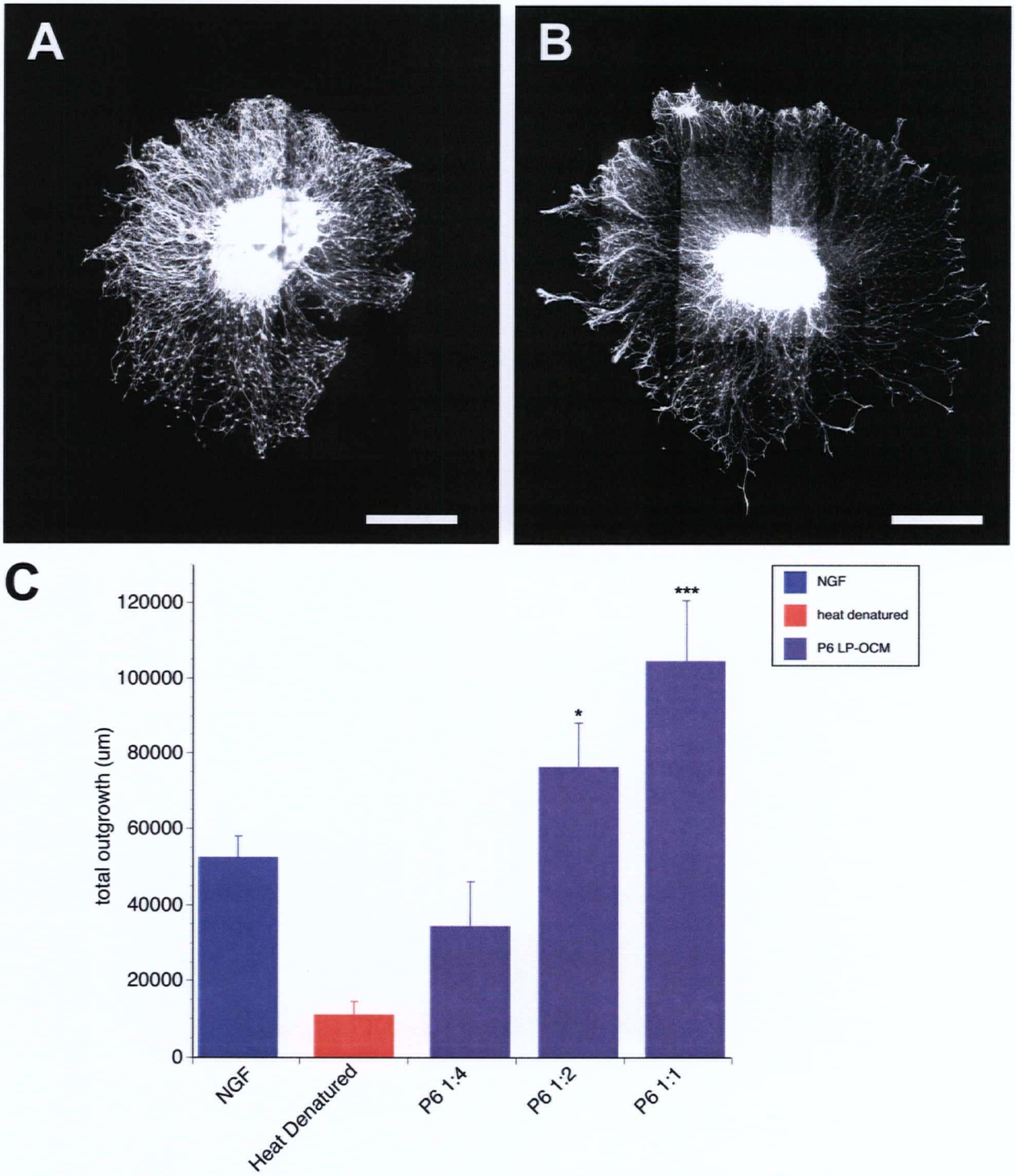
A
B
C
120000
100000
80000
60000
40000
20000
0
total outgrowth (um)
***
*
NGF
heat denatured
P6 LP-OCM
NGF
Heat Denatured
P6 1:4
P6 1:2
P6 1:1

FIGURE 4.9

FIGURE 4.9

Comparison of Baseline NGF conditions with Baseline Supplemented with Passage 6 Conditioned Media

Embryonic DRG explants were cultured in (A) baseline NGF (1.5 ng/ml) or (B) baseline NGF supplemented with passage 6 conditioned media (1:1 concentration). (C) Total outgrowth quantified for baseline NGF (blue), heat-denatured conditioned media (red) and various concentrations of passage 6 conditioned media (purple). All explants were labeled with neurofilament heavy chain antibody (NF/H). Scalebar represents 500 microns. Asterisks: * is $p < 0.05$; * is $p < 0.005$; *** is $p < 0.0005$.

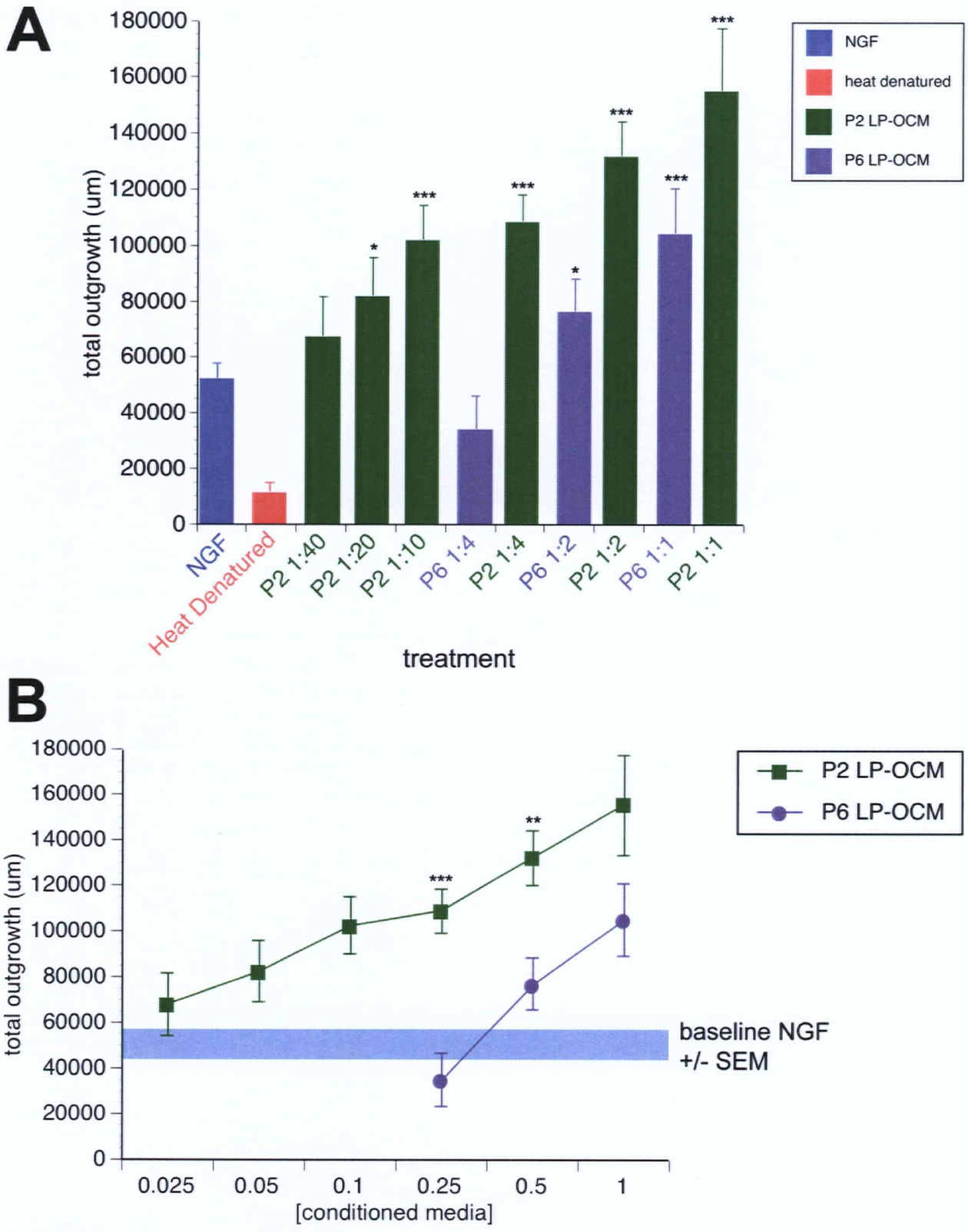
A
180000
160000
140000
120000
100000
80000
60000
40000
20000
0
total outgrowth (um)
NGF
heat denatured
P2 LP-OCM
P6 LP-OCM
*
***
***
*
***
***
NGF
Heat Denatured
P2 1:40
P2 1:20
P2 1:10
P6 1:4
P2 1:4
P6 1:2
P2 1:2
P6 1:1
P2 1:1
treatment
B
180000
160000
140000
120000
100000
80000
60000
40000
20000
0
total outgrowth (um)
P2 LP-OCM
P6 LP-OCM
**
***
baseline NGF
+/- SEM
0.025
0.05
0.1
0.25
0.5
1
[conditioned media]

FIGURE 4.10

FIGURE 4.10

Comparing the Biological Activity of Passage 2 and Passage 6 Conditioned Media

(A) Total outgrowth quantified for baseline NGF (blue), heat-denatured conditioned media (red), various concentrations of passage 2 conditioned media (green) and various concentrations of passage 6 conditioned media (purple). (B) Same data as in (A) plotted as a line graph. Passage 2 media (green), passage 6 media (purple) and baseline NGF +/- SEM (blue stripe). Asterisks: * is $p < 0.05$; * is $p < 0.005$; *** is $p < 0.0005$.

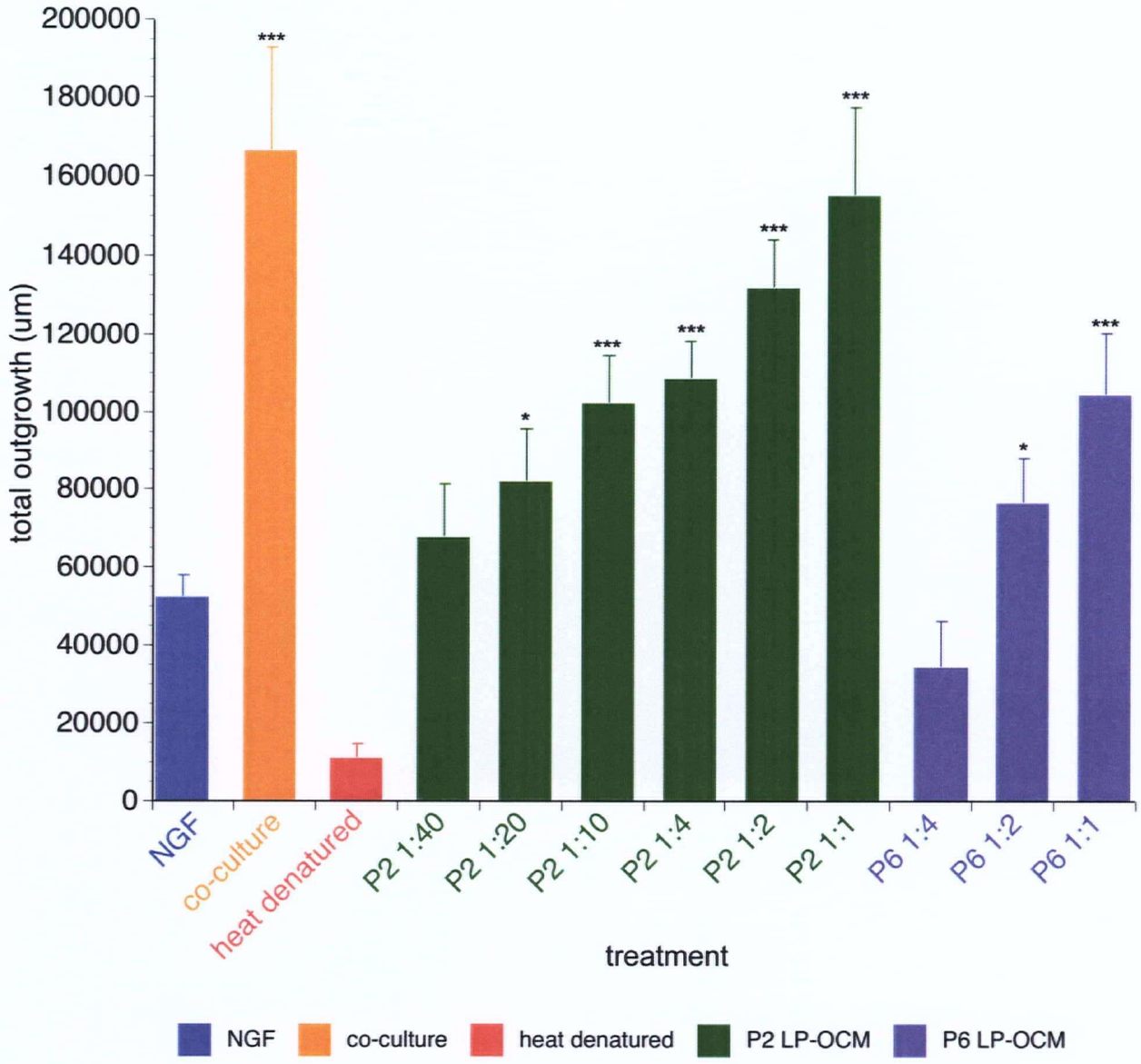

FIGURE 4.11

Summary of Total Outgrowth in All Conditions Assayed

Total outgrowth quantified for baseline NGF (blue), LP-OEC co-culture (orange), heat-denatured conditioned media (red), various concentrations of passage 2 conditioned media (green) and various concentrations of passage 6 conditioned media (purple). Asterisks: * is $p < 0.05$; * is $p < 0.005$; *** is $p < 0.0005$.

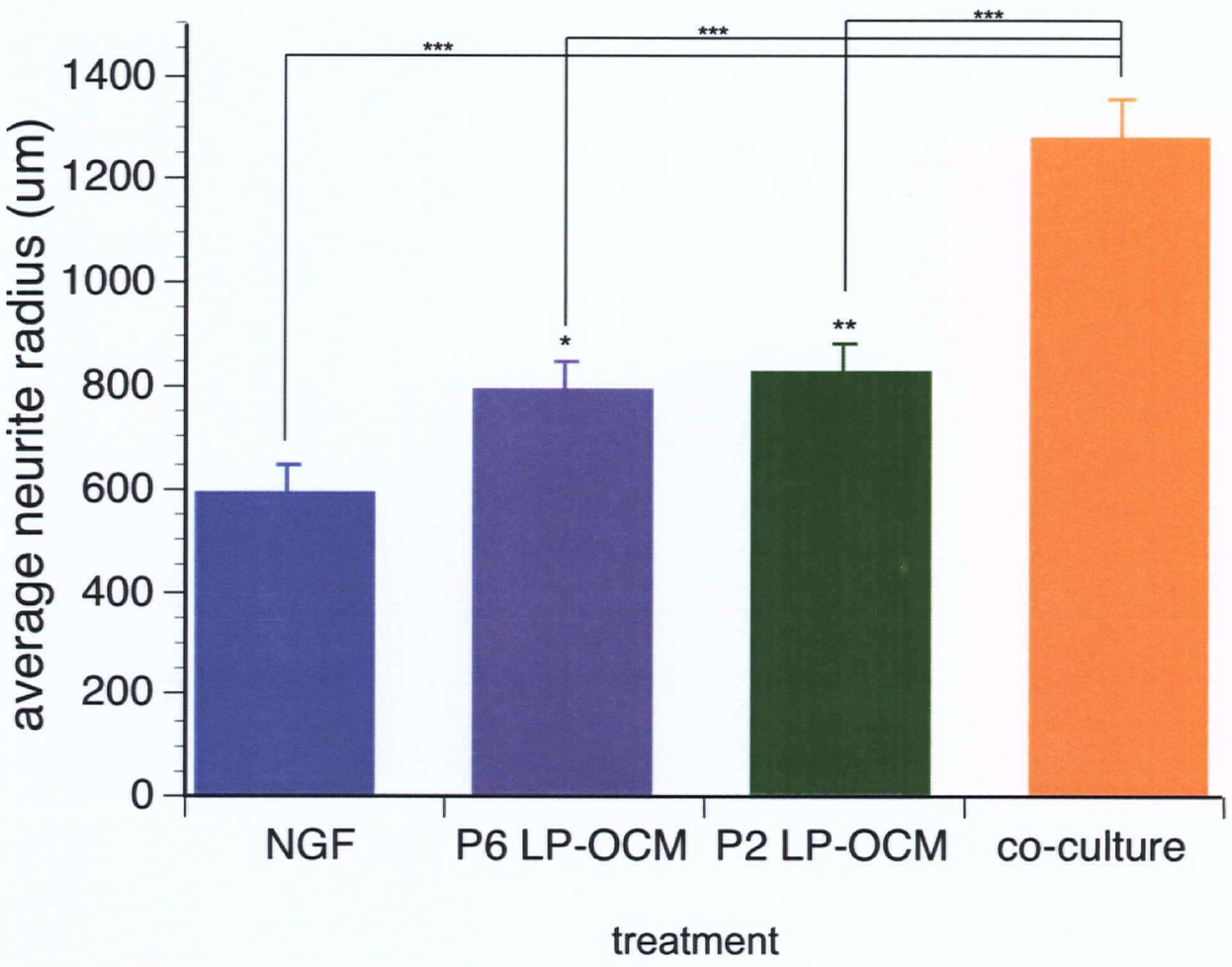

FIGURE 4.12

Comparing Average Neurite Radius of NGF Baseline, Conditioned Media and LP-OEC Co-culture

Average neurite radius quantified as described in figure 4.1B. Baseline NGF (blue), LP-OEC co-culture (orange), 1:1 concentration of passage 2 conditioned media (green) and 1:1 concentration of passage 6 conditioned media (purple). Asterisks: * is $p < 0.05$; * is $p < 0.005$; *** is $p < 0.0005$.

Chapter 5: Analysis of Conditioned Media Samples by Isotope Coded Affinity Tags Proteomics

5.1 Introduction

5.1.1 Rationale for Proteomic Analysis

While the in vitro assay can measure the ability of OECs to promote neurite outgrowth, a bridge is needed between the functional data and potential candidates responsible for OEC activity. To accomplish this, it was decided that potential mediators of OEC biological activity would be identified using a screen approach (see section 5.1.2 and figure 5.1). Proteomics was chosen as the screening method for a variety of reasons, and it has advantages and disadvantages compared with other methods such as microarray and SAGE (serial analysis of gene expression). Perhaps the most compelling argument in favour of proteomics is that it directly identifies the factors responsible for the biological activity. The other two methods mentioned are indirect in that it must be inferred that the mRNA (messenger ribonucleic acid) is properly translated and trafficked by the cell. No such assumption is required with proteomics – the protein is either present or absent in the sample. In this study, proteomics was particularly appropriate, because of the nature of the sample analyzed: Since OEC conditioned media contains the proteins being secreted by OECs, it was not necessary to deal with whether candidate factors were truly being trafficked out of the cell. Instead, by virtue of their being in the conditioned media, there was a strong likelihood that they were part of the OEC 'secreteome'. This approach can bypass problems encountered in another study looking for neurotrophic factor expression in OECs by a ribonuclease protection assay (Lipson et al., 2003). While the presence of transcripts for known neurotrophic factors were detected, with documented biological effects on the neuronal populations assayed (peripheral sensory and autonomic ganglion explants), the authors did not find a biological effect from the conditioned

media and postulated that the neurotrophins were not being secreted or secreted at too low levels for bioactivity.

As with any screen approach, there are also inherent difficulties with employing a proteomic approach to study OEC function, the most obvious issue being what if the factor(s) responsible for the biological activity is not proteinaceous? There are controls that can be built-in to the experimental design to test this possibility. But even if this were the case, microarray and/or SAGE may not fare any better in this respect. Second, proteomics tends to be less sensitive than other screening methods. A direct cross-comparison of yeast proteins analyzed by 2-D gel electrophoresis and mass spectroscopic sequencing and found that there was a definite bias for detecting high abundance proteins based on codon bias (Gygi et al., 1999b). Third, proteomic techniques can have issues resolving proteins with extremes in isoelectric point and hydrophobicity (reviewed in Haynes and Yates, 2000). Fourth, proteomics has issues with processing large, complex samples due to limitations in mass spectrometer cycling frequency and data processing speed (Aebersold and Mann, 2003).

5.1.2 Using ICAT to Analyze Conditioned Media Samples

ICAT proteomics is well suited to compare the differences between passage 2 and passage 6 LP-OCM. ICAT not only provides the identities of the constituent proteins, but also provide relative quantitation (section 5.1.3). So even if the two samples of conditioned media have identical protein constituents, differences in protein levels could be informative for identifying key candidate factors. Since the two conditioned media samples were derived from the same cell population, separated only by age in culture, analysis of the ICAT dataset for differences should be greatly simplified.

Whether the active factors in the conditioned media were proteins was tested by heat denaturing the conditioned media prior to bioassay. If the activity was lost, there is a

strong likelihood of a protein-based mechanism; and indeed this is what was observed (see figures 4.8 and 4.9). An assumption was made that sufficient quantities of the proteins responsible for the activity would be presnt to be detected by ICAT. Also the active factors would have to contain cysteine residues. Otherwise, regardless of expression level, ICAT would not identify the protein.

5.1.3 Isotope-Coded Affinity Tags Proteomics

Isotope coded affinity tags (ICAT) proteomics is a tandem mass spectroscopic method that integrates protein sequencing and relative quantitation (Gygi et al., 1999a). ICAT has several advantages that made it particularly suitable for analyzing OEC function. First, ICAT proteomics uses a stable isotope tag to differentiate the samples to be analyzed, in contrast with metabolic labeling which has been used previously with yeast (Oda et al., 1999), which could have adverse effects on the OECs as they incorporate the ^{15}N isotope. Instead, ICAT reagent is added after the sample has been collected and it binds covalently to the protein sample. Second ICAT proteomics is quantitative, adding another dimension to the data set by cross-comparing the relative quantities of a given protein between samples rather than just absence/presence. Third, ICAT proteomics has practical advantages over traditional 2-D gel electrophoretic (2-DE) techniques. Not limited to separating the proteins by isolectric point, as is the case with 2-DE, ICAT can work in line with any number of HPLC (high pressure liquid chromatography) columns which separate samples by various criteria (Gygi and Aebersold, 2000). This enables ICAT to analyze a broader range of protein samples.

The general principle behind ICAT is that two samples are analyzed concurrently by tandem mass spectroscopy (MS-MS), giving information on the identity and relative quantity of the constituent proteins in both samples (Gygi et al., 1999a) (see figure 5.2A). First, the two samples are differentially labeled with ICAT reagent, of which there are two forms: heavy and light. In the light form, the nine carbons that make up the backbone of the isotope-labeling region (see figure 5.2B) are common ^{12}C carbon atoms. In the heavy form, the nine carbons are ^{13}C carbon isotope atoms, which makes it nine

atomic mass units (amu) heavier than the light form. ICAT reagent covalently binds to cysteines in the two samples via alkylation of the sulfhydryl R-group residue.

Next, the protein sample is separated from the unbound ICAT reagent by SDS-PAGE (sodium dodecyl sulphate - polyacrylamide gel electrophoresis) and then digested with trypsin. Trypsin cleaves proteins at the peptide bond on the C-terminus end of lysine and arginine residues and breaks the proteins down into small peptide fragments in a stochastic manner. The fragments from both light- and heavy-labeled samples are mixed together and passed through a monomeric avidin affinity column. Peptides covalently labeled by ICAT reagent are retained on the column via biotin-avidin complex formation. The bound fraction is eluted in a mild formic acid solution and the peptides are dried by evaporation under vacuum. To minimize steric hindrance, the biotin tag is cleaved at the acid cleavable linker region by reconstituting the peptides in a solution containing trifluoroacetic acid (Applied Biosystems).

The mixture is then loaded into an HPLC (high pressure liquid chromatography) reverse phase column. Reverse phase chromatography separates peptides by size and hydrophobicity and like peptides elute directly into the first MS. Mass spectrometer #1 measures the signal amplitudes of the eluted peptides and measures their mass to charge ratio (m/z) (see figure 5.3A). Like peptides differently labeled with light and heavy ICAT reagent and can be distinguished as paired peaks typically 9 amu apart (assuming the peptide contains one cysteine residue or is singly labeled). The mass spectrometer measures the height of each peak as a measure of peptide abundance. As the paired peaks continue to elute from the HPLC, the entire elution profile is measured and thus, the area under the elution curve is the measure of peptide abundance (see figure 5.3B). This method of quantitation is particularly valid because the peptides measured are almost completely identical to one another and act as their own internal controls.

As mass spectrometer #1 measures peak height and sorts b m/z ratio, a peak is selected for analysis by mass spectrometer #2. Peak selection is an automated process (Yi et al., 2005). First the largest peak is analyzed and then subsequently smaller peaks are

analyzed in succession. While the process cycles relatively quickly between MS#1 and MS#2, there is a strong likelihood that very low abundance proteins will be missed, especially if their elution profile is shallow, resulting in generally low signal amplitude. In MS#2, the peak is selected by its mass/charge ratio and fragmented by electron spray ionization. Using this method, the majority of the peptides are broken between peptide bonds resulting in N-terminus (γ+ ions) and C-terminus (β+ ions) fragments. Theoretically, this process is purely stochastic. However there are tendencies for fragmentation influenced by R-groups and, in the case of a tryptic digest like this, there is a bias towards γ+ ions due to the positive charged lysine or arginine at the C-terminus (reviewed in Mann and Pandey, 2001). The γ+ and β+ ions are measured by MS#2 to produce collision induced (CID) spectra. These spectra provide information about the mass of the ions, which can then be used to determine its amino acid composition (known as mass fingerprinting). In addition, the spectrum as whole is analyzed to provide information about the amino acid sequence. This is accomplished using a series of algorithms that attempt to 'best fit' the data with computer-derived theoretical CID spectra. The combined use of both mass fingerprinting and 'best fit' spectral analyses can provide the sequence of the peptide with a corresponding statistical margin of error. The cycle repeats between MS#1 and MS#2 to analyze all of the peptides that elute from the HPLC. The data is processed and compiled after collection using the software programs SEQUEST, Peptide Prophet and ASAPRatio. SEQUEST matches CID spectra and mass fingerprints to peptide sequences and correlates the sequence with a database to deduce protein identity (Ducret et al., 1998). The nature of the database is flexible; it can be protein, genomic or EST (expressed sequence tagged). Peptide Prophet uses statistical models to assign a margin of error to the SEQUEST results (Keller et al., 2002) and ASAPRatio matches the quantitative data with the SEQUEST results and gives an estimated margin of error (Li et al., 2003a). The data is presented in a graphical user interface (INTERACT) to effectively navigate and filter the dataset.

There are several assumptions made in ICAT proteomics. First is that a small peptide fragment can uniquely identify the protein that it belongs to. Second, the protein of interest contains a cysteine residue, to which the ICAT reagent binds. Third, proteins

present in one sample are also present in the other sample. Absence/presence of proteins cannot easily be interpreted because there is no basis for relative comparison. Fourth, due to the bias towards high abundance proteins, it must be assumed that one's protein(s) of interest is at a detectable level.

5.2 Results

5.2.1 ICAT Dataset

The proteomic dataset reported a large number of proteins detected in the two conditioned media samples. However, not all of these proteins were reported with high confidence. I set my cut-off for high confidence to be a peptide probability score greater than 0.9. The peptide probability is based on the clarity and quality of the fragment mass spectrum, which directly impacts the certainty with which peptide sequence can be assigned. The statistical model also takes into account the number of peptides identifying a given protein. Thus, the individual probabilities of each peptide increase as the number of peptides also identifying the same protein increase (Nesvizhskii et al., 2003). As such, I decided to look at all proteins identified by peptides with probability scores greater than 0.9 regardless of how many unique peptides indicate the same protein. A cut-off of 0.9, while to a degree arbitrary, provides a sound compromise between sensitivity and accuracy. Nesviszhskii and coworkers found with their positive control protein sample that a cut-off of 0.9 yielded negligible error rates (>1%) while still accounting for approximately 90% of the proteins detected.

With this cut-off alone, the number of peptides in the dataset shrinks from 755 peptides (corresponding to 702 unique proteins) to 97 peptides (corresponding to 63 unique proteins). These data have been included in spreadsheet format in the Appendix (see Table 5.1). This indicates that the dataset generated from the conditioned media was not nearly as robust as that generated by Nesvizhskii and coworkers. This has been represented graphically in figure 5.4. In general, the error and sensitivity graphs as

modeled by the method of Nesvizhskii et al. (2003) indicate that the data was of poorer quality than the well-defined mixture of proteins used by the authors. The drop in quality is not due to error rate; in this respect the datasets are comparable. The main difference is that the Nesviszhskii et al. dataset has far superior sensitivity. This may be because a conditioned media sample, even though it has been concentrated by ultrafiltration prior to analysis, is more dilute than is ideal. Nonetheless, it is important to note that with the stringent cut-off of 0.9, I have reduced my dataset sensitivity to approximately 50%. Dropping the cut-off to 0.6 raises the false positive error rate to approximately 7.5% but increases the sensitivity to almost 70%. I examined the datasets at multiple cut-offs in an attempt to identify candidate factors. The trade-off between error rate and sensitivity is an obvious consideration but also important was to look for trends with respect to proteins and the peptides uniquely identifying them. I needed to consider questions such as: As the cut-off drops, are the same proteins being represented by peptides of lower probability or are new proteins making the cut, represented by peptides of lower scores? In general, the latter was the case. Thus, I stayed with the 0.9 cut-off, despite its obvious drawbacks, to minimize false positives at the expense of low abundance proteins. That is not to say that the data was not useful; only that it is important to note that by using a stringent cut-off of 0.9, it is possible that key proteins were not considered as potential candidate factors.

In a subsequent ICAT run, using the same cut-off of 0.9 peptide probability score, only 42 peptides remained. They corresponded to 24 unique proteins. Cross comparing the 24 proteins with the 63 identified in the first run, 10/24 were found on the shortlist of 63. There is a high likelihood that all 10 of these proteins were correctly identified since they were found in both ICAT runs and passed the cut-off criteria of 0.9. Two other proteins from the list of 24 were found in the full list of 702 proteins from the first run. Both of these proteins had low peptide probability scores reported in the first run.

These results can be interpreted in a number of ways. One is that the ICAT runs were not entirely successful in identifying the protein constituents of the conditioned media samples. Likely, further optimization may be required to generate a more comprehensive

list. Two, the conditioned media sample is relatively simple with few constituent proteins. A silver stained gel of passage 2 and passage 6 conditioned media samples can be found in the appendix (see Appendix 4). Qualitatively, the mixture looks fairly complex but it is difficult to assign identities to individual bands because there is the possibility that there may be a laddering effect due to heat denaturation or protein breakdown. Three, as mentioned previously (see section 5.1.3) there are limitations to the sensitivity and detection range of ICAT and this may simply be a shortcoming of the technique chosen. Four, even though some of the proteins were detected with high probability, they were not likely secreted by OECs, but rather a product of cell lysis as the conditioned media was being generated (for example: poly(A) binding protein II, Table 5.1). Cell lysate proteins were highly variable between the two ICAT runs and added an extra level of background that needed to be accounted for when analyzing the dataset. Overall however, the ICAT data provided me with ample data to identify candidate proteins responsible for the biological activity of the conditioned media.

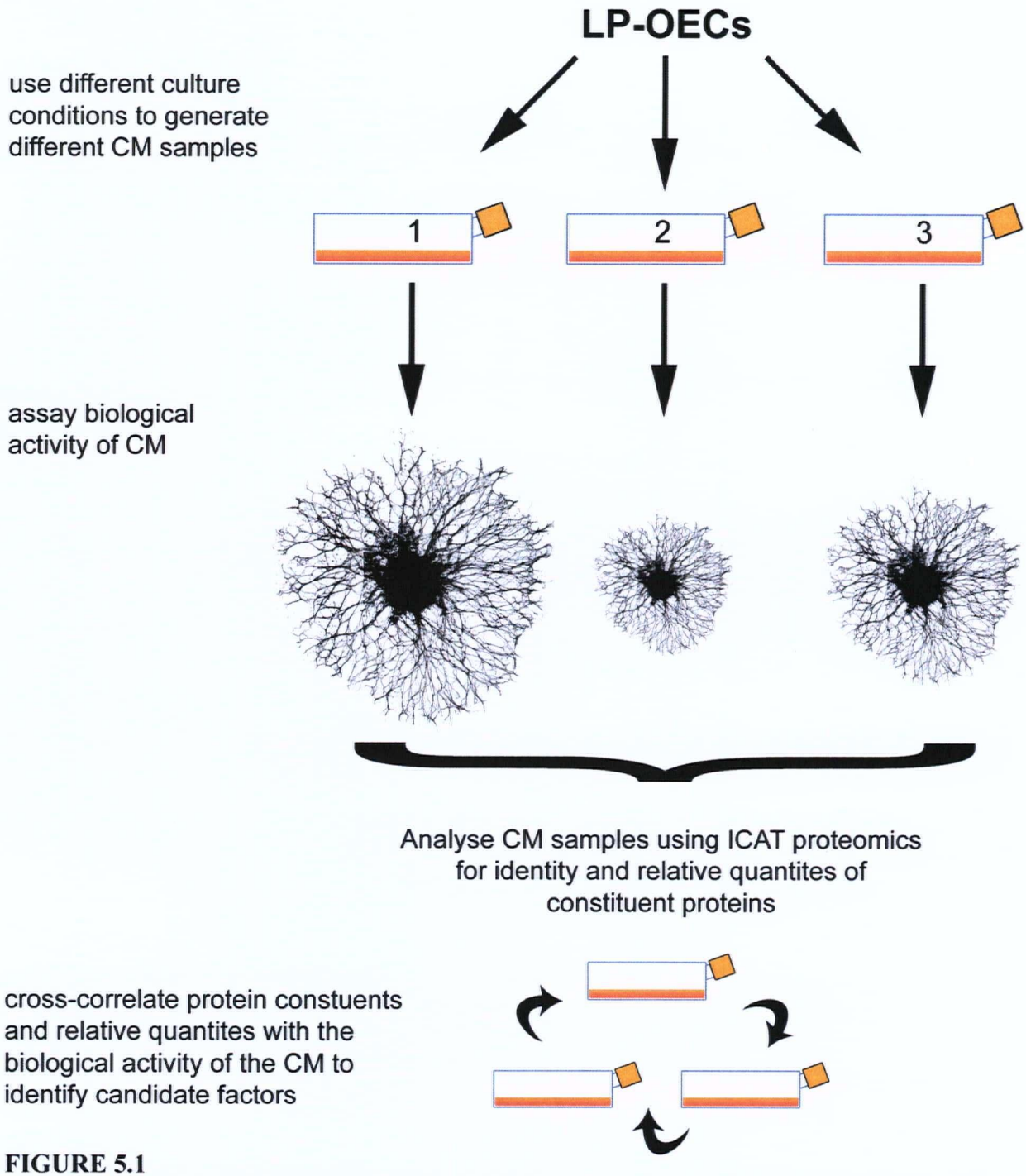

FIGURE 5.1
Schematic of Experimental Approach to Find Candidate Secreted Factors Important in OEC-Mediated Neurite Outgrowth
Starting with a purified population of lamina propria-derived OECs (LP-OECs), the cells are cultured under different conditions. Conditioned media (CM) is harvested and assayed for biological activity by a neurite outgrowth assay. CM is analysed by ICAT (isotope coded affinity tagged) proteomics. The identity and relative quantities of the constituent proteins within the CM samples are compared and correlated with their respective biological activity.

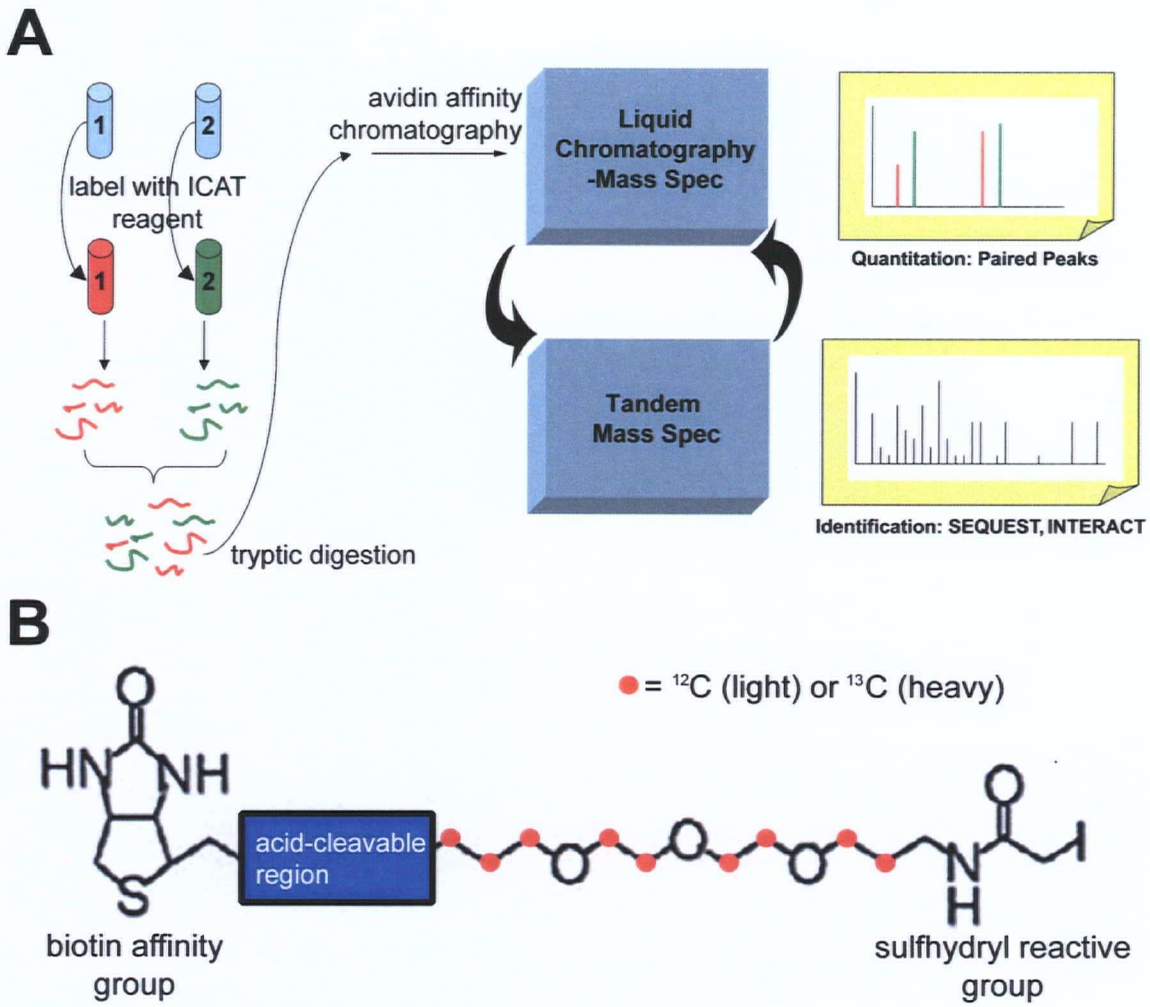

FIGURE 5.2
Schematic of Isotope-Coded Affinity Tags Proteomic Procedure
(A) Two samples are labeled with either light (red) or heavy (green) isotope-coded affinity tags (ICAT) reagent. The samples are mixed together and digested with trypsin. The digest is run through an avidin affinity column, and labeled peptides are released via acid cleavage. The peptides are separated by reverse phase liquid chromatography in-line with the first mass spectrometer (MS). The first MS measures peptide amplitudes to determine relative quantity and then cycles to the second MS which fragments and sequences the peptide to provide protein identity. All data is collected and compiled via SEQUEST software suite and presented in a graphical user interface by INTERACT. (B) Salient features of the ICAT reagent. Biotin affinity group is connected to the isotope-labeled region via an acid cleavable group. Upon binding to an avidin affinity column, the biotin group is cleaved to reduce steric hindrance. The isotope-labeled region either contains 9 normal 12C atoms (light) or 9 13C atoms (heavy) giving a difference of 9 atom mass units between the two reagents. A sulfhydryl reactive group covalently binds to cysteine residues in the sample.

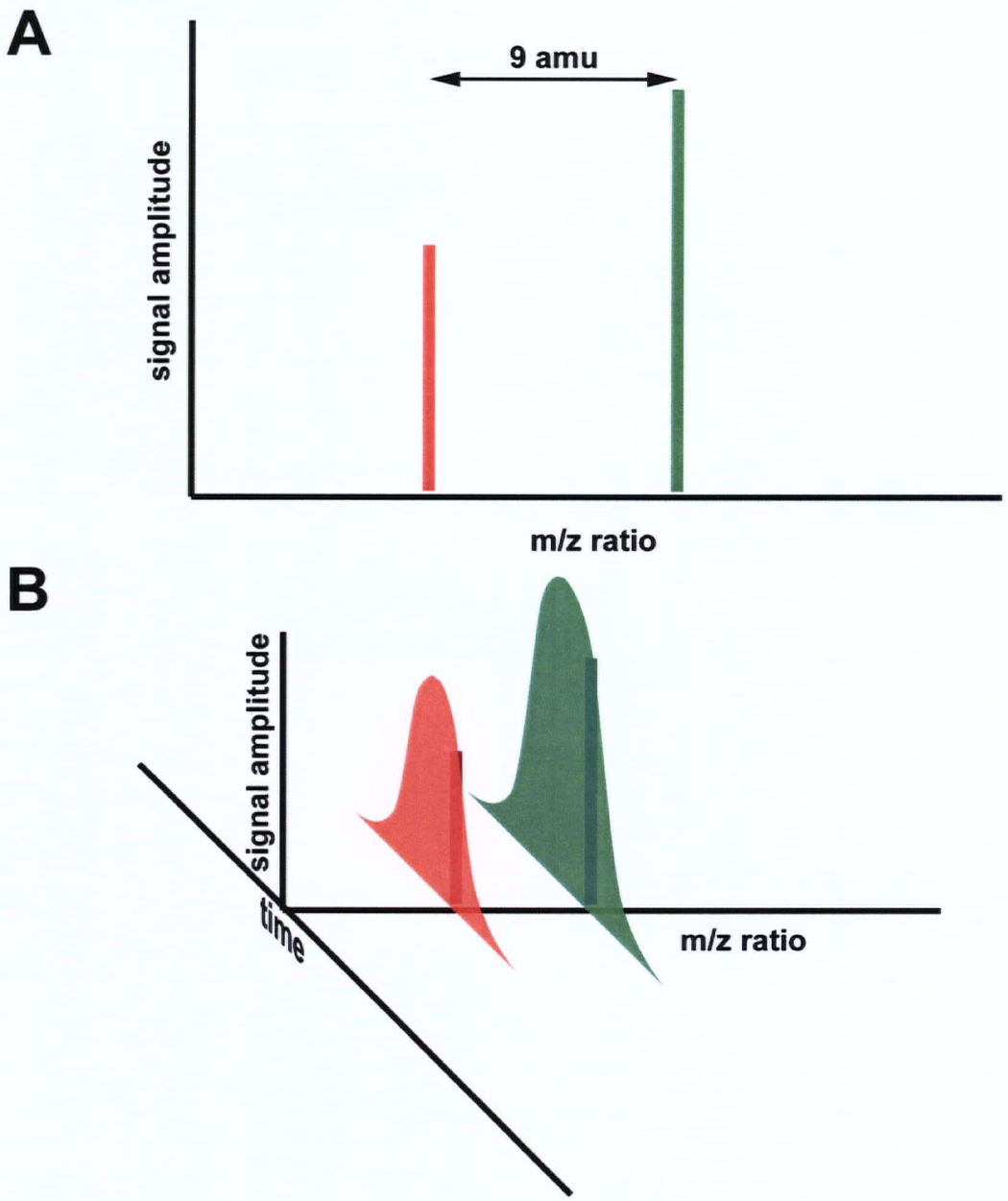

FIGURE 5.3
Relative Quantitation Using ICAT Proteomics
(A) Two identical peptides are eluted from the HPLC. One peptide is labeled with heavy reagent (green) and the other with light (red). They are detected by the mass spectrometer as two peaks, 9 atomic mass units (amu) apart. (B) To quantify the peptide abundances, the entire elution profile is analyzed such that the areas under the entire elution curves, not the peak height at any given time, corresponds to relative quantity.

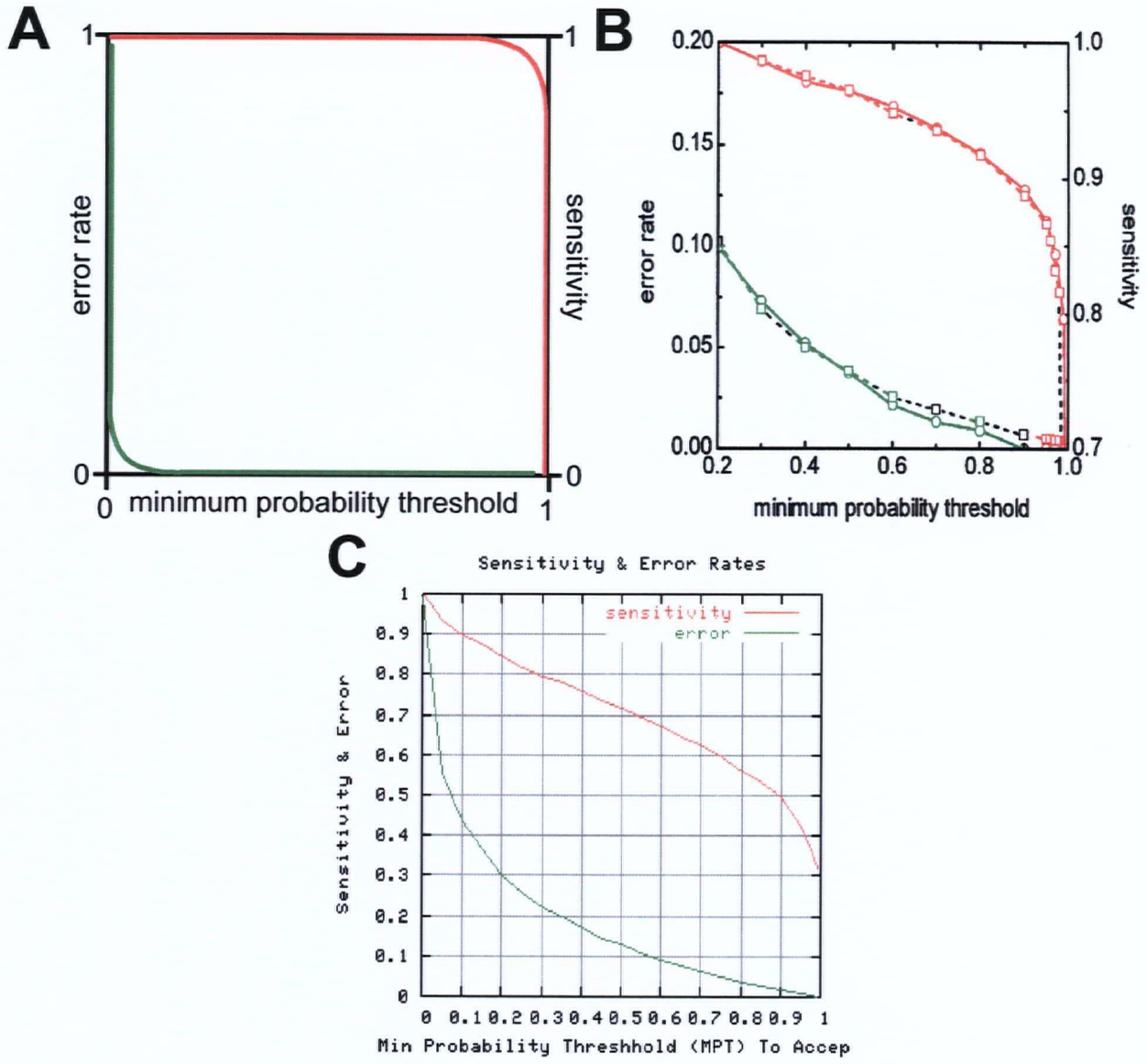

FIGURE 5.4

Sensitivity and False Positive Identification Error Rate Plots

Sensitivity to false positive identification error rate plots are a graphical representation of ICAT data quality. The x-axis is the minimum cut-off for acceptable data. As the cut-off decreases, the false positive and sensitivity rates both increase. (A) represents an idealized plot with very low false positive rates and very high sensitivity. (B) Taken from Nesvishskii et al (2003) Analytical Chemistry 75(17): 4646-4658. Shows the plot of a known protein mixture processed by ICAT (solid lines) compared to a theoretical plot based on mathematical modeling (dashed lines). (C) Error and Sensitivity plot for ICAT dataset from P2 and P6 LP-OCM.

TABLE 5.1 List of ICAT Results using 0.9 Protein Probability Cut-Off

protein probability	Protein Name	IPI Protein DB #
0.9989	Insulin-like growth factor binding protein 4 precursor	IPI00112487
1		IPI00112487
0.9281		IPI00112487
1		IPI00112487
0.9928	2810025A12Rik protein	IPI00112492
0.9993	Polydom protein precursor	IPI00112858
0.9805		IPI00112858
1	72 kDa type IV collagenase precursor	IPI00112904
1		IPI00112904
0.9922		IPI00112904
1		IPI00112904
0.9993	CYR61 protein precursor	IPI00113117
0.9465	Fibronectin precursor	IPI00113539
1		IPI00113539
0.999		IPI00113539
0.973		IPI00113539
0.9981		IPI00113539
0.9047	Recombining binding protein suppressor of hairless-like protein	IPI00114954
0.9238	Serine proteinase inhibitor NK13	IPI00116247
0.903	Splice isoform 1 of P35329 B-cell receptor CD22 precursor	IPI00117413
0.9374	None Mouse germ cell-less haploid specific	IPI00118128
0.9106	Tumor necrosis factor, alpha-induced protein 2	IPI00119978
1	Procollagen C-proteinase enhancer protein precursor	IPI00120176
0.9996		IPI00120176
1		IPI00120176

protein probability	Protein Name	IPI Protein DB #
0.9676	Procollagen type V alpha 2	IPI00121120
0.9773		IPI00121120
0.9217	Nonmuscle heavy chain myosin II-A	IPI00123181
0.9452		IPI00123181
0.9741		IPI00123181
0.9979	Biglycan precursor	IPI00123194
0.9997		IPI00123194
0.9423		IPI00123194
0.9186		IPI00123194
0.9665		IPI00123194
0.999		IPI00123194
0.998		IPI00123194
0.9834	Follistatin-related protein 1 precursor	IPI00124707
0.9978	Protein kinase A anchoring protein 11	IPI00125322
0.9906		IPI00125322
0.9863		IPI00125322
0.9858	SPARC precursor	IPI00126343
0.9831		IPI00126343
0.9212		IPI00126343
0.9665		IPI00126343
0.9754		IPI00126343
0.9972		IPI00126343
1		IPI00126343
1		IPI00126343
0.9783		IPI00126343
0.9896		IPI00126343
0.9956		IPI00126343
0.9235		IPI00126343
0.9244		IPI00126343
0.9436		IPI00126343
0.9232		IPI00126343
1		IPI00126343
1		IPI00126343
1		IPI00126343
1		IPI00126343

protein probability	Protein Name	IPI Protein DB #
0.9995	SPARC precursor	IPI00126343
0.9796		IPI00126343
1		IPI00126343
0.9757		IPI00126343
0.9925		IPI00126343
0.9995		IPI00126343
0.9995		IPI00126343
0.9979		IPI00126343
0.9974		IPI00126343
0.9962		IPI00126343
0.9986		IPI00126343
0.9918		IPI00126343
1		IPI00126343
0.999		IPI00126343
0.9426		IPI00126343
0.9955		IPI00126343
0.9999		IPI00126343
1		IPI00126343
0.988		IPI00126343
1		IPI00126343
0.9689		IPI00126343
0.997		IPI00126343
0.9982		IPI00126343
0.9206	Serine/threonine protein kinase SSTK	IPI00126982
0.9759	Chondroitin 6-sulfotransferase	IPI00128074
0.9901		IPI00128074
1	None 5'-3' exonuclease	IPI00129132
0.9996	RPE-retinal G protein-coupled receptor	IPI00130998
0.9156	Splice isoform 1 of P54265 Myotonin-protein kinase	IPI00133497
1	Splice isoform 1 of Q9QX66 Zinc-finger protein neuro-d4	IPI00134511
1	Poly(A) binding protein II	IPI00136169

protein probability	Protein Name	IPI Protein DB #
0.9998	Serotransferrin precursor	IPI00139788
1		IPI00139788
1		IPI00139788
0.9997		IPI00139788
1		IPI00139788
0.9816		IPI00139788
1		IPI00139788
1		IPI00139788
0.988		IPI00139788
1		IPI00139788
0.9995		IPI00139788
1		IPI00139788
0.9908		IPI00139788
1		IPI00139788
0.9814		IPI00139788
1		IPI00139788
0.9829		IPI00139788
0.9997		IPI00139788
0.9998		IPI00139788
0.9998		IPI00139788
0.9998		IPI00139788
0.9988		IPI00139788
0.9996		IPI00139788
1		IPI00139788
0.9996		IPI00139788
0.9959		IPI00139788
0.9998		IPI00139788
0.9996		IPI00139788
0.9978		IPI00139788
0.9988		IPI00139788
0.9938		IPI00139788
0.9728		IPI00139788
0.993		IPI00139788
1		IPI00139788
0.9982		IPI00139788
0.9979		IPI00139788
1		IPI00139788
0.9893		IPI00139788
0.9727		IPI00139788
1		IPI00139788

protein probability	Protein Name	IPI Protein DB #
0.9508	Serotransferrin precursor	IPI00139788
0.9999		IPI00139788
0.9999		IPI00139788
0.9996		IPI00139788
1		IPI00139788
0.9994		IPI00139788
0.996		IPI00139788
0.9991		IPI00139788
1		IPI00139788
1		IPI00139788
0.9343		IPI00139788
0.9994		IPI00139788
0.947		IPI00139788
0.9106		IPI00139788
0.9998		IPI00139788
0.9995		IPI00139788
0.9987		IPI00139788
0.9998		IPI00139788
0.9317		IPI00139788
0.9999		IPI00139788
1		IPI00139788
0.9557		IPI00139788
0.9976		IPI00139788
0.9762	Similar to RIKEN cDNA 1700008D07 gene	IPI00153305
0.9735	Tumor-related protein	IPI00165849
1	Similar to follicle stimulating hormone primary response gene 1	IPI00169777
0.951	Inducible 6-phosphofructo-2-kinase homolog	IPI00177072
0.996		IPI00177072
0.9722		IPI00177072
0.9899		IPI00177072
0.9621		IPI00177072
0.9617		IPI00177072
0.9896		IPI00177072
0.9403	NS1-associated protein 1	IPI00221655

protein probability	Protein Name	IPI Protein DB #
1	Similar to CUBITUS INTERRUPTUS	IPI00222006
1	procollagen, type I, alpha 2	IPI00222188
0.9988		IPI00222188
0.9998		IPI00222188
0.9977		IPI00222188
0.9975		IPI00222188
0.9933		IPI00222188
1		IPI00222188
0.9144	Hypothetical fibronectin type III domain containing protein	IPI00225355
0.9258	MKIAA0826 protein	IPI00229629
0.9905	Splice isoform 2 of Q61701 ELAV-like protein 4	IPI00229977
0.9998	cytochrome c, testis	IPI00230033
0.9104	Ensembl_locations(Chr-bp):14-114366276	IPI00261268
0.9127	MKIAA0734 protein	IPI00264338
0.964	Ensembl_locations(Chr-bp):7-34268464	IPI00271619
1	Ensembl_locations(Chr-bp):5-106198580	IPI00273479
1	Tissue inhibitor of metalloproteinase 2	IPI00310128
0.9808		IPI00310128
0.9998		IPI00310128
0.9997		IPI00310128
0.9526	Similar to interleukin-1 receptor-associated kinase 2	IPI00311613
1	Insulin-like growth factor binding protein 2 precursor	IPI00313327
0.984		IPI00313327
0.9413		IPI00313327
0.9989		IPI00313327
0.9757		IPI00313327
1		IPI00313327
0.9794		IPI00313327

protein probability	Protein Name	IPI Protein DB #
0.9984	Insulin-like growth factor binding protein 2 precursor	IPI00313327
1		IPI00313327
0.9925		IPI00313327
1		IPI00313327
0.9967	iIPI00313327	
0.9922		IPI00313327
0.9967		IPI00313327
0.9958		IPI00313327
0.9998		IPI00313327
0.9534		IPI00313327
1		IPI00313327
0.9959		IPI00313327
0.9959		IPI00313327
0.9123		IPI00313327
0.99		IPI00313327
1		IPI00313327
0.9952		IPI00313327
0.9988		IPI00313327
0.9124	Lactotransferrin	IPI00317340
1	Angiotensinogen precursor	IPI00320617
0.9958	Connective tissue growth factor precursor	IPI00322594
0.9968		IPI00322594
0.971		IPI00322594
0.9947	Fibulin-5 precursor	IPI00323035
0.9944	procollagen, type I, alpha 1	IPI00329872
0.9936		IPI00329872
0.9869		IPI00329872
1		IPI00329872
0.9903		IPI00329872
1		IPI00329872
0.9981		IPI00329872
0.9686		IPI00329872
1		IPI00329872
1	Pigment epithelium-derived factor	IPI00331088

protein probability	Protein Name	IPI Protein DB #
0.9815	Pigment epithelium-derived factor	IPI00331088
1		IPI00331088
0.9999	Collagen alpha 1(VI) chain precursor	IPI00339885
0.9999		IPI00339885
0.922	similar to RIKEN cDNA 2610028H07	IPI00341459
0.9761	RIKEN cDNA 2410003A14	IPI00346015
1	gene model 252	IPI00350399
0.9908	Latent transforming growth factor beta binding protein, isoform 1S precursor	IPI00352982
0.9972	fibrillin 1	IPI00353445
0.9733		IPI00353445
0.9573	similar to glyceraldehyde-3-phosphate dehydrogenase	IPI00353598
0.9475	similar to Melanoma-associated antigen B3 (MAGE-B3 antigen)	IPI00355959
0.9471	Similar to Bernardinelli-Seip congenital lipodystrophy 2	IPI00377352
1	similar to placenta-specific 4	IPI00378092
0.9062	similar to Pro-Pol-dUTPase polyprotein	IPI00378297
0.9452	similar to Transcription factor BTF3 (RNA polymerase B transcription factor 3)	IPI00379807
0.9523		IPI00379807
0.9664	similar to cytochrome P450 monooxygenase CYP2T1	IPI00379809
0.9438	similar to Munc13-1	IPI00381088
0.9513	Spermatid-specific heat shock protein 70	IPI00387394

protein probability	Protein Name	IPI Protein DB #
0.9441	procollagen, type III, alpha 1	IPI00387550
0.9981		IPI00387550
0.9306		IPI00387550

Note: The mass spectroscopic data was analyzed using the International Protein Index Database. Its website can be found at: http://www.ebi.ac.uk/IPI/IPIhelp.html

Summary Table of ICAT Dataset

ECM and ECM-interacting molecules
Fibronectin precursor
Procollagen type V alpha 2
Biglycan precursor
Procollagen type I, alpha 2
Hypothetical fibronectin type III domain containing
Fibrillin 1
Procollagen type III alpha 1
Collagen alpha 1 (IV) chain precursor
SPARC precursor
Fibulin-5
Latent transforming growth factor beta binding protein, isoform 1 S precursor

Growth Factor/Growth Factor-Related
Polydom protein precursor
CYR61 protein precursor
Follistatin-related precursor protein 1 precursor
Similar to follicle stimulating hormone primary response gene 1
Insulin-like growth factor binding protein 2 precursor
Angiotensinogen precursor
Connective tissue growth factor precursor
Pigment epithelium-derived factor

Note: proteins excluded from summary table either have no known function or are likely not secreted but rather from lysed cell contaminants

Chapter 6: Functional Studies on Secreted Protein Acidic Rich in Cysteine

6.1 Introduction

6.1.1 Secreted Protein Acidic Rich in Cysteine

After a thorough analysis of the ICAT dataset from passage 2 and 6 LP-OCM, SPARC (secreted protein acidic rich in cysteine) was determined to be the most promising candidate factor responsible for the biological activity. Based on relative quantity, SPARC fit the profile of a molecule that could account for the difference in activity between the two samples. ICAT reported higher levels of SPARC in passage 2 versus passage 6 conditioned media (by approximately 30%). An important caveat however, is that there is a considerable bias for SPARC by ICAT analysis. As the name implies, SPARC contains a disproportionate number of cysteine residues and therefore is overrepresented in the ICAT dataset. That does not, however, affect SPARC's high peptide probability scores or overall quantitative ratio reported in both datasets. Also, there were several aspects about SPARC a priori that suggested it was a potentially important factor in conditioned media (described below).

6.1.1.1 General Features of SPARC

SPARC belongs to the matricellular family of proteins. Matricellular proteins, which include thrombospondin-1 and 2 and tenascin-C, and do not contribute to extracellular matrix structure but rather modulate cellular interactions with ECM molecules (reviewed in Brekken and Sage, 2001). SPARC is made up of three domains (see figure 6.1A): (1) an acidic calcium-binding domain, (2) a follistatin-like domain and (3) an extracellular calcium-binding domain. Each domain has specific functions and some of the functions

overlap between domains suggesting cooperativity. SPARC has many different effects on different systems and in different contexts. In general, SPARC has been reported to decrease cell adhesion, affect angiogenesis and cell migration and modulate growth factor activity and cell proliferation.

SPARC is a widely expressed protein in development. It has been found in heart, cartilage, bone, gut epithelium, skin and blood vessels (Holland et al., 1987; Sage et al., 1989). Its expression in adulthood however is confined primarily to tissue undergoing continual turnover or following injury such as bone and gut. In this regard, with its neuronal population undergoing constant turnover, it is not surprising that the olfactory system retains SPARC expression postnatally. In fact, SPARC mRNA was detected by differential display in an olfactory cell line, OLF442 grown in serum and serum-starved conditions (Zehntner et al., 1998).

6.1.1.2 SPARC Interaction with ECM Molecules

Like other members of the matricellular protein family, SPARC binds to ECM molecules. Its third domain, extracellular-calcium binding (E-C) domain, is largely responsible for this activity and mediates SPARC binding to collagen, thrombospondin-1, vitronectin and entactin/nidogen (reviewed in Brekken and Sage, 2001). SPARC also binds to laminin-1 via its E-C domain (Sweetwyne et al., 2004). The biological significance of SPARC-ECM binding is only beginning to be understood. Analysis of the SPARC null mouse reveals defects in collagen fibril formation (Bradshaw et al., 2003) and collagen α1 deficient *mov*-13 mice show mis-targeting of SPARC (Iruela-Arispe et al., 1996). SPARC can be specifically cleaved at leucine-197 and leucine-198 by a number of matrix metalloproteases (several of which were detected in the ICAT run, Table 5.1) in vitro resulting in a significantly higher affinity for collagen (Sasaki et al., 1997).

There is evidence that laminin can augment SPARC activity (Rempel et al., 2001). In an examination of glioma cell line division, attachment and migration on various ECM substrates normally found in the CNS, SPARC slowed proliferation and increased cell

attachment to different degrees depending on the substrate. SPARC had the most effect on collagen and laminin. Collagen and laminin substrates also interacted with SPARC to modulate glioma cell migration but the trend was not dose-dependent. Mid levels of SPARC increased migration and low levels were similar to control migration rates. High SPARC levels decreased migration rate; an effect the authors propose may be due to increased attachment. These data indicate that the interplay of SPARC with different ECM molecules is complex and likely dependent on context.

6.1.1.3 SPARC Modulation of Growth Factor Activity

SPARC has also been shown to modulate the activity and expression of a number of different growth factors most notably bFGF, PDGF, VEGF and TGFβ. In the case of PDGF and VEGF, there is evidence of direct physical interaction with SPARC. SPARC can bind PDGF-AB and PDGF-BB dimers to prevent growth factor-receptor binding resulting in decreased smooth muscle cell proliferation (Raines et al., 1992). There is also evidence that SPARC may also bind PDGF-AA (Gohring et al., 1998). SPARC binds to VEGF via its E-C domain and can inhibit endothelial cell proliferation (Kupprion et al., 1998). SPARC can also interfere with bFGF signaling although not through direct interaction with the growth factor. It was suggested that SPARC does not interfere with bFGF2-FGFR ligand-receptor interaction but rather indirectly interferes with downstream signal transduction pathways including PKA activation (Motamed et al., 2003). It is possible that SPARC itself may have a receptor whose signaling pathway interferes with the bFGF MAPK pathway. To date, however the identity of the putative SPARC receptor has not been reported. SPARC also interacts with TGFβ. While there is no evidence of a direct interaction, it has been suggested that there may be an indirect interaction via ECM (Bradshaw and Sage, 2001; Nunes et al., 1997). Indirect or otherwise, there appears to be a link between their expression levels. Increasing TGFβ levels induce increased SPARC and collagen-1 expression (Reed et al., 1994) while adding SPARC to SPARC null mesangial cells can restore TGFβ to normal levels (Francki et al., 1999). Upregulation of TGFβ can have multiple downstream effects depending on cell type and environment (see section 6.3.6).

It has also been suggested that certain portions of SPARC may have intrinsic growth

factor function. SPARC expression is coincident with angiogenesis (Iruela-Arispe et al., 1991) and in a subsequent study the same group found that fragments (including (K)GHK; see figure 6.1A) of SPARC were potent activators of endothelial cell differentiation and proliferation (Lane et al., 1994). More recently, it was found that SPARC is a substrate for matrix metalloprotease-3 which cleaves SPARC into 3 fragments one of which is (K)GHK (Sage et al., 2003). The resulting fragment was able to mediate angiogenesis in a dose dependent manner.

6.1.1.4 The Effect of SPARC on Cell Differentiation

With the modulatory effect of SPARC on growth factors and ECM molecules, it is not surprising that SPARC also impacts cell differentiation. The effect of SPARC, or more accurately its lack thereof, on cell differentiation is hypothesized to be the underlying cause of the most pronounced phenotype in SPARC null mice: Null mutants experience early onset cataract formation with 100% penetrance (Norose et al., 1998). SPARC is localized to the normal lens capsule to which immature cells of the lens remain attached prior to differentiation. Upon differentiation, lens cells elongate and detach from the basement membrane of the capsule, lose their organelles and become the well-ordered transparent cells of the lens. The lens cells in SPARC null mice are irregularly shaped and disordered suggesting a defect in differentiation and/or cell organization. Delany and coworkers (2000) have reported defects in bone formation resulting in late onset osteopenia in SPARC null mice. SPARC is a major component of bone and the phenotype suggests that SPARC plays a role in osteoclast and osteoblast differentiation. By blocking bFGF, PDGF and VEGF signaling and augmenting TGFβ levels (see section 6.1.1.3), SPARC likely impacts the differentiation of a host of other cell types.

6.1.1.5 SPARC and Wound Healing

Wound healing is a multifactorial and complex biological process that involves cell migration, ECM re-modeling a host of cytokines, growth factors and matrix metalloproteases (reviewed in Singer and Clark, 1999). With its ability to modulate many of these processes, it is not surprising that SPARC expression is increased at sites of injury (Reed et al., 1993). There are conflicting reports about the ability of SPARC

null mutants to recover from dermal wounds. Basu and coworkers (2001) found deficits in wound healing both in vivo and in vitro using fibroblasts cultured from SPARC null mice. The authors attribute the effect to poor cell migration which could be rescued by exogenous SPARC. Bradshaw and coworkers (2002) found that SPARC null mice exhibited faster than normal wound closure. The authors hypothesize that the effect is secondary with defects in collagen fibril formation resulting in weaker skin tensile strength and easier wound closure. Differences in the severity of the wound could help account for the discrepancies between the two studies. The effect of SPARC on wound healing may be complex and context dependent. With SPARC having an antagonistic effect on PDGF, bFGF and VEGF (all of whom have been documented to contribute to wound healing (reviewed in Bradshaw and Sage, 2001), levels of SPARC and the severity of the injury may tip the balance on the role of SPARC in wound repair. It is possible that, as in dermal wounds, SPARC may also be upregulated following nervous system injury. To support this idea, a study by Mendis and coworkers (1998) found increased SPARC mRNA levels following traumatic brain injury. Gillen and coworkers (1995) also observed upregulation of SPARC coincident with Wallerian degeneration in the peripheral nervous system.

SPARC is a multifunctional protein that is retained in tissues undergoing constant turnover, making it likely expressed by olfactory ensheathing cells to accommodate ORN turnover. SPARC can modify cell-ECM interaction, modulate growth factor activity and expression levels and influence angiogenesis and wound healing. All of these features could potentially help OECs to maintain a plastic environment for ORN axons and may also contribute to the regeneration and functional recovery found after OEC transplantation into spinal cord injury models (see section 1.2.6.1.2). With all of these considerations in mind, I decided to investigate the role of SPARC in the biological activity of LP-OEC conditioned media.

6.2 Results

6.2.2 Examining SPARC Expression in Cultured LP-OECs

Of the ten high certainty candidates, one of the most well represented was secreted protein acidic rich in cysteine (SPARC). To confirm the results of the ICAT screen, I initially looked for the presence of SPARC mRNA from passage 2 and passage 6 cell pellets used to generate conditioned media as well as postnatal day 5 olfactory epithelium, the tissue used to culture the LP-OECs. RNA was purified from all three samples and used as the template for reverse transcriptase reactions using a poly d-T primer to obtain cDNA. PCR reactions using SPARC primers confirmed the presence of SPARC in all three samples (figure 6.2A). By immunohistochemistry using a goat anti-SPARC antibody, SPARC was also expressed in cultured LP-OECs (figure 6.2B). Conditioned media was loaded normalized to the number of cells generating the media – in essence, to mimic the levels used in the outgrowth assays (Chapter 4). SPARC was detected in both samples and was detected at greater levels (33% ± 9.8% as determined by densitometry, n=3) in passage 2 compared to passage 6 conditioned media (figure 6.2C). However, when the cell pellets were analyzed for SPARC expression, there was considerably more SPARC detected in passage 6 LP-OECs than passage2, suggesting that older cells may retain rather than secrete SPARC (figure 6.2D). The blot was re-probed with anti-β actin to confirm equal loading

6.2.3 SPARC Expression in the Olfactory System

To further confirm SPARC expression by olfactory ensheathing cells, I examined the expression of SPARC in the olfactory system during development and maturity. It has been previously reported that SPARC is expressed in cartilage and bone (Sage et al., 1989) and not surprisingly, SPARC was detected in cartilaginous turbinates as well as the cribriform plate in the olfactory system (figure 6.3). At E14.5, cells immunolabelled with

SPARC were detected along GAP-43 positive ORN axons en-route to the olfactory bulb (figure 6.3A and 6.3B). SPARC was also expressed by ensheathing cell processes that surround ORN nerve bundles (figure 6.3D). Of note, SPARC signal overlaps with laminin in the lamina propria suggesting perhaps a functional relationship between the two (figure 6.3C). SPARC was also detected in OB-OECs aligned parallel to the nerve fibre layer (figure 6.3E) and along ORN axons entering glomeruli (see Appendix 6) and in the glomeruli themselves (figure 6.3E). In the adult, SPARC expression is decreased coincident with a more quiescent mature olfactory system (figure 6.3F).

6.2.4 SPARC Expression in the Injured Nervous System

It was possible that SPARC downregulation in adulthood reflects less ORN growth and pathfinding associated with a low basal rate of ORN turnover. To test this hypothesis I examined the expression of SPARC 12 days following unilateral bulbectomy, a timepoint during which ORN regeneration is robust (Struble et al., 2001). I wanted to examine if a synchronous wave of ORN regeneration would result in a coincident increase in SPARC expression. SPARC levels in ensheathing cells were elevated on both the lesioned and unlesioned sides following a unilateral bulbectomy compared to uninjured animals (figure 6.4A) but SPARC expression was more concentrated and potentially more highly expressed on the lesioned side by comparison (figure 6.4A and 6.4B). This expression pattern is consistent with ensheathing cell expression of SPARC being involved in ORN growth. Could the same be happening with OECs transplanted into spinal cord injury? In control animals 7 days post injury, there is a modest increase in SPARC levels likely expressed by GFAP-positive astrocytes (figure 6.4C). In the OEC-treated spinal cord, there is considerably more SPARC detected and neurofilament-positive axon sprouting into the lesion site is coincident with areas high in SPARC expression (figure 6.4D). While there is only a correlative relationship between SPARC and neural regeneration, it further suggested that SPARC might be an important contributor to the effect of LP-OEC conditioned media.

6.2.5 Gain-of-Function Studies with SPARC

Based on the data above, it was clear that SPARC was expressed in LP-OECs and in their conditioned media. In the olfactory system, SPARC was expressed in olfactory ensheathing cells of the lamina propria and olfactory bulb and expression appeared to be developmentally regulated. SPARC expression could be re-upregulated after bulbectomy and OECs transplanted into spinal cord injured animals appeared to express high levels of SPARC. This was sufficient evidence to suggest that SPARC may be an important component in LP-OCM. Therefore I decided to test the effect of SPARC on my outgrowth assay. Two forms of SPARC were used: recombinant mouse SPARC and recombinant human SPARC.

I generated recombinant mouse SPARC from the PCR product using RT reaction template obtained from passage 2 LP-OECs. The primers included additional flanking sequences for restriction sites to allow for directional insertion, a signal peptide to facilitate secretion and a c-terminus glycine hinge to minimize steric hindrance from V5 and His tag epitopes (figure 6.2B). The sequence was inserted into a pcDNA vector with C-terminus V5 epitope and 6xHis tag and lipofected into cos-7 cells. Cos-7 conditioned media was harvested and recombinant mouse SPARC (rmSPARC) was batch purified using nickel resin (for a more detailed description see section 2.7). Recombinant human SPARC (rhSPARC) was a gift from Dr. E. Helene Sage (University of Washington) (Bradshaw et al., 2000). Sf9 cells were transfected with baculovirus containing the human SPARC inserted into the gp67 coat protein gene for efficient expression. Conditioned media from sf9 cells was harvested and SPARC was purified using anion exchange chromatography. The authors reported that rhSPARC was properly glycosylated and biologically active as assayed by endothelial cell proliferation and mesangial cell collagen production. The Sage lab and others have since used the protein in subsequent studies as a reliable source of SPARC (for example: Sweetwyne et al., 2004; Yan et al., 2005).

Both rmSPARC and rhSPARC mediated significant increase in neurite outgrowth over NGF baseline levels (figure 6.5). Overall, rhSPARC (figure 6.5A) was more effective than rmSPARC (figure 6.5B), likely due a higher level of protein purity. The SPARC generated by the Sage lab was reported to be 95% pure as measured by circular dichroism (Bradshaw et al., 2000). rmSPARC was purified by nickel affinity chromatography from serum-containing media and was likely a less pure sample. Both SPARC samples exhibited a high degree of biological activity at 5 ng/ml and the effect dropped somewhat at 10 ng/ml.

6.2.6 Loss of Function Studies with SPARC

The Sage lab also generously provided function-blocking antibodies against different forms of SPARC (Sweetwyne et al., 2004). Antibody clone 236 (Ab 236) specifically blocks rhSPARC activity. Mouse SPARC (purified from parietal yolk sac; (Sage et al., 1989)) was specifically blocked by antibody clone 255 (Ab 255). By pre-incubating rhSPARC and rmSPARC with a 20-fold molar excess of Ab 236 and 255 respectively, the outgrowth activity was abolished (figure 6.6A). Reversing the antibodies did not affect rh- or rmSPARC outgrowth activity, which demonstrated the species specificity of Ab 236 and Ab 255 and acted as ideal isotype controls (figure 6.6A). Having worked out effective conditions to block SPARC activity, I applied these conditions to passage 2 and passage 6 conditioned media (figure 6.6B). In both cases, there was a general decrease in outgrowth when Ab 255 was added. No effect on outgrowth was detected when antibody was added alone. However, only in passage 2 conditioned media was there a statistically significant decrease. Additionally, LP-OECs were cultured from SPARC null mice (Norose et al., 1998) and passage 2 conditioned media was harvested from them. Antigenically, SPARC null LP-OECs appeared normal when labeled with anti-S100β, anti-GFAP and anti-p75, although there may be some subtle differences in cell adhesion (noticeable when passaging the cells). The biological activity of passage 2 SPARC null conditioned media was significantly less than passage 2 conditioned media from wild type LP-OECs, supporting the function-blocking experiments. However, the decrease in

total outgrowth for SPARC null mice is somewhat deceptive since the nature of the outgrowth was different. SPARC null conditioned media treated explants had less dense and potentially less branched outgrowth compared to wildtype (figures 6.7 A and B vs. C and D) but the average neurite carpet radius of SPARC null conditioned media is statistically indistinguishable from wild type passage 2 conditioned media and both conditions exhibited longer neurites than NGF baseline (figure 6.7E).

6.2.7 Studying the Mechanisms of SPARC Activity

Having established that SPARC promotes neurite outgrowth in my assay system, and that it is an important factor in the biological activity of LP-OEC conditioned media, I wanted to examine how SPARC was mediating this effect. Was the increase in outgrowth due to a direct effect of SPARC on neurites or was there a secondary effect on dividing cells that ultimately resulted in neurite outgrowth? I initially wanted to test this using a Campenot compartment culture system whereby neurites would be separated from cell bodies and I could not only examine the effect of SPARC on neurons alone but also individually examine the effect on cell body versus neurites. Unfortunately, I found that the growth was not reliable enough for quantitative analysis so I decided to use a much simpler method: kill the dividing cells in my assay prior to adding SPARC. To do so, I plated the explants in cytosine arabinoside (AraC) for two days baseline conditions before switching them to normal media with and without SPARC; this regimen eliminated approximately 85% of the dividing cells, even with the 2 extra days to recover in AraC-free media. Under these conditions, I found that the effect of SPARC was eliminated suggesting that SPARC may be acting secondarily via the dividing cells of the explant.

The effect of NGF on DRG explants is twofold. NGF not only mediates neurite outgrowth but also survival (reviewed in Bothwell, 1995). These two effects can be separated by using the MAP kinase inhibitor PD98059, which inhibits NGF-mediated outgrowth but not survival or spontaneous outgrowth when used at 50 μM (Sjogreen et al., 2000). In the presence of PD 98059, NGF baseline levels were largely the same as

untreated (figure 6.8B), suggesting that 1.5 ng/ml NGF is sufficient for survival but has little impact on outgrowth. NGF was necessary for DRG survival since in the absence of NGF or by using a pan-trk inhibitor K252a (Berg et al., 1992) no outgrowth was ever observed (data not shown). SPARC was still able to significantly increase outgrowth in the presence of PD, but the effect was greatly diminished compared to SPARC without PD. This suggests that SPARC may be acting through both a MAPK dependent and independent pathways to mediate outgrowth.

Since SPARC can be modulated by its association with ECM molecules (see section 6.1.1.2), I also examined the effect of removing laminin substrate from the outgrowth assay (figure 6.8C); all other parameters were kept the same only that the DRGs were grown on poly-L-lysine alone. Under these conditions, the outgrowth activity of SPARC was diminished significantly. Although there was a trend towards increased outgrowth, the difference was not statistically significant over NGF control levels. This result suggests that the outgrowth activity of SPARC is dependent on laminin and the modest increase in outgrowth with SPARC is likely due to laminin production by dividing cells in the explant.

These data suggest that the activity of SPARC is sensitive to the parameters of the assay. When the dividing cells were eliminated or laminin was removed from the assay, the ability of SPARC to promote neurite outgrowth was greatly diminished. Therefore it is likely that SPARC increases outgrowth via a secondary effect mediated by the dividing cells in the explant (predominantly Schwann cells). The effect appears to be dependent on laminin for its activity and signals partially but not entirely through the MAP kinase pathway.

6.2.8 Correlating Dividing Cell Number with Total Outgrowth

For some of the outgrowth assay conditions, I also labeled the dividing cell nuclei with DAPI (4'6-diamidino-2-phenylindole) to see if there was an effect on dividing cell number, density and distribution in response to SPARC. The dividing cells, most of

which are Schwann cells when explants of this age are cultured (Banker, 1998), should divide in proportion to the total amount of neurite outgrowth since neuregulin expression by neurites regulates Schwann cell number by acting as the rate limiting source of mitogens (reviewed in Lobsiger et al., 2002). To examine this relationship, I tested the correlation between total outgrowth and the total number of DAPI nuclei in the neurite carpet in NGF and SPARC-treated conditions (figure 6.9). Figure 6.9A and B show representative montages of DAPI nuclei associated with the explant. The ganglion and its associated DAPI signal was excluded and only the nuclei in the surrounding region were counted. A scatter plot correlating individual explant total growth versus DAPI nuclei number shows a significant difference between NGF baseline and SPARC-treated groups (figure 6.9C). There is much more outgrowth per dividing cell in the SPARC-treated versus NGF baseline condition. Grouping all of the data together as a ratio of total outgrowth divided by DAPI number, demonstrates that the difference between the two groups is statistically significant. There is a possibility that the disparity between the two ratios was due to a difference in DAPI nuclei density. To account for this, the number of DAPI nuclei per explant was divided by the neurite carpet area (figure 4.1C) to determine nuclei density. By this measurement, SPARC also had a lower DAPI nuclei density (figure 6.9D). Thus, the total amount of outgrowth attributed to each DAPI nuclei is significantly greater in SPARC-treated outgrowth assays, suggesting that SPARC may influence the phenotype dividing cells making them better able to promote neurite outgrowth.

I then tested if this correlation holds true for the outgrowth assays where SPARC's effect was greatly diminished or altogether abolished (figures 6.6 and 6.8). That is, I wanted to see if under those conditions if the total outgrowth attributed to each DAPI nucleus was similar to its NGF baseline control. Figure 6.10 compares the ratio of total outgrowth divided by total DAPI nuclei in outgrowth assays where SPARC activity is disrupted. In all of these conditions, the ratio of outgrowth to DAPI number is similar between SPARC-treated and NGF control groups. In both AraC- and PD 98059-treated groups, the ratio outgrowth to DAPI number is high because in both groups, there are fewer dividing cells in general. With AraC the reason is obviously that the mitotically active

cells are being killed off while with PD 98059, the decrease in cell number is most likely due to inhibition of the MAP kinase pathway. Maurel and Salzer (2000) demonstrated that neuregulin-based Schwann cell proliferation is dependent on PI3 kinase activation of the MAP kinase pathway. Regardless, the ratio of outgrowth to DAPI number is statistically indistinguishable between NGF baseline and SPARC-treated conditions in both AraC and PD-treated groups (figure 6.10A and B). There is a trend towards higher ratios in the PD and SPARC-treated group however. The outgrowth assay where laminin was not included in the substrate, SPARC outgrowth was abolished and this was coincident with equal ratio of outgrowth to DAPI number between control and treated groups (figure 6.10C). In the assay involving SPARC null conditioned media, the difference between ratios is also statistically insignificant (6.10D).

Figure 6.11 shows the relative difference in ratios of outgrowth per DAPI number between SPARC and NGF control groups. By showing the relative difference between the two ratios, there is a positive correlation between the difference in outgrowth per DAPI nucleus and the resulting total outgrowth. This correlation also supports the hypothesis that the role of SPARC is to increase the ability of dividing cells to promote outgrowth.

6.3 Discussion

6.3.1 SPARC expression in the olfactory system

SPARC is expressed at higher levels during the development of the olfactory system than in maturity. This trend makes sense with regard to the degree of turnover and ORN growth during embryonic development and neonatally and the lower, basal rate exhibited during adulthood. A molecule known for 'loosening up' ECM, modulating growth factor activity, cell adhesion and angiogenesis (see section 6.1.1.1) would certainly be useful and conducive to ORN pathdfinding and growth. And certainly, OECs are advantageously situated to provide SPARC when needed. It has also been suspected that SPARC may play a role in establishing synaptic connections (Mendis et al., 1995) and expression of SPARC in developing glomeruli also suggests that this may be the case.

A unilateral bulbectomy lesion to the olfactory system causes a distal axotomy of all ORNs that have reached the nerve fibre layer of the olfactory bulb. ORNs die rapidly following injury, leaving a void for newly generated ORNs to attempt to grow back into the olfactory bulb. SPARC is upregulated by OECs in this scenario, likely to re-create an environment conducive to ORN axon growth. SPARC was also upregulated on the uninjured side, although not to the same degree, consistent with previous studies where growth and survival factors were upregulated bilaterally following unilateral bulbectomy (reviewed in Carter and Roskams, 2002). This pattern of expression also suggests that SPARC could be involved in the outgrowth-promoting properties of SPARC.

6.3.2 The Role of SPARC in OEC Repair of Spinal Cord Injury?

Perhaps even more intriguingly, the ability of OEC to upregulate SPARC expression following injury could have multiple effects in cell transplantation experiments into spinal cord injury. Firstly, OECs reduce cavitation and in its place is a lesion site into which many axons sprout (see section 1.2.6.1.2). SPARC could be modulating the local

ECM environment within the lesion site resulting a more 'porous', less adhesive environment through which to grow. Secondly, SPARC can be cleaved by matrix metalloprotease-3 to yield a highly angiogenic (K)GHK peptide (Sage et al., 2003). Ramer and coworkers (2004) report increased local angiogenesis that appeared to radiate from the lesion site – potentially, SPARC could be involved in this phenomenon. Thirdly, several groups have reported Schwann cell infiltration following spinal cord injury (Boyd et al., 2004; Ramer et al., 2004b; Ruitenberg et al., 2003; Sasaki et al., 2004; Takami et al., 2002). In the context of the neurite outgrowth assay, SPARC appears to act secondarily by making Schwann cells more neurotrophic. Might the same phenomenon be taking place at the lesion? Of course, with Schwann cells and OECs sharing so many of the same characteristics (see section 1.2.5.1), SPARC could also be having an autocrine/paracrine effect signalling OECs to become more neurotrophic as well.

6.3.3 SPARC Gain- and Loss-of-Function Experiments Using the Outgrowth Assay

Gain-of-function experiments strongly suggest that SPARC increases the total outgrowth in this neurite outgrowth assay. Comparing the total growth in passage 2 LP-OCM with SPARC at optimal concentration (5 ng/ml), they are very similar (155315 μm to 170780 μm). In fact, they are statistically indistinguishable ($p = 0.588$). One interpretation is that all of the outgrowth-promoting properties of LP-OCM can be attributed to SPARC. This is however unlikely. Conditioned media from SPARC null mice was still able to increase total outgrowth, although not to the degree of wild type conditioned media. Also, an analysis of average neurite carpet radius between SPARC null and wild type P2 LP-OCM shows that both conditions increase neurite above control levels and the difference between the two is not significant. Both data are suggestive of other factors present in conditioned media that also contribute to the biological activity of LP-OCM. The fact that SPARC alone was able to increase outgrowth to levels similar to P2 LP-OCM, suggests that there could be inhibitors of neurite outgrowth also present in conditioned media.

The function-blocking antibody studies strongly suggest that SPARC plays a significant role on in the biological activity of LP-OEC conditioned media. Addition of Ab255 to the cultures reduced total outgrowth in both passage 2 and passage 6 conditioned media-treated explants (figure 6.6B). Even with Ab 255, passage 2 conditioned media was still able to promote outgrowth significantly above NGF baseline. Again, this suggests that other factors may contribute to the biological activity of LP-OCM. In the case of passage 6 media however, the effect of the Ab255 was not statistically significant. This suggests that SPARC is a less important component of the outgrowth activity in passage 6 conditioned media.

By ICAT analysis and confirmed by Western blotting, passage 2 conditioned media contains more SPARC than passage 6. Counter to this, passage 6 LP-OEC cell lysates contained more SPARC than passage 2. In both cases, the samples were normalized to cell number and in the case of the cell lysate, were confirmed by re-probing with β-actin. These results are not readily reconcilable. It is possible that there were errors in counting the cell numbers generating the media or making up the cell lysate. However, SPARC was more strongly detected in passage 2 conditioned media and yet far less SPARC was detected in passage 2 cell lysate. This would have required a gross miscounting of cell number. The other explanation is that passage 6 LP-OECs, as a result of senescence, lose the ability to effectively traffic and secrete SPARC. Intracellular localization of SPARC in lens epithelial cells (Yan et al., 2005) and Xenopus embryos (Huynh et al., 2000) has been reported. In the case of cultured lens epithelial cells, they actively internalize exogenous rhSPARC. The function of intracellular SPARC is not well understood and why passage 6 LP-OEC would retain or actively take up SPARC is an interesting question. Perhaps SPARC is internalized upon binding to its receptor to effect downstream signaling pathways and LP-OECs are more responsive to SPARC as they sensesce in culture.

The manner in which SPARC null LP-OCM promotes outgrowth bears further discussion. While there is less total outgrowth, the neurite radius is still similar to wild type passage 2 media. A closer look at the neurites in SPARC null and wild type

conditioned media-treated explants suggests that the neurites are less branched and overall less dense. It is interesting to speculate that two distinct modes of neurite outgrowth promotion could be at play between the two conditioned media samples. Perhaps SPARC, in addition to increasing length, also promotes branching and plasticity while unknown factor(s) present in SPARC null conditioned media only increases length without promoting branching. Perhaps the unknown factor is present in wildtype conditioned media but its effect is masked by SPARC. Or alternatively, this unknown factor is upregulated by SPARC null OECs as a compensatory mechanism in the absence of SPARC. This is an issue that should be examined in future as it could have important implications for OEC-mediated spinal cord repair. Factors that can increase branching and neurite length could be useful for initiating novel local neural circuitry. Factors that just drive neurite length alone are useful to possibly repair axon tracts where branching would be undesirable. Perhaps by identifying these types of factors with different ways of promoting growth, more directed methods could be used for treating injury in the CNS.

6.3.4 Studying Mechanisms of SPARC Activity By Using the Modularity of the Outgrowth Assay

In retrospect, the parameters of the outgrowth assay provided an ideal platform for elucidating mechanisms underlying SPARC activity. The dorsal root ganglion explant proved to be a robust culture system with multiple components that could be removed piece-by-piece to show if each piece was necessary for the activity of the growth factor.

6.3.4.1 Removal of Nerve Growth Factor

The first component I removed was NGF. I took away the outgrowth-promoting properties of NGF and looked to see if the bioactivity of SPARC was left intact. I found that while SPARC-treated explants still grew significantly better than controls, its effect

was significantly diminished compared to SPARC without PD 98059 inhibitor (see figure 6.8B). This finding can be interpreted in a number of ways. (1) SPARC's action is partially dependent on the MAP kinase pathway. (2) With inhibition of MAPK, Schwann cell proliferation was greatly affected resulting in decreased outgrowth by SPARC. (3) The neurotrophic support given by the Schwann cells acts through the MAPK pathway. Without additional experiments, it is not easy to interpret the results. I do, however, favour the second hypothesis because there is a noticeable decrease in DAPI-positive nuclei in explants treated with PD 98059. In addition to inhibiting NGF's outgrowth ability, I also used K252A, a pan-trk inhibitor (Berg et al., 1992) to block all NGF signaling. With every explant grown with either the inhibitor or in the absence of NGF, no growth was observed. I tried these conditions supplemented with passage 2, passage 6, SPARC null and rhSPARC also with no explant survival. Thus, I conclude that NGF is necessary for this outgrowth assay and the conditioned media used in its present concentrations was not able to mediate embryonic DRG survival.

6.3.4.2 Removal of Dividing Cells

The second component of the outgrowth assay I removed was the dividing cells. The neurites grow on a carpet of Schwann cells (predominantly, but also fibroblasts) that migrate out of the explant to where neurites are present. There are complex interactions occurring between the two cell types with axonal neuregulin regulating Schwann cell number and differentiation (reviewed in Lobsiger et al., 2002) and Schwann cells influencing neuronal survival and growth (reviewed in Corfas et al., 2004). Schwann cells were eliminated by adding AraC to the media for two days, followed by two days growth with SPARC. Under these conditions, the ability of SPARC to promote outgrowth was abolished (figure 6.8A). The simplest explanation is that SPARC acts on Schwann cells, which are then more effective in promoting outgrowth. Another possibility is that AraC could have rendered the neurites incapable of responding to SPARC, thus NGF control and SPARC-treated groups would exhibit similar outgrowth. This is unlikely since many groups have shown that cultured neurons are responsive to

growth factors for differentiation, growth and survival even when grown in the presence of AraC (for example: MacInnis and Campenot, 2002; Tucker et al., 2005). At high concentrations, AraC has been reported to induce neuronal apoptosis (Leeds et al., 2005; Martin et al., 1990) however only at concentrations 10-50 times the concentration used in this study (10 μM). Also, the AraC is washed from the culture before testing SPARC – after 2 days in 10 μM AraC, the media was changed to SPARC-containing media without AraC for an additional 2 days. Subjectively, the overall health of the cultures was not noticeably different than the explants grown in other conditions.

That SPARC is nullified by removing dividing cells from the culture is consistent with the DAPI analysis results. Under normal conditions, axonal neuregulin drives Schwann cell proliferation and regulates their population size and maturity (reviewed in Lobsiger, 2002). SPARC appears to interfere with this relationship since the density of DAPI nuclei is significantly reduced (figure 6.9E). This correlates with increased outgrowth overall and therefore increased outgrowth per Schwann cell. It is possible that the decrease in Schwann cell proliferation and increase in outgrowth are linked. The data suggest that the proliferation via neuregulin is being affected by SPARC. Could SPARC also be affecting Schwann cell differentiation – perhaps keeping them in a more growth-promoting state? The capacity for promoting axon growth at different stages of Schwann cell maturity is not well understood. However, based on what is known about SPARC and its downstream effects and the factors that regulate Schwann cell differentiation, possible links can be made (see section 6.3.6).

6.3.4.2 Removal of Laminin

The final component that I removed from the outgrowth system was laminin in the substrate. When the explants were grown on poly-L-lysine alone, even with everything else still in place, the effect of SPARC was greatly attenuated if not entirely eliminated (figure 6.8C). With SPARC activity intertwined with ECM binding, perhaps this result is not entirely surprising. The small increase in outgrowth observed in the SPARC-treated

versus NGF baseline group can be attributed to laminin or other ECM molecules produced by the dividing cells. Based on these results, I tried looking at SPARC-laminin binding from another angle. SPARC was added with the substrate and incubated overnight. I hoped that SPARC would have a chance to form a strong attachment to the laminin and when the explant was grown on this substrate, it would mimic the effect of having SPARC in the media. Unfortunately, I did not find a difference between this condition and NGF baseline controls. It is possible that in the process of washing the substrate, the relatively weak interaction between SPARC and laminin was disrupted and most of the SPARC washed off.

6.3.5 Correlation Between Schwann Cell Number and Total Outgrowth

In SPARC-treated explants an inverse trend emerges between Schwann cell density and total outgrowth (figure 6.9-6.11) resulting in increased outgrowth per DAPI-positive nucleus. As components of the outgrowth assay are systematically removed, the outgrowth activity of SPARC is attenuated or altogether eliminated, accompanied by outgrowth to DAPI ratios indistinguishable from NGF controls (figures 6.10 A-C). The two effects mirror one another through all of the conditions such that as the total amount of outgrowth per DAPI nucleus increases, so does the total outgrowth in total (figure 6.11) and the trend continues with SPARC null conditioned media (figure 6.10D). This strongly suggests that total outgrowth and SPARC's influence on Schwann cells are interrelated.

6.3.6 A Putative Pathway for SPARC Outgrowth Activity

The outgrowth assay used to test LP-OEC conditioned media can be thought of as a modular system. Taking away a module, any module, undermines SPARC's ability to mediate neurite outgrowth. The dependence of SPARC on NGF, Schwann cells in the explant as well as laminin is telling of its mode of action. SPARC appears to act

indirectly by influencing Schwann cells. It appears to slow or prevent their proliferation and the result is an overall increase in both total neurite outgrowth as well as increased neurite length. It does not appear to be a stand-alone survival factor for embryonic DRG neurons as it cannot compensate for a lack of NGF or when grown with K252A trk inhibitor. Its influence on Schwann cells both with respect to regulating cell density and total outgrowth appears to require laminin.

These results can be reconciled by previous studies on SPARC's downstream effects and Schwann cell development. As mentioned previously in section 6.1.1.3, SPARC can influence TGF-β expression. The two factors have been reported to have a positive feedback loop where expression of one increases the expression of the other (Francki et al., 1999; Reed et al., 1994). It has been proposed that TGF-β interacts with SPARC via an intermediate protein: latent TGF-β binding protein (LTBP-1, reported in the ICAT dataset, Table 5.1) (reviewed in Bradshaw and Sage, 2001) leading downstream to release of TGF-β from its latent complex thereby activating it (Annes et al., 2004; Nunes et al., 1997). LTBP-1 and the bound, inactive form of TGF-β are associated with ECM via transglutaminase-mediated cross-linking. SPARC is also a substrate for transglutaminase (Aeschlimann et al., 1995) and it may be via this crosslinking that the two pathways intersect. The association with ECM by both molecules could account for SPARC's dependence on laminin. The prevalent view in the field is that fibronectin is the intervening ECM molecule (Annes et al., 2004; Taipale et al., 1996). It might be worthwhile to see if fibronectin can replace or even improve upon laminin as a partner in SPARC-mediated outgrowth. Additionally, Francki and coworkers (2004) have found interaction of SPARC TGF-β and TGF receptor II but only when all three components are present. The authors suggest that the interaction may be via a SPARC-receptor complex, which leads to increased downstream effect upon ligand binding. Therefore, SPARC may also potentiate the effect TGF-β signaling.

6.3.6.1 The Effect of TGF-β on Schwann Cells

SPARC activation of TGF-β in Schwann cells could be having multiple effects and

interpretation is made more difficult by the conflicting data as to the role of TGF-β in Schwann cell biology. When grown as a purified culture, TGF-β is a potent Schwann cell mitogen (Eccleston et al., 1989; Watabe et al., 1994). However, in co-culture with neurons, TGF-β inhibits Schwann cell proliferation (Einheber et al., 1995; Guenard et al., 1995b), consistent with SPARC inhibiting Schwann cell proliferation in the explant (figure 6.9). TGF-β1 has also been shown to both be necessary for proper myelination (Day et al., 2003) and also inhibitory to a pro-myelinating phenotype (Atanasoski et al., 2004; Awatramani et al., 2002; Guenard et al., 1995a). TGF-β also regulates Schwann cell production of growth factors and cell adhesion molecules. In purified Schwann cell cultures, TGF-β decreases NT-3 mRNA stability (Cai et al., 1999), and upregulates LIF (leukemia inhibitory factor) expression (Matsuoka et al., 1997). NCAM and L1 are also upregulated in purified Schwann cells in response to TGF-β (Stewart et al., 1995). TGF-β, in combination with TNF-α, has also been implicated in Schwann cell apoptosis (Skoff et al., 1998).

While these results appear disparate, even contradictory, it is possible that they can be reconciled. In cultures of Schwann cells alone, TGF-β appears to induce proliferation and upregulate pro-survival factors such as LIF and growth promotive CAMs such as L1 and NCAM (Stewart et al., 1995). This makes biological sense with respect to Schwann cells forming a growth tube following peripheral nerve injury in the absence of axonal contact (reviewed in Liuzzi and Tedeschi, 1991). Cytokines such as TNF-α are also upregulated shortly following injury, and in combination with TGF-β, could be facilitating Wallerian degeneration. However, when Schwann cells are in contact with axons, the effect of TGF-β is altogether different. Here TGF-β in some ways antagonizes the effects caused by axon contact. Consistent with this, TGF-β expression by Schwann cells is downregulated upon contact with axons (Einheber et al., 1995). However, myelination is not normal in the absence of TGF-β (Day et al., 2003) which suggests that it may be required again later on in Schwann cell maturity. A similar relationship exists with Schwann cells and neuregulin where it is needed as a mitogen early on (reviewed in Lobsiger et al., 2002) and then later to regulate myelin sheath size (Michailov et al.,

2004).

6.3.6.2 SPARC-Mediated Neurite Outgrowth Via TGF-β Signaling

Given this, how does SPARC's influence on TGF-β expression and signaling result in increased neurite outgrowth? The effect of TGF-β on purified cultures of Schwann cells is not directly applicable to the outgrowth assay. The outgrowth assay has a more complex neuron-glia relationship where myelination and neuregulin-mediated Schwann cell proliferation are reportedly disrupted (Einheber et al., 1995). In this system, I propose three alternate hypotheses through which SPARC via TGF-β could be promoting neurite outgrowth (figure 6.12B). (1) SPARC increases TGF-β expression (Francki et al., 1999; Reed et al., 1994) and therefore increases TGF-β signaling. (2) SPARC releases TGF-β from its latent state by its co-localization with ECM via LTBP-1 (LTBP-1 was found in the ICAT dataset, Table 5.1). This may account for why the effect of SPARC is eliminated when laminin is not added to the system. (3) SPARC potentiates TGF-β signaling via modulation of ligand-receptor interactions (Francki et al., 2004). These three hypotheses are not mutually exclusive. In fact, all three could be happening concurrently.

It has been suggested that TGF-β induces Schwann cells in co-culture to adopt a non-myelinating phenotype (Guenard et al., 1995a; Mews and Meyer, 1993) and defects in myelination have been observed when exogenous TGF-β is added to an in vitro myelination system (Einheber et al., 1995; Guenard et al., 1995a). I hypothesize that in addition to its role in regulating myelination, SPARC increases TGF-β signaling even in the presence of neurons. This interferes with neuregulin signaling and consequently interferes with Schwann cell transition to a pro-myelinating phenotype. Instead, the Schwann cells either adopt or retain a growth tube-like, outgrowth promoting state which results in increased total outgrowth and decreased Schwann cell proliferation (see figure 6.12). This assertion is supported by the following: When purified Schwann cells are

treated with TGF-β, they proliferate and express growth-promoting molecules such as L1 and NCAM (Stewart et al., 1995). After sciatic nerve injury, treatment of the distal stump with TGF-β results in improved nerve regeneration (Rufer et al., 1994). Upon contact with axons, TGF-β is downregulated and loss of contact leads to upregulation. It has been suggested that TGF-β may drive Schwann cell differentiation to a growth-promoting state as it coincided with formation of Schwann cell growth tubes following neural injury (Rogister et al., 1993; Scherer et al., 1993). More recent work has also corroborated these conclusions (Gordon et al., 2003; Sulaiman and Gordon, 2002). In these studies the authors treated denervated distal stumps with TGF-β and waited long periods of time (up to 6 months). Normally, with prolonged denervation, regeneration back into the distal stump is poor. In the TGF-β treated groups, the recovery was significantly better. Therefore, while SPARC may also be affecting other processes in the outgrowth assay, these studies strongly indicate that TGF-β signaling should be examined further.

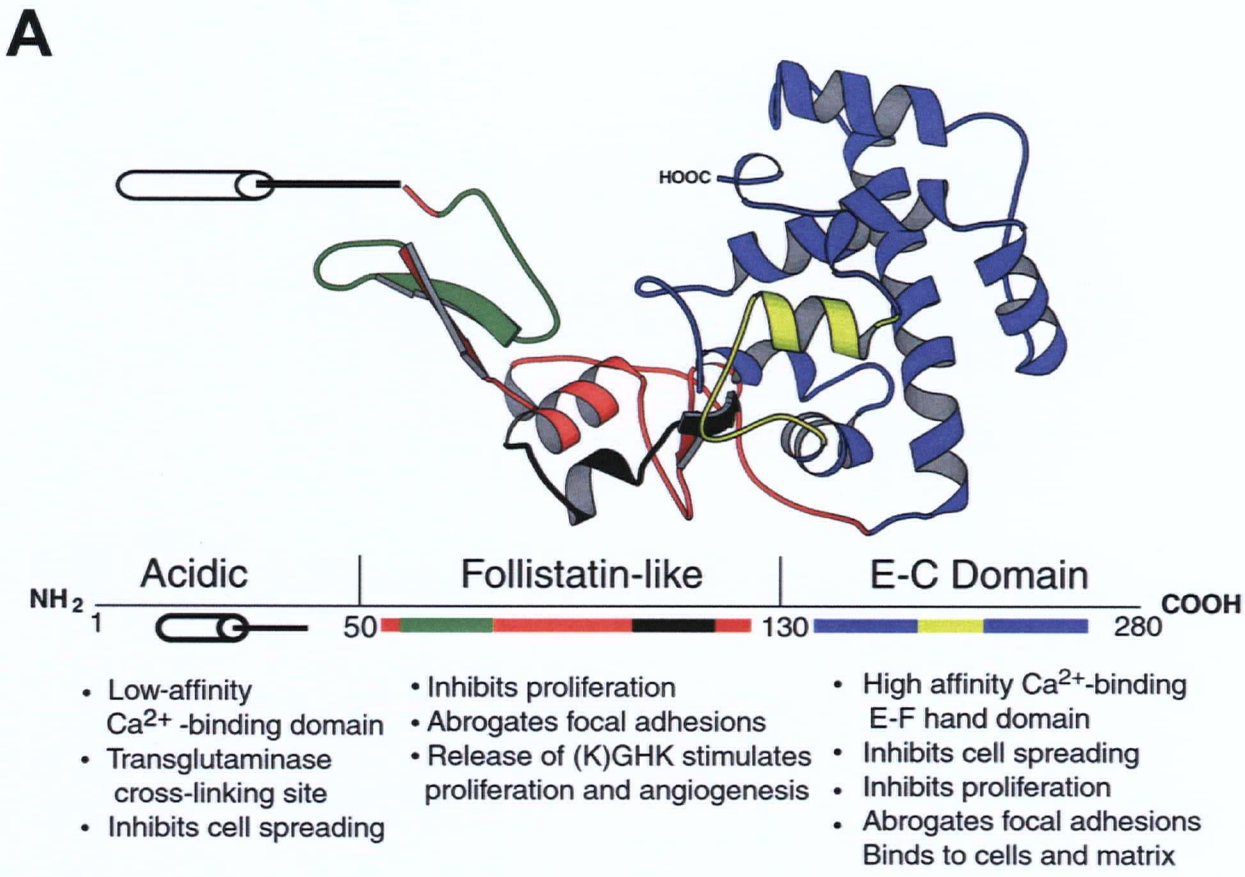

FIGURE 6.1
Schematic Diagrams of SPARC and Recombinant Mouse SPARC
(A) Secreted protein acidic rich in cysteine (SPARC) has three domains: (1) an N-terminus acidic domain (white), (2) a follistatin domain (red and black) and (3) a C-terminus extracellular matrix binding domain (blue and yellow). Summarized below each domain are its putative functions. From Bradshaw and Sage (2001) Journal of Clinical Investigation 109(9): 1045-1054. (B) A schematic diagram of recombinant mouse SPARC used in this study. The mouse SPARC sequence was obtained from passage 2 LP-OEC reverse transcriptase product. Flanking the sequence from the N-terminus is a start site (green) and an Ig-k chain leader sequence to facilitate secretion (blue). On the C-terminus, a glycine hinge (purple, to minimize steric hindrance) joins SPARC to a V5 epitope (light blue), a 6xHis tag (lime green) and a stop codon (red).

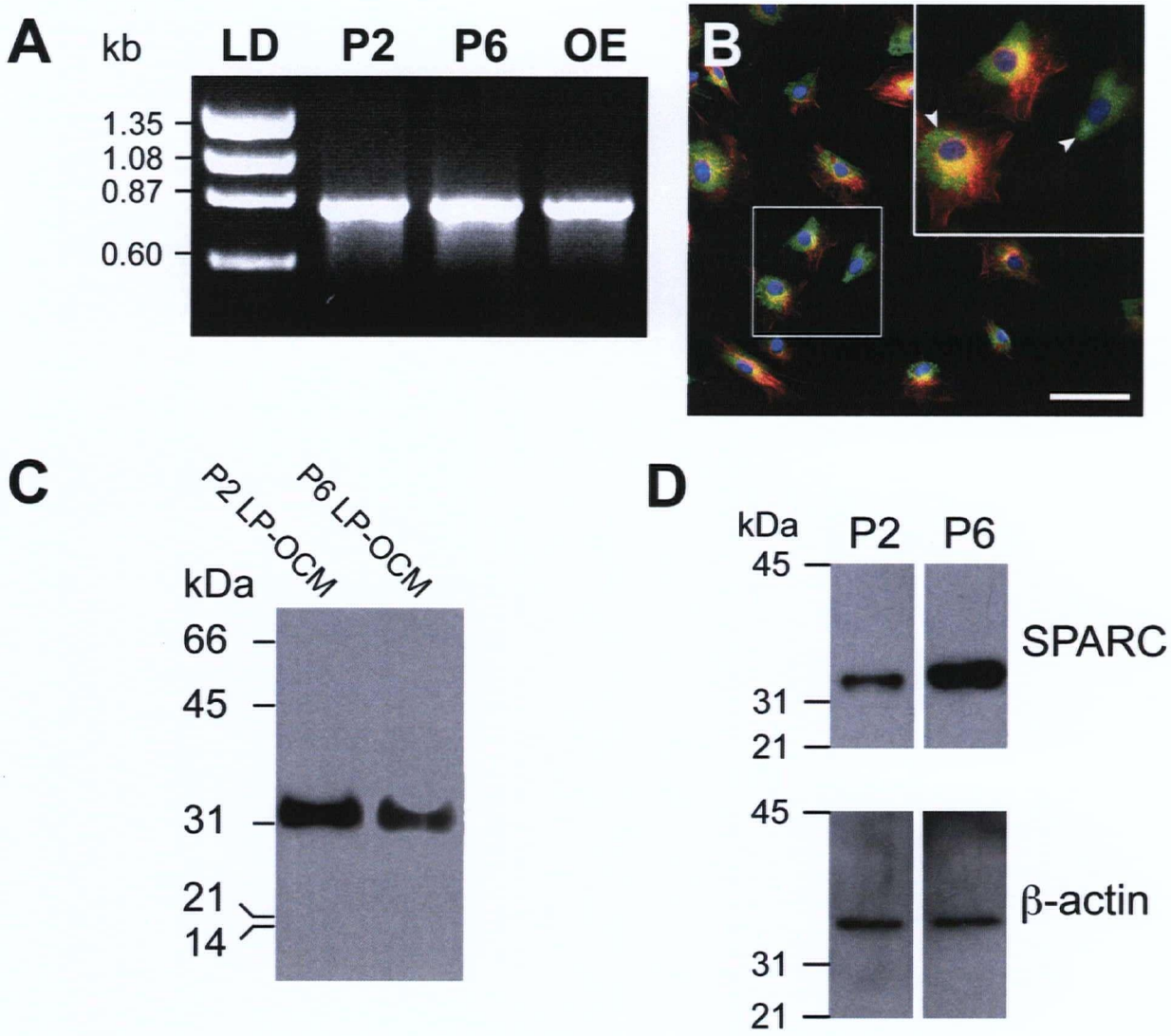

FIGURE 6.2
SPARC Expression in Cultured LP-OECs and LP-OEC Conditioned Media
(A) SPARC PCR product from RT reactions obtained from passage 2 and passage 6 LP-OECs and postnatal day 5 olfactory mucosa tissue. (B) LP-OECs are labeled with S100β (red), SPARC (green; yellow is overlap) and DAPI (blue). Inset is a higher magnification of box showing SPARC-containing vesicles (arrowheads). (C) Western blot of passage2 and passage 6 conditioned media probed with goat anti-SPARC. Sample loading was normalized to number of cells (30 000 LP-OECs) generating media. (D) Western blot of passage 2 and passage 6 cell pellets probed with mouse anti-b actin and goat anti-SPARC. Abbreviations: LD = DNA ladder; P2 = passage 2; P6 = passage 6; LP-OCM = lamina propria derived olfactory ensheathing cell conditioned media. Scalebar represents 100 microns.

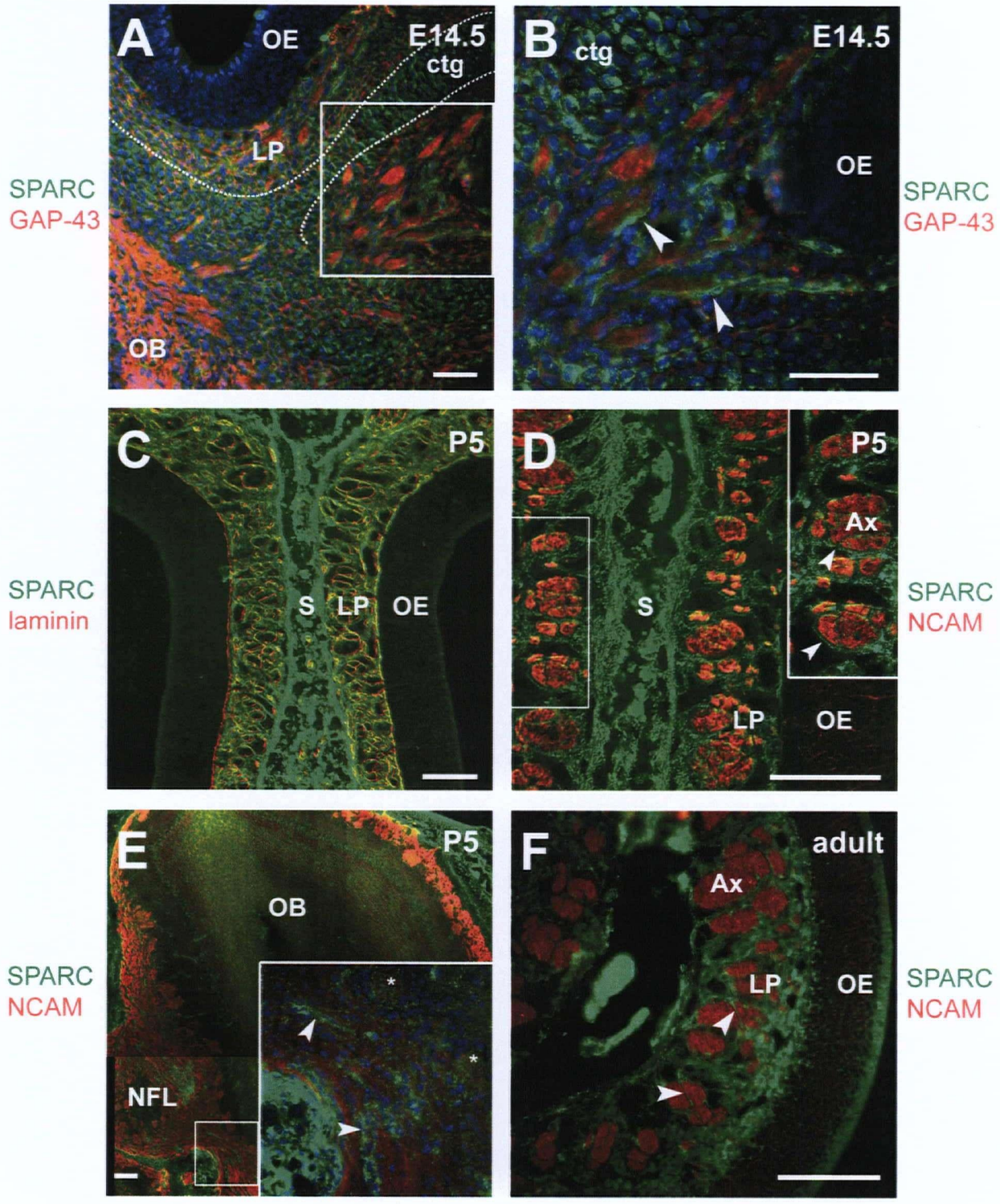
A
OE
E14.5
ctg
LP
OB
B
ctg
E14.5
OE
SPARC
GAP-43
SPARC
GAP-43
C
P5
S
LP
OE
D
P5
Ax
S
LP
OE
SPARC
laminin
SPARC
NCAM
E
P5
OB
NFL
F
adult
Ax
LP
OE
SPARC
NCAM
SPARC
NCAM

FIGURE 6.3

FIGURE 6.3
SPARC Expression in the Olfactory System
SPARC is expressed by olfactory ensheathing cells developmentally and also in adulthood. (A and B) The olfactory system at embryonic day 14.5 is immunolabeled with GAP-43 (red), SPARC (green) and DAPI (blue). OECs and cartilage are labeled with goat anti-SPARC (green) (B) Higher magnification of box in A. Arrowheads indicate OECs co-migrating with growing ORNs (red). (C and D) Postnatal day 5 olfactory mucosa immunolabeled with SPARC (green). (C) SPARC expression overlaps with laminin (red). (D) SPARC immunolabels OEC ensheathement (green, arrowhead) of NCAM positive ORN axon bundles (red). (E) Postnatal day 5 olfactory bulb immunolabeled with SPARC (green) and NCAM (red). SPARC is found in OB-OECs along the nerve fibre layer (arrowheads) as well as in the glomeruli (asterisks). (F) Adult olfactory mucosa labeled with SPARC (green) and NCAM (red). Arrowheads indicate OEC ensheathement (green). Abbreviations: OE = olfactory epithelium; LP = lamina propria; S = nasal septum; ctg = cartilage; Ax = axon bundle; OB = olfactory bulb; OEC = olfactory ensheathing cell; ORN = olfactory receptor neuron; NCAM = neural cell adhesion molecule; GAP-43 = growth associated protein 43 kDa. All scalebars represent 100 μm.

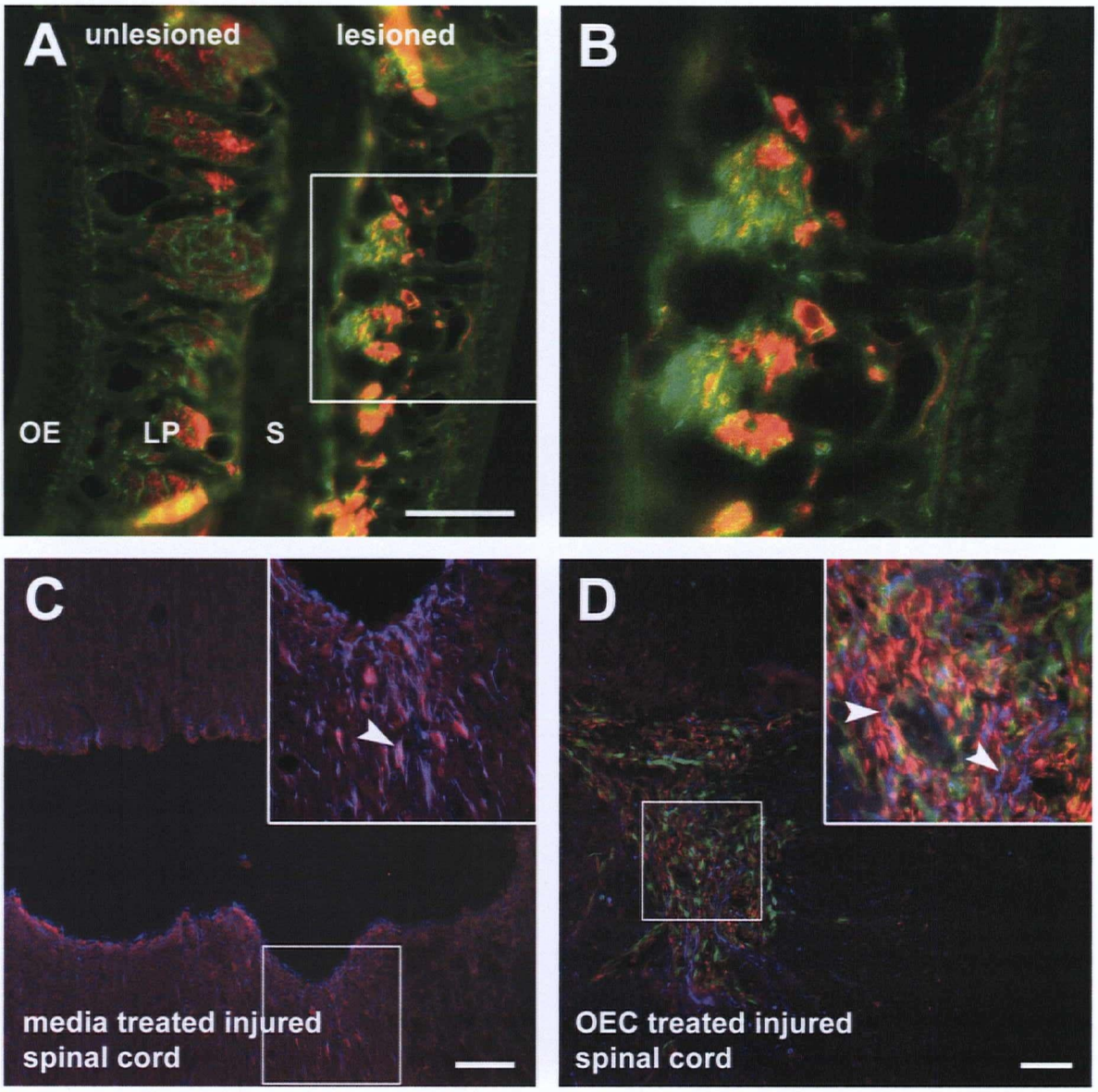

FIGURE 6.4
SPARC Expression After Nervous System Injury
(A and B) Adult mouse olfactory mucosa at the septum 12 days following bulbectomy is labelled with GAP-43 (red) and SPARC (green). SPARC signal in ensheathing cells is stronger on the lesioned side. (B) Higher magnification of box in A. (C and D) Transverse section of spinal cord 7 days following rubrospinal crush lesion. (C) Media-injected control animal immunolabeled with GFAP (blue), SPARC (red) and a large cavity is present (black). Higher magnification inset show GFAP-positive astrocytes (blue, arrowhead) co-labeled with SPARC (red). (D) OEC-treated animal immunolabeled with neurofilament (blue) and SPARC (red); olfactory ensheathing cells express GFP (green). Higher magnification inset shows OECs (green) co-labeled with SPARC (red) and neurofilament-positive axons (blue, arrowheads) growing in SPARC-rich regions (red).

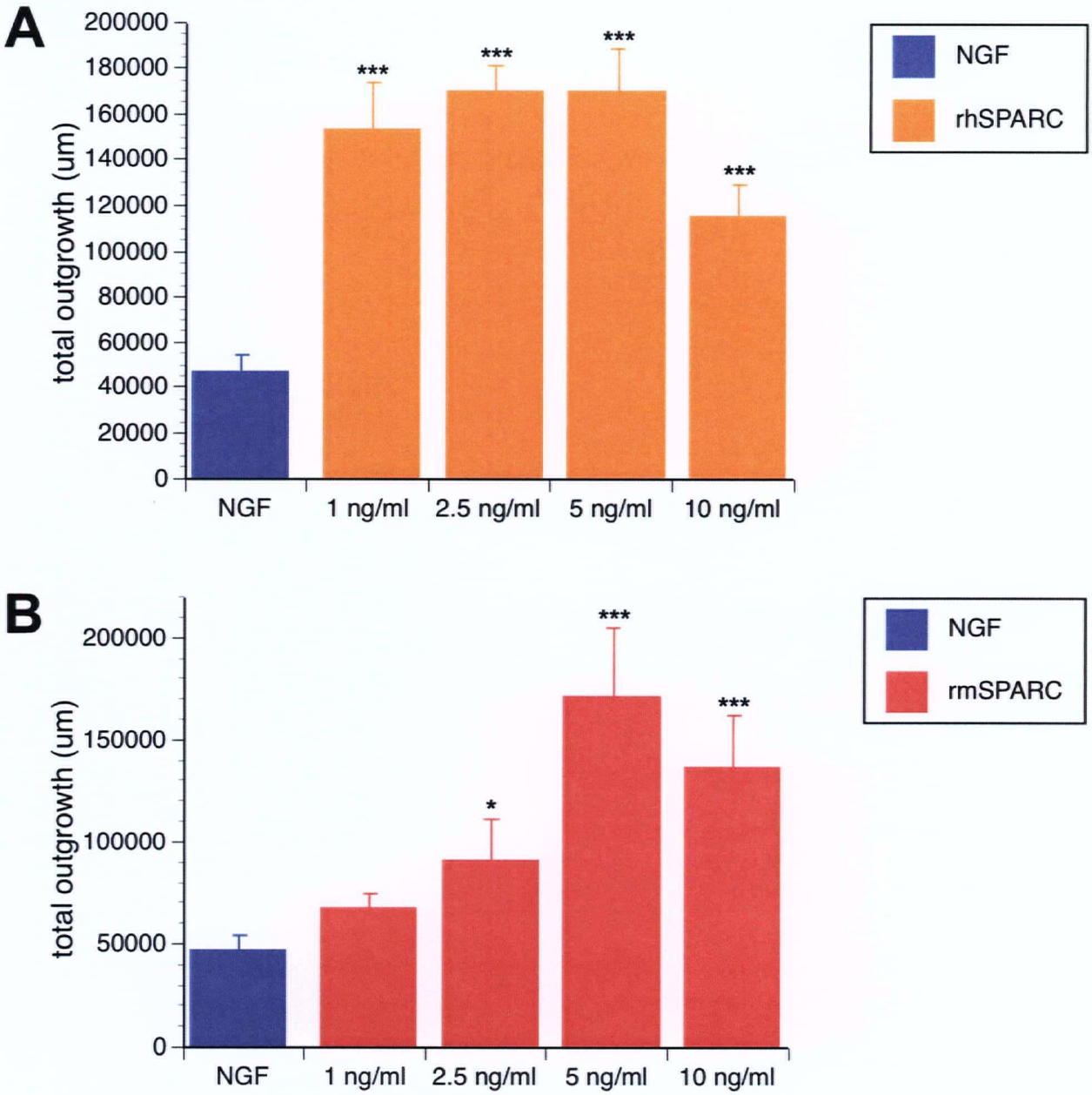

FIGURE 6.5

Recombinant Human and Recombinant Mouse SPARC Promote Neurite Outgrowth

(A) Recombinant human SPARC (rhSPARC, orange) and (B) recombinant mouse SPARC (rmSPARC, red) was added to baseline outgrowth conditions at increasing concentrations. All concentrations of rhSPARC and three of the rmSPARC concentrations tested exhibited significantly increased outgrowth over NGF baseline (blue). Asterisks: * is $p < 0.05$; * is $p < 0.005$; *** is $p < 0.0005$.

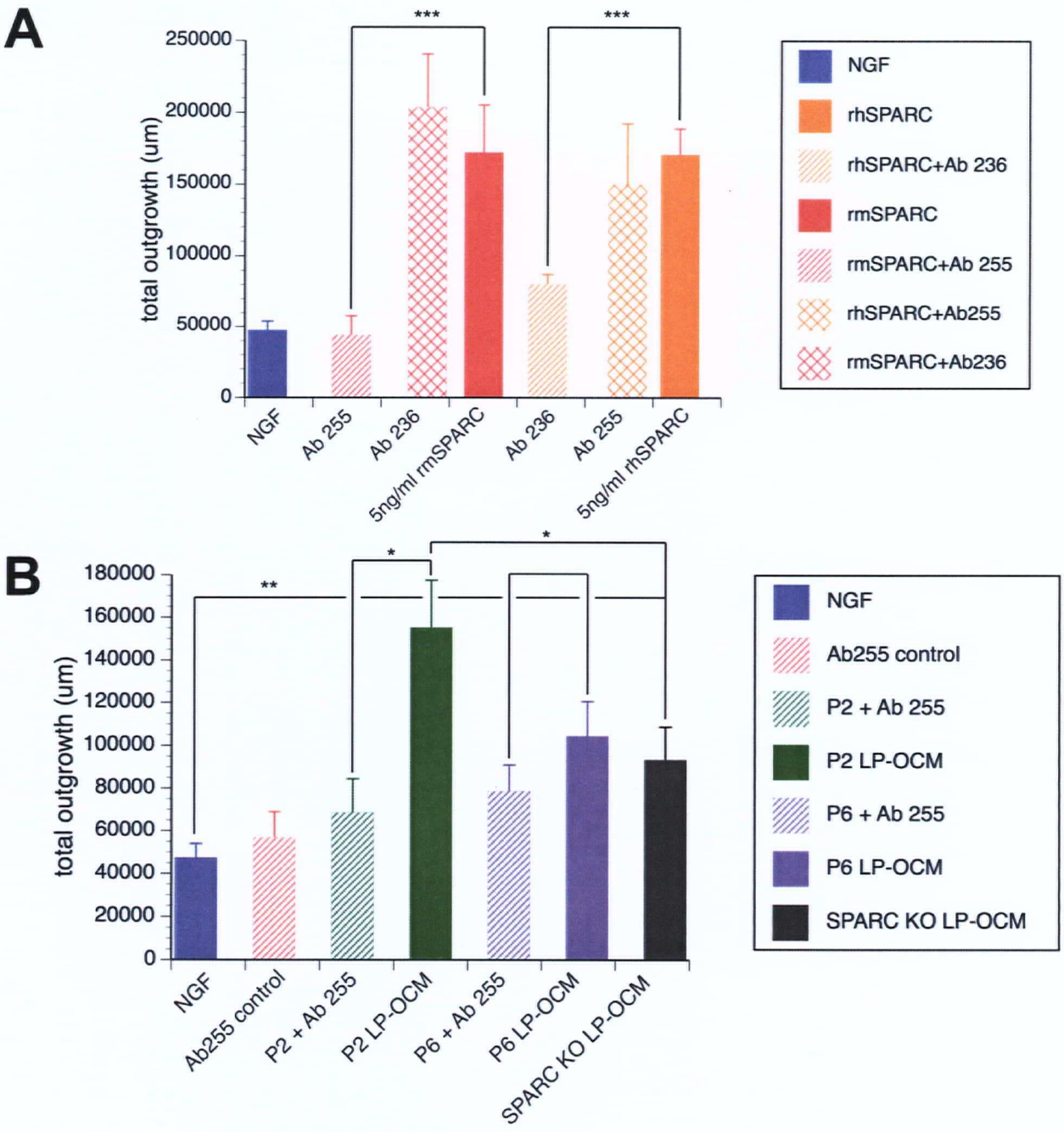

FIGURE 6.6
SPARC Loss-of-Function Experiments
(A) The increase in neurite outgrowth by both recombinant mouse (rmSPARC) and recombinant human (rhSPARC) SPARC is attenuated by adding function-blocking antibodies specific to mouse (Ab 255) and human (Ab 236) SPARC. (B) Addition of Ab 255 to passage 2 and passage 6 conditioned media decreases total outgrowth. Passage 2 conditioned media generated from SPARC knockout LP-OECs promotes neurite outgrowth above baseline levels but significantly less than wild type passage 2 conditioned media. Asterisks: * is $p < 0.05$; * is $p < 0.005$; *** is p

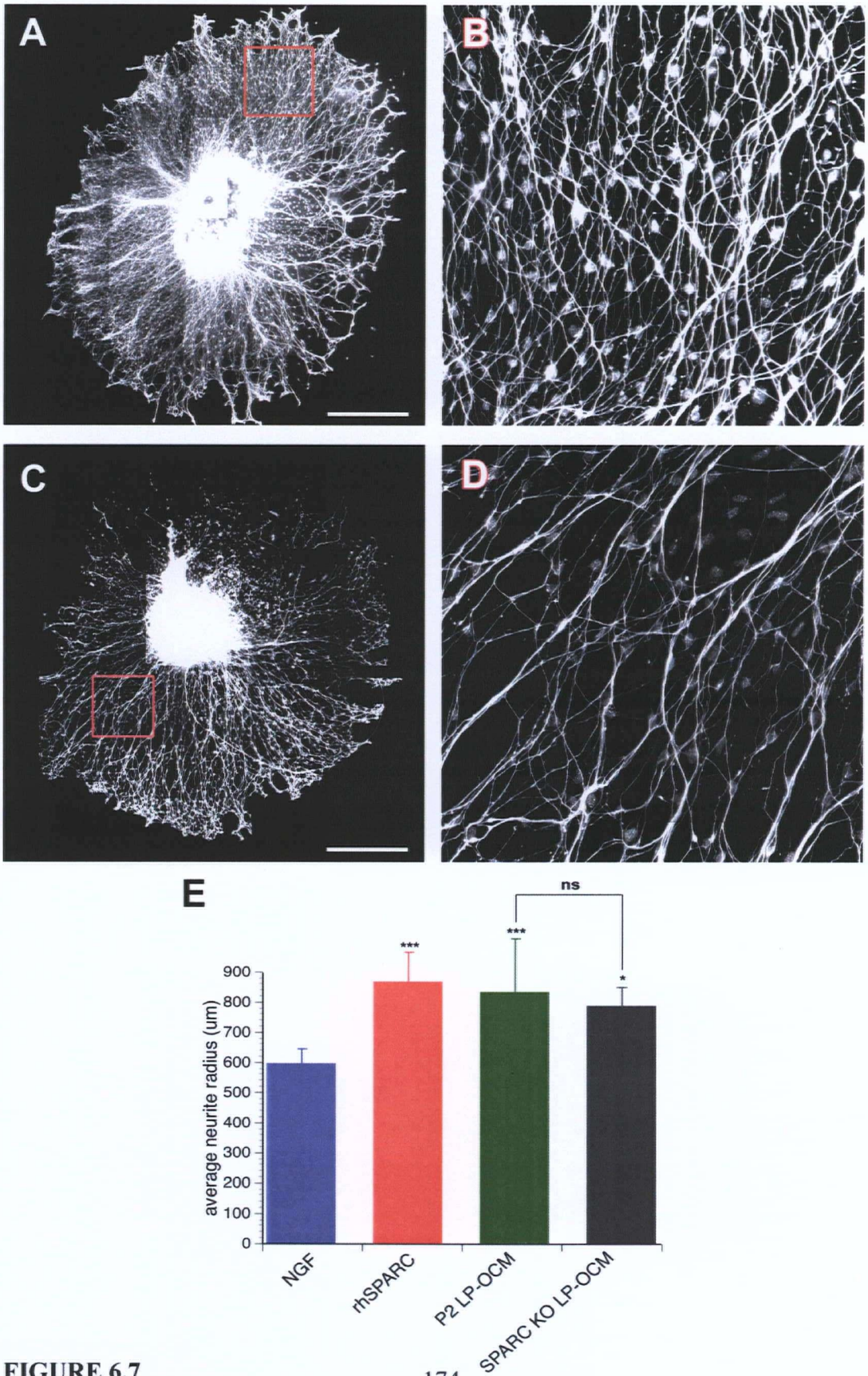
A
B
C
D
E
ns
***
***
*
900
800
700
600
500
400
300
200
100
0
average neurite radius (um)
NGF
rhSPARC
P2 LP-OCM
SPARC KO LP-OCM

FIGURE 6.7

FIGURE 6.7

Comparison of Average Neurite Carpet Radius Between Wild Type and SPARC Knockout Conditioned Media

(A and C) Representative montages of DRG explants grown in (A) P2 LP-OCM and (C) SPARC null P2 LP-OCM. (B and D) Higher magnifications of (B) red box in (A) and (D) red box in (C). (E) rhSPARC, passage 2 wild type and passage 2 SPARC KO conditioned media increase the average length of neurites over the NGF baseline control. There is no statistical significance between the 2 conditioned media groups. Asterisks: * is $p < 0.05$; * is $p < 0.005$; *** is $p < 0.0005$; ns= not statistically significant. Scalebar represents 500 μm.

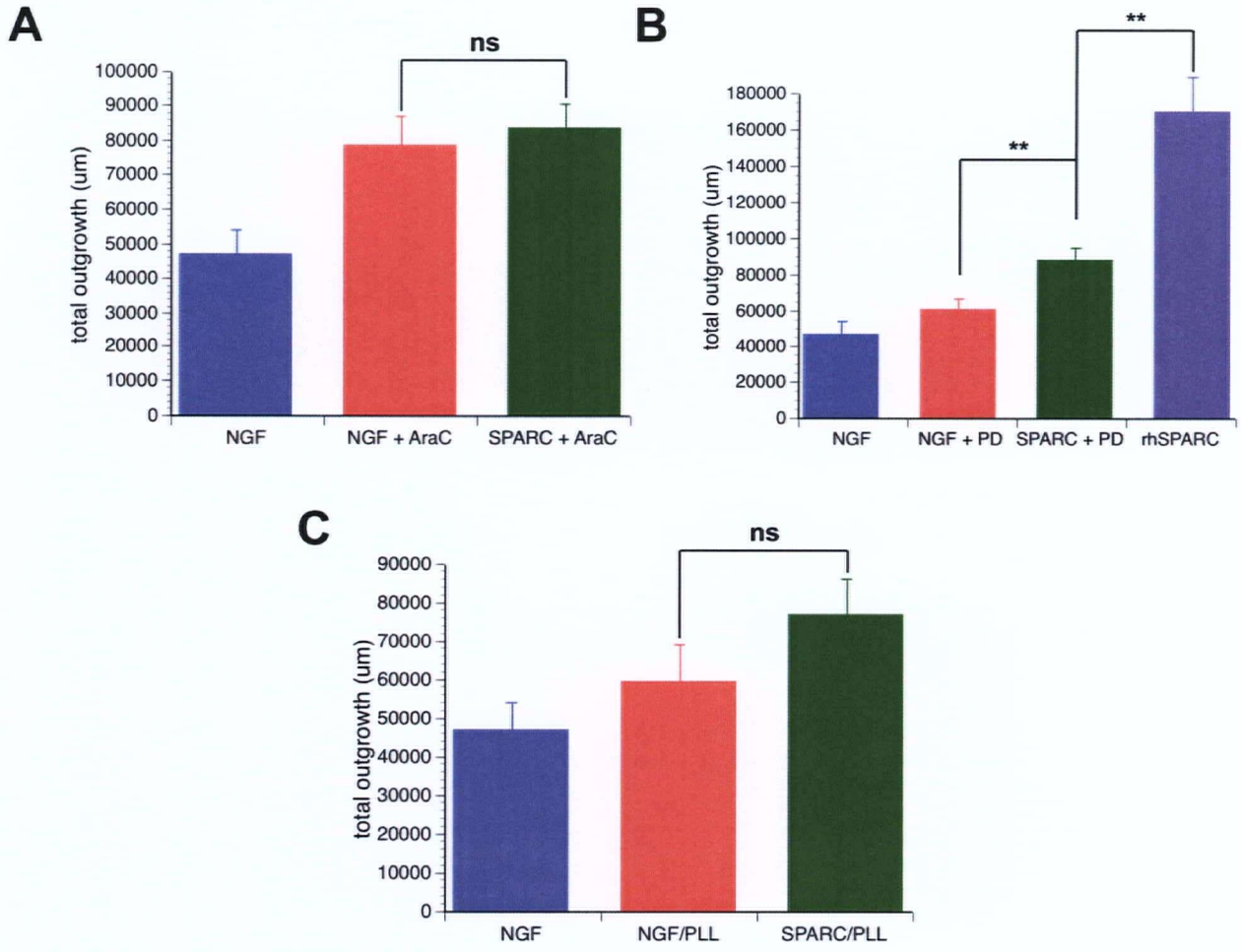

FIGURE 6.8

The Effect of SPARC can be Attenuated By Altering the Parameters of the Neurite Outgrowth Assay

(A) Cytosine arabinoside (AraC) was added to the assay for two days to kill dividing cells. The media was changed and the explants received either NGF (red) or NGF and SPARC (green). (B) The MAP kinase inhibitor PD 98059 was added for the duration of the assay to inhibit NGF-mediated outgrowth. NGF alone (red) or NGF and SPARC (green) were tested with the inhibitor. (C) The assay was performed excluding laminin as a substrate and NGF baseline (red) was tested against NGF with SPARC (green). Asterisks: * is $p < 0.05$; * is $p < 0.005$; *** is $p < 0.0005$; ns= not statistically significant.

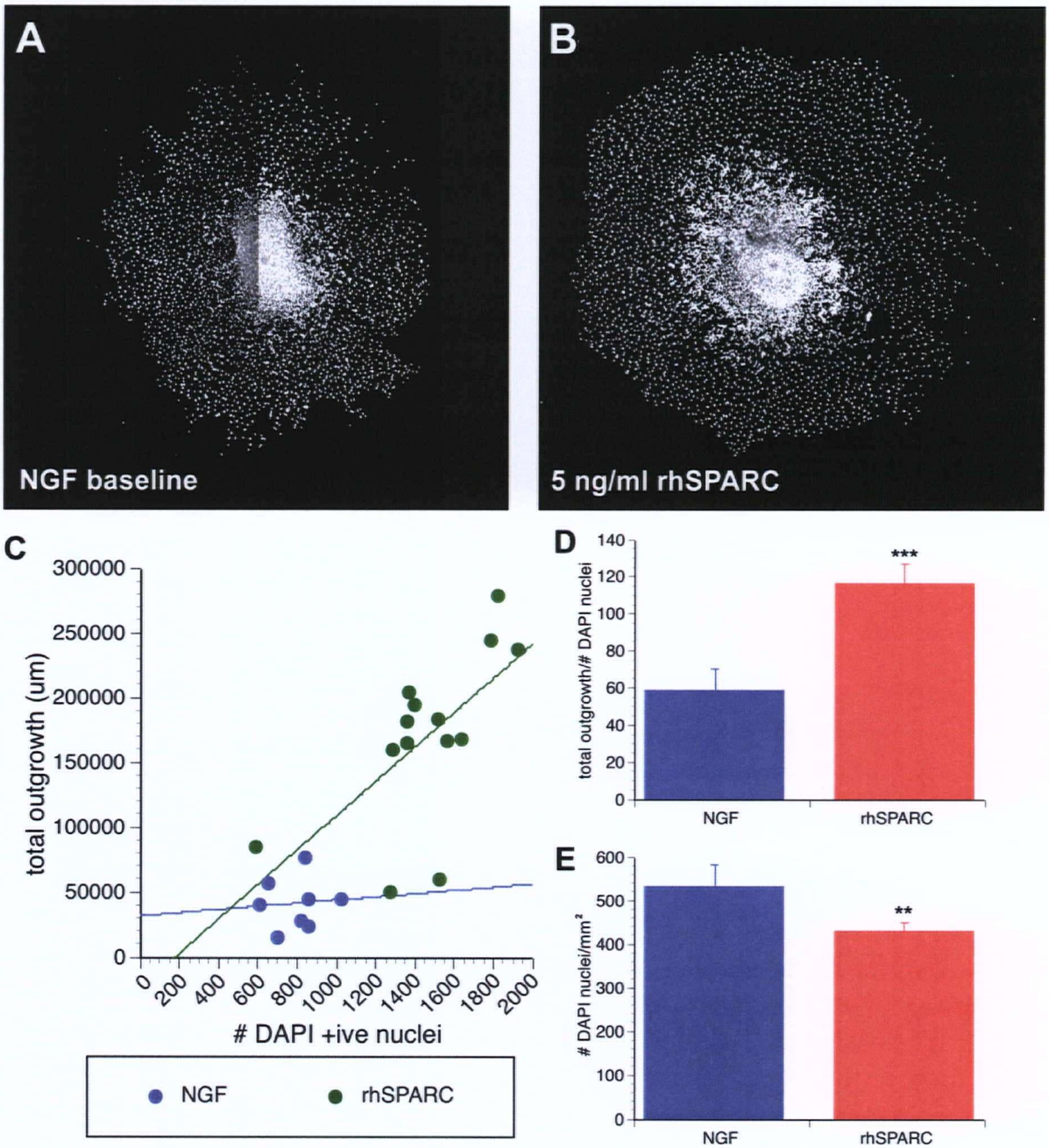

FIGURE 6.9

Correlation Between Number of Dividing Cells and Total Outgrowth

(A and B) Representative montages of DAPI labeled explants grown in (A) NGF baseline conditions or (B) NGF and 5ng/ml SPARC. (C) Scatter plot of number of DAPI nuclei versus total outgrowth. SPARC-treated group (green) tends to have more outgrowth per number of DAPI nuclei than NGF baseline group (blue). (D) Average ratio of total outgrowth per DAPI nuclei in NGF (blue) and SPARC-treated (red) groups. (E) The DAPI nuclei density of NGF (blue) versus SPARC-treated (red) groups.

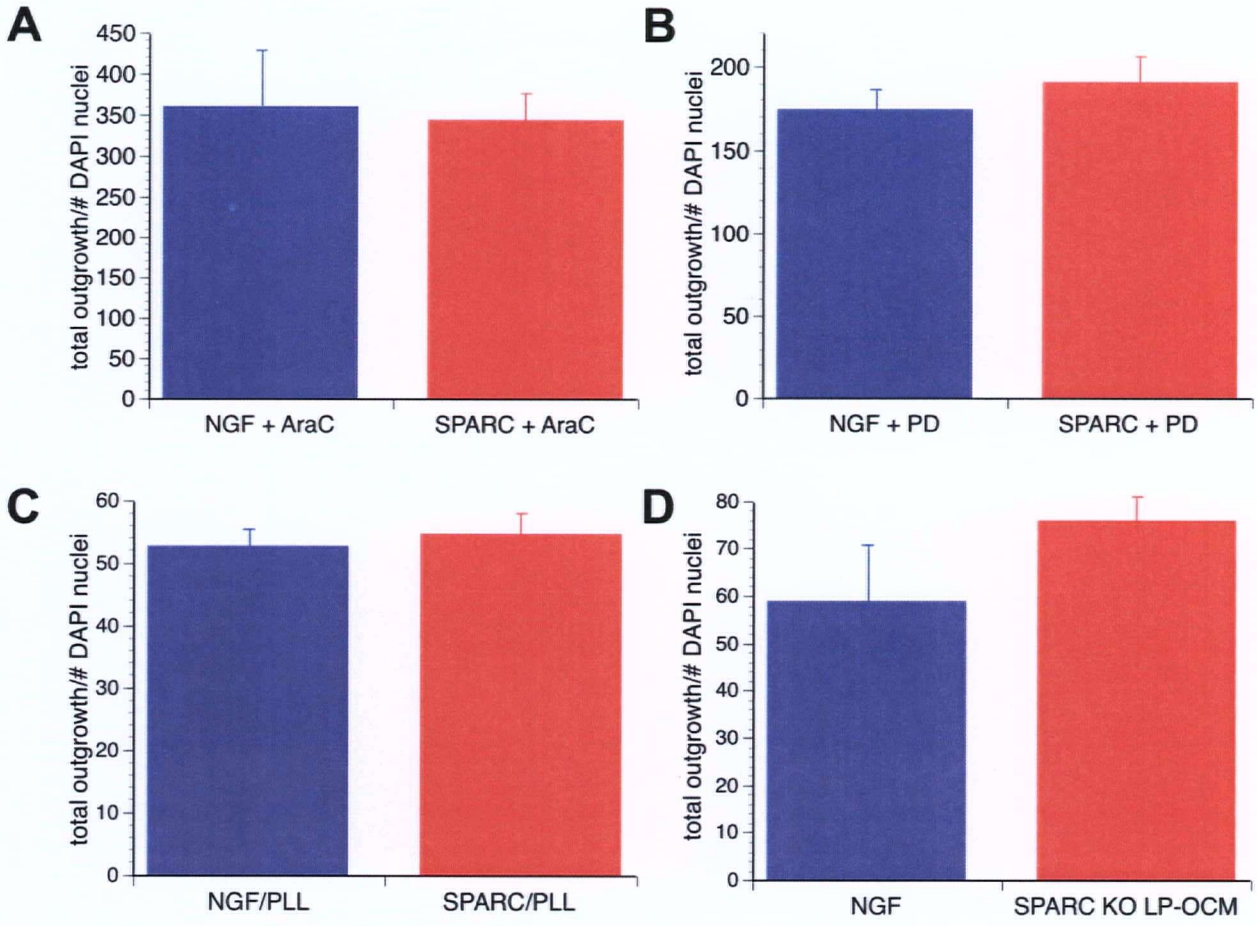

FIGURE 6.10
Correlation Between Number of Dividing Cells and Total Outgrowth When SPARC Activity is Distrupted
Ratio of outgrowth per dividing cell in (A) AraC-treated explants, (B) PD 98059-treated explants, (C) grown on PLL alone and (D) grown in SPARC null conditioned media. Blue bars are NGF control and red bars are 5 ng/ml rhSPARC treated.

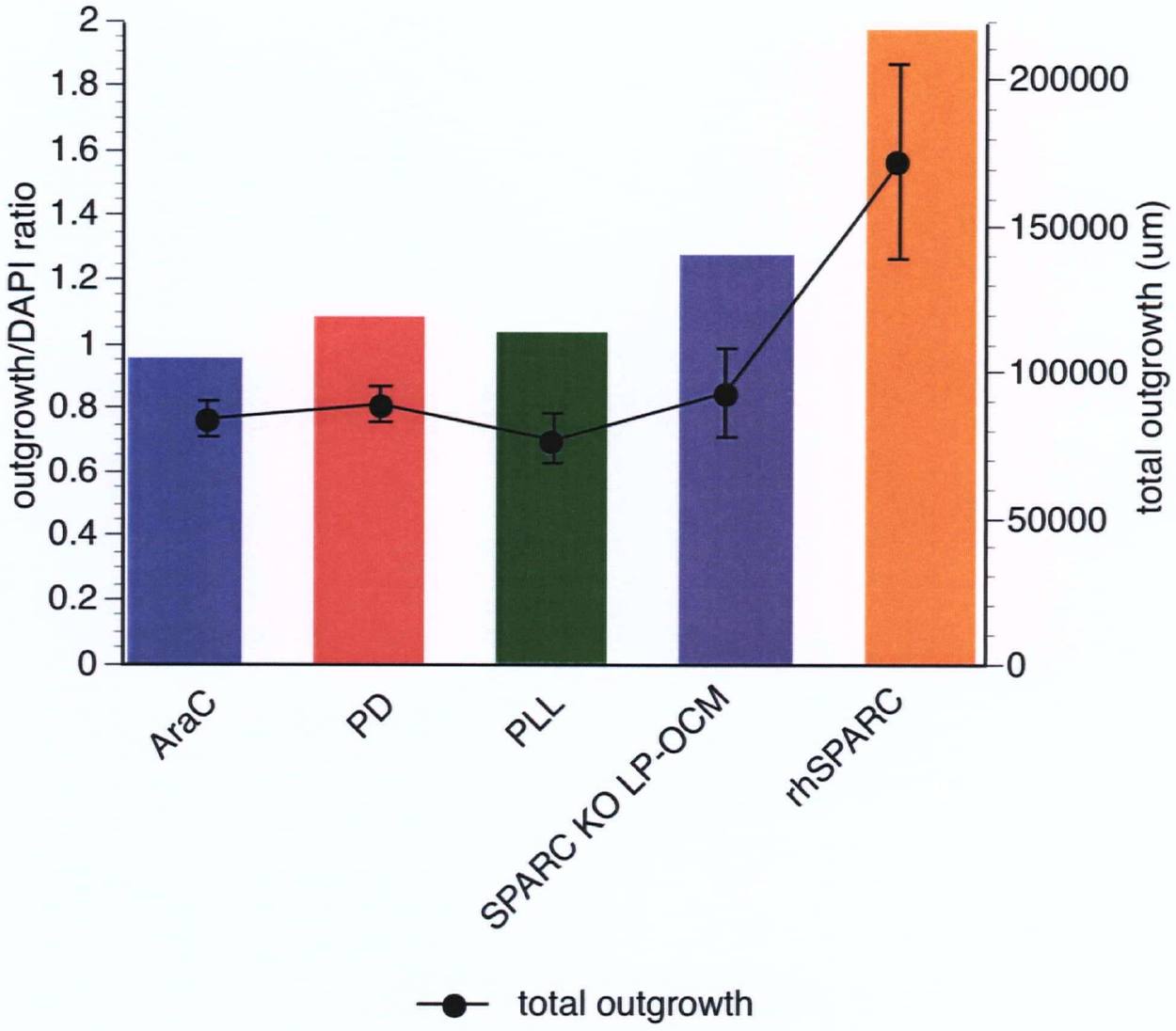

FIGURE 6.11
Correlation Between Outgrowth/DAPI # Ratios and Resulting Outgrowth
The outgrowth/DAPI# ratios of SPARC-treated groups were divided by the outgrowth/DAPI# ratios of their corresponding NGF control groups. The resulting ratio is compared with the total outgrowth of the SPARC-treated group in each condition (black line).

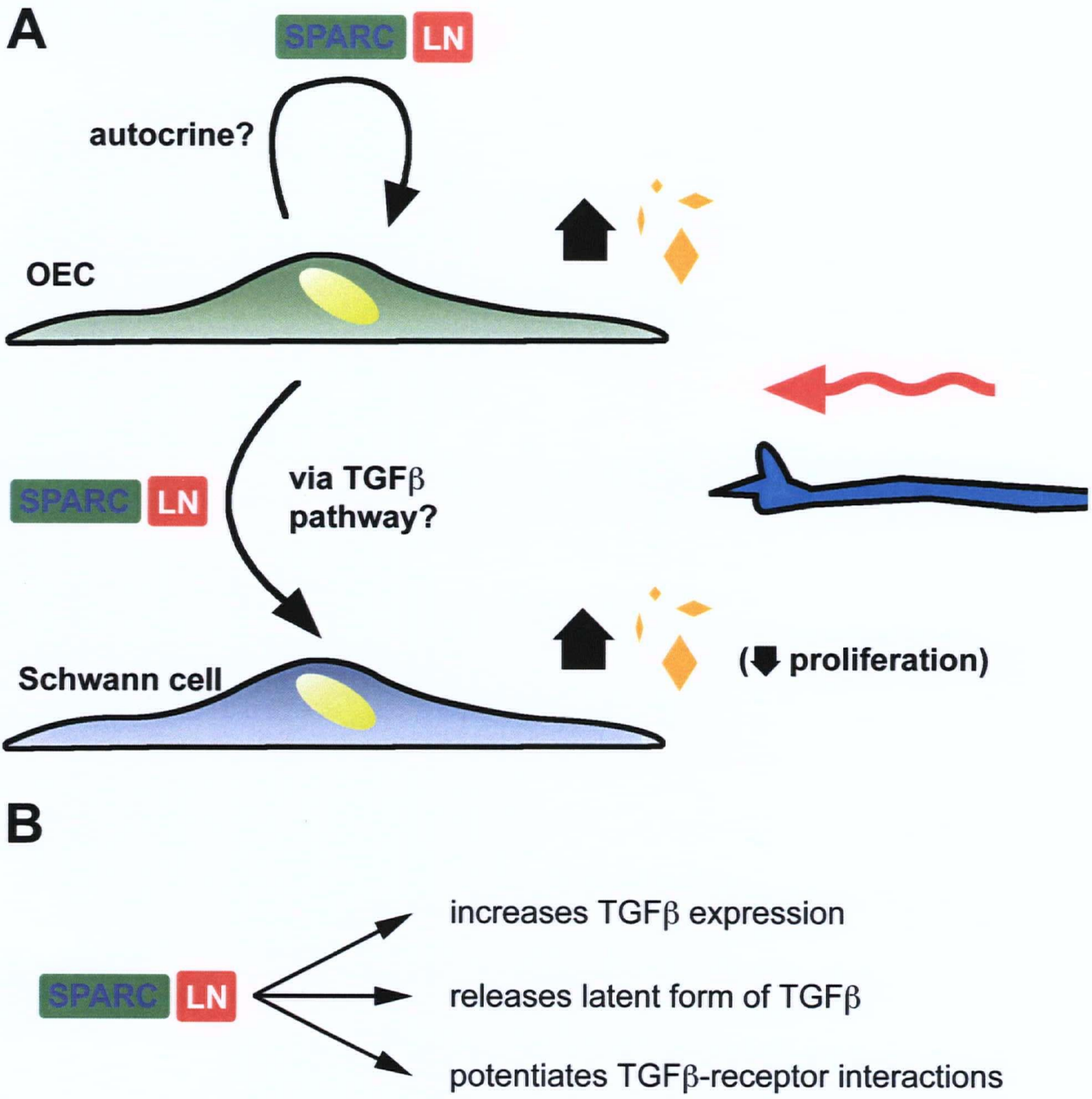

FIGURE 6.12
Putative Mechanism of SPARC-Mediated Neurite Outgrowth
(A) SPARC is secreted by OECs (green) and affects Schwann cells (blue), potentially in an autocrine manner. Laminin (LN, red) is shown directly interacting with the ECM binding domain of SPARC. The pathway initiated by SPARC, which may signal via TGFβ, results in increased expression of ougrowth-promoting molecules (orange) and decreased Schwann cell proliferation. (B) Three potential mechanisms by which SPARC impinges on TGFβ: 1) increases expression level, 2) releases latent form and 3) modulates ligand-receptor interactions.

Chapter 7: Conclusions

Chapter 3 Purification and Characterization of Olfactory Ensheathing Cells In Vivo and In Vitro

SUMMARYOF RESULTS

- Olfactory ensheathing cells residing in the lamina propria express many of the same markers as OECs residing the olfactory bulb in vivo in postnatal day 5 mice
- LP-OECs can be cultured from P5 mouse olfactory mucosa
- In vitro, LP-OECs express many of the same antigens reported in OB-OECs by other groups
- The primary culture starts as an approximately 80% glial population
- By actively eliminating fibroblast contaminants, the culture achieves a purity level of 95% as measured by S100β positivity
- LP-OECs can proliferate in the absence of exogenous mitogens but basic fibroblast growth factor was found to be a potent mitogen
- With successive passaging, LP-OECs lose their capacity to proliferate, likely due to senescence
- LP-OECs express novel markers CD44, β1 integrin, P200, NG2, VEGF, PACAP, Notch 3, CBP300 in vitro
- CD44 expression in vivo is restricted to OECs residing in the lamina propria

CONCLUSIONS

- Both in vivo and in vitro, LP-OECs are very similar to OB-OECs supporting the work of others that they share a common origin
- LP-OECs can robustly proliferate in serum-containing media in the absence of mitogens while OB-OECs are reported to be dependent on mitogens for

proliferation. This suggests that LP-OECs may be more immature than OB-OECs and it is possible that there is a developmental gradient of glial cell maturity from the lamina propria to the nerve fibre layer.

- Despite their propensity to proliferate, LP-OECs their proliferative capacity over time
- With their greater ability to proliferate and their expression of developmentally-regulated markers, LP-OECs appear to be a more plastic, immature glial cell type

Chapter 4 Assessing Neurite Outgrowth Promotion by Lamina Propria-Derived Olfactory Ensheathing Cells

SUMMARY OF RESULTS

- Four methods of quantifying neurite outgrowth were compared: skeletonization, average neurite radius, neurite carpet surface area, total neurite carpet signal
- Of these methods, skeletonization and total neurite carpet signal were found to be the most sensitive
- E13.5 DRGs grown on a monolayer of LP-OECs grew more robustly than DRGs grown on PLL-laminin alone
- LP-OECs can be grown in serum-free media by gradually stepping down serum concentration and stepping up plating density. With this method, serum-free conditioned media libraries can be generated.
- Adding conditioned media from LP-OECs increase total neurite outgrowth above baseline NGF conditions in a dose dependent manner
- The effect is protein based since heat denaturation abolishes the effect
- Passage 2 and Passage 6 conditioned media promote neurite outgrowth differentially such that P2 LP-OCM has a more effective dose response curve
- By measuring total outgrowth, P2 LP-OCM is as effective as co-culturing on a monolayer of LP-OECs
- However, co-cultured DRGs exhibited longer neurites as measured by average neurite radius

CONCLUSIONS

- LP-OECS promote robust neurite outgrowth both in co-culture and also by the secreted factors present in conditioned media
- As the cells age in culture, their ability to produce secreted factors that promote neurite outgrowth diminishes
- This is an ideal model system with which to analyze the conditioned media by ICAT proteomics. By analysis of proteins differentially expressed in the two samples, candidate factors important in OEC-mediated neurite outgrowth may be identified.

Chapter 6 Expression and Functional Studies on Secreted Protein Acidic Rich in Cysteine

SUMMARY OF RESULTS

- By analyzing ICAT results, SPARC was identified as a likely candidate underlying the biological activity of LP-OCM
- SPARC expression in LP-OECs was confirmed by RT-PCR, immunocytochemistry and western blot analysis of conditioned media and cell pellet lysates
- SPARC is expressed in LP-OECs in vivo at all stages of development in both the LP and OB. Expression levels drop with age.
- In response to bulbectomy, SPARC expression is upregulated globally and more so on the injured side
- Recombinant human and mouse SPARC added to the neurite outgrowth assay robustly increases total outgrowth
- Human- and mouse-specific function-blocking antibodies to SPARC can block the SPARC-mediated increase in outgrowth

- Mouse-specific function-blocking antibody can greatly attenuate the biological activity of P2 and P6 LP-OCM
- P2 SPARC null LP-OCM is less effective in promoting total neurite outgrowth compared with wild type P2 LP-OCM.
- However, the average neurite radius of SPARC null LP-OCM treated groups is greater than NGF baseline levels
- Removal of dividing cells using AraC ablates the outgrowth effect of SPARC
- The outgrowth effect of SPARC is attenuated by removing laminin from the assay or by adding the MAPK inhibitor PD 98059
- In SPARC-treated groups, the density of DAPI nuclei in the neurite carpet is decreased and the amount of neurite outgrowth per DAPI nucleus is increased.
- In outgrowth assays where laminin was removed, PD 98059 was added or SPARC null LP-OCM was used, there is no significant effect on DAPI density or outgrowth per nucleus

CONCLUSIONS

- With its differential expression between P2 and P6 LP-OCM and a priori data on SPARC's involvement in growth factor modulation and plasticity, SPARC was determined to be a promising candidate factor
- Expression of SPARC is developmentally regulated. However, SPARC is still expressed at low levels in adulthood, likely to accommodate the re-modeling required for continual ORN turnover
- Following bulbectomy when a synchronous wave of ORNs re-grows towards the olfactory bulb, SPARC expression is re-upregulated suggesting its importance in mediating ORN axon growth
- In the neurite outgrowth assay, SPARC greatly increases neurite outgrowth
- Using function-blocking antibodies, SPARC was found to be an important contributor to the biological activity of LP-OCM

- The effect of SPARC is dependent on the presence of dividing cells and laminin substrate. The removal of either all but eliminates the outgrowth effect of SPARC.
- When SPARC is added, dividing cells are less proliferative and the total neurite outgrowth ascribed to each cell is significantly increased. This suggests that SPARC increases the neurotrophic properties of the dividing cells in the explant.
- As the effect of SPARC is attenuated, the outgrowth per DAPI nucleus ratio also drops. This is strongly suggesting that SPARC's outgrowth properties act secondarily via the dividing cells of the explant.

Chapter 8: General Discussion and Future Directions

8.1 A Critique of Thesis Results

At the onset of my thesis there were two main questions I wanted to address. One, I wanted to study olfactory ensheathing cells residing in the lamina propria, since at the time very little was known about them. There had been two reports indirectly examining glial cells cultured from nasal mucosa (Barnett et al., 1993; Ramon-Cueto and Nieto-Sampedro, 1992) but without carefully characterizing them as had been done with olfactory bulb OECs (2003). Two, I wanted to study mechanistically how OECs promote axon growth. The question was interesting to me because of the remarkable degree of ORN axon growth still possible in the adult olfactory system and also because of the growing interest in using OECs to mediate spinal cord repair. I felt that while many groups observed regeneration in both systems, how exactly OECs contributed to this process was poorly understood. Perhaps with more insight into how OECs work, they could be more effectively employed to restore function in the spinal cord and the olfactory system. To that end, I have included a critique of how successful (and unsuccessful) I have been in addressing these two issues.

8.1.1 Culture and Characterization of Lamina Propria-Derived Olfactory Ensheathing Cells

This portion of my thesis was largely successful in that it provided a solid basis from which to proceed. The culture of OECs from olfactory mucosa proved to be robust and repeatable giving me a sufficient supply of cells with which to examine OEC function. Also, I found that LP-OECs are very similar to what has been previously reported for OB-OECs in vitro. Subsequent work from the Roskams lab comparing OB-OECs and

LP-OECs has also supported this (Richter et al, manuscript under review). This is perhaps not surprising since embryonically both populations are derived from the olfactory placode (see section 1.2.2) and they are situated continuously along the length of ORN axons from the OE to glomeruli. I noted in vivo that LP-OECs but not OB-OECs express CD44, the hyaluronic acid receptor, known to have anti-adhesive properties (figure 3.6) and that they proliferate in serum-containing media without the aid of additional mitogens. This suggests that there may be some subtle differences between the two cell types, perhaps a maturity gradient where younger, more proliferative OECs reside in the LP and migrate towards the olfactory bulb to become more mature OB-OECs.

Setting aside the practical considerations of having developed a robust model system, there is still much to be done to address the differences between OB- and LP-OECs. There are likely many important differences between the two cell types functionally given that they associate with different subdomains of ORN axons. Even within the nerve fibre layer, there are subsets of OB-OECs that serve to promote axon growth or facilitate pathfinding (Au et al., 2002). It is an important issue to address given the relative accessibility of LP-OECs and inaccessibility of OB-OECs for autotransplantation strategies – is it especially worthwhile to harvest OECs from the olfactory bulb because of their unique properties over LP-OECs? In section 7.2.1 I speculate on different strategies to address the differences between the two cell types later.

The purification, culture and characterization of lamina propria-derived OECs resolved an important question in the field: Are OECs residing in the lamina propria and olfactory bulb similar, as has been suspected but not proven, or fundamentally different? The answer appears to be that they are largely similar, however, the fact that LP-OECs appear to have a greater capacity to proliferate and reside in a more accessible region for harvest and autotransplantion, argue in favour of LP-OECs as a potentially superior candidate for mediating neuronal repair. The data in chapter 3 also suggests that there may be a gradient of maturity along the olfactory neuraxis where peripheral OECs are more immature than OECs of the olfactory bulb. One can imagine newly generated LP-OECs

migrating with new ORN axons en-route to the olfactory bulb and then undergoing differentiation to become OB-OECs to accommodate ORN targeting. This would be certainly be consistent with the observation that different subtypes of OB-OECs reside in the nerve fibre layer coincident with ORN growth, defasciculation and targeting (Au et al., 2002).

8.1.2 The Neurite Outgrowth Assay

In retrospect, there are several aspects of the neurite outgrowth assay that were particularly fortuitous given the properties of SPARC. Counting in favour of the assay, it was robust, reproducible and very sensitive to adding exogenous factors (such as more NGF or LP-OCM). In that regard, it proved to be a reliable screen for the bioactivity of LP-OEC conditioned media. Its robustness also allowed it to be somewhat modular such that components (laminin for example) could be removed or added (for example, an OEC monolayer) to suit and address different questions. Because of the modularity I was able to determine that SPARC required both the presence of Schwann cells and laminin to effectively promote outgrowth. Also, the assay reflected the question I was interested in, namely how do OECs promote axon growth in the context of spinal cord injury and in the olfactory system? In both of these cases, glial cells are present and play an active role in the outcome. Because the Schwann cells were kept in the assay, the interaction between neurons and glia remained intact, more accurately modeling the situation in the spinal cord and olfactory system.

There were however, aspects of the outgrowth assay that were less satisfactory. For one, the primary method of quantification was measuring total outgrowth by skeletonization. While this method is very sensitive for detecting changes in neurite outgrowth, it doesn't provide information on other potentially important parameters such as neurite length, fasciculation and branching. To try and account for this, I also reported average neurite length in conditions where total outgrowth was misrepresenting the differences between groups (see figures 4.12 and 6.7). The degree of branching and fasciculation are

inherently difficult to measure, especially in an explant with such high density growth. Measuring branching is better suited to a low-density dissociated neuronal culture, where one can tell the difference between branching and two neurites simply crossing over one another.

There is also the issue that the outgrowth assay does not distinguish increased survival versus increased outgrowth. Here, while not definitive, something can be gleaned from the experiments involving NGF inhibitors. First, in the absence of NGF or using the pan-trk inhibitor K252a, no outgrowth was ever observed even when supplemented with P2, P6 LP-OCM or SPARC. This suggests that if LP-OCM or SPARC mediates increased outgrowth via increased survival, it does so in an NGF-dependent manner. Second, in the presence of a MAPK inhibitor (PD 98059) ostensibly to block NGF-mediated outgrowth while leaving NGF-mediated survival intact, the effect of SPARC was greatly attenuated (figure 6.8B). Thus, even with NGF survival pathways intact, SPARC was considerably less effective. This could be interpreted as a dependence on the MAPK pathway for SPARC-mediated neuronal survival or that SPARC acts to increase outgrowth with at least a partial dependence on MAPK. With the many processes through which MAPK is involved, it is difficult to interpret further.

Finally, it should be mentioned that there is an inherent bias in how the outgrowth assay was set up. The assay was used to screen the biological activity of LP-OCM and candidate factors with the highest degree of sensitivity possible. At 1.5 ng/ml NGF, the explant was growing well enough to survive but not so well as to mask the effect of factors added to the assay. As such, effects of LP-OCM and SPARC were presented in the best light possible and not necessarily representing their relative importance in vivo. It will be important to test the biological effect of SPARC using in vivo models in order to truly validate its impact on OEC-mediated axon growth.

There have been conflicting reports as to the ability of OEC conditioned media to promote neurite outgrowth (Chung et al., 2004; Kafitz and Greer, 1999; Lipson et al., 2003). I have found that at least with LP-OECs grown in serum-free media, the

biological activity of LP-OCM is considerable; it has proven to be a rich source from which to search for novel candidate molecules that underlie its functional activity. There is likely much more that we can learn from LP-OEC conditioned media. For example, in addition to its neurite outgrowth-promoting properties, LP-OCM appears to robustly promote neuronal differentiation of progenitors cultured from the olfactory epithelium (Roskams lab, unpublished observations). Based on candidates found in the ICAT dataset, as well as additional candidates that can be identified by straight MS sequencing, other processes potentially involving OEC signaling (neuronal survival, maturation and differentiation, to name but a few) may be elucidated in future. LP-OCM, by virtue of its purity and relatively simple composition, could prove to be a valuable starting material with which to identify key molecules and mechanisms regulating fundamental processes in the olfactory system.

8.1.3 The Use of ICAT Proteomics to Screen for Factors In Vitro

The use of ICAT proteomics to deduce mechanisms of OEC function is appealing on several levels. One, it is a prospective approach unbiased by what has been previously reported in the literature about OEC growth factors. At its core, the question was reduced to: Given that there is a biological activity in LP-OCM, what factors are present in LP-OCM and how can we simplify or shorten the list of candidate factors irrespective of what those factors are? Two, the approach helped to simplify the question from a complex biological interaction between different cell types to that of a biochemical question where a well-defined fraction (LP-OCM) has a given activity and the agent(s) responsible need only be isolated and tested systematically. Three, this particular question was inherently well suited for proteomic analysis. The conditioned media was relatively simple (compared with say, a whole cell lysate), it could be readily isolated by harvesting the media from the cells and the validation of candidates only involved adding the protein back to the outgrowth assay. In this manner, it may have been the simplest possible approach to tackle a seeming very difficult biological question. The promise of

using proteomics to meaningfully address black box issues in biology is considerable. This study has demonstrated that a prospective screening approach is potentially feasible if the parameters of the question synergize with the strengths of the technique used.

On the downside, the datasets provided by ICAT were less than ideal (see figure 5.1C). This is probably due to the limited to the sensitivity of ICAT (because of its requirement for cysteine labeling) and that the protocol for analyzing LP-OCM needs further optimization. There are probably other candidate factors in LP-OCM that were either not detected or detected with low confidence and therefore not carefully scrutinized. As a complement to the ICAT data, it is probably a good idea to analyze LP-OCM using mass spectroscopy or 2-D electrophoresis without pre-screening with ICAT reagent, to get better overall coverage of the proteins present. Also, there is something to be said for the cysteine bias in the ICAT dataset. Perhaps fortuitously, there was an overrepresentation of SPARC in the dataset because, as its name implies, it is rich in cysteine residues. Even so, SPARC was readily detectable by Western blotting and even without the unusually high cysteine content, would have been seriously considered as a potential candidate much in the same way as say, pigment epithelium derived factor (see Table 5.1). Finally, it is worth commenting on the conditioned media samples analyzed. Even with the stringent cut-off, one can see that there are proteins reported that are not likely secreted (for example: non-muscle heavy myosin chain II-A, Table 5.1). This is probably due to cell lysis while generating the conditioned media and not a failing of ICAT as a technique, but it did make analysis of the dataset somewhat more difficult.

8.1.4 SPARC as a Significant Contributor to the Biological Activity of LP-OCM

ICAT and western blotting confirms that SPARC is expressed at different levels in P2 and P6 LP-OCM; its higher levels in P2 LP-OCM certainly suggest that it could account for the difference in biological activity between the two samples. Based on the gain- and loss-of-function experiments using SPARC, SPARC null conditioned media and function-blocking antibodies there is a strong case for SPARC playing a significant role

in LP-OCM activity. At optimal concentration, the total outgrowth with SPARC is statistically indistinguishable from passage 2 conditioned media. Its expression developmentally (figure 6.3) and its upregulation following injury in the olfactory system (figures 6.4A and B) suggest that it is important in olfactory regeneration and re-modeling. Although its effect appears to act secondarily via Schwann cells, there is a potential TGFβ pathway that could link the two pathways together.

What is lacking about SPARC as a candidate factor is that it raises more questions than it answers. One, what are the growth factors/preferential substrates etc. that are upregulated in Schwann cells as a result of SPARC that directly impact neurite outgrowth? Two, is there an autocrine/paracrine effect of SPARC on OECs? Three, SPARC, especially developmentally, is widely expressed and it is unclear how it could signal for migration, and differentiation in one cell type while signaling for axon growth in another. Potentially context could be important, for example by association with ECM molecules. In the outgrowth assay, laminin appears to be important in SPARC-mediated outgrowth. Laminin expression pattern also closely mimics SPARC expression in the olfactory system (figure 6.3C), suggesting perhaps such a signaling partnership is also important in vivo.

The identification of SPARC as a key component in OEC-mediated outgrowth is an important contribution to the OEC field as a whole. Other studies have proposed secreted factor based mechanisms testing for known neurotrophic factors (Lipson et al., 2003; Woodhall et al., 2001). Here, SPARC was identified prospectively by using an approach that directly links candidate secreted factors with the biological activity of the conditioned media as a whole. Moreover, SPARC provides a novel mechanism of neurite, and potentially axon, growth employed by OECs that may facilitate ORN turnover throughout adult life. That SPARC appears to work secondarily through glial cells may also help explain how OECs promote regeneration in the injured spinal cord via infiltrating Schwann cells (Boyd et al., 2004; Ramer et al., 2004a; Sasaki et al., 2004). Also, what is known about SPARC and its modulation of growth factor and ECM, suggests it may also play a role in maintaining the plasticity of the olfactory system

(sections 5.1.2.2 and 5.1.2.3) and that this role may also carry over to the spinal cord lesion site.

In conclusion, I have characterized LP-OECs, a poorly understood cell population, and employed them as a model system for deducing OEC mechanisms. Starting first with biological activity, both in co-culture and also in two conditioned media samples, I employed ICAT proteomics to elucidate a key component of OEC-mediated neurite outgrowth. In so doing, I have revealed a novel pathway of glial-neuronal interaction through which OECs may be facilitating ORN axon growth and neural regeneration in the spinal cord.

8.2 Future Directions

The findings in this thesis clear the way for a number of new directions and raise issues to be addressed in future. This section has been divided into three categories: (1) OB- vs. LP-OECs: what are potential ways that one can highlight the key differences and fundamental similarities between these two populations? (2) Mechanisms of OEC function: are there other ways to extend the approach used in this thesis to better elucidate OEC function. (3) Mechanisms of SPARC activity: how can we more definitively understand how SPARC promotes neurite outgrowth and validate its function in vivo?

8.2.1 OB- vs. LP-OECs

Resolving the origin of LP- and OB-OECs will go a long way to understanding the relationship between the two cell types. Do the cells have a long lifespan and replenish their populations slowly by dividing in situ or is there a dedicated population of OEC progenitors. If it is the latter, is there a separate progenitor population for OB- and LP-

OECs? With the proliferative capabilities of LP-OECs seemingly greater than OB-OECs in vitro, it is possible that there is a progenitor population residing peripherally from which both OB- and LP-OECs arise. To test this possibility, an S100β-GFP-IRES-thymidine kinase mouse could be generated similar to the S100β-GFP mouse generated previously (Vives et al., 2003). A localized injection of gancyclovir would be administered to the olfactory bulb intracranially, selectively ablating OB-OECs and creating the need for OEC replacement. Along with the gancyclovir, a halogenated thymidine analog, IdU (iododeoxyuridine) could be co-administered. Some time later, another BrdU-like analog, CldU (chlorodeoxyuridine) could be administered systemically. The two analogs can be distinguished by different antibodies (Vega and Peterson, 2005). The general idea is to temporally and spatially distinguish the cells that move in and replenish the OB-OECs thereby deducing the source of OEC progenitors. If the source of OEC progenitors can be identified, it may be possible to follow the development and maturation of OECs using a promoter-specific CRE-ER system to fate map the cells in adulthood. Already with the mouse developed by Vives and coworkers (2003) or the one used in Storan and Key (2004), such experiments can be performed embryonically. Perhaps by tracing their lineage, functional differences between OEC subtypes can be brought to light.

8.2.2 Mechanisms of OEC Function

Making use of the fact that LP-OECs senesce in culture is only one of many ways in which one can generate LP-OCM with different biological activities. Another method I attempted, but did not get the chance to analyze is stimulating LP-OECs with axon membrane shards to mimic axon contact. In this way, OECs secrete factors as if they are in contact with neurons without the confounding issue of neurons also secreting factors into the media. When I tested the biological activity of P2 LP-OCM vs. axon-stimulated P2 LP-OCM, I found a trend towards greater neurite outgrowth with axon-stimulated media over and above P2 LP-OCM (Appendix 7). It would certainly be interesting to compare the constituents of the two media samples and possibly identify novel candidates

responsible for this effect. Other potential media conditions that could be compared include adult vs. neonate OECs or OECs cultured from intact and bulbectomized animals. OEC cell surface factors could also be examined but there are practical issues such as how to generate and store libraries of cell surface factors and also how to test factors individually for biological activity.

8.2.3 Mechanisms of SPARC Activity

More work should be done to elucidate how SPARC impacts neurite outgrowth. The potentiation of the TGFβ pathway is an attractive hypothesis but requires further examination. For example, there are three potential mechanisms by which SPARC could be modulating TGFβ activity: (1) increasing overall TGFβ levels, (2) promoting the release of latent TGFβ or (3) potentiation of TGFβ ligand-receptor interactions as has been suggested by Franki and coworkers (2004). These possibilities can be explored by analysis of conditioned media and cell lysates of DRG explants grown with or without SPARC. Overall TGFβ levels and free vs. latent TGFβ could be examined by ELISA. Probing for phosphorylated Smad2 could assess TGFβ signaling. To complete the story, in vivo studies should be performed to assay the relative importance of SPARC on OEC function. To that end, OECs from SPARC null and wild type mice could be transplanted into a spinal cord injury model and assessed for ability to promote regeneration. Also, bulbectomies could be performed on SPARC null and wild type mice and ORN regenerative response could be examined by DiI labeling the gelfoam used to plug the cavity where the OB used to be.

References

. Cleavable ICAT Reagent Kit for Protein Labeling (Foster City, CA, USA., Applied Biosystems).

Aebersold, R., and Mann, M. (2003). Mass spectrometry-based proteomics. Nature *422*, 198-207.

Aeschlimann, D., Kaupp, O., and Paulsson, M. (1995). Transglutaminase-catalyzed matrix cross-linking in differentiating cartilage: identification of osteonectin as a major glutaminyl substrate. J Cell Biol *129*, 881-892.

Alexander, C. L., Fitzgerald, U. F., and Barnett, S. C. (2002). Identification of growth factors that promote long-term proliferation of olfactory ensheathing cells and modulate their antigenic phenotype. Glia *37*, 349-364.

Amemori, T., Soukup, T., and Bures (1987). Olfactory neuroepithelium transplanted onto the parietal cortex of rats: electroolfactogram in absence of connections with the host brain. Int J Neurosci *34*, 35-48.

Andrews, M. R., and Stelzner, D. J. (2004). Modification of the regenerative response of dorsal column axons by olfactory ensheathing cells or peripheral axotomy in adult rat. Exp Neurol *190*, 311-327.

Angeletti, R. H., Bradshaw, R. A., and Wade, R. D. (1971). Subunit structure and amino acid composition of mouse submaxillary gland nerve growth factor. Biochemistry *10*, 463-469.

Ankeny, D. P., McTigue, D. M., and Jakeman, L. B. (2004). Bone marrow transplants provide tissue protection and directional guidance for axons after contusive spinal cord injury in rats. Exp Neurol *190*, 17-31.

Annes, J. P., Chen, Y., Munger, J. S., and Rifkin, D. B. (2004). Integrin alphaVbeta6-mediated activation of latent TGF-beta requires the latent TGF-beta binding protein-1. J Cell Biol *165*, 723-734.

Astic, L., Pellier-Monnin, V., and Godinot, F. (1998). Spatio-temporal patterns of ensheathing cell differentiation in the rat olfactory system during development. Neuroscience *84*, 295-307.

Astic, L., Pellier-Monnin, V., Saucier, D., Charrier, C., and Mehlen, P. (2002). Expression of netrin-1 and netrin-1 receptor, DCC, in the rat olfactory nerve pathway during development and axonal regeneration. Neuroscience *109*, 643-656.

Atanasoski, S., Notterpek, L., Lee, H. Y., Castagner, F., Young, P., Ehrengruber, M. U., Meijer, D., Sommer, L., Stavnezer, E., Colmenares, C., and Suter, U. (2004). The protooncogene Ski controls Schwann cell proliferation and myelination. Neuron *43*, 499-511.

Au, E., and Roskams, A. J. (2002). Culturing olfactory ensheathing glia from the mouse olfactory epithelium. Methods Mol Biol *198*, 49-54.

Au, E., and Roskams, A. J. (2003). Olfactory ensheathing cells of the lamina propria in vivo and in vitro. Glia *41*, 224-236.

Au, W. W., Treloar, H. B., and Greer, C. A. (2002). Sublaminar organization of the mouse olfactory bulb nerve layer. J Comp Neurol *446*, 68-80.

Awatramani, R., Shumas, S., Kamholz, J., and Scherer, S. S. (2002). TGFbeta1 modulates the phenotype of Schwann cells at the transcriptional level. Mol Cell Neurosci *19*, 307-319.
Banker, G. G., K, ed. (1998). Culturing Nerve Cells, 2nd edn (Cambridge, MA, The MIT Press).
Barber, P. C. (1982). Regeneration of olfactory sensory axons into transplanted segments of peripheral nerve. Neuroscience *7*, 2677-2685.
Barber, P. C., and Dahl, D. (1987). Glial fibrillary acidic protein (GFAP)-like immunoreactivity in normal and transected rat olfactory nerve. Exp Brain Res *65*, 681-685.
Barber, P. C., Jensen, S., and Zimmer, J. (1982). Differentiation of neurons containing olfactory marker protein in adult rat olfactory epithelium transplanted to the anterior chamber of the eye. Neuroscience *7*, 2687-2695.
Barber, P. C., and Lindsay, R. M. (1982). Schwann cells of the olfactory nerves contain glial fibrillary acidic protein and resemble astrocytes. Neuroscience *7*, 3077-3090.
Barnett, S. C., Alexander, C. L., Iwashita, Y., Gilson, J. M., Crowther, J., Clark, L., Dunn, L. T., Papanastassiou, V., Kennedy, P. G., and Franklin, R. J. (2000). Identification of a human olfactory ensheathing cell that can effect transplant-mediated remyelination of demyelinated CNS axons. Brain *123 (Pt 8)*, 1581-1588.
Barnett, S. C., and Chang, L. (2004). Olfactory ensheathing cells and CNS repair: going solo or in need of a friend? Trends Neurosci *27*, 54-60.
Barnett, S. C., Hutchins, A. M., and Noble, M. (1993). Purification of olfactory nerve ensheathing cells from the olfactory bulb. Dev Biol *155*, 337-350.
Barnett, S. C., and Roskams, A. J. (2002). Olfactory ensheathing cells. Isolation and culture from the rat olfactory bulb. Methods Mol Biol *198*, 41-48.
Bartolomei, J. C., and Greer, C. A. (2000). Olfactory ensheathing cells: bridging the gap in spinal cord injury. Neurosurgery *47*, 1057-1069.
Basu, A., Kligman, L. H., Samulewicz, S. J., and Howe, C. C. (2001). Impaired wound healing in mice deficient in a matricellular protein SPARC (osteonectin, BM-40). BMC Cell Biol *2*, 15.
Baudet, C., Mikaels, A., Westphal, H., Johansen, J., Johansen, T. E., and Ernfors, P. (2000). Positive and negative interactions of GDNF, NTN and ART in developing sensory neuron subpopulations, and their collaboration with neurotrophins. Development *127*, 4335-4344.
Berg, M. M., Sternberg, D. W., Parada, L. F., and Chao, M. V. (1992). K-252a inhibits nerve growth factor-induced trk proto-oncogene tyrosine phosphorylation and kinase activity. J Biol Chem *267*, 13-16.
Bewick, G. S., Rowlerson, A., Tonge, D. A., and Holder, N. (1991). Organization of motor units in the axolotl: a continuously growing animal. J Comp Neurol *303*, 551-562.
Bibel, M., Hoppe, E., and Barde, Y. A. (1999). Biochemical and functional interactions between the neurotrophin receptors trk and p75NTR. Embo J *18*, 616-622.
Boruch, A. V., Conners, J. J., Pipitone, M., Deadwyler, G., Storer, P. D., Devries, G. H., and Jones, K. J. (2001). Neurotrophic and migratory properties of an olfactory ensheathing cell line. Glia *33*, 225-229.
Bothwell, M. (1995). Functional interactions of neurotrophins and neurotrophin receptors. Annu Rev Neurosci *18*, 223-253.

Bottenstein, J., Hayashi, I., Hutchings, S., Masui, H., Mather, J., McClure, D. B., Ohasa, S., Rizzino, A., Sato, G., Serrero, G., *et al.* (1979). The growth of cells in serum-free hormone-supplemented media. Methods Enzymol *58*, 94-109.
Boyd, J. G., Lee, J., Skihar, V., Doucette, R., and Kawaja, M. D. (2004). LacZ-expressing olfactory ensheathing cells do not associate with myelinated axons after implantation into the compressed spinal cord. Proc Natl Acad Sci U S A *101*, 2162-2166.
Bradbury, E. J., McMahon, S. B., and Ramer, M. S. (2000). Keeping in touch: sensory neurone regeneration in the CNS. Trends Pharmacol Sci *21*, 389-394.
Bradshaw, A. D., Bassuk, J. A., Francki, A., and Sage, E. H. (2000). Expression and purification of recombinant human SPARC produced by baculovirus. Mol Cell Biol Res Commun *3*, 345-351.
Bradshaw, A. D., Puolakkainen, P., Dasgupta, J., Davidson, J. M., Wight, T. N., and Helene Sage, E. (2003). SPARC-null mice display abnormalities in the dermis characterized by decreased collagen fibril diameter and reduced tensile strength. J Invest Dermatol *120*, 949-955.
Bradshaw, A. D., Reed, M. J., and Sage, E. H. (2002). SPARC-null mice exhibit accelerated cutaneous wound closure. J Histochem Cytochem *50*, 1-10.
Bradshaw, A. D., and Sage, E. H. (2001). SPARC, a matricellular protein that functions in cellular differentiation and tissue response to injury. J Clin Invest *107*, 1049-1054.
Brekken, R. A., and Sage, E. H. (2001). SPARC, a matricellular protein: at the crossroads of cell-matrix communication. Matrix Biol *19*, 816-827.
Brockes, J. P., Fields, K. L., and Raff, M. C. (1979). Studies on cultured rat Schwann cells. I. Establishment of purified populations from cultures of peripheral nerve. Brain Res *165*, 105-118.
Brummendorf, T., and Rathjen, F. G. (1995). Cell adhesion molecules 1: immunoglobulin superfamily. Protein Profile *2*, 963-1108.
Cai, F., Campana, W. M., Tomlinson, D. R., and Fernyhough, P. (1999). Transforming growth factor-beta1 and glial growth factor 2 reduce neurotrophin-3 mRNA expression in cultured Schwann cells via a cAMP-dependent pathway. Brain Res Mol Brain Res *71*, 256-264.
Calof, A. L., Holcomb, J. D., Mumm, J. S., Haglwara, N., Tran, P., Smith, K. M., and Shelton, D. (1996). Factors affecting neuronal birth and death in the mammalian olfactory epithelium. Ciba Found Symp *196*, 188-205; discussion; 205-110.
Cao, L., Liu, L., Chen, Z. Y., Wang, L. M., Ye, J. L., Qiu, H. Y., Lu, C. L., and He, C. (2004). Olfactory ensheathing cells genetically modified to secrete GDNF to promote spinal cord repair. Brain *127*, 535-549.
Carey, D. J., and Stahl, R. C. (1990). Identification of a lipid-anchored heparan sulfate proteoglycan in Schwann cells. J Cell Biol *111*, 2053-2062.
Carter, L. A., MacDonald, J. L., and Roskams, A. J. (2004). Olfactory horizontal basal cells demonstrate a conserved multipotent progenitor phenotype. J Neurosci *24*, 5670-5683.
Carter, L. A., and Roskams, A. J. (2002). Neurotrophins and their receptors in the primary olfactory neuraxis. Microsc Res Tech *58*, 189-196.
Chakrabortty, S., Kitada, M., Matsumoto, N., Taketomi, M., Kimura, K., and Ide, C. (2000). Choroid plexus ependymal cells enhance neurite outgrowth from dorsal root ganglion neurons in vitro. J Neurocytol *29*, 707-717.

Chan, H. M., and La Thangue, N. B. (2001). p300/CBP proteins: HATs for transcriptional bridges and scaffolds. J Cell Sci *114*, 2363-2373.
Chernousov, M. A., Scherer, S. S., Stahl, R. C., and Carey, D. J. (1999). p200, a collagen secreted by Schwann cells, is expressed in developing nerves and in adult nerves following axotomy. J Neurosci Res *56*, 284-294.
Chernousov, M. A., Stahl, R. C., and Carey, D. J. (2001). Schwann cell type V collagen inhibits axonal outgrowth and promotes Schwann cell migration via distinct adhesive activities of the collagen and noncollagen domains. J Neurosci *21*, 6125-6135.
Chuah, M. I., and Au, C. (1991). Olfactory Schwann cells are derived from precursor cells in the olfactory epithelium. J Neurosci Res *29*, 172-180.
Chuah, M. I., and Au, C. (1993). Cultures of ensheathing cells from neonatal rat olfactory bulbs. Brain Res *601*, 213-220.
Chuah, M. I., and Au, C. (1994). Olfactory cell cultures on ensheathing cell monolayers. Chem Senses *19*, 25-34.
Chuah, M. I., Choi-Lundberg, D., Weston, S., Vincent, A. J., Chung, R. S., Vickers, J. C., and West, A. K. (2004). Olfactory ensheathing cells promote collateral axonal branching in the injured adult rat spinal cord. Exp Neurol *185*, 15-25.
Chuah, M. I., Cossins, J., Woodhall, E., Tennent, R., Nash, G., and West, A. K. (2000). Glial growth factor 2 induces proliferation and structural changes in ensheathing cells. Brain Res *857*, 265-274.
Chuah, M. I., and Teague, R. (1999). Basic fibroblast growth factor in the primary olfactory pathway: mitogenic effect on ensheathing cells. Neuroscience *88*, 1043-1050.
Chung, R. S., Woodhouse, A., Fung, S., Dickson, T. C., West, A. K., Vickers, J. C., and Chuah, M. I. (2004). Olfactory ensheathing cells promote neurite sprouting of injured axons in vitro by direct cellular contact and secretion of soluble factors. Cell Mol Life Sci *61*, 1238-1245.
Clemence, A., Mirsky, R., and Jessen, K. R. (1989). Non-myelin-forming Schwann cells proliferate rapidly during Wallerian degeneration in the rat sciatic nerve. J Neurocytol *18*, 185-192.
Cloutier, J. F., Sahay, A., Chang, E. C., Tessier-Lavigne, M., Dulac, C., Kolodkin, A. L., and Ginty, D. D. (2004). Differential requirements for semaphorin 3F and Slit-1 in axonal targeting, fasciculation, and segregation of olfactory sensory neuron projections. J Neurosci *24*, 9087-9096.
Coloma, M. J., Hastings, A., Wims, L. A., and Morrison, S. L. (1992). Novel vectors for the expression of antibody molecules using variable regions generated by polymerase chain reaction. J Immunol Methods *152*, 89-104.
Connolly, G. P. (2001). Cell imaging and morphology: application to studies of inherited purine metabolic disorders. Pharmacol Ther *90*, 267-281.
Corfas, G., Velardez, M. O., Ko, C. P., Ratner, N., and Peles, E. (2004). Mechanisms and roles of axon-Schwann cell interactions. J Neurosci *24*, 9250-9260.
Couly, G. F., and Le Douarin, N. M. (1985). Mapping of the early neural primordium in quail-chick chimeras. I. Developmental relationships between placodes, facial ectoderm, and prosencephalon. Dev Biol *110*, 422-439.
Cowan, W. M. (2001). Viktor Hamburger and Rita Levi-Montalcini: the path to the discovery of nerve growth factor. Annu Rev Neurosci *24*, 551-600.

Cutforth, T., Moring, L., Mendelsohn, M., Nemes, A., Shah, N. M., Kim, M. M., Frisen, J., and Axel, R. (2003). Axonal ephrin-As and odorant receptors: coordinate determination of the olfactory sensory map. Cell *114*, 311-322.
Davies, R., Hayat, S., Wigley, C. B., and Robbins, J. (2004). The calcium influx pathway in rat olfactory ensheathing cells shows TRPC channel pharmacology. Brain Res *1023*, 154-156.
Day, W. A., Koishi, K., and McLennan, I. S. (2003). Transforming growth factor beta 1 may regulate the stability of mature myelin sheaths. Exp Neurol *184*, 857-864.
Delany, A. M., Amling, M., Priemel, M., Howe, C., Baron, R., and Canalis, E. (2000). Osteopenia and decreased bone formation in osteonectin-deficient mice. J Clin Invest *105*, 1325.
Delree, P., Leprince, P., Schoenen, J., and Moonen, G. (1989). Purification and culture of adult rat dorsal root ganglia neurons. J Neurosci Res *23*, 198-206.
Denis-Donini, S., and Estenoz, M. (1988). Interneurons versus efferent neurons: heterogeneity in their neurite outgrowth response to glia from several brain regions. Dev Biol *130*, 237-249.
Devon, R., and Doucette, R. (1992). Olfactory ensheathing cells myelinate dorsal root ganglion neurites. Brain Res *589*, 175-179.
Devon, R., and Doucette, R. (1995). Olfactory ensheathing cells do not require L-ascorbic acid in vitro to assemble a basal lamina or to myelinate dorsal root ganglion neurites. Brain Res *688*, 223-229.
Dingwell, K. S., Holt, C. E., and Harris, W. A. (2000). The multiple decisions made by growth cones of RGCs as they navigate from the retina to the tectum in Xenopus embryos. J Neurobiol *44*, 246-259.
Dong, Z., Dean, C., Walters, J. E., Mirsky, R., and Jessen, K. R. (1997). Response of Schwann cells to mitogens in vitro is determined by pre-exposure to serum, time in vitro, and developmental age. Glia *20*, 219-230.
Dono, R. (2003). Fibroblast growth factors as regulators of central nervous system development and function. Am J Physiol Regul Integr Comp Physiol *284*, R867-881.
Doucette, J. R. (1984). The glial cells in the nerve fiber layer of the rat olfactory bulb. Anat Rec *210*, 385-391.
Doucette, J. R., Kiernan, J. A., and Flumerfelt, B. A. (1983a). The re-innervation of olfactory glomeruli following transection of primary olfactory axons in the central or peripheral nervous system. J Anat *137 (Pt 1)*, 1-19.
Doucette, J. R., Kiernan, J. A., and Flumerfelt, B. A. (1983b). Two different patterns of retrograde degeneration in the olfactory epithelium following transection of primary olfactory axons. J Anat *136 (Pt 4)*, 673-689.
Doucette, R. (1989). Development of the nerve fiber layer in the olfactory bulb of mouse embryos. J Comp Neurol *285*, 514-527.
Doucette, R. (1990). Glial influences on axonal growth in the primary olfactory system. Glia *3*, 433-449.
Doucette, R. (1991). PNS-CNS transitional zone of the first cranial nerve. J Comp Neurol *312*, 451-466.
Doucette, R. (1993). Glial cells in the nerve fiber layer of the main olfactory bulb of embryonic and adult mammals. Microsc Res Tech *24*, 113-130.

Doucette, R. (1996). Immunohistochemical localization of laminin, fibronectin and collagen type IV in the nerve fiber layer of the olfactory bulb. Int J Dev Neurosci *14*, 945-959.
Ducret, A., Van Oostveen, I., Eng, J. K., Yates, J. R., 3rd, and Aebersold, R. (1998). High throughput protein characterization by automated reverse-phase chromatography/electrospray tandem mass spectrometry. Protein Sci *7*, 706-719.
Eccleston, P. A., Jessen, K. R., and Mirsky, R. (1989). Transforming growth factor-beta and gamma-interferon have dual effects on growth of peripheral glia. J Neurosci Res *24*, 524-530.
Edstrom, A., Sjoberg, J., and Kanje, M. (1986). The use of whole-mount preparations of nerves labelled with axonally transported radioactive proteins to study regeneration. J Neurosci Methods *16*, 19-27.
Einheber, S., Hannocks, M. J., Metz, C. N., Rifkin, D. B., and Salzer, J. L. (1995). Transforming growth factor-beta 1 regulates axon/Schwann cell interactions. J Cell Biol *129*, 443-458.
Fairless, R., Frame, M. C., and Barnett, S. C. (2005). N-cadherin differentially determines Schwann cell and olfactory ensheathing cell adhesion and migration responses upon contact with astrocytes. Mol Cell Neurosci *28*, 253-263.
Farbman, A. I. (1990). Olfactory neurogenesis: genetic or environmental controls? Trends Neurosci *13*, 362-365.
Farbman, A. I., and Margolis, F. L. (1980). Olfactory marker protein during ontogeny: immunohistochemical localization. Dev Biol *74*, 205-215.
Farbman, A. I., and Squinto, L. M. (1985). Early development of olfactory receptor cell axons. Brain Res *351*, 205-213.
Fawcett, J. W., and Asher, R. A. (1999). The glial scar and central nervous system repair. Brain Res Bull *49*, 377-391.
Fehlings, M. G., and Tator, C. H. (1995). The relationships among the severity of spinal cord injury, residual neurological function, axon counts, and counts of retrogradely labeled neurons after experimental spinal cord injury. Exp Neurol *132*, 220-228.
Feiner, L., Koppel, A. M., Kobayashi, H., and Raper, J. A. (1997). Secreted chick semaphorins bind recombinant neuropilin with similar affinities but bind different subsets of neurons in situ. Neuron *19*, 539-545.
Field, P., Li, Y., and Raisman, G. (2003). Ensheathment of the olfactory nerves in the adult rat. J Neurocytol *32*, 317-324.
Fraher, J. P. (1992). The CNS-PNS transitional zone of the rat. Morphometric studies at cranial and spinal levels. Prog Neurobiol *38*, 261-316.
Franceschini, I. A., and Barnett, S. C. (1996). Low-affinity NGF-receptor and E-N-CAM expression define two types of olfactory nerve ensheathing cells that share a common lineage. Dev Biol *173*, 327-343.
Francki, A., Bradshaw, A. D., Bassuk, J. A., Howe, C. C., Couser, W. G., and Sage, E. H. (1999). SPARC regulates the expression of collagen type I and transforming growth factor-beta1 in mesangial cells. J Biol Chem *274*, 32145-32152.
Francki, A., McClure, T. D., Brekken, R. A., Motamed, K., Murri, C., Wang, T., and Sage, E. H. (2004). SPARC regulates TGF-beta1-dependent signaling in primary glomerular mesangial cells. J Cell Biochem *91*, 915-925.

Franklin, R. J. (2002). Remyelination of the demyelinated CNS: the case for and against transplantation of central, peripheral and olfactory glia. Brain Res Bull *57*, 827-832.
Franklin, R. J. (2003). Remyelination by transplanted olfactory ensheathing cells. Anat Rec B New Anat *271*, 71-76.
Franklin, R. J., Gilson, J. M., Franceschini, I. A., and Barnett, S. C. (1996). Schwann cell-like myelination following transplantation of an olfactory bulb-ensheathing cell line into areas of demyelination in the adult CNS. Glia *17*, 217-224.
Franzen, R., Martin, D., Daloze, A., Moonen, G., and Schoenen, J. (1999). Grafts of meningeal fibroblasts in adult rat spinal cord lesion promote axonal regrowth. Neuroreport *10*, 1551-1556.
Fryer, R. H., Kaplan, D. R., and Kromer, L. F. (1997). Truncated trkB receptors on nonneuronal cells inhibit BDNF-induced neurite outgrowth in vitro. Exp Neurol *148*, 616-627.
Garcia-Alias, G., Lopez-Vales, R., Fores, J., Navarro, X., and Verdu, E. (2004). Acute transplantation of olfactory ensheathing cells or Schwann cells promotes recovery after spinal cord injury in the rat. J Neurosci Res *75*, 632-641.
Gershon, M. D., Chalazonitis, A., and Rothman, T. P. (1993). From neural crest to bowel: development of the enteric nervous system. J Neurobiol *24*, 199-214.
Gheusi, G., Cremer, H., McLean, H., Chazal, G., Vincent, J. D., and Lledo, P. M. (2000). Importance of newly generated neurons in the adult olfactory bulb for odor discrimination. Proc Natl Acad Sci U S A *97*, 1823-1828.
Gillen, C., Gleichmann, M., Spreyer, P., and Muller, H. W. (1995). Differentially expressed genes after peripheral nerve injury. J Neurosci Res *42*, 159-171.
Gohring, W., Sasaki, T., Heldin, C. H., and Timpl, R. (1998). Mapping of the binding of platelet-derived growth factor to distinct domains of the basement membrane proteins BM-40 and perlecan and distinction from the BM-40 collagen-binding epitope. Eur J Biochem *255*, 60-66.
Gomez, V. M., Averill, S., King, V., Yang, Q., Perez, E. D., Chacon, S. C., Ward, R., Nieto-Sampedro, M., Priestley, J., and Taylor, J. (2003). Transplantation of olfactory ensheathing cells fails to promote significant axonal regeneration from dorsal roots into the rat cervical cord. J Neurocytol *32*, 53-70.
Gong, Q., Bailey, M. S., Pixley, S. K., Ennis, M., Liu, W., and Shipley, M. T. (1994). Localization and regulation of low affinity nerve growth factor receptor expression in the rat olfactory system during development and regeneration. J Comp Neurol *344*, 336-348.
Gong, Q., and Shipley, M. T. (1996). Expression of extracellular matrix molecules and cell surface molecules in the olfactory nerve pathway during early development. J Comp Neurol *366*, 1-14.
Gong, S. G. (2001). Characterization of olfactory nerve abnormalities in Twirler mice. Differentiation *69*, 58-65.
Goodman, M. N., Silver, J., and Jacobberger, J. W. (1993). Establishment and neurite outgrowth properties of neonatal and adult rat olfactory bulb glial cell lines. Brain Res *619*, 199-213.
Gordon, T., Sulaiman, O., and Boyd, J. G. (2003). Experimental strategies to promote functional recovery after peripheral nerve injuries. J Peripher Nerv Syst *8*, 236-250.

Graziadei, G. A., and Graziadei, P. P. (1979a). Neurogenesis and neuron regeneration in the olfactory system of mammals. II. Degeneration and reconstitution of the olfactory sensory neurons after axotomy. J Neurocytol *8*, 197-213.
Graziadei, P. P., and Graziadei, G. A. (1979b). Neurogenesis and neuron regeneration in the olfactory system of mammals. I. Morphological aspects of differentiation and structural organization of the olfactory sensory neurons. J Neurocytol *8*, 1-18.
Graziadei, P. P., Levine, R. R., and Graziadei, G. A. (1978). Regeneration of olfactory axons and synapse formation in the forebrain after bulbectomy in neonatal mice. Proc Natl Acad Sci U S A *75*, 5230-5234.
Graziadei, P. P., and Monti Graziadei, A. G. (1983). Regeneration in the olfactory system of vertebrates. Am J Otolaryngol *4*, 228-233.
Graziadei, P. P., and Monti Graziadei, G. A. (1976). Olfactory epithelium of Necturus maculosus and Ambystoma tigrinum. J Neurocytol *5*, 11-32.
Graziadei, P. P., and Monti Graziadei, G. A. (1986). Neuronal changes in the forebrain of mice following penetration by regenerating olfactory axons. J Comp Neurol *247*, 344-356.
Grothe, C., Schulze, A., Semkova, I., Muller-Ostermeyer, F., Rege, A., and Wewetzer, K. (2000). The high molecular weight fibroblast growth factor-2 isoforms (21,000 mol. wt and 23,000 mol. wt) mediate neurotrophic activity on rat embryonic mesencephalic dopaminergic neurons in vitro. Neuroscience *100*, 73-86.
Gudino-Cabrera, G., and Nieto-Sampedro, M. (1999). Estrogen receptor immunoreactivity in Schwann-like brain macroglia. J Neurobiol *40*, 458-470.
Guenard, V., Gwynn, L. A., and Wood, P. M. (1995a). Transforming growth factor-beta blocks myelination but not ensheathment of axons by Schwann cells in vitro. J Neurosci *15*, 419-428.
Guenard, V., Rosenbaum, T., Gwynn, L. A., Doetschman, T., Ratner, N., and Wood, P. M. (1995b). Effect of transforming growth factor-beta 1 and -beta 2 on Schwann cell proliferation on neurites. Glia *13*, 309-318.
Guntinas-Lichius, O., Angelov, D. N., Tomov, T. L., Dramiga, J., Neiss, W. F., and Wewetzer, K. (2001). Transplantation of olfactory ensheathing cells stimulates the collateral sprouting from axotomized adult rat facial motoneurons. Exp Neurol *172*, 70-80.
Guntinas-Lichius, O., Wewetzer, K., Tomov, T. L., Azzolin, N., Kazemi, S., Streppel, M., Neiss, W. F., and Angelov, D. N. (2002). Transplantation of olfactory mucosa minimizes axonal branching and promotes the recovery of vibrissae motor performance after facial nerve repair in rats. J Neurosci *22*, 7121-7131.
Gygi, S. P., and Aebersold, R. (2000). Mass spectrometry and proteomics. Curr Opin Chem Biol *4*, 489-494.
Gygi, S. P., Rist, B., Gerber, S. A., Turecek, F., Gelb, M. H., and Aebersold, R. (1999a). Quantitative analysis of complex protein mixtures using isotope-coded affinity tags. Nat Biotechnol *17*, 994-999.
Gygi, S. P., Rochon, Y., Franza, B. R., and Aebersold, R. (1999b). Correlation between protein and mRNA abundance in yeast. Mol Cell Biol *19*, 1720-1730.
Hansel, D. E., May, V., Eipper, B. A., and Ronnett, G. V. (2001). Pituitary adenylyl cyclase-activating peptides and alpha-amidation in olfactory neurogenesis and neuronal survival in vitro. J Neurosci *21*, 4625-4636.

Hayat, S., Thomas, A., Afshar, F., Sonigra, R., and Wigley, C. B. (2003a). Manipulation of olfactory ensheathing cell signaling mechanisms: effects on their support for neurite regrowth from adult CNS neurons in coculture. Glia *44*, 232-241.
Hayat, S., Wigley, C. B., and Robbins, J. (2003b). Intracellular calcium handling in rat olfactory ensheathing cells and its role in axonal regeneration. Mol Cell Neurosci *22*, 259-270.
Haynes, P. A., and Yates, J. R., 3rd (2000). Proteome profiling-pitfalls and progress. Yeast *17*, 81-87.
Hegg, C. C., Au, E., Roskams, A. J., and Lucero, M. T. (2003). PACAP is present in the olfactory system and evokes calcium transients in olfactory receptor neurons. J Neurophysiol *90*, 2711-2719.
Heredia, M., Gascuel, J., Ramon-Cueto, A., Santacana, M., Avila, J., Masson, C., and Valverde, F. (1998). Two novel monoclonal antibodies (1.9.E and 4.11.C) against olfactory bulb ensheathing glia. Glia *24*, 352-364.
Hermanns, S., Klapka, N., and Muller, H. W. (2001). The collagenous lesion scar--an obstacle for axonal regeneration in brain and spinal cord injury. Restor Neurol Neurosci *19*, 139-148.
Hiraizumi, Y., Transfeldt, E. E., Kawahara, N., Sung, J. H., Knighton, D., and Fiegel, V. D. (1993). In vivo angiogenesis by platelet-derived wound-healing formula in injured spinal cord. Brain Res Bull *30*, 353-357.
Holcomb, J. D., Mumm, J. S., and Calof, A. L. (1995). Apoptosis in the neuronal lineage of the mouse olfactory epithelium: regulation in vivo and in vitro. Dev Biol *172*, 307-323.
Holland, P. W., Harper, S. J., McVey, J. H., and Hogan, B. L. (1987). In vivo expression of mRNA for the Ca++-binding protein SPARC (osteonectin) revealed by in situ hybridization. J Cell Biol *105*, 473-482.
Horie, H., Kadoya, T., Hikawa, N., Sango, K., Inoue, H., Takeshita, K., Asawa, R., Hiroi, T., Sato, M., Yoshioka, T., and Ishikawa, Y. (2004). Oxidized galectin-1 stimulates macrophages to promote axonal regeneration in peripheral nerves after axotomy. J Neurosci *24*, 1873-1880.
Hossain, W. A., and Morest, D. K. (2000). Fibroblast growth factors (FGF-1, FGF-2) promote migration and neurite growth of mouse cochlear ganglion cells in vitro: immunohistochemistry and antibody perturbation. J Neurosci Res *62*, 40-55.
Hsu, P., Yu, F., Feron, F., Pickles, J. O., Sneesby, K., and Mackay-Sim, A. (2001). Basic fibroblast growth factor and fibroblast growth factor receptors in adult olfactory epithelium. Brain Res *896*, 188-197.
Huynh, M. H., Hong, H., Delovitch, S., Desser, S., and Ringuette, M. (2000). Association of SPARC (osteonectin, BM-40) with extracellular and intracellular components of the ciliated surface ectoderm of Xenopus embryos. Cell Motil Cytoskeleton *47*, 154-162.
Ikeda, K., Nakao, J., Asou, H., Toya, S., Shinoda, J., and Uyemura, K. (1996). Expression of CD44H in the cells of neural crest origin in peripheral nervous system. Neuroreport *7*, 1713-1716.
Illing, N., Boolay, S., Siwoski, J. S., Casper, D., Lucero, M. T., and Roskams, A. J. (2002). Conditionally immortalized clonal cell lines from the mouse olfactory placode differentiate into olfactory receptor neurons. Mol Cell Neurosci *20*, 225-243.

Imaizumi, T., Lankford, K. L., Burton, W. V., Fodor, W. L., and Kocsis, J. D. (2000a). Xenotransplantation of transgenic pig olfactory ensheathing cells promotes axonal regeneration in rat spinal cord. Nat Biotechnol *18*, 949-953.
Imaizumi, T., Lankford, K. L., and Kocsis, J. D. (2000b). Transplantation of olfactory ensheathing cells or Schwann cells restores rapid and secure conduction across the transected spinal cord. Brain Res *854*, 70-78.
Imaizumi, T., Lankford, K. L., Waxman, S. G., Greer, C. A., and Kocsis, J. D. (1998). Transplanted olfactory ensheathing cells remyelinate and enhance axonal conduction in the demyelinated dorsal columns of the rat spinal cord. J Neurosci *18*, 6176-6185.
Iruela-Arispe, M. L., Hasselaar, P., and Sage, H. (1991). Differential expression of extracellular proteins is correlated with angiogenesis in vitro. Lab Invest *64*, 174-186.
Iruela-Arispe, M. L., Vernon, R. B., Wu, H., Jaenisch, R., and Sage, E. H. (1996). Type I collagen-deficient Mov-13 mice do not retain SPARC in the extracellular matrix: implications for fibroblast function. Dev Dyn *207*, 171-183.
Itoh, H., Aso, Y., Furuse, M., Noishiki, Y., and Miyata, T. (2001). A honeycomb collagen carrier for cell culture as a tissue engineering scaffold. Artif Organs *25*, 213-217.
Jessen, K. R., and Mirsky, R. (1985). Glial fibrillary acidic polypeptides in peripheral glia. Molecular weight, heterogeneity and distribution. J Neuroimmunol *8*, 377-393.
Jessen, K. R., and Mirsky, R. (1991). Schwann cell precursors and their development. Glia *4*, 185-194.
Jessen, K. R., and Mirsky, R. (2002). Signals that determine Schwann cell identity. J Anat *200*, 367-376.
Joosten, E. A., Veldhuis, W. B., and Hamers, F. P. (2004). Collagen containing neonatal astrocytes stimulates regrowth of injured fibers and promotes modest locomotor recovery after spinal cord injury. J Neurosci Res *77*, 127-142.
Julliard, A. K., and Hartmann, D. J. (1998). Spatiotemporal patterns of expression of extracellular matrix molecules in the developing and adult rat olfactory system. Neuroscience *84*, 1135-1150.
Jung, W., Castren, E., Odenthal, M., Vande Woude, G. F., Ishii, T., Dienes, H. P., Lindholm, D., and Schirmacher, P. (1994). Expression and functional interaction of hepatocyte growth factor-scatter factor and its receptor c-met in mammalian brain. J Cell Biol *126*, 485-494.
Kafitz, K. W., and Greer, C. A. (1998). The influence of ensheathing cells on olfactory receptor cell neurite outgrowth in vitro. Ann N Y Acad Sci *855*, 266-269.
Kafitz, K. W., and Greer, C. A. (1999). Olfactory ensheathing cells promote neurite extension from embryonic olfactory receptor cells in vitro. Glia *25*, 99-110.
Kawano, H., Li, H. P., Sango, K., Kawamura, K., and Raisman, G. (2005). Inhibition of collagen synthesis overrides the age-related failure of regeneration of nigrostriatal dopaminergic axons. J Neurosci Res *80*, 191-202.
Keller, A., Nesvizhskii, A. I., Kolker, E., and Aebersold, R. (2002). Empirical statistical model to estimate the accuracy of peptide identifications made by MS/MS and database search. Anal Chem *74*, 5383-5392.
Key, B., and St John, J. (2002). Axon navigation in the mammalian primary olfactory pathway: where to next? Chem Senses *27*, 245-260.

Key, B., Treloar, H. B., Wangerek, L., Ford, M. D., and Nurcombe, V. (1996). Expression and localization of FGF-1 in the developing rat olfactory system. J Comp Neurol *366*, 197-206.
Keyvan-Fouladi, N., Raisman, G., and Li, Y. (2003). Functional repair of the corticospinal tract by delayed transplantation of olfactory ensheathing cells in adult rats. J Neurosci *23*, 9428-9434.
Kiryushko, D., Berezin, V., and Bock, E. (2004). Regulators of neurite outgrowth: role of cell adhesion molecules. Ann N Y Acad Sci *1014*, 140-154.
Kleinman, H. K., McGarvey, M. L., Hassell, J. R., Star, V. L., Cannon, F. B., Laurie, G. W., and Martin, G. R. (1986). Basement membrane complexes with biological activity. Biochemistry *25*, 312-318.
Klimaschewski, L., Nindl, W., Pimpl, M., Waltinger, P., and Pfaller, K. (2002). Biolistic transfection and morphological analysis of cultured sympathetic neurons. J Neurosci Methods *113*, 63-71.
Koh, S., Oyler, G. A., and Higgins, G. A. (1989). Localization of nerve growth factor receptor messenger RNA and protein in the adult rat brain. Exp Neurol *106*, 209-221.
Kornblum, H. I., Raymon, H. K., Morrison, R. S., Cavanaugh, K. P., Bradshaw, R. A., and Leslie, F. M. (1990). Epidermal growth factor and basic fibroblast growth factor: effects on an overlapping population of neocortical neurons in vitro. Brain Res *535*, 255-263.
Kott, J. N., Westrum, L. E., Raines, E. W., Sasahara, M., and Ross, R. (1994). Olfactory ensheathing glia and platelet-derived growth factor B-chain reactivity in the transplanted rat olfactory bulb. Int J Dev Neurosci *12*, 315-323.
Krasnoselsky, A., Massay, M. J., DeFrances, M. C., Michalopoulos, G., Zarnegar, R., and Ratner, N. (1994). Hepatocyte growth factor is a mitogen for Schwann cells and is present in neurofibromas. J Neurosci *14*, 7284-7290.
Kumar, R., Hayat, S., Felts, P., Bunting, S., and Wigley, C. (2005). Functional differences and interactions between phenotypic subpopulations of olfactory ensheathing cells in promoting CNS axonal regeneration. Glia *50*, 12-20.
Kupprion, C., Motamed, K., and Sage, E. H. (1998). SPARC (BM-40, osteonectin) inhibits the mitogenic effect of vascular endothelial growth factor on microvascular endothelial cells. J Biol Chem *273*, 29635-29640.
Kwon, B. K., and Tetzlaff, W. (2001). Spinal cord regeneration: from gene to transplants. Spine *26*, S13-22.
Lacroix, S., and Tuszynski, M. H. (2000). Neurotrophic factors and gene therapy in spinal cord injury. Neurorehabil Neural Repair *14*, 265-275.
Lakatos, A., Barnett, S. C., and Franklin, R. J. (2003a). Olfactory ensheathing cells induce less host astrocyte response and chondroitin sulphate proteoglycan expression than Schwann cells following transplantation into adult CNS white matter. Exp Neurol *184*, 237-246.
Lakatos, A., Franklin, R. J., and Barnett, S. C. (2000). Olfactory ensheathing cells and Schwann cells differ in their in vitro interactions with astrocytes. Glia *32*, 214-225.
Lakatos, A., Smith, P. M., Barnett, S. C., and Franklin, R. J. (2003b). Meningeal cells enhance limited CNS remyelination by transplanted olfactory ensheathing cells. Brain *126*, 598-609.

Lane, T. F., Iruela-Arispe, M. L., Johnson, R. S., and Sage, E. H. (1994). SPARC is a source of copper-binding peptides that stimulate angiogenesis. J Cell Biol *125*, 929-943.
Le Roux, P. D., and Reh, T. A. (1994). Regional differences in glial-derived factors that promote dendritic outgrowth from mouse cortical neurons in vitro. J Neurosci *14*, 4639-4655.
Lee, R., Kermani, P., Teng, K. K., and Hempstead, B. L. (2001). Regulation of cell survival by secreted proneurotrophins. Science *294*, 1945-1948.
Leeds, P., Leng, Y., Chalecka-Franaszek, E., and Chuang, D. M. (2005). Neurotrophins protect against cytosine arabinoside-induced apoptosis of immature rat cerebellar neurons. Neurochem Int *46*, 61-72.
Levine, J. M., and Stallcup, W. B. (1987). Plasticity of developing cerebellar cells in vitro studied with antibodies against the NG2 antigen. J Neurosci *7*, 2721-2731.
Levine, J. M., Stincone, F., and Lee, Y. S. (1993). Development and differentiation of glial precursor cells in the rat cerebellum. Glia *7*, 307-321.
Li, Q., Xiao, H., and Isobe, K. (2002). Histone acetyltransferase activities of cAMP-regulated enhancer-binding protein and p300 in tissues of fetal, young, and old mice. J Gerontol A Biol Sci Med Sci *57*, B93-98.
Li, X. J., Zhang, H., Ranish, J. A., and Aebersold, R. (2003a). Automated statistical analysis of protein abundance ratios from data generated by stable-isotope dilution and tandem mass spectrometry. Anal Chem *75*, 6648-6657.
Li, Y., Carlstedt, T., Berthold, C. H., and Raisman, G. (2004). Interaction of transplanted olfactory-ensheathing cells and host astrocytic processes provides a bridge for axons to regenerate across the dorsal root entry zone. Exp Neurol *188*, 300-308.
Li, Y., Decherchi, P., and Raisman, G. (2003b). Transplantation of olfactory ensheathing cells into spinal cord lesions restores breathing and climbing. J Neurosci *23*, 727-731.
Li, Y., Field, P. M., and Raisman, G. (1997). Repair of adult rat corticospinal tract by transplants of olfactory ensheathing cells. Science *277*, 2000-2002.
Li, Y., Field, P. M., and Raisman, G. (1998). Regeneration of adult rat corticospinal axons induced by transplanted olfactory ensheathing cells. J Neurosci *18*, 10514-10524.
Lipson, A. C., Widenfalk, J., Lindqvist, E., Ebendal, T., and Olson, L. (2003). Neurotrophic properties of olfactory ensheathing glia. Exp Neurol *180*, 167-171.
Liu, K. L., Chuah, M. I., and Lee, K. K. (1995). Soluble factors from the olfactory bulb attract olfactory Schwann cells. J Neurosci *15*, 990-1000.
Liu, Y., and Rao, M. S. (2004). Glial progenitors in the CNS and possible lineage relationships among them. Biol Cell *96*, 279-290.
Liuzzi, F. J., and Tedeschi, B. (1991). Peripheral nerve regeneration. Neurosurg Clin N Am *2*, 31-42.
Lobsiger, C. S., Taylor, V., and Suter, U. (2002). The early life of a Schwann cell. Biol Chem *383*, 245-253.
Lu, J., Feron, F., Mackay-Sim, A., and Waite, P. M. (2002). Olfactory ensheathing cells promote locomotor recovery after delayed transplantation into transected spinal cord. Brain *125*, 14-21.
Lundkvist, J., and Lendahl, U. (2001). Notch and the birth of glial cells. Trends Neurosci *24*, 492-494.
MacInnis, B. L., and Campenot, R. B. (2002). Retrograde support of neuronal survival without retrograde transport of nerve growth factor. Science *295*, 1536-1539.

Mackay-Sima, A., and Chuahb, M. I. (2000). Neurotrophic factors in the primary olfactory pathway. Prog Neurobiol *62*, 527-559.
Magrassi, L., and Graziadei, P. P. (1985). Interaction of the transplanted olfactory placode with the optic stalk and the diencephalon in Xenopus laevis embryos. Neuroscience *15*, 903-921.
Malatesta, P., Hack, M. A., Hartfuss, E., Kettenmann, H., Klinkert, W., Kirchhoff, F., and Gotz, M. (2003). Neuronal or glial progeny: regional differences in radial glia fate. Neuron *37*, 751-764.
Manitt, C., and Kennedy, T. E. (2002). Where the rubber meets the road: netrin expression and function in developing and adult nervous systems. Prog Brain Res *137*, 425-442.
Mann, M., and Pandey, A. (2001). Use of mass spectrometry-derived data to annotate nucleotide and protein sequence databases. Trends Biochem Sci *26*, 54-61.
Marin-Padilla, M., and Amieva, M. R. (1989). Early neurogenesis of the mouse olfactory nerve: Golgi and electron microscopic studies. J Comp Neurol *288*, 339-352.
Martin, D. P., Wallace, T. L., and Johnson, E. M., Jr. (1990). Cytosine arabinoside kills postmitotic neurons in a fashion resembling trophic factor deprivation: evidence that a deoxycytidine-dependent process may be required for nerve growth factor signal transduction. J Neurosci *10*, 184-193.
Matsuoka, I., Nakane, A., and Kurihara, K. (1997). Induction of LIF-mRNA by TGF-beta 1 in Schwann cells. Brain Res *776*, 170-180.
Matsuyama, A., Iwata, H., Okumura, N., Yoshida, S., Imaizumi, K., Lee, Y., Shiraishi, S., and Shiosaka, S. (1992). Localization of basic fibroblast growth factor-like immunoreactivity in the rat brain. Brain Res *587*, 49-65.
Maurel, P., and Salzer, J. L. (2000). Axonal regulation of Schwann cell proliferation and survival and the initial events of myelination requires PI 3-kinase activity. J Neurosci *20*, 4635-4645.
McMahon, S. B., Armanini, M. P., Ling, L. H., and Phillips, H. S. (1994). Expression and coexpression of Trk receptors in subpopulations of adult primary sensory neurons projecting to identified peripheral targets. Neuron *12*, 1161-1171.
Mendis, D. B., Ivy, G. O., and Brown, I. R. (1998). SPARC/osteonectin mRNA is induced in blood vessels following injury to the adult rat cerebral cortex. Neurochem Res *23*, 1117-1123.
Mendis, D. B., Malaval, L., and Brown, I. R. (1995). SPARC, an extracellular matrix glycoprotein containing the follistatin module, is expressed by astrocytes in synaptic enriched regions of the adult brain. Brain Res *676*, 69-79.
Mews, M., and Meyer, M. (1993). Modulation of Schwann cell phenotype by TGF-beta 1: inhibition of P0 mRNA expression and downregulation of the low affinity NGF receptor. Glia *8*, 208-217.
Michailov, G. V., Sereda, M. W., Brinkmann, B. G., Fischer, T. M., Haug, B., Birchmeier, C., Role, L., Lai, C., Schwab, M. H., and Nave, K. A. (2004). Axonal neuregulin-1 regulates myelin sheath thickness. Science *304*, 700-703.
Michel, D., Moyse, E., Brun, G., and Jourdan, F. (1994). Induction of apoptosis in mouse [correction of rat] olfactory neuroepithelium by synaptic target ablation. Neuroreport *5*, 1329-1332.

Miragall, F., Kadmon, G., and Schachner, M. (1989). Expression of L1 and N-CAM cell adhesion molecules during development of the mouse olfactory system. Dev Biol *135*, 272-286.
Miwa, T., Horikawa, I., Uramoto, N., Ishimaru, T., Yamamoto, K., Furukawa, M., Kato, T., and Moriizumi, T. (1998). TrkA expression in mouse olfactory tract following axotomy of olfactory nerves. Acta Otolaryngol Suppl *539*, 79-82.
Mombaerts, P. (2001). How smell develops. Nat Neurosci *4 Suppl*, 1192-1198.
Mombaerts, P., Wang, F., Dulac, C., Chao, S. K., Nemes, A., Mendelsohn, M., Edmondson, J., and Axel, R. (1996). Visualizing an olfactory sensory map. Cell *87*, 675-686.
Monti Graziadei, A. G., and Graziadei, P. P. (1989). Experimental studies on the olfactory marker protein. V. Olfactory marker protein in the olfactory neurons transplanted within the olfactory bulb. Brain Res *484*, 157-167.
Monti Graziadei, A. G., and Morrison, E. E. (1988). Experimental studies on the olfactory marker protein. IV. Olfactory marker protein in the olfactory neurons transplanted within the brain. Brain Res *455*, 401-406.
Morrison, S. J., Perez, S. E., Qiao, Z., Verdi, J. M., Hicks, C., Weinmaster, G., and Anderson, D. J. (2000). Transient Notch activation initiates an irreversible switch from neurogenesis to gliogenesis by neural crest stem cells. Cell *101*, 499-510.
Motamed, K., Blake, D. J., Angello, J. C., Allen, B. L., Rapraeger, A. C., Hauschka, S. D., and Sage, E. H. (2003). Fibroblast growth factor receptor-1 mediates the inhibition of endothelial cell proliferation and the promotion of skeletal myoblast differentiation by SPARC: a role for protein kinase A. J Cell Biochem *90*, 408-423.
Mu, X., Silos-Santiago, I., Carroll, S. L., and Snider, W. D. (1993). Neurotrophin receptor genes are expressed in distinct patterns in developing dorsal root ganglia. J Neurosci *13*, 4029-4041.
Nash, H. H., Borke, R. C., and Anders, J. J. (2001). New method of purification for establishing primary cultures of ensheathing cells from the adult olfactory bulb. Glia *34*, 81-87.
Nash, H. H., Borke, R. C., and Anders, J. J. (2002). Ensheathing cells and methylprednisolone promote axonal regeneration and functional recovery in the lesioned adult rat spinal cord. J Neurosci *22*, 7111-7120.
Navarro, X., Valero, A., Gudino, G., Fores, J., Rodriguez, F. J., Verdu, E., Pascual, R., Cuadras, J., and Nieto-Sampedro, M. (1999). Ensheathing glia transplants promote dorsal root regeneration and spinal reflex restitution after multiple lumbar rhizotomy. Ann Neurol *45*, 207-215.
Nesvizhskii, A. I., Keller, A., Kolker, E., and Aebersold, R. (2003). A statistical model for identifying proteins by tandem mass spectrometry. Anal Chem *75*, 4646-4658.
Newman, M. P., Feron, F., and Mackay-Sim, A. (2000). Growth factor regulation of neurogenesis in adult olfactory epithelium. Neuroscience *99*, 343-350.
Nguyen Ba-Charvet, K. T., Brose, K., Marillat, V., Kidd, T., Goodman, C. S., Tessier-Lavigne, M., Sotelo, C., and Chedotal, A. (1999). Slit2-Mediated chemorepulsion and collapse of developing forebrain axons. Neuron *22*, 463-473.
Norose, K., Clark, J. I., Syed, N. A., Basu, A., Heber-Katz, E., Sage, E. H., and Howe, C. C. (1998). SPARC deficiency leads to early-onset cataractogenesis. Invest Ophthalmol Vis Sci *39*, 2674-2680.

Novoselov, V. I., Bragin, A. G., Novikov, J. V., Nesterov, V. I., and Fesenko, E. E. (1983). Transplants of olfactory mucosa in the anterior chamber of the eye: morphology, electrophysiology and biochemistry. Dev Neurosci *6*, 317-324.
Nunes, I., Gleizes, P. E., Metz, C. N., and Rifkin, D. B. (1997). Latent transforming growth factor-beta binding protein domains involved in activation and transglutaminase-dependent cross-linking of latent transforming growth factor-beta. J Cell Biol *136*, 1151-1163.
Nykjaer, A., Willnow, T. E., and Petersen, C. M. (2005). p75(NTR) -- live or let die. Curr Opin Neurobiol *15*, 49-57.
O'Leary, D. D., and Wilkinson, D. G. (1999). Eph receptors and ephrins in neural development. Curr Opin Neurobiol *9*, 65-73.
Oda, Y., Huang, K., Cross, F. R., Cowburn, D., and Chait, B. T. (1999). Accurate quantitation of protein expression and site-specific phosphorylation. Proc Natl Acad Sci U S A *96*, 6591-6596.
Ono, K., Tomasiewicz, H., Magnuson, T., and Rutishauser, U. (1994). N-CAM mutation inhibits tangential neuronal migration and is phenocopied by enzymatic removal of polysialic acid. Neuron *13*, 595-609.
Orr-Urtreger, A., and Lonai, P. (1992). Platelet-derived growth factor-A and its receptor are expressed in separate, but adjacent cell layers of the mouse embryo. Development *115*, 1045-1058.
Pascual, J. I., Gudino-Cabrera, G., Insausti, R., and Nieto-Sampedro, M. (2002). Spinal implants of olfactory ensheathing cells promote axon regeneration and bladder activity after bilateral lumbosacral dorsal rhizotomy in the adult rat. J Urol *167*, 1522-1526.
Pataky, D. M., Borisoff, J. F., Fernandes, K. J., Tetzlaff, W., and Steeves, J. D. (2000). Fibroblast growth factor treatment produces differential effects on survival and neurite outgrowth from identified bulbospinal neurons in vitro. Exp Neurol *163*, 357-372.
Patel, K., Nash, J. A., Itoh, A., Liu, Z., Sundaresan, V., and Pini, A. (2001). Slit proteins are not dominant chemorepellents for olfactory tract and spinal motor axons. Development *128*, 5031-5037.
Pini, A. (1993). Chemorepulsion of axons in the developing mammalian central nervous system. Science *261*, 95-98.
Plant, G. W., Christensen, C. L., Oudega, M., and Bunge, M. B. (2003). Delayed transplantation of olfactory ensheathing glia promotes sparing/regeneration of supraspinal axons in the contused adult rat spinal cord. J Neurotrauma *20*, 1-16.
Plant, G. W., Currier, P. F., Cuervo, E. P., Bates, M. L., Pressman, Y., Bunge, M. B., and Wood, P. M. (2002). Purified adult ensheathing glia fail to myelinate axons under culture conditions that enable Schwann cells to form myelin. J Neurosci *22*, 6083-6091.
Pollock, G. S., Franceschini, I. A., Graham, G., Marchionni, M. A., and Barnett, S. C. (1999). Neuregulin is a mitogen and survival factor for olfactory bulb ensheathing cells and an isoform is produced by astrocytes. Eur J Neurosci *11*, 769-780.
Powell, E. M., Muhlfriedel, S., Bolz, J., and Levitt, P. (2003). Differential regulation of thalamic and cortical axonal growth by hepatocyte growth factor/scatter factor. Dev Neurosci *25*, 197-206.
Raines, E. W., Lane, T. F., Iruela-Arispe, M. L., Ross, R., and Sage, E. H. (1992). The extracellular glycoprotein SPARC interacts with platelet-derived growth factor (PDGF)-

AB and -BB and inhibits the binding of PDGF to its receptors. Proc Natl Acad Sci U S A *89*, 1281-1285.
Raisman, G. (2001). Olfactory ensheathing cells - another miracle cure for spinal cord injury? Nat Rev Neurosci *2*, 369-375.
Ramer, L. M., Au, E., Richter, M. W., Liu, J., Tetzlaff, W., and Roskams, A. J. (2004a). Peripheral olfactory ensheathing cells reduce scar and cavity formation and promote regeneration after spinal cord injury. J Comp Neurol *473*, 1-15.
Ramer, L. M., Ramer, M. S., and Steeves, J. D. (2005). Setting the stage for functional repair of spinal cord injuries: a cast of thousands. Spinal Cord *43*, 134-161.
Ramer, L. M., Richter, M. W., Roskams, A. J., Tetzlaff, W., and Ramer, M. S. (2004b). Peripherally-derived olfactory ensheathing cells do not promote primary afferent regeneration following dorsal root injury. Glia *47*, 189-206.
Ramon-Cueto, A., and Avila, J. (1998). Olfactory ensheathing glia: properties and function. Brain Res Bull *46*, 175-187.
Ramon-Cueto, A., Cordero, M. I., Santos-Benito, F. F., and Avila, J. (2000). Functional recovery of paraplegic rats and motor axon regeneration in their spinal cords by olfactory ensheathing glia. Neuron *25*, 425-435.
Ramon-Cueto, A., and Nieto-Sampedro, M. (1992). Glial cells from adult rat olfactory bulb: immunocytochemical properties of pure cultures of ensheathing cells. Neuroscience *47*, 213-220.
Ramon-Cueto, A., and Nieto-Sampedro, M. (1994). Regeneration into the spinal cord of transected dorsal root axons is promoted by ensheathing glia transplants. Exp Neurol *127*, 232-244.
Ramon-Cueto, A., Perez, J., and Nieto-Sampedro, M. (1993). In vitro enfolding of olfactory neurites by p75 NGF receptor positive ensheathing cells from adult rat olfactory bulb. Eur J Neurosci *5*, 1172-1180.
Ramon-Cueto, A., Plant, G. W., Avila, J., and Bunge, M. B. (1998). Long-distance axonal regeneration in the transected adult rat spinal cord is promoted by olfactory ensheathing glia transplants. J Neurosci *18*, 3803-3815.
Reed, M. J., Puolakkainen, P., Lane, T. F., Dickerson, D., Bornstein, P., and Sage, E. H. (1993). Differential expression of SPARC and thrombospondin 1 in wound repair: immunolocalization and in situ hybridization. J Histochem Cytochem *41*, 1467-1477.
Reed, M. J., Vernon, R. B., Abrass, I. B., and Sage, E. H. (1994). TGF-beta 1 induces the expression of type I collagen and SPARC, and enhances contraction of collagen gels, by fibroblasts from young and aged donors. J Cell Physiol *158*, 169-179.
Rempel, S. A., Golembieski, W. A., Fisher, J. L., Maile, M., and Nakeff, A. (2001). SPARC modulates cell growth, attachment and migration of U87 glioma cells on brain extracellular matrix proteins. J Neurooncol *53*, 149-160.
Renzi, M. J., Feiner, L., Koppel, A. M., and Raper, J. A. (1999). A dominant negative receptor for specific secreted semaphorins is generated by deleting an extracellular domain from neuropilin-1. J Neurosci *19*, 7870-7880.
Renzi, M. J., Wexler, T. L., and Raper, J. A. (2000). Olfactory sensory axons expressing a dominant-negative semaphorin receptor enter the CNS early and overshoot their target. Neuron *28*, 437-447.

Riddell, J. S., Enriquez-Denton, M., Toft, A., Fairless, R., and Barnett, S. C. (2004). Olfactory ensheathing cell grafts have minimal influence on regeneration at the dorsal root entry zone following rhizotomy. Glia *47*, 150-167.
Robinson, M., Parsons Perez, M. C., Tebar, L., Palmer, J., Patel, A., Marks, D., Sheasby, A., De Felipe, C., Coffin, R., Livesey, F. J., and Hunt, S. P. (2004). FLRT3 is expressed in sensory neurons after peripheral nerve injury and regulates neurite outgrowth. Mol Cell Neurosci *27*, 202-214.
Rodriguez-Tebar, A., Dechant, G., and Barde, Y. A. (1990). Binding of brain-derived neurotrophic factor to the nerve growth factor receptor. Neuron *4*, 487-492.
Rodriguez-Tebar, A., Dechant, G., Gotz, R., and Barde, Y. A. (1992). Binding of neurotrophin-3 to its neuronal receptors and interactions with nerve growth factor and brain-derived neurotrophic factor. Embo J *11*, 917-922.
Rogister, B., Delree, P., Leprince, P., Martin, D., Sadzot, C., Malgrange, B., Munaut, C., Rigo, J. M., Lefebvre, P. P., Octave, J. N., and et al. (1993). Transforming growth factor beta as a neuronoglial signal during peripheral nervous system response to injury. J Neurosci Res *34*, 32-43.
Roskams, A. J., Bethel, M. A., Hurt, K. J., and Ronnett, G. V. (1996). Sequential expression of Trks A, B, and C in the regenerating olfactory neuroepithelium. J Neurosci *16*, 1294-1307.
Rufer, M., Flanders, K., and Unsicker, K. (1994). Presence and regulation of transforming growth factor beta mRNA and protein in the normal and lesioned rat sciatic nerve. J Neurosci Res *39*, 412-423.
Ruit, K. G., Elliott, J. L., Osborne, P. A., Yan, Q., and Snider, W. D. (1992). Selective dependence of mammalian dorsal root ganglion neurons on nerve growth factor during embryonic development. Neuron *8*, 573-587.
Ruitenberg, M. J., Levison, D. B., Lee, S. V., Verhaagen, J., Harvey, A. R., and Plant, G. W. (2005). NT-3 expression from engineered olfactory ensheathing glia promotes spinal sparing and regeneration. Brain *128*, 839-853.
Ruitenberg, M. J., Plant, G. W., Hamers, F. P., Wortel, J., Blits, B., Dijkhuizen, P. A., Gispen, W. H., Boer, G. J., and Verhaagen, J. (2003). Ex vivo adenoviral vector-mediated neurotrophin gene transfer to olfactory ensheathing glia: effects on rubrospinal tract regeneration, lesion size, and functional recovery after implantation in the injured rat spinal cord. J Neurosci *23*, 7045-7058.
Sage, E. H., Reed, M., Funk, S. E., Truong, T., Steadele, M., Puolakkainen, P., Maurice, D. H., and Bassuk, J. A. (2003). Cleavage of the matricellular protein SPARC by matrix metalloproteinase 3 produces polypeptides that influence angiogenesis. J Biol Chem *278*, 37849-37857.
Sage, H., Vernon, R. B., Decker, J., Funk, S., and Iruela-Arispe, M. L. (1989). Distribution of the calcium-binding protein SPARC in tissues of embryonic and adult mice. J Histochem Cytochem *37*, 819-829.
Salzer, J. L., Williams, A. K., Glaser, L., and Bunge, R. P. (1980). Studies of Schwann cell proliferation. II. Characterization of the stimulation and specificity of the response to a neurite membrane fraction. J Cell Biol *84*, 753-766.
Sasahara, A., Kott, J. N., Sasahara, M., Raines, E. W., Ross, R., and Westrum, L. E. (1992). Platelet-derived growth factor B-chain-like immunoreactivity in the developing and adult rat brain. Brain Res Dev Brain Res *68*, 41-53.

Sasaki, M., Lankford, K. L., Zemedkun, M., and Kocsis, J. D. (2004). Identified olfactory ensheathing cells transplanted into the transected dorsal funiculus bridge the lesion and form myelin. J Neurosci *24*, 8485-8493.
Sasaki, T., Gohring, W., Mann, K., Maurer, P., Hohenester, E., Knauper, V., Murphy, G., and Timpl, R. (1997). Limited cleavage of extracellular matrix protein BM-40 by matrix metalloproteinases increases its affinity for collagens. J Biol Chem *272*, 9237-9243.
Saxod, R., and Bizet, M. C. (1988). Substrate effects on the dynamics of neurite growth in vitro: a quantitative multi-parametric analysis. Int J Dev Neurosci *6*, 177-191.
Schellinck, H. M., Arnold, A., and Rafuse, V. F. (2004). Neural cell adhesion molecule (NCAM) null mice do not show a deficit in odour discrimination learning. Behav Brain Res *152*, 327-334.
Scherer, S. S., Kamholz, J., and Jakowlew, S. B. (1993). Axons modulate the expression of transforming growth factor-betas in Schwann cells. Glia *8*, 265-276.
Schmid, R. S., Graff, R. D., Schaller, M. D., Chen, S., Schachner, M., Hemperly, J. J., and Maness, P. F. (1999). NCAM stimulates the Ras-MAPK pathway and CREB phosphorylation in neuronal cells. J Neurobiol *38*, 542-558.
Schmid, R. S., Pruitt, W. M., and Maness, P. F. (2000). A MAP kinase-signaling pathway mediates neurite outgrowth on L1 and requires Src-dependent endocytosis. J Neurosci *20*, 4177-4188.
Schwanzel-Fukuda, M., and Pfaff, D. W. (1989). Origin of luteinizing hormone-releasing hormone neurons. Nature *338*, 161-164.
Schwarting, G. A., Kostek, C., Bless, E. P., Ahmad, N., and Tobet, S. A. (2001). Deleted in colorectal cancer (DCC) regulates the migration of luteinizing hormone-releasing hormone neurons to the basal forebrain. J Neurosci *21*, 911-919.
Schwarting, G. A., Raitcheva, D., Bless, E. P., Ackerman, S. L., and Tobet, S. (2004). Netrin 1-mediated chemoattraction regulates the migratory pathway of LHRH neurons. Eur J Neurosci *19*, 11-20.
Schwartz, M. A. (2001). Integrin signaling revisited. Trends Cell Biol *11*, 466-470.
Singer, A. J., and Clark, R. A. (1999). Cutaneous wound healing. N Engl J Med *341*, 738-746.
Sjogreen, B., Wiklund, P., and Ekstrom, P. A. (2000). Mitogen activated protein kinase inhibition by PD98059 blocks nerve growth factor stimulated axonal outgrowth from adult mouse dorsal root ganglia in vitro. Neuroscience *100*, 407-416.
Skoff, A. M., Lisak, R. P., Bealmear, B., and Benjamins, J. A. (1998). TNF-alpha and TGF-beta act synergistically to kill Schwann cells. J Neurosci Res *53*, 747-756.
Skold, M., Cullheim, S., Hammarberg, H., Piehl, F., Suneson, A., Lake, S., Sjogren, A., Walum, E., and Risling, M. (2000). Induction of VEGF and VEGF receptors in the spinal cord after mechanical spinal injury and prostaglandin administration. Eur J Neurosci *12*, 3675-3686.
Smale, K. A., Doucette, R., and Kawaja, M. D. (1996). Implantation of olfactory ensheathing cells in the adult rat brain following fimbria-fornix transection. Exp Neurol *137*, 225-233.
Smith, P. M., Lakatos, A., Barnett, S. C., Jeffery, N. D., and Franklin, R. J. (2002). Cryopreserved cells isolated from the adult canine olfactory bulb are capable of extensive remyelination following transplantation into the adult rat CNS. Exp Neurol *176*, 402-406.

Smith, P. M., Sim, F. J., Barnett, S. C., and Franklin, R. J. (2001). SCIP/Oct-6, Krox-20, and desert hedgehog mRNA expression during CNS remyelination by transplanted olfactory ensheathing cells. Glia *36*, 342-353.
Sonigra, R. J., Brighton, P. C., Jacoby, J., Hall, S., and Wigley, C. B. (1999). Adult rat olfactory nerve ensheathing cells are effective promoters of adult central nervous system neurite outgrowth in coculture. Glia *25*, 256-269.
Sonigra, R. J., Kandiah, S. S., and Wigley, C. B. (1996). Spontaneous immortalisation of ensheathing cells from adult rat olfactory nerve. Glia *16*, 247-256.
Squinto, S. P., Stitt, T. N., Aldrich, T. H., Davis, S., Bianco, S. M., Radziejewski, C., Glass, D. J., Masiakowski, P., Furth, M. E., Valenzuela, D. M., and et al. (1991). trkB encodes a functional receptor for brain-derived neurotrophic factor and neurotrophin-3 but not nerve growth factor. Cell *65*, 885-893.
St John, J. A., and Key, B. (2001). EphB2 and two of its ligands have dynamic protein expression patterns in the developing olfactory system. Brain Res Dev Brain Res *126*, 43-56.
St John, J. A., Pasquale, E. B., and Key, B. (2002). EphA receptors and ephrin-A ligands exhibit highly regulated spatial and temporal expression patterns in the developing olfactory system. Brain Res Dev Brain Res *138*, 1-14.
Stewart, H. J., Rougon, G., Dong, Z., Dean, C., Jessen, K. R., and Mirsky, R. (1995). TGF-betas upregulate NCAM and L1 expression in cultured Schwann cells, suppress cyclic AMP-induced expression of O4 and galactocerebroside, and are widely expressed in cells of the Schwann cell lineage in vivo. Glia *15*, 419-436.
Storan, M. J., and Key, B. (2004). Target tissue influences the peripheral trajectory of mouse primary sensory olfactory axons. J Neurobiol *61*, 175-188.
Struble, R. G., Beckman, S. L., Fesser, E., and Nathan, B. P. (2001). Volumetric and horseradish peroxidase tracing analysis of rat olfactory bulb following reversible olfactory nerve lesions. Chem Senses *26*, 971-981.
Studer, L., Spenger, C., Luthman, J., and Seiler, R. W. (1994). NGF increases neuritic complexity of cholinergic interneurons in organotypic cultures of neonatal rat striatum. J Comp Neurol *340*, 281-296.
Sulaiman, O. A., and Gordon, T. (2002). Transforming growth factor-beta and forskolin attenuate the adverse effects of long-term Schwann cell denervation on peripheral nerve regeneration in vivo. Glia *37*, 206-218.
Sweetwyne, M. T., Brekken, R. A., Workman, G., Bradshaw, A. D., Carbon, J., Siadak, A. W., Murri, C., and Sage, E. H. (2004). Functional analysis of the matricellular protein SPARC with novel monoclonal antibodies. J Histochem Cytochem *52*, 723-733.
Taipale, J., Saharinen, J., Hedman, K., and Keski-Oja, J. (1996). Latent transforming growth factor-beta 1 and its binding protein are components of extracellular matrix microfibrils. J Histochem Cytochem *44*, 875-889.
Takami, T., Oudega, M., Bates, M. L., Wood, P. M., Kleitman, N., and Bunge, M. B. (2002). Schwann cell but not olfactory ensheathing glia transplants improve hindlimb locomotor performance in the moderately contused adult rat thoracic spinal cord. J Neurosci *22*, 6670-6681.
Tennent, R., and Chuah, M. I. (1996). Ultrastructural study of ensheathing cells in early development of olfactory axons. Brain Res Dev Brain Res *95*, 135-139.

Thewke, D. P., and Seeds, N. W. (1996). Expression of hepatocyte growth factor/scatter factor, its receptor, c-met, and tissue-type plasminogen activator during development of the murine olfactory system. J Neurosci *16*, 6933-6944.
Thompson, R. J., Roberts, B., Alexander, C. L., Williams, S. K., and Barnett, S. C. (2000). Comparison of neuregulin-1 expression in olfactory ensheathing cells, Schwann cells and astrocytes. J Neurosci Res *61*, 172-185.
Tisay, K. T., and Key, B. (1999). The extracellular matrix modulates olfactory neurite outgrowth on ensheathing cells. J Neurosci *19*, 9890-9899.
Tomasiewicz, H., Ono, K., Yee, D., Thompson, C., Goridis, C., Rutishauser, U., and Magnuson, T. (1993). Genetic deletion of a neural cell adhesion molecule variant (N-CAM-180) produces distinct defects in the central nervous system. Neuron *11*, 1163-1174.
Tonge, D., Edstrom, A., and Ekstrom, P. (1998). Use of explant cultures of peripheral nerves of adult vertebrates to study axonal regeneration in vitro. Prog Neurobiol *54*, 459-480.
Treloar, H., Tomasiewicz, H., Magnuson, T., and Key, B. (1997). The central pathway of primary olfactory axons is abnormal in mice lacking the N-CAM-180 isoform. J Neurobiol *32*, 643-658.
Treloar, H. B., Nurcombe, V., and Key, B. (1996). Expression of extracellular matrix molecules in the embryonic rat olfactory pathway. J Neurobiol *31*, 41-55.
Tucker, B. A., Rahimtula, M., and Mearow, K. M. (2005). Integrin activation and neurotrophin signaling cooperate to enhance neurite outgrowth in sensory neurons. J Comp Neurol *486*, 267-280.
Valverde, F., Santacana, M., and Heredia, M. (1992). Formation of an olfactory glomerulus: morphological aspects of development and organization. Neuroscience *49*, 255-275.
Vaudry, D., Gonzalez, B. J., Basille, M., Anouar, Y., Fournier, A., and Vaudry, H. (1998). Pituitary adenylate cyclase-activating polypeptide stimulates both c-fos gene expression and cell survival in rat cerebellar granule neurons through activation of the protein kinase A pathway. Neuroscience *84*, 801-812.
Vega, C. J., and Peterson, D. A. (2005). Stem cell proliferative history in tissue revealed by temporal halogenated thymidine analog discrimination. Nat Methods *2*, 167-169.
Vickland, H., Westrum, L. E., Kott, J. N., Patterson, S. L., and Bothwell, M. A. (1991). Nerve growth factor receptor expression in the young and adult rat olfactory system. Brain Res *565*, 269-279.
Vincent, A. J., Taylor, J. M., Choi-Lundberg, D. L., West, A. K., and Chuah, M. I. (2005). Genetic expression profile of olfactory ensheathing cells is distinct from that of Schwann cells and astrocytes. Glia.
Vives, V., Alonso, G., Solal, A. C., Joubert, D., and Legraverend, C. (2003). Visualization of S100B-positive neurons and glia in the central nervous system of EGFP transgenic mice. J Comp Neurol *457*, 404-419.
Wang, S., and Barres, B. A. (2000). Up a notch: instructing gliogenesis. Neuron *27*, 197-200.
Wang, Y. Z., Meng, J. H., Yang, H., Luo, N., Jiao, X. Y., and Ju, G. (2003). Differentiation-inducing and protective effects of adult rat olfactory ensheathing cell conditioned medium on PC12 cells. Neurosci Lett *346*, 9-12.

Watabe, K., Fukuda, T., Tanaka, J., Toyohara, K., and Sakai, O. (1994). Mitogenic effects of platelet-derived growth factor, fibroblast growth factor, transforming growth factor-beta, and heparin-binding serum factor for adult mouse Schwann cells. J Neurosci Res *39*, 525-534.
Whitesides, J. G., 3rd, and LaMantia, A. S. (1996). Differential adhesion and the initial assembly of the mammalian olfactory nerve. J Comp Neurol *373*, 240-254.
Williams, E. J., Walsh, F. S., and Doherty, P. (1994). The production of arachidonic acid can account for calcium channel activation in the second messenger pathway underlying neurite outgrowth stimulated by NCAM, N-cadherin, and L1. J Neurochem *62*, 1231-1234.
Williams, S. K., Gilbey, T., and Barnett, S. C. (2004). Immunohistochemical studies of the cellular changes in the peripheral olfactory system after zinc sulfate nasal irrigation. Neurochem Res *29*, 891-901.
Wilson, P. O., Barber, P. C., Hamid, Q. A., Power, B. F., Dhillon, A. P., Rode, J., Day, I. N., Thompson, R. J., and Polak, J. M. (1988). The immunolocalization of protein gene product 9.5 using rabbit polyclonal and mouse monoclonal antibodies. Br J Exp Pathol *69*, 91-104.
Woodhall, E., West, A. K., and Chuah, M. I. (2001). Cultured olfactory ensheathing cells express nerve growth factor, brain-derived neurotrophic factor, glia cell line-derived neurotrophic factor and their receptors. Brain Res Mol Brain Res *88*, 203-213.
Yan, H., Bunge, M. B., Wood, P. M., and Plant, G. W. (2001a). Mitogenic response of adult rat olfactory ensheathing glia to four growth factors. Glia *33*, 334-342.
Yan, H., Nie, X., and Kocsis, J. D. (2001b). Hepatocyte growth factor is a mitogen for olfactory ensheathing cells. J Neurosci Res *66*, 698-704.
Yan, Q., and Johnson, E. M., Jr. (1988). An immunohistochemical study of the nerve growth factor receptor in developing rats. J Neurosci *8*, 3481-3498.
Yan, Q., Weaver, M., Perdue, N., and Sage, E. H. (2005). Matricellular protein SPARC is translocated to the nuclei of immortalized murine lens epithelial cells. J Cell Physiol *203*, 286-294.
Yi, E. C., Li, X. J., Cooke, K., Lee, H., Raught, B., Page, A., Aneliunas, V., Hieter, P., Goodlett, D. R., and Aebersold, R. (2005). Increased quantitative proteome coverage with (13)C/(12)C-based, acid-cleavable isotope-coded affinity tag reagent and modified data acquisition scheme. Proteomics *5*, 380-387.
Yuan, W., Zhou, L., Chen, J. H., Wu, J. Y., Rao, Y., and Ornitz, D. M. (1999). The mouse SLIT family: secreted ligands for ROBO expressed in patterns that suggest a role in morphogenesis and axon guidance. Dev Biol *212*, 290-306.
Zanger, K., Radovick, S., and Wondisford, F. E. (2001). CREB binding protein recruitment to the transcription complex requires growth factor-dependent phosphorylation of its GF box. Mol Cell *7*, 551-558.
Zehntner, S. P., Mackay-Sim, A., and Bushell, G. R. (1998). Differentiation in an olfactory cell line. Analysis via differential display. Ann N Y Acad Sci *855*, 235-239.
Zhang, Z., and Guth, L. (1997). Experimental spinal cord injury: Wallerian degeneration in the dorsal column is followed by revascularization, glial proliferation, and nerve regeneration. Exp Neurol *147*, 159-171.
Zhang, Z., Yoo, R., Wells, M., Beebe, T. P., Jr., Biran, R., and Tresco, P. (2005). Neurite outgrowth on well-characterized surfaces: preparation and characterization of chemically

and spatially controlled fibronectin and RGD substrates with good bioactivity. Biomaterials *26*, 47-61.

Appendices

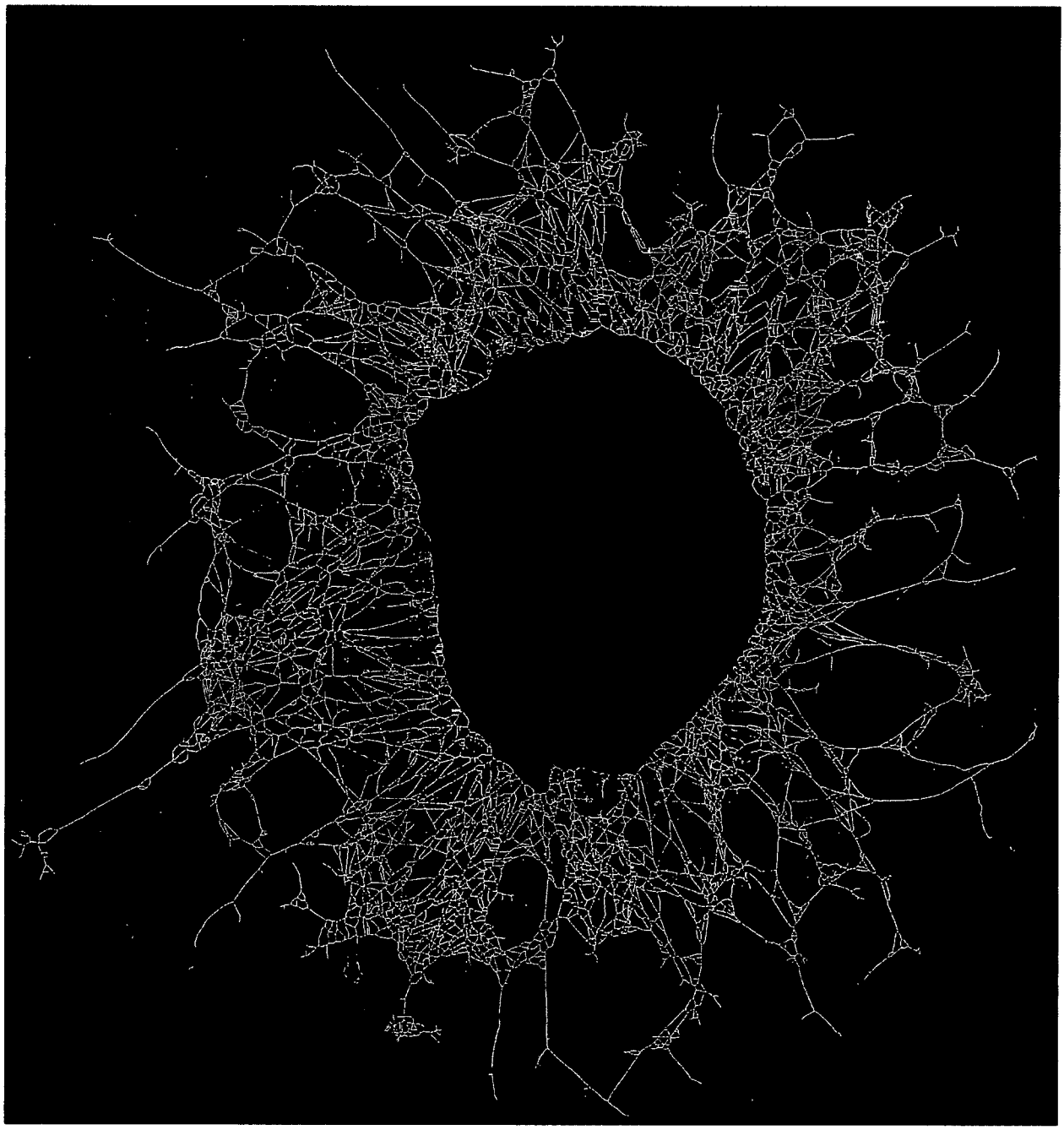

APPENDIX 1
A Skeletonized DRG Explant

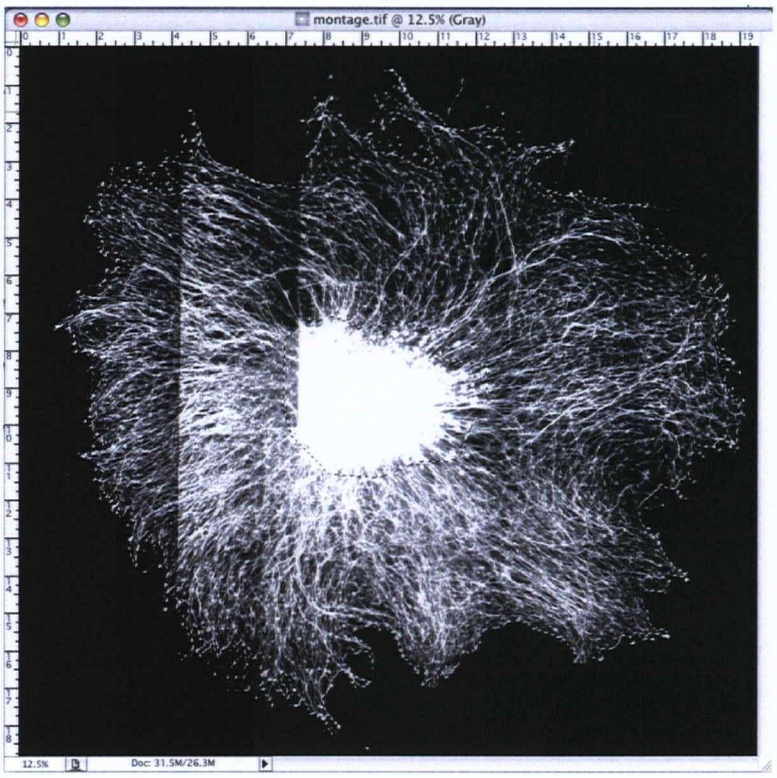

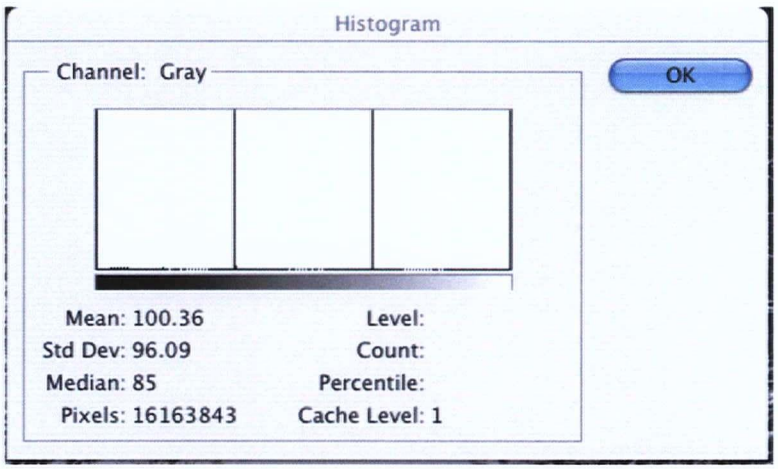

APPENDIX 2
Measuring Neurite Carpet Surface Area

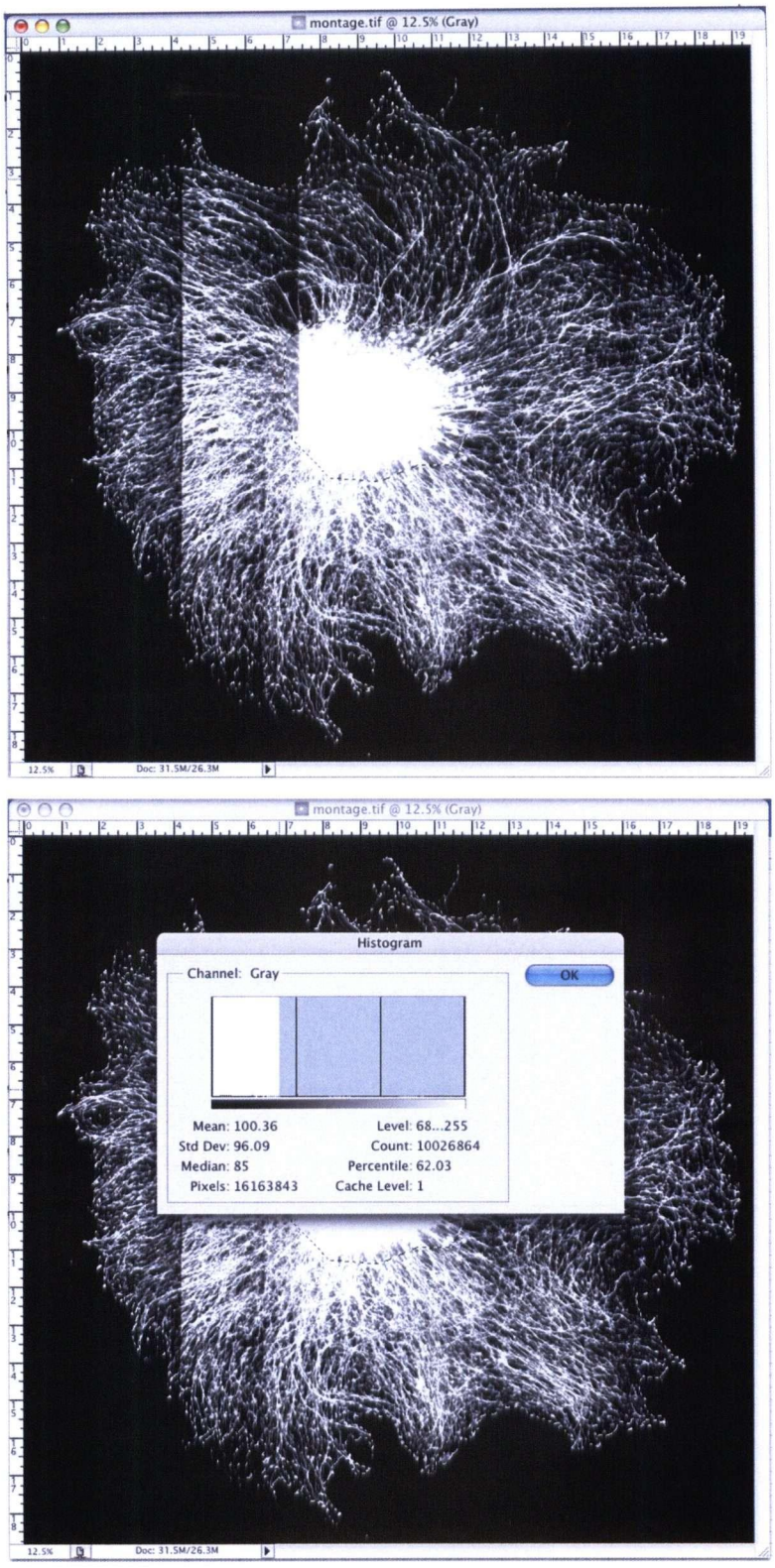

APPENDIX 3
Measuring Total Neurite Pixels

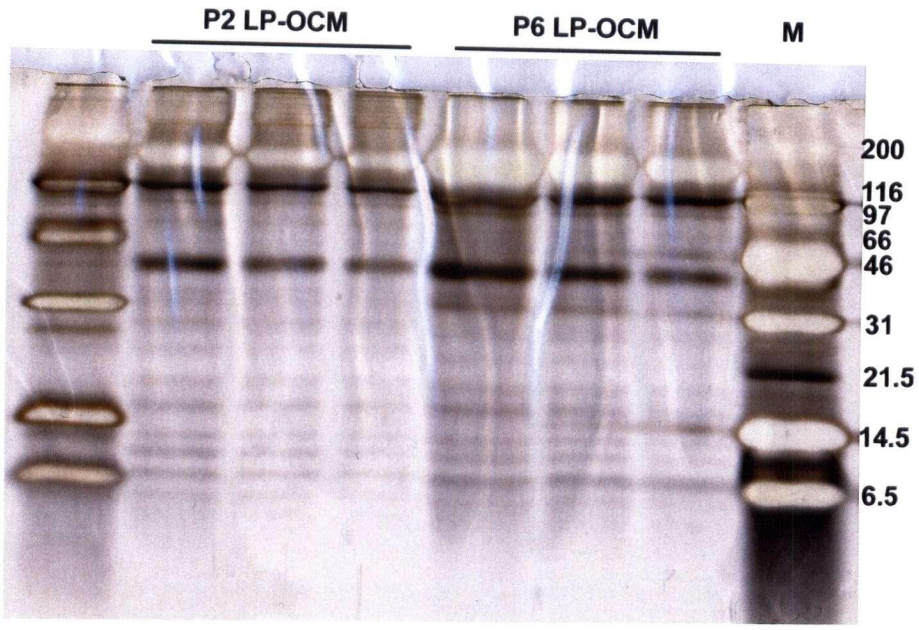

APPENDIX 4
Silverstain of P2 and P6 LP-OCM

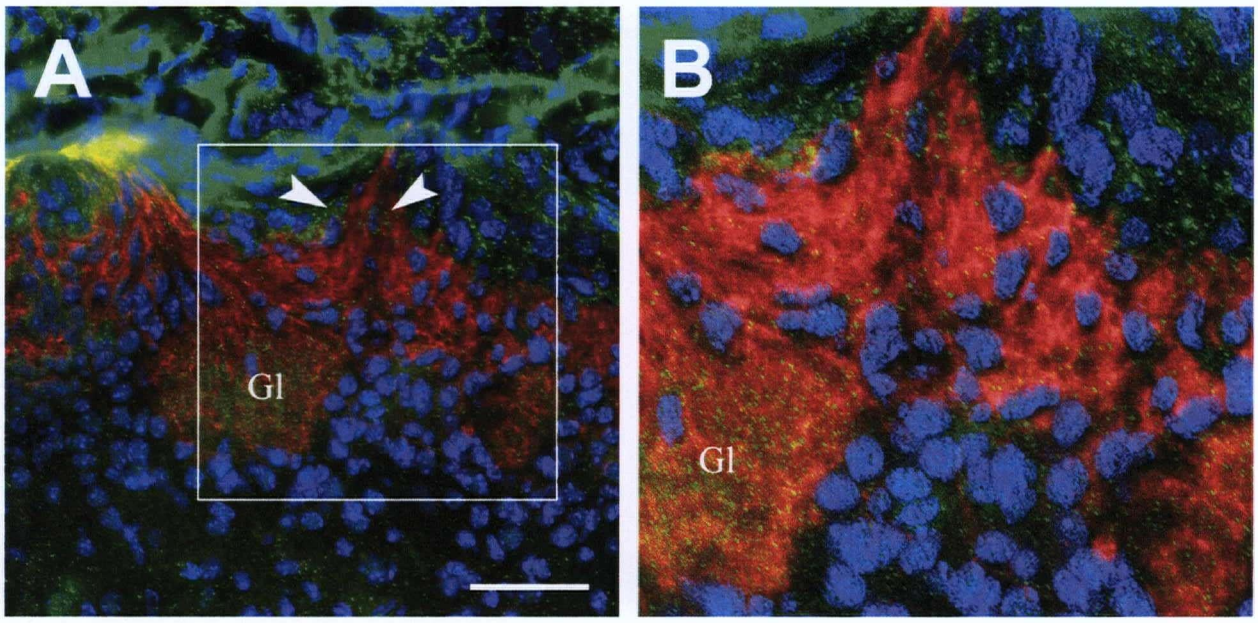

APPENDIX 5

Alternate Image of SPARC Expression in the Olfactory Bulb

(A and B) Postnatal day 5 olfactory nerve fibre layer and glomeruli (Gl) immunolabeled with NCAM (red), SPARC (green) and DAPI (blue). Arrowheads indicate SPARC-positive OB-OEC accompanying ORN axons towards glomeruli. (B) is higher magnification of box in (A). Scale-bar represents 100 microns.

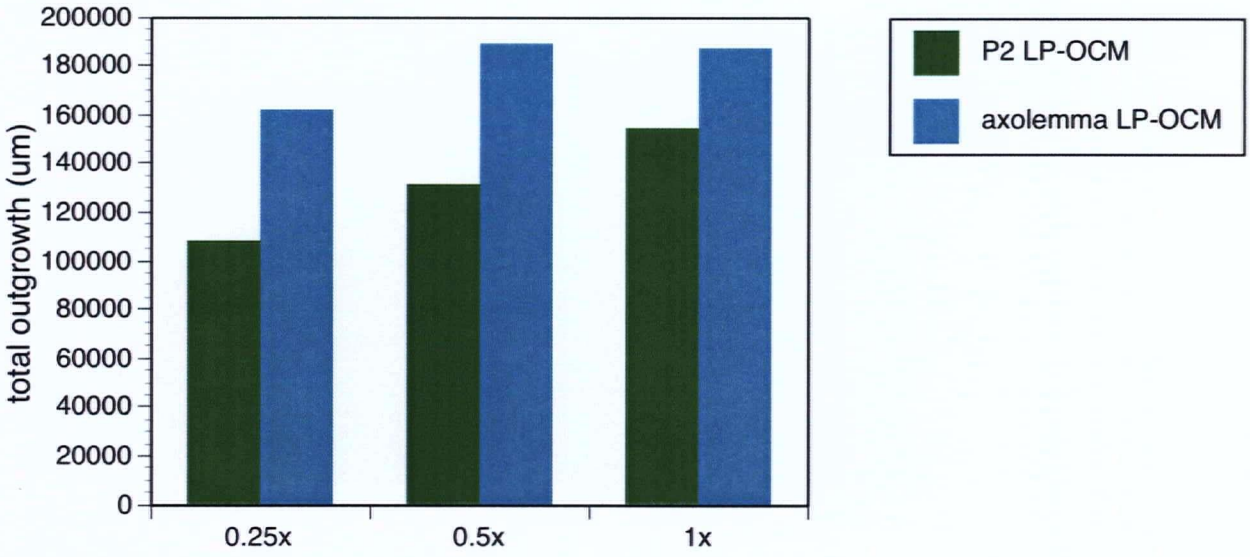

APPENDIX 6

Comparison of P2 LP-OCM and Axolemma-stimulated LP-OCM

Total outgrowth for passage 2 (dark green) and axolemma-stimulate passage 2 (teal) media at various concentrations.